Regulation of Protein Degradation at the Endoplasmic Reticulum

Anna Sophie Dickson

Newnham College

This dissertation is submitted for the degree of Doctor of Philosophy

June 2020

Department of Medicine

Cambridge Institute for Medical Research/Cambridge Institute of Therapeutic, Immunology and Infectious Disease

University of Cambridge

UNIVERSITY OF CAMBRIDGE

Declaration

This dissertation is the result of my own work and includes nothing which is the outcome of work done in collaboration except as declared in the Preface and specified in the text.

It is not substantially the same as any that I have submitted, or, is being concurrently submitted for a degree or diploma or other qualification at the University of Cambridge or any other University or similar institution except as declared in the Preface and specified in the text. I further state that no substantial part of my dissertation has already been submitted, or, is being concurrently submitted for any such degree, diploma or other qualification at the University of Cambridge or any other University or similar institution except as declared in the Preface and specified in the text.

It does not exceed the prescribed word limit for the relevant Degree Committee.

Anna Sophie Dickson

Regulation of Protein Degradation at the Endoplasmic Reticulum

Endoplasmic reticulum (ER) associated degradation (ERAD) is important for removing damaged or misfolded proteins at the ER membrane, and is central to the physiological regulation of proteins such as HMG-CoA Reductase (HMGCR), the rate limiting enzyme in cholesterol biosynthesis. Under sterol rich conditions, HMGCR is rapidly degraded through ERAD, however, when sterols are limited, HMGCR is stabilised through decreased degradation and increased transcription by the transcription factor SREBP2. As well as being tightly regulated by sterol levels, the cholesterol synthesis pathway is highly oxygen dependent; however, how oxygen levels affect the regulation of this pathway is largely unknown. Here, using a combination of fluorescent reporters, genetic approaches, and cellular assays, I determine the role of hypoxia in the regulation of cholesterol synthesis, and also characterise the ubiquitination machinery for an ERAD pathway involving the degradation of misfolded cytosolic proteins. Under low sterol conditions, I show that low oxygen availability overrides the stabilisation of HMGCR. This is not dependent upon the canonical mammalian hypoxia response, driven by hypoxia-inducible factors (HIFs), but instead relies on SREBP2. I find that SREBP2 protein levels are reduced in hypoxia which are partially rescued by proteasome inhibition, suggesting that SREBP2 protein degradation occurs when oxygen is scarce. Recently, using forward genetic screens to probe for the ERAD machinery required to degrade a model misfolded protein, the CL1 degron, the Nathan group identified that two ER E3 ligases, MARCH6 and TRC8, were also potentially involved in the degradation of SREBP2. Here I show that the ubiquitin conjugating enzyme UBE2J2, is involved in this pathway, and identify a role for the ER membrane complex (EMC) in regulating the membrane insertion of UBE2J2. My data also shows that in hypoxia, depletion of MARCH6 and TRC8 partially rescues HMGCR levels, consistent with a role for SREBP2 protein degradation in regulating cholesterol synthesis. Together, these studies demonstrate the importance of hypoxia in the regulation of cholesterol synthesis, which could have broad implications for our understating of how solid cancerous tumours adapt to their hypoxic and nutrient deprived environments.

Acknowledgements

I would like to thank all those who kindly donated reagents that were used in the preparation of this thesis. In particular I would like to thank Sandra Stefanovic-Barret, Sam Menzies, Norbert Volkmar, Stephen Burr, Peter Bailey, and Dick van den Boomen (Nathan and Lehner laboratories, CIMR/CITIID, Cambridge), for kindly providing cell lines which are detailed and acknowledged in this thesis, and Ian Brierley for his help carrying out the polysome profiling and advice interpreting the data.

I am especially grateful to my supervisor, James Nathan, for his support, guidance and advice throughout my PhD, and with the preparation of this work. I would also like to thank all members of the Nathan laboratory, past and present, for their on-going support, advice and friendship through my PhD. In particular I would like to thank Sandra Stefanovic-Barrett, for teaching me many laboratory techniques at the beginning of my PhD and for always being on hand to answer my questions, and Peter Bailey, for helping analyse my CRISPR screen sequencing data. I would also like to thank Paul Lehner for his helpful advice during my PhD as well as all members of his group. In particular I would like to thank Sam Menzies and Norbert Volkmar for helping me find my feet in experimental the world of cholesterol synthesis, and Stuart Bloor, who along with Sam Menzies and Peter Bailey, gave me helpful advice and support carrying out and analysing the data from the forward genetic screens. This work was funded by the Medical Research Council and the Wellcome Trust.

On a personal note, I would like to thank my partner Jonathan for his constant support throughout my PhD, and for enduring me writing this thesis through some of the COVID-19 lockdown. Finally, I am eternally grateful to my parents, Moyra and Colin, and my sister, Emily, for their never ending support, encouragement and patience in all my endeavours.

Publications arising from work from this thesis

1. Stefanovic-Barrett. S., **Dickson. A. S**., Burr. S. P., Williamson. J. C., Lobb. I. T., van den Boomen. D. J., Lehner. P. J., Nathan. J. A. (2018). MARCH6 and TRC8 facilitate the quality control of cytosolic tail-anchored proteins. *EMBO Reports.* 19(5).

2. Menzies. S. A., Volkmar. N., van den Boomen. D. J., Timms. R. T., **Dickson. A. S**., Nathan. J. A., Lehner. P. J. (2018). *eLife*. DOI: 10.7554/eLife.40009

3. Signes. A., Cerutti. R., **Dickson. A. S**., Benincá. C., Hinchy. E. C.,Ghezzi. D., Carrozzo. R., Bertini. E., Murphy. M. P., Nathan. J. A., Viscomi. C., Fernandez-Vizarra. E., Zeviani. M. (2019). *EMBO Molecular Medicine*. 11(1).

Abbreviations

2-OGDD	2-Oxoglutarate-Dependent Dioxygenase
ATP	Adenosine triphosphate
β2M	Beta-2 Microglobulin
BiP	Binding Immunoglobulin Protein
BSA	Bovine Serum Albumin
Btz	Bortezomib (Velcade)
CAIX	Carbonic Anhydrase 9
Cas9	CRISPR-Associated Protein 9
cDNA	Complimentary DNA
CHOP	C/EBP-Homologous Protein 10
Co-IP	Co-immunoprecipitation
CRISPR	Clustered Regularly Interspaced Short Palindromic Repeat
CFTR	Cystic Fibrosis Transmembrane conductor Regulator
DMEM	Dulbecco's Modified Eagle's Medium
DMOG	Dimethyloxalylglycine
DMSO	Dimethyl Sulfoxide
DNA	Deoxyribonucleic Acid
DTT	Dithiothreitol
E.coli	Escherichia coli
ECL	Enhanced Chemiluminescence
EGFR	Epidermal Growth Factor Receptor
eIF	Eukaryotic Translation Initiation Factor
EMC	Endoplasmic reticulum Membrane Complex
ER	Endoplasmic Reticulum
ERAD	Endoplasmic Reticulum Associated Degradation
FACS	Fluorescence-Activated Cell Sorting

FCS	Foetal Calf Serum
FH	Familial Hypocholesterolemia
GBM	Glioblastoma
GFP	Green Fluorescent Protein
Gp78	Glycoprotein 78
GTP	Guanosine Triphosphate
HA	Hemagglutinin
HECT	Homologous to the E6AP Carboxyl Terminus
HEK	Humanembryonic Kidney
HeLa	Henrietta Lacks
HEPG2	Hepatoma G2
HCMV	Human Cytomegalovirus
HIF	Hypoxia-Inducible transcription Factor
HMCGR	3-Hydroxy-3-Methylglutaryl-CoA Reductase
HMGCS1	3-Hydroxy-3-Methylglutaryl-CoA Synthase 1
Hrd1	HMG-CoA Reductase Degradation 1 Homologue
HRE	Hypoxia Response Element
IF	Immunofluorescence
INSIG	Insulin Induced Gene
IP	Immunoprecipitation
IRES	Internal Ribosome Entry site
ISRIB	Integrated Stress Response Inhibitor
KO	Knock-Out
LB	Lysogeny Broth
LDLR	Low-Density Lipoprotein Receptor
LPDS	Lipoprotein Deficient Serum
LXR	Liver X Receptor
mAb	Monoclonal Antibody

MARCH6	Membrane Associated Ring-CH-Type Finger 6
MBCD	Methyl-β-cyclodextrin
MHC	Major Histocompatibility Complex
MOI	Multiplicity of Infection
mRNA	Messenger Ribonucleic Acid
mTOR	Mammalian Target of Rapamycin
PBS	Phosphate Buffered Saline
PCR	Polymerase Chain Reaction
PFA	Paraformaldehyde
PHD	Proyl Hydroxylase Domain
RING	Really Interesting New Gene
RNF145	Ring Finger Protein 145
ROS	Reactive Oxygen Species
RT-qPCR	Quantitative Reverse Transcription Polymerase Chain Reaction
SCAP	SREBP Cleavage Activating Protein
SD	Sterol Depletion
SDS-PAGE	Sodium Dodecyl Sulphate Polyacrylamide Gel Electrophoresis
sgRNA	Single Guide RNA
siRNA	Small Interfering RNA
SOC	Super Optimal Broth
SREBP	Sterol Regulatory Element-Binding Protein
SSD	Sterol Sensing Domain
TBS	Tris Buffered Saline
TMD	Transmembrane Domain
TNM	Theonellamides
TRC	Transmembrane Recognition Complex
TRC8	Translocation in Renal Carcinoma, Chromosome 8
Tsc	Tuberous Sclerosis Complex

Ub	Ubiquitin
UPR	Unfolded Protein Response
UPS	Ubiquitin Proteasome System
UTR	Untranslated Region
VCP/p97	Valosin-Containing Protein
VHL	Von Hippel–Lindau tumour suppressor protein
WT	Wildtype

Table of Contents

List of Figures

List of Tables

Chapter 1: Introduction

1.1. Intracellular protein quality control and degradation

Intracellular protein quality control is an essential process within cells to ensure survival and limit toxicity (Balchin *et al.*, 2016). Protein quality control involves several pathways within the endoplasmic reticulum (ER) and cytosol to ensure that misfolded or damaged proteins are removed or refolded. However, genetic defects, drug toxicity, conditions associated with a lack of folding capacity in the ER, or protein aggregation can overwhelm the cell's intrinsic quality control mechanisms (reviewed in Hartl & Hayer-Hartl, 2009). As a result, misfolded proteins can accumulate within cells and can cause pathological toxicity. This is apparent in diseases including lysosomal storages disorders (Sawkar *et al.*, 2006) and a number of neurodegenerative diseases such as Alzheimer's and Parkinson's disease (Aguzzi & O'Connor, 2010).

Within mammalian cells the ubiquitin proteasome system (UPS) and autophagy are the two major intracellular quality control pathways that maintain protein homeostasis by removing misfolded or damaged proteins. Most soluble misfolded or damaged proteins are typically removed through the UPS, whereas bulk degradation of larger cellular components including damaged or aggregated proteins, damaged organelles and intracellular pathogens are removed from the cell through the process of autophagy. The UPS involves the selective ubiquitination of protein substrates preceding degradation by the multi-subunit ATP-dependent protease, the 26S proteasome (Collins & Goldberg, 2017; Grice & Nathan, 2016). Autophagy involves the formation of a cytosolic intracellular membrane (termed autophagosome), which is able to engulf cargo and ultimately target it for lysosomal degradation (Glick *et al.*, 2010). Alongside these protein degradation pathways are cellular responses to promote protein folding, such as the ER stress response. The ER stress response is triggered upon an accumulation of misfolded proteins, and the cell responds by increasing the folding capacity of the ER and decreasing general protein synthesis, in an attempt to restore protein homeostasis (Ron & Walter, 2007). For this thesis I will be focusing on specific

degradation pathways associated with the UPS and in particular protein degradation at the ER membrane.

1.1.1. The ubiquitin proteasome system

Post translational modification of proteins by the 76 amino acid protein ubiquitin (Ub) is used to regulate several fundamental cellular processes such as: protein degradation, protein localisation, and protein-protein interactions (Komander & Rape, 2012). Ubiquitination involves an enzymatic cascade involving three main groups: ubiquitin activating enzymes (E1), ubiquitin conjugating enzymes (E2) and ubiquitin ligase enzymes (E3). These enzymes work together to transfer ubiquitin onto a specific substrate, usually attaching ubiquitin to a lysine residue. Firstly, the E1 enzyme activates ubiquitin in an ATP dependent manner, then the activated ubiquitin binds to a ubiquitin conjugating enzyme (E2). Finally, the E3 ligase recruits the E2 enzyme and allows transfer of ubiquitin onto the substrate (Hershko *et al*., 1983; Pickart, 2001) **(Figure 1.1)**.

Specific modification of a substrate with ubiquitin can require just one ubiquitin (monoubiquitination), or multiple ubiquitin moieties (polyubiquitination); both of which have important roles in cellular processes. For example, monoubiquination has been shown to be important during the sorting of proteins within the endocytic pathway (Haglund & Dikic, 2012), whilst polyubiquitination is known to be important in protein stability and degradation. For polyubiquitination, ubiquitin can be conjugated to itself through one of its seven lysine residues (K6, K11, K27, K29, K31, K48 and K63) or it's N-terminus, forming distinct ubiquitin chains which act as unique signals. For example, K48-linked chains are the canonical signal for proteasomal degradation, whereas K63-linked chains are typically involved in cell signalling and DNA repair (Haglund & Dikic, 2005; Nathan *et al*., 2013).

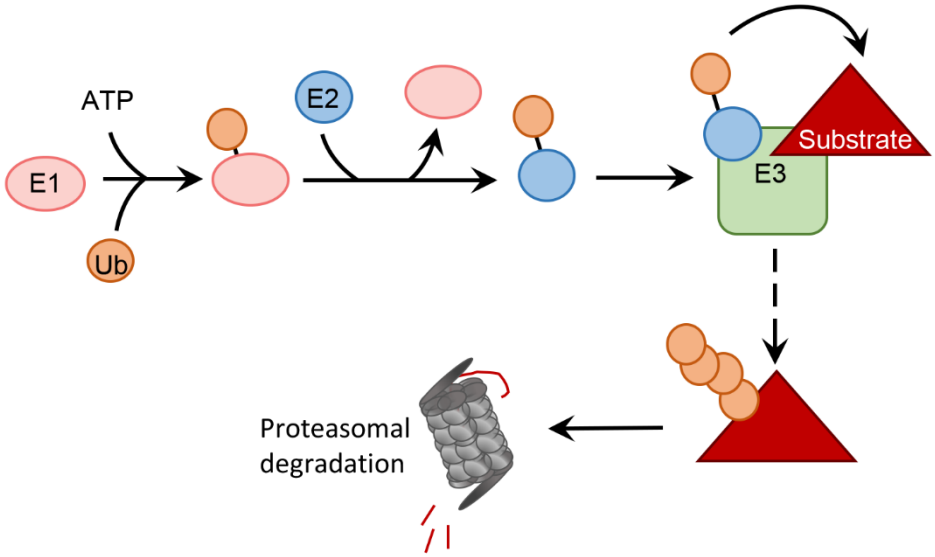

Figure 1.1. The enzymatic cascade of substrate ubiquitination as a signal for proteasomal degradation.

Ubiquitination is a common signal in eukaryote cells for proteasomal degradation. Substrate ubiquitination involves a signalling cascade of E1 ubiquitin activating, E2 ubiquitin conjugating and E3 ubiquitin ligase enzymes. Ubiquitin (Ub) is firstly activated by the E1 enzyme, before being transferred to an E2 enzyme. The E3 ligase then recruits the E2 and transfers ubiquitin onto the substrate to target it for degradation by the multi-subunit ATP-dependent protease, the 26S proteasome.

The best described role for ubiquitination is for protein degradation through the UPS. The specific ubiquitination of protein substrates for proteasome mediated degradation provides a highly selective mechanism for removing proteins form the cell. The human genome encodes approximately 2 E1s, 40 E2s and over 600 E3 ligases (Li *et al.*, 2008). Due to the abundance of distinct ligases, E3 ligases are principally responsible for substrate recognition within cells, although the interaction with E2s can also be important in increasing substrate specificity. There are two main families of E3 ligases, the homologous to the E6AP carboxyl terminus (HECTs), and the really interesting new genes (RINGs). RING E3 ligases, mediate direct transfer of ubiquitin from the E2 to the substrate, whereas HECT family members accept the ubiquitin from the E2 forming a thioester intermediate, before transferring ubiquitin to the substrate (reviewed by Metzger *et al.*, 2012). Although much is known about ubiquitination and the UPS, understanding how E3 ligases selectively bind their substrates, and the role of different polyubiquitin chains remains poorly understood and is an area of intense research interest.

1.1.2. Endoplasmic reticulum associated degradation

Endoplasmic reticulum associated degradation (ERAD) is a specialised form of proteasomal degradation which targets terminally misfolded secretory or ER membrane proteins and some cytosolic proteins for degradation, as well as controlling the cellular concentration of specific proteins **(Figure 1.2)**. The most commonly studied role of ERAD is the removal of terminally misfolded secretory, or membrane proteins within the ER. Proteins with an ER signal sequence at their N-terminus can enter the ER through the sec61 translocon (Görlich *et al*., 1992; Osborne *et al*., 2005). However, this pathway is inaccessible to tail-anchored proteins, which have an ER targeting sequence at their C-terminus, so these proteins enter the ER post translationally via the transmembrane recognition complex (TRC) 40 pathway (Stefanovic & Hegde, 2007) or the ER membrane complex (EMC) (Guna *et al*., 2018). Once proteins are in the ER, protein folding occurs facilitated by ER chaperones such as binding immunoglobulin protein (BiP), which prevent the aggregation of unfolded proteins (reviewed in Ron & Walter, 2007; Sun & Brodsky, 2019). When folding is complete, proteins destined for the secretory pathway then leave the ER. However, it is estimated that up to 30% of proteins in mammalian cells fail to fold correctly (Schubert *et al*., 2000). These misfolded proteins often display exposed hydrophobic domains that would normally be buried within membranes, and exposure of these domains can lead to an increased propensity for protein aggregation. ER chaperones readily recognise and bind to these domains in an attempt to limit any toxicity caused by aggregation (reviewed in Hartl & Hayer-Hartl, 2009). Eventually, terminally misfolded proteins are retrotranslocated across the ER membrane into the cytosol where they are polyubiquitinated, extracted from the membrane, and degraded by the proteasome (Brodsky & Vembar, 2008).

Aside from ERAD's role in maintaining proteostasis, it is involved in many diseases. For example, in cystic fibrosis a genetic germline mutation causing deletion of amino acid 508 in the cystic fibrosis transmembrane conductor regulator (CFTR) protein disrupts the folding ability of CFTR within the ER, and is the most common cause of the disease. The mutant CFTR protein is targeted for ERAD (Ward *et al*., 1995) to limit toxicity, but this does not restore CFTR function, and it is the loss of this protein through degradation which leads to cystic fibrosis.

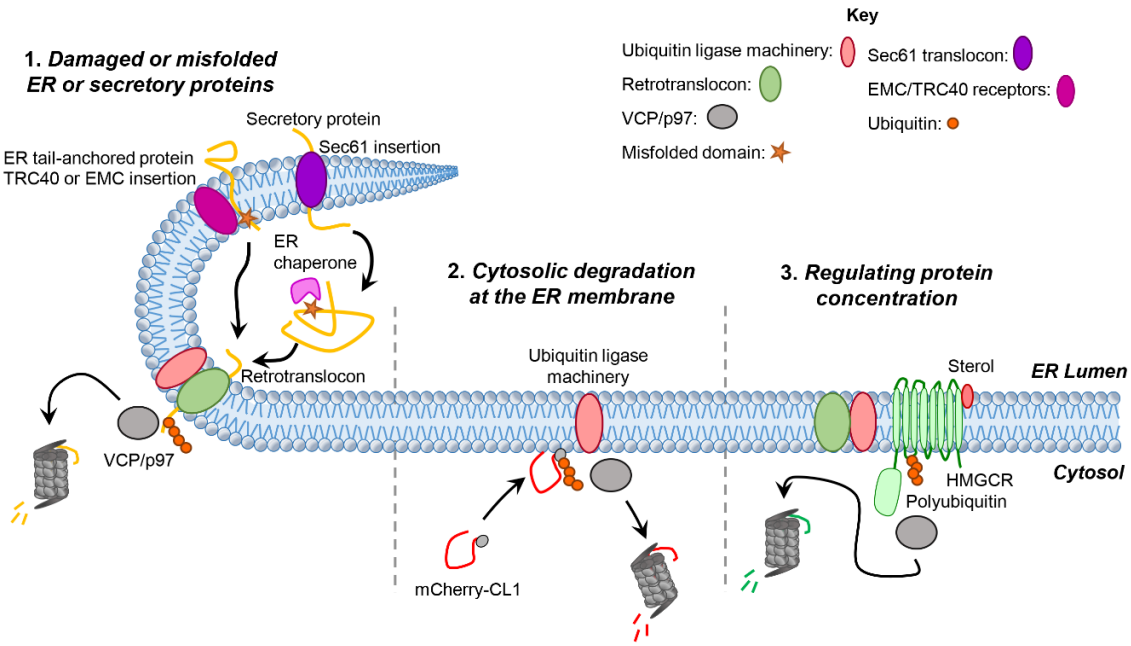

Figure 1.2. The role of endoplasmic reticulum associated degradation in protein homeostasis. Endoplasmic reticulum associated degradation (ERAD) is a specialised form of proteasomal degradation which regulates the degradation of damaged or misfolded ER or secretory proteins **(1)**, the degradation of some cytosolic proteins **(2)**, and regulates the physiological level of some proteins **(3)**. **1.** Soluble secretory proteins enter the ER through through the Sec61 translocation channel, whilst tail-anchored proteins enter the ER membrane post translationally through interaction with the transmembrane receptor complex (TRC) 40 pathway, or the ER membrane complex (EMC). Proteins within the ER that are recognised as misfolded, are retrotranslocated into the cytosol, ubiquitinated, extracted from the membrane and degraded by the proteasome. **2.** Some misfolded cytosolic proteins e.g. the CL1 degron, a model misfolded protein, associate with the ER membrane, are ubiquitnated, extracted and degraded by the proteasome. **3.** ERAD degrades some correctly folded proteins to control cellular protein concentration, e.g. HMG-CoA Reductase (HMGCR). When sterols are present within the ER membrane, HMGCR is ubiquitinated, extracted from the membrane and degraded by the proteasome.

As well as genetic mutations affecting ERAD, some viruses have evolved to hijack ERAD to increase their chances of infecting mammalian cells and evade the host's immune response. This is well described for the human cytomegalovirus (HCMV). Following infection with HCMV the expression of the viral protein US11 causes the degradation the major histocompatibility complex (MHC) class 1 (MHC-1) protein, enabling these virally infected cells to escape recognition by the immune system and cause increased infection (van den Boomen & Lehner, 2015; Wiertz *et al.*, 1996).

1.1.3. The machinery involved in endoplasmic reticulum associated degradation

In budding yeast, *Saccharomyces cerevisiae (S. cerevisiae)*, two ERAD complexes exist within the ER membrane consisting of two separate E3 ligases, Doa10p (Swanson *et al*., 2001) and Hrd1p (Bays *et al*., 2001), which function with a variety of other proteins to degrade ERAD substrates. These two complexes generally work to degrade separate substrates, with Doa10p monitoring the cytosolic portion of membrane proteins (ERAD-C), whilst Hrd1p recognises misfolded luminal (ERAD-L) and transmembrane regions (ERAD-M) of ER membrane proteins (Carvalho *et al*., 2006). The E2 enzymes generally involved in ERAD in *S. cerevisiae*, are Ubc6, which is an ER transmembrane protein, and Ubc7, which is associate with the ER through the ER anchor protein Cue1p. These E2 enzymes work independently with both ligases dependent upon the substrate (Christianson & Ye, 2014). In yeast, ERAD has also been implicated outside of the ER but in membrane compartments continuous to the ER such as the nuclear membrane. The E3 Asi complex works with Ubc6 and Ubc7 to degrade proteins within the inner nuclear membrane via ERAD (Foresti *et al*., 2014; Khmelinskii *et al*., 2014).

Whilst yeast only uses two E3 ligases for classical ERAD, in mammalian cells the E3 ligases involved in ERAD have rapidly expanded, probably due to increased protein complexity within the ER. Many mammalian E3 ligases have been implicated in ERAD, with a wide range of substrates. These include ER resident E3 ligases Hrd1 (Kikkert *et al*., 2004; Nadav *et al*., 2003) and gp78 (Fang *et al*., 2001; Menzies *et al*., 2018) (orthologues of Hrd1p), MARCH6 (Membrane Associated ubiquitin Ring-CH-Type finger 6) (orthologue of Doa10p) (Hassink *et al*., 2005; Stefanovic-Barrett *et al*., 2018), TRC8 (Stagg *et al*., 2009; Stefanovic-Barrett *et al*., 2018), TMEM129 (van den Boomen *et al*., 2014) and RNF145 (Jiang *et al*., 2018; Menzies *et al*., 2018). The E2 conjugating enzymes primarily implicated in mammalian ERAD have not rapidly expanded from those observed in yeast. The predominant E2 enzymes involved in ERAD include UBE2J1 (Mueller *et al*., 2008) and UBE2J2 (Stefanovic-Barrett *et al*., 2018) (orthologues of Ubc6), which are single pass ER tail-anchored proteins, and UBE2G2 (orthologue of Ubc7) (Menzies *et al*., 2018; Stefanovic-Barrett *et al*., 2018), which is an ER associated cytosolic protein recruited to the ER by Ancient Ubiquitous Protein 1 (AUP1) (Spandl *et al*., 2011). AUP1 is associated with the membranes of the ER and lipid droplets through its N-terminal hydrophobic region, and the G2 binding region (G2BR) at its C-terminus

has been shown to recruit the E2 enzyme UBE2G2, intrinsically linking AUP1 to the ERAD process (Spandl *et al*., 2011).

ER proteins destined for degradation are retrotranslocated into the cytosol for ubiquitination and subsequent proteasomal degradation. This process is an energy dependent process, requiring the AAA ATPase Cdc48 in yeast, or the mammalian orthologue vasolin-containing protein (VCP)/p97 (Ye *et al*., 2001). For many years, the mechanism by which misfolded proteins cross the ER membrane remained controversial, but more recently Hrd1p was identified as a likely candidate in *S. cerevisiae* (Baldridge & Rapoport, 2016; Carvalho *et al*., 2010). Schoebel *et al*., (2017) revealed that Hrd1p forms an aqueous cavity across the ER membrane, suggesting that it could function as a retrotranslocation channel. In mammalian cells, Hrd1 and gp78 are both orthologues of Hrd1p, and a number of other ligases, including RNF145 and TRC8, show sequence similarities to Hrdp1 (Schoebel *et al*., 2017; Wu & Rapoport, 2018). This suggests that these ligases could function in a similar manner, however, further experimental evidence is needed to show this.

1.1.4. Cytosolic degradation at the endoplasmic reticulum membrane

ER protein quality control and the involvement of the UPS in ERAD is reasonably well understood for ER membrane and secretory proteins, although new pathways and substrates are frequently identified. However, less is generally known about the substrates and machinery involved in the quality control and proteasomal degradation of cytosolic misfolded proteins, which could have huge implications in diseases involving the accumulation and aggregation of misfolded proteins.

Endogenous or artificial substrate reporter systems are useful for studying protein quality control. The cytosolic CL1 degron was initially identified in *S. cerevisiae* in a genetic screen to identify peptide sequences that promote rapid proteasomal degradation (Gilon *et al*., 1998). Gilon *et al* identified the CL1 degron as a 16 amino acid sequence that is thought to represent an exposed hydrophobic domain, in the form of an amphipathic helix. This domain is analogous to misfolded or damaged cellular proteins and is rapidly degraded by the proteasome (Balchin *et al*., 2016). The CL1 degron has been used in genetic screens to identify

genes involved in cytosolic protein quality control and protein aggregate formation (Bence *et al*., 2005). In yeast, attachment of CL1 to the cytosolic protein Urap3, leads to rapid degradation which requires the ER resident E3 ligase Doa10p, and the E2 enzymes Ubc6 and Ubc7, suggesting that access to the cytosolic face of the ER membrane is required for CL1 degradation (Gilon *et al*., 1998; Metzger *et al*., 2008). However, in mammalian cells CL1 fusion proteins have typically been used as proteasome reporters for cytosolic protein aggregates and the membrane localisation of CL1 fusion proteins had not been described (Bennett *et al*., 2005). Misfolded proteins with exposed hydrophobic residues are often bound by chaperones to limit protein aggregation and toxicity. The cytosolic chaperone Bag6 is involved in the TRC pathway, which mediates the ER insertion of tail-anchored proteins, and has been implicated in the degradation of CL1 in mammalian cells (Minami *et al*., 2010). Recently, the Nathan laboratory combined the use of a fluorescent CL1 reporter and genetic screens to study the membrane localisation and proteasomal degradation of the CL1 degron. It was shown that CL1 is degraded at the cytosolic face of the ER membrane, independently of Bag6, and requires ERAD machinery for full proteasomal degradation, supporting a role for ERAD in cytosolic protein quality control in mammalian cells (Stefanovic-Barrett *et al*., 2018) **(Figure 1.2) (see 1.4.2 and Chapter 3)**.

1.1.5. The role of ERAD in regulating protein concentrations

Further to the role of ERAD in removing misfolded or damaged proteins both within the cytosol and the secretory pathway, ERAD is also important in regulating some physiological pathways by recognising and degrading correctly folded proteins in order to regulate protein concentration. This is observed with apolipoprotein-B (apoB). ApoB is a major component of circulating lipids, and when cellular lipids are low, ApoB is almost immediately degraded by ERAD following its co-translational insertion in to the ER membrane (Fisher *et al*., 2011). Another example of physiological regulation by ERAD is within the cholesterol synthesis pathway, where levels of the enzyme involved in the first rate limiting step, 3-Hydroxy-3-Methylglutaryl-CoA Reductase (HMGCR), are tightly regulated through ERAD **(Figure 1.2)**. This pathway will be discussed in detail in **section 1.2**.

1.2. The regulation of cholesterol in mammalian cells

Within the cell, cholesterol has several vital functions. It is fundamental for maintaining the normal structure, fluidity and permeability of cell membranes, and is therefore required for cell growth. Additionally, cholesterol is involved in several metabolic pathways including the production of steroid hormones, bile and vitamin D (reviewed in Simons & Ikonen, 2000). Whilst cholesterol is necessary for cell survival, elevated levels of circulating cholesterol is a risk factor for a number of diseases including cardiovascular disease, hypertension and diabetes, therefore understanding how to modulate cholesterol levels is important in many clinical settings (reviewed by Seo & Choi, 2015).

Cholesterol is primarily synthesised and used in the liver in a series of reactions that occur at the ER membrane. Cholesterol is the major sterol component within mammalian cell membranes, however, within the cell, membrane cholesterol levels are not homogenous. Over 90% of a cell's membrane cholesterol is enriched in the latter stages of the secretory pathway, primarily located at the plasma membrane. Interestingly, the ER membrane, where the majority of cellular *de novo* cholesterol synthesis occurs, contains very low levels of cholesterol, as following synthesis, it is rapidly transported elsewhere (Maxfield & van Meer, 2010). Under physiological conditions cholesterol levels are tightly regulated through two interconnected pathways, cholesterol uptake and synthesis. This is to ensure appropriate levels of cholesterol for cell growth and survival, whilst also ensuring that levels do not exceed cellular requirements.

1.2.1. Two pathways to regulate intracellular cholesterol levels: uptake and synthesis

The *de novo* cholesterol synthesis and uptake pathways work together within cells to maintain cellular cholesterol homeostasis. The cholesterol uptake pathway involves the low-density lipoprotein (LDL), a lipoprotein complex that carries circulating dietary cholesterol around the body, and its receptor, LDLR. Following the receptor mediated internalisation of circulating LDL, the complex is processed in the lysosome, where cholesterol is released from LDL to be utilised by the cell (reviewed by Goldstein & Brown, 2009). The second way cholesterol levels are maintained is through the synthesis of cholesterol from Acetyl-CoA **(Figure 1.3)**. This biosynthetic pathway was delineated in the 1940-60s (Bloch, 1965; Bloch & Rittenberg, 1942) and occurs at the ER membrane.

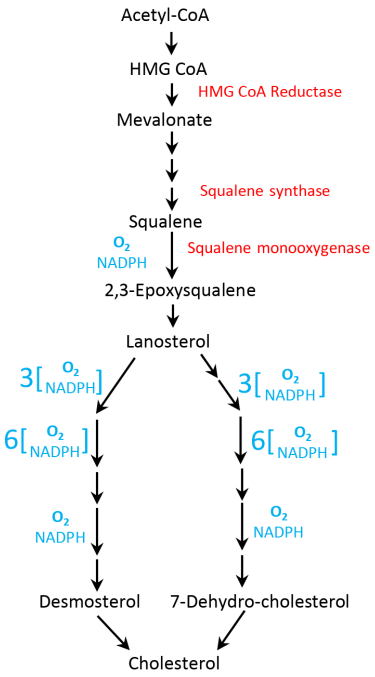

Figure 1.3. The *de novo* cholesterol synthesis pathway.

Basic schematic representing the *de novo* cholesterol synthesis pathway in mammalian cells from Acetyl-CoA which consumes 11 molecules of oxygen. The oxygen consuming steps have been highlighted in blue, and important enzymes required for some reactions are highlighted in red.

Figure 1.3 (page 29) has been adapted with permission from DeBose-Boyd, 2008, (Licence number 4937651432215); Springer Nature, Cell Research, Feedback regulation of cholesterol synthesis: Sterol-accelerated ubiquitination and degradation of HMG CoA reductase. Cell Research, 18(6), 609–621. © (2008).

Although separate pathways, the cholesterol uptake and synthesis pathways are tightly connected through feedback mechanisms to ensure cellular cholesterol homeostasis is maintained. The importance of this coordination is highlighted in some patients with familial hypercholesterolemia (FH). Patients with FH have genetic mutations which cause their LDLR to be non-functional, and are therefore unable to uptake cholesterol from their environment. Consequently, these patients have high levels of circulating cholesterol increasing their risk of atherosclerosis and cardiovascular disease. At a cellular level in FH patients, their cholesterol uptake pathway is perturbed, therefore their cells synthesise much more cholesterol to compensate for this loss to ensure that cellular cholesterol homeostasis is maintained (Brown & Goldstein, 1976; Goldstein & Brown, 1973).

1.2.2. The regulation of mammalian HMG-CoA reductase

Due to the importance of cholesterol for cell growth and survival, cellular levels are very tightly regulated at multiple steps. Regulation particularly involves the enzyme that catalyses the rate limiting step of *de novo* cholesterol synthesis, HMGCR **(Figure 1.3)**. HMGCR is a polytopic ER membrane glycoprotein with 8 transmembrane domains (TMDs), which is highly controlled by a sterol regulated feedback system which operates at both the transcriptional and post-translational level **(Figure 1.4)**. Highlighting the importance of this enzyme and the cholesterol synthesis pathway, homozygous deletion of HMGCR is lethal at an early embryonic stage (Ohashi *et al*., 2003). Under normal conditions most cells express relatively low levels of HMGCR, as sufficient cholesterol is generated through the processing of the LDL and low level synthesis. However, when sterols are limited HMGCR is rapidly transcriptionally activated and stabilised within the ER membrane.

Crucial to the sterol responsive feedback regulation of HMGCR are: the resident ER polytypic proteins, insulin-induced genes 1 and 2 (INSIG1/2); the transcription factor, sterol response element binding protein 2 (SREBP2); and the binding partner of SREBP2, SREBP2 cleavage activating protein (SCAP). The INSIG proteins contain 6 TMDs and help to regulate HMGCR levels both transcriptionally and post translationally (reviewed by Dong & Tang, 2010). The transcription factor SREBP2 is a hairpin ER membrane protein which interacts with SCAP, an

ER membrane protein with 8 TMDs. The interaction between SREBP2 and SCAP is crucial for the sterol mediated regulation of the transcription factor, as TMDs 2-6 within SCAP comprise a sterol sensing domain which facilitates SREBP2 activation when cellular sterols are low (Hua *et al*., 1996).

1.2.3. Regulation of SREBP2 mediated HMGCR transcription

Under conditions where sterols are limiting, the cell need to synthesis more cholesterol. Therefore, transcription of HMGCR is induced through the activation of SREBP2, which binds to sterol responsive elements (SREs) in the promoter region of HMGCR (Osborne, 1991). When sterols are present within the ER membrane, they bind to the SSD of SCAP which enables SCAP to bind to the INSIGs (Yang *et al*., 2002). This interaction renders the SCAP/SREBP2 complex inactive and retained within the ER. A lack of sterols within the ER membrane triggers the dissociation of the SCAP/SREBP2 complex from the INSIGs, and the SCAP/SREBP2 complex is trafficked to the Golgi apparatus (Golgi) through COPII mediated transport (Espenshade *et al*., 2002) **(Figure 1.4)**. This vesicular transport was shown to require a hexapeptide sequence (MELADL) in the cytoplasmic loop of SCAP (Sun *et al*., 2005), which becomes inaccessible to the COPII machinery following the sterol mediated interaction between SCAP and the INSIGs. At the Golgi the SREBP2 transcription factor is released through proteolytic cleavage by site-1 and site-2 proteases, releasing the N-terminus of SREBP2 (Sakai *et al*., 1996) **(Figure 1.4)**. This active transcription factor is able to activate the transcription of genes involved in the cholesterol synthesis pathway such HMGCR, in an attempt to restore cellular cholesterol levels when sterols are limiting. The release of SREBP2 from the ER and subsequent transcription of its target genes is tightly regulated by cholesterol levels within the ER membrane. The cholesterol content of the ER membrane is inherently low and therefore small changes can be closely monitored. One study demonstrated that when cholesterol levels within the ER membrane drop to below 5%, a rapid switch like response is triggered to activate SREBP2 transcription, which is turned off once the level of cholesterol within the ER membrane had been restored to above 5% (Radhakrishnan *et al*., 2008).

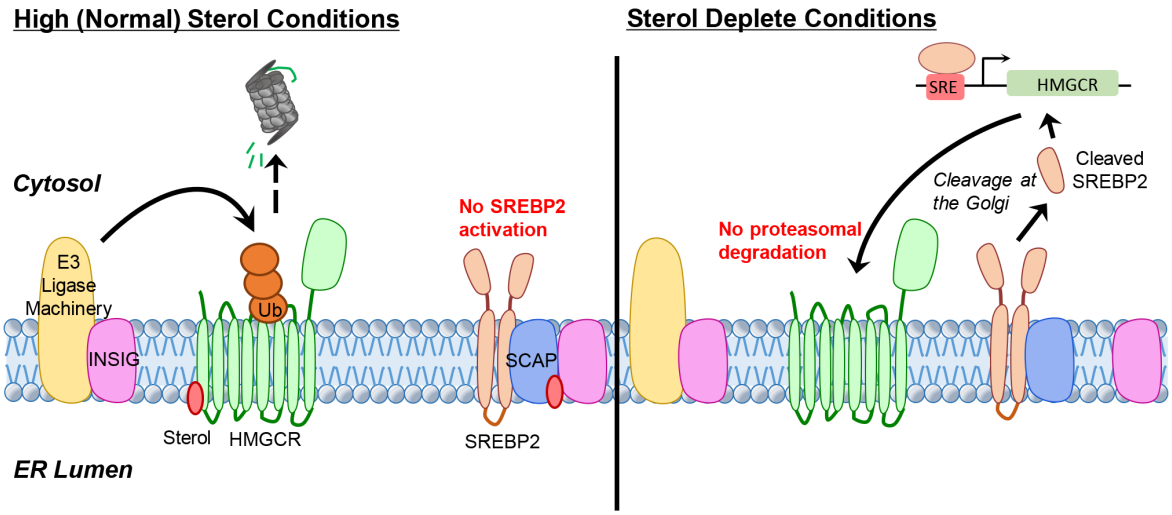

Figure 1.4. Regulation of HMGCR at the ER membrane under high and low sterol conditions.

Under high sterol conditions (left), levels of cellular HMGCR are kept low. Sterols within the ER membrane are able to interact the sterol sensing domain (SSD) of SCAP, causing the SCAP/SREBP2/INSIG complex to be retained within the ER. Additionally, sterols are able to interact with the SSD of HMGCR, enabling HMGCR to interact with its degradation machinery via INSIGs, and be degraded via ERAD. When sterols are limited (right), cellular HMGCR levels are increased. The lack of sterols causes the SCAP/SREBP2 complex to be trafficked to the Golgi where SREBP2 is cleaved, releasing the active transcription factor which transcribes genes including HMGCR. Additionally, HMGCR does not interact with its degradation machinery and is therefore not proteasomally degraded.

Ub = Ubiquitin, SRE = sterol response element

1.2.4. Regulation of HMGCR stability within the ER membrane

Post-translationally HMGCR is regulated by the UPS through ERAD (Ravid *et al.*, 2000). When sterols are limiting, the half-life of HMGCR is over 10 hours, however, once intracellular sterol levels have been restored, HMGCR is rapidly degraded with a half-life of less than two hours (Brown *et al.*, 1973; Gil *et al.*, 1985; Goldstein & Brown, 1990). Like SCAP, HMGCR contains a SSD in TMDs 2-6 (Hua *et al.*, 1996). Interaction of sterols with HMGCR accelerates its degradation through interaction with the INSIGs (Gil *et al.*, 1985; Sever *et al.*, 2003b). Degradation of HMGCR has been shown to be dependent on the interaction with INSIGs, and

their association with ER membrane bound ubiquitination machinery (Sever *et al*., 2003a). SCAP and HMGCR appear to interact with the same site on the INSIGs, as overexpression of SCAP inhibits the sterol mediated degradation of HMGCR (Sever *et al*., 2003a). Interestingly, interaction with the INSIGs leads to very different outcomes for SCAP and HMGCR, with SCAP being retained in the ER, whilst HMGCR is polyubiquitinated and degraded (Sever *et al*., 2003a; Sever *et al*., 2003b; Yang *et al*., 2002). These effects work together to ensure that levels of HMGCR are kept low when intracellular sterols are in excess, and enables rapid accumulation of HMGCR when sterols are limiting.

The INSIGs are crucial to the regulation of HMGCR and affect both its degradation and transcription, however, different sterols appear to preferably initiate different effects. Under sterol rich conditions, cholesterol itself has been shown to bind to the SSD of SCAP, causing the SCAP/SREBP2 complex to bind to the INSIGs and be retained in the ER (Radhakrishnan *et al*., 2004). However other sterols, such as lanosterol, the first sterol intermediate in *de novo* cholesterol synthesis, have been shown to be ineffective at initiating this interaction between SCAP and the INSIGs (Song *et al*., 2005a). Conversely, cholesterol has very low potency in stimulating the interaction between HMGCR and the INSIGs prior to its degradation, whereas lanosterol has been shown to rapidly stimulate this interaction and therefore HMGCR degradation (Song *et al*., 2005a). Thus, ER membrane lanosterol, rather than cholesterol, appears to be important for mediating HMGCR degradation, whilst ER membrane cholesterol is key to retaining the SCAP/SREBP2 complex within the ER thereby repressing SREBP2 transcription.

1.2.5. What degradation machinery is required for HMGCR turnover?

In budding yeast, *S. cerevisiae*, the orthologue of HMGCR, Hmg2p, is also regulated by ERAD (Hampton & Rine, 1994). The degradation machinery required for Hmg2p is well defined, with Hrd1p (orthologue of mammalian Hrd1) being the predominant E3 ligase (Hampton *et al*., 1996), working with the E2 enzyme Ubc7 (orthologue of mammalian UBE2G2) (Hampton & Bhakta, 1997). In mammalian cells, although the role of ERAD in regulating the cellular level of HMGCR is well described, the degradation machinery required has remained controversial.

Prior studies had implicated the E3 ligases gp78 (a mammalian orthologue of Hrd1p) (Song *et al*., 2005b) and TRC8 (Jo *et al*., 2011) in the sterol regulated degradation of HMGCR. However, Tsai *et al*., (2012) addressed discrepancies in these finding, observing that siRNA depletion of either gp78 or TRC8 alone did not stabilise HMGCR. To address these discrepancies, recently the Lehner laboratory carried out two unbiased CRISPR (clustered regulatory interspaced short palindromic repeats) Cas9 forward genetic screens, and uncovered that three E3 ligases, RNF145, gp78 and Hrd1, regulate HMGCR degradation all using the E2 enzyme UBE2G2 (Menzies *et al*., 2018) **(see section 1.4.3.)**. Jiang *et al*., (2018) also showed an involvement of RNF145 in this pathway.

1.2.6. The cholesterol synthesis pathway as a therapeutic target

The cholesterol synthesis pathway is important therapeutically as increased cellular levels of cholesterol are associated with the development of cardiovascular diseases, and have been associated with the progression of some cancers (Clendening *et al*., 2010; Gidding & Allen, 2019; Stopsack *et al*., 2016). Therefore, alongside reducing dietary intake of cholesterol, reducing the activity of the cholesterol synthesis pathway has been an important therapeutic target, particularly for treating cardiovascular diseases. As HMGCR is involved in the rate limiting step of cholesterol synthesis, converting HMG-CoA to mevalonate, it was an attractive drug target for lowering cholesterol levels in patients **(Figure 1.3)**. In the 1970s, research to inhibit sterol synthesis in microbes in order to limit their growth, led to Akira Endo isolating a compound from fungi, termed compactin (mevastatin), which was identified to be a competitive inhibitor of HMGCR (Endo, 2010; Endo *et al*., 1976). Highlighting the importance of this in human health, today, there multiple statin varieties available, and they are one of the most commonly prescribed drugs for patients with cardiovascular disease to reduce their risk of angina, heart attack, and stroke (Byrne *et al*., 2019).

Other components of the cholesterol synthesis pathway are also attractive therapeutic targets. Squalene monooxygenase, which is an enzyme often referred to as being involved in the second rate limiting step of cholesterol synthesis, is also regulated in a cholesterol dependent manner, being degraded when cholesterol is in excess (Chua *et al*., 2019; Gill *et al*.,

2011). Targeting the orthologue of squalene monooxygenase in yeast (ERG1), inhibits the sterol synthesis pathway and is effectively used clinically as an antifungal treatment (e.g. terbinafine) (Rodrigues, 2018). Recently in humans, altered gene expression of squalene monoxygenase has been associated with tumour progression and perturbed cholesterol synthesis (Stopsack *et al*., 2016). This has highlighted squalene monooxygenase as a potential drug target, however, inhibitors are still under investigation in mammalian cells although some specific inhibitors have been identified including a small molecule competitive inhibitor NB-598 (Horie *et al*., 1990; Padyana *et al*., 2019).

1.3. The mammalian hypoxic response

Mammals are regularly exposed to, and can survive in, a wide range of atmospheric oxygen tensions, from 21% oxygen at sea level to 11% oxygen at 5000 meters above sea level. As well as varying atmospheric oxygen tensions, the oxygen levels within the human body vary from approximately 1% in the digestive system, to 21% in the trachea, therefore requiring cells and tissues to be specifically adapted to their oxygen environments (Carreau *et al*., 2011). Limited oxygen availability contributes to some of the leading causes of death in the developed world, such as strokes, ischemic heart disease, and cancer (reviewed in Semenza, 2014). Therefore, mammalian cells have evolved with the ability to rapidly adapt to their oxygen environments in an attempt to limit any damage caused by any unexpected shift in oxygen tensions. Central to the metazoan response to oxygen tensions are the hypoxia inducible transcription factors (HIFs). HIFs are stabilised in response to low oxygen concentrations, which leads to the transcription of a myriad of genes involved in hypoxic cell survival such as angiogenesis, cell growth, and glucose metabolism (Chen & Sang, 2016; Maxwell & Ratcliffe, 2002). More broadly, HIFs have been implicated in the regulation of immune cells (Taylor & Colgan, 2017), and transcriptional activation of HIF target genes are implicated in a number of disease processes such as tumour growth and metastasis, angiogenesis, and pulmonary hypertension (Maxwell & Ratcliffe, 2002; Wielockx & Meneses, 2016). Although activation of HIFs is the best studied response to hypoxia in mammalian cells, it is important to note that oxygen also acts as a cofactor in many enzymatic reactions in multiple metabolic pathways. Therefore, it is also important to understand the role of low oxygen tension beyond that of the HIFs in both physiological and pathophysiological conditions.

1.3.1. The hypoxia-inducible transcription factors

HIFs were first identified as transcription factors that upregulate specific gene transcription in hypoxia through purification by DNA affinity chromatography, with erythropoietin (EPO) being the first target gene identified of HIF1 (Semenza & Wang, 1992). Purification revealed that HIF1 exists predominantly in a heterodimeric complex, composed of HIFα (120 KDa) and

HIFβ/Aryl hydrocarbon Receptor Nuclear Translocator (ARNT) (91-94 KDa) (Wang & Semenza, 1995). The mechanism of HIF activation under conditions of low oxygen was uncovered through experiments carried out by Peter Ratcliffe, William Kaelin, Greg Semenza, and their colleagues (Maxwell *et al*., 1999; Ohh *et al*., 2000; Wang *et al*., 1995). They demonstrated that the HIFα subunit is dynamically regulated by oxygen levels, whilst HIFβ remains constitutively expressed and not sensitive to oxygen. Under conditions where oxygen is present the HIFα subunit is rapidly degraded by the UPS, however, in response to low oxygen conditions, the HIFα subunit is stabilised so it is able to bind to HIFβ and activate target gene transcription.

The presence of nuclear localisation signals (NLS) in both HIFα and HIFβ enables their independent translocation to the nucleus (Chilov *et al*., 1999; Eguchi *et al*., 1997). Following their dimerization under conditions of hypoxia, the dimer is able to bind to the hypoxia response element (HRE) consensus sequence - 5'-(A/G)CGTG-3', in promoter regions of over 600 HIF target genes (Mole *et al*., 2009; Wenger *et al*., 2005). Interestingly, the HRE sequence is highly abundant in the mammalian genome, however, less than 1% of potential sites are occupied by HIFs in response to hypoxia, suggesting that other factors apart from the DNA sequence contribute to gene activation (reviewed by Dengler *et al*., 2014).

In addition to HIF1α, in mammals the HIFα subunit was found to be encoded by two additional genes termed HIF2α and HIF3α (Ema *et al*., 1997; Gu *et al*., 1998). These isoforms share some sequence homology, but have different tissue specificity. HIF1α is largely ubiquitously expressed throughout the body, whilst HIF2α is more specific to tissues such as lung, heart and kidney (Ema *et al*., 1997). Similarly to HIF1α, HIF2α is stabilised in low oxygen conditions, is able to heterodimarise with HIF1β, and activates gene transcription in an oxygen dependent manner (Wiesener *et al*., 1998; Wiesener *et al*., 2003). The function and localisation of HIF3α is less well understood. Some studies have shown that expression of HIF3α can negatively regulate the transcriptional activation of HIF1α and 2α, and that HIF3α can compete with HIF1α and 2α for binding to HIF1β (Hara *et al*., 2001; Makino *et al*., 2001). Although HIF3α shares structural similarities to the other HIF isoforms, it lacks a C-terminal DNA binding domain, which is thought to account for its distinct functions. Additionally, depletion of either HIF1α or HIF2α results in early embryonic lethality (Compernolle *et al*., 2002; Kotch *et al*., 1999), whereas HIF3α depletion embryos are viable, with very mild defects (Yamashita *et al*., 2008), suggesting that HIF1α and HIF2α carry out fundamental roles in development.

1.3.2. The regulation of HIF1α by the ubiquitin proteasome system

HIF1α is constitutively expressed in cells, but is dynamically regulated by cellular oxygen levels **(Figure 1.5)**. Under normal oxygen tensions HIF1α is rapidly turned over, with a half-life of <10 minutes (Wang *et al*., 1995). Salceda & Caro, (1997) later confirmed that the turnover of HIF1α was mediated by ubiquitination and proteasomal degradation. This was shown to require both proline hydroxylation on HIF1α, mediated by the prolyl hydroxylase enzymes (PHDs) (Bruick & McKnight, 2001; Epstein *et al*., 2001), and ubiquitination by the von-Hippel Lindau (pVHL) E3 ligase complex (Maxwell *et al*., 1999).

The PHDs are members of the 2-oxoglutarate (2-OG) dependent dioxygenase (2-OGDD) superfamily. Many of the >60 identified 2-OGDDs have undefined functions, but all require 2-OG, oxygen and iron for their enzymatic activity (Loenarz & Schofield, 2008). The PHDs, of which there are three isoforms (PHD 1-3), are the best described 2-OGDDs in mammalian cells, and PHD2 appears to be the isoform principally responsible for regulating the stability of HIF1α (Epstein *et al*., 2001). HIF1α contains an oxygen-dependent degradation (ODD) domain, which was shown to be required for its oxygen dependent degradation (Huang *et al*., 1998). Within this domain, the PHDs recognise a conserved LXXLAP motif (Berra *et al*., 2003), and in oxygen rich conditions HIF1α is rapidly prolyl-hydroxylated on two proline residues (P402 and P564) (Bruick & McKnight, 2001; Epstein *et al*., 2001). Hydroxylated HIF1α is recognised by the E3 ligase pVHL, initiating its proteasomal degradation (Maxwell *et al*., 1999) **(Figure 1.5, left)**. Under conditions where the PHD enzymes are inhibited, such as low oxygen or iron chelation, HIF1α is no longer hydroxylated and therefore escapes pVHL mediated proteasomal degradation and is able to activate the transcription of genes required for hypoxic survival (Jiang *et al*., 1996) **(Figure 1.5, right)**.

pVHL is a tumour suppressor protein, which was first identified in patients with the inherited autosomal dominant condition VHL disease, where patients only have one functioning pVHL allele (Latif *et al*., 1993). These patients have an increased risk of benign and malignant tumours, which are commonly located within the kidney (Kaelin & Maher, 1998). Studies went on to show that pVHL null cells display increased HIF1α stabilisation and target gene transcription, and that the VHL E3 ligase complex is required for the ubiquitination and

subsequent proteasomal degradation of HIF1α in oxygen rich conditions (Maxwell *et al.*, 1999). The multi-protein VHL E3 ligase complex contains pVHL, which is involved in substrate recognition; the regulatory subunits Elongins B and C; the scaffold protein Cullin-2; and the RING H2 finger protein (RBX1) which binds to the E2 enzyme and transfers ubiquitin onto the substrate (Iwai *et al.*, 1999; Kamura *et al.*, 1999; Lonergan *et al.*, 1998; Pause *et al.*, 1997). Overall, the PHDs and VHL E3 ligase complex regulate the stability of HIF1α within cells to ensure that transcriptional activation of its target genes only occurs when necessary. This is vitally important in cells as aberrant stabilisation of HIF is associated with multiple pathophysiological processes.

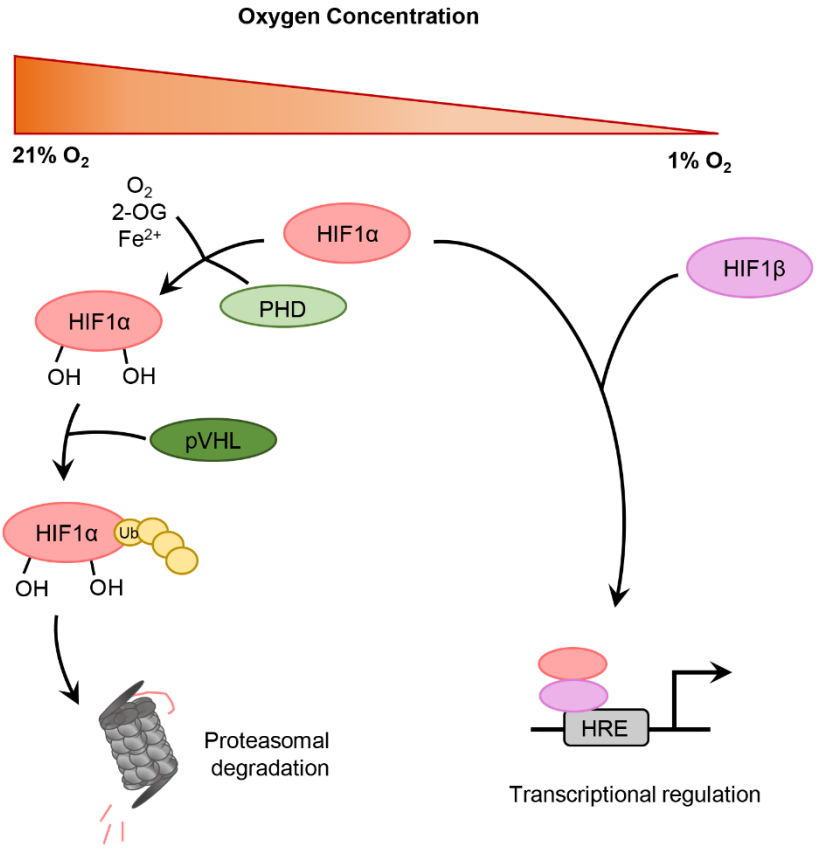

Figure 1.5. Schematic of HIF1α regulation under different oxygen tensions.

Under normal oxygen tensions (left) HIF1α is hydroxylated (OH) at two proline residues by the PHD enzymes. To carry out this reaction the prolyl hydroxylase enzymes (PHD) require oxygen (O_2), 2-oxoglutarate (2-OG) and iron (Fe^{2+}). Hydroxylated HIF1α is polyubiquitinated by the von-Hippel Lindau (pVHL) E3 ligase complex which targets HIF1α for proteasomal mediated degradation. When oxygen is limiting (right), the PHD enzymes are inactive and unable to hydroxylate HIF1α. Therefore HIF1α accumulates and forms a heterodimer with HIF1β, translocates to the nucleus and upregulates gene transcription through DNA binding at hypoxia response elements (HRE). *Ub = ubiquitin*

1.3.3. Oxygen regulation independent of the HIFs

Although activation of the HIFs is the best described mammalian response to low oxygen conditions, levels of oxygen are also important in other physiological process which are affected in hypoxia independent of the HIFs. The carotid body is a cluster of chemoreceptors which detect changes in arterial oxygen levels and signal the respiratory system to increase ventilation when necessary. The mechanism by which these cells sense oxygen is largely unknown, however, studies have shown that their depolarisation and activation through the inhibition of potassium channels during hypoxia, is independent of the HIFs (reviewed by (López-Barneo *et al*., 2008). Additionally, the energy dependent process of protein translation is reduced in hypoxia. One mechanism for this is the decrease in ATP production through oxidative phosphorylation, leading a global reduction in translation (Liu & Simon, 2004). Furthermore, oxygen is also critical in many enzymatic reactions involved in metabolic pathways such as the *de novo* cholesterol synthesis pathway, which requires 11 molecules of oxygen to generate one molecule of cholesterol **(Figure 1.3, oxygen sensitive steps highlighted in blue)** (reviewed by DeBose-Boyd, 2008). The importance of oxygen in the regulation of sterol synthesis has been shown throughout evolution, with both fungi and mammals displaying oxygen regulated steps (Hwang *et al*., 2017; Lee *et al*., 2011). Although some studies have shown that low oxygen conditions affect the cholesterol synthesis pathway in a number of ways, the full extent to which this occurs is relatively unknown.

1.3.4. The role of hypoxia in the cholesterol synthesis pathway in fission yeast

While cholesterol is the major sterol in eukaryote cells, ergosterol is the most abundant sterol found in fungal cell membranes. Ergosterol is structurally similar to cholesterol and carries out related functions, with both sterols being crucial for membrane maintenance. Like cholesterol, ergosterol is vital for fungal survival, and is therefore tightly regulated. The central role of ergosterol in fungi growth is demonstrated by the inhibition of ergosterol synthesis being an effective antifungal treatment (Rodrigues, 2018). In contrast to mammalian cells and *S. cerevisiae*, in fission yeast, *Schizosaccharomyces pombe (S. pombe)*, the orthologue of

HMGCR, Hmg1 is not regulated by SREBP2 mediated transcription or INSIG mediated degradation. Instead, Ins1 (orthologue of INSIG1) regulates the activity of Hmg1 by controlling the MAP kinase mediated phosphorylation on Hmg1, with phosphorylation inhibiting the activity of Hmg1 under conditions of nutrient stress (Burg *et al.*, 2008). However, a similar SREBP2 processing pathway does exist in fission yeast, involving, Sre1 and Scp1 which are the orthologues of mammalian SREBP2 and SCAP, respectively. Akin to SREBP2 processing, Sre1 is cleaved and activated in response to sterol depletion in a Scp1 dependent manner, releasing the active transcription factor Sre1N, which transcribes some genes involved in ergosterol synthesis, but does not activate the transcription of Hmg1 (Lee *et al.*, 2011).

Aside from the sterol regulation of Sre1, Hughes *et al.*, (2005) demonstrated that Sre1 is also activated under conditions of low oxygen, upregulating genes involved in both ergosterol synthesis and those required for survival in low oxygen conditions. More recently the regulation of Sre1N has been shown to be dependent on a 2-OGDD family member, Ofd1, which is regulated by oxygen. Ofd1 regulates Sre1N stability, causing rapid degradation in 21% oxygen, whilst under low oxygen conditions, Ofd1 is unable to bind and regulate Sre1N, enabling Sre1N to activate gene transcription (Lee *et al.*, 2011). This demonstrates a mechanism by which sterol synthesis in yeast is regulated by oxygen levels, and highlights the importance of studying the role of oxygen in the mammalian cholesterol synthesis pathway.

1.3.5. The role of hypoxia in the cholesterol synthesis pathway in mammalian cells

While an analogous pathway to Sre1N has not been identified in metazoans, DeBose-Boyd and colleagues have demonstrated a role for hypoxia in regulating the degradation of HMGCR through HIF1α stabilisation and lanosterol accumulation (Hwang *et al.*, 2017; Nguyen *et al.*, 2007). HIF1α dependent regulation of HMGCR has been shown through the chemical stabilisation of HIF1α. Inhibition of the PHD enzymes using the drug DMOG (Dimethylocalyglycine), is well known to lead to HIF1α stabilisation. Following stabilisation, an increase in INSIG2 protein levels were observed, and this was shown to increase the interaction between HMGCR and its degradation machinery even when sterols are limited

(Hwang *et al*., 2017) **(Figure 1.6)**. Furthermore, HIF stabilisation through PHD inhibition has been shown clinically to reduce circulating cholesterol levels in patients (Chen *et al*., 2019). Additionally, lanosterol levels have been shown to accumulate under conditions of low oxygen, due to the requirement of oxygen in processing lanosterol to cholesterol **(Figure 1.3)**. As lanosterol is able to interact with the SSD of HMGCR and trigger its degradation (Song *et al*., 2005a), increased cellular levels of lanosterol have been shown to increase the degradation of HMGCR under conditions of sterol depletion and low oxygen (Nguyen *et al*., 2007).

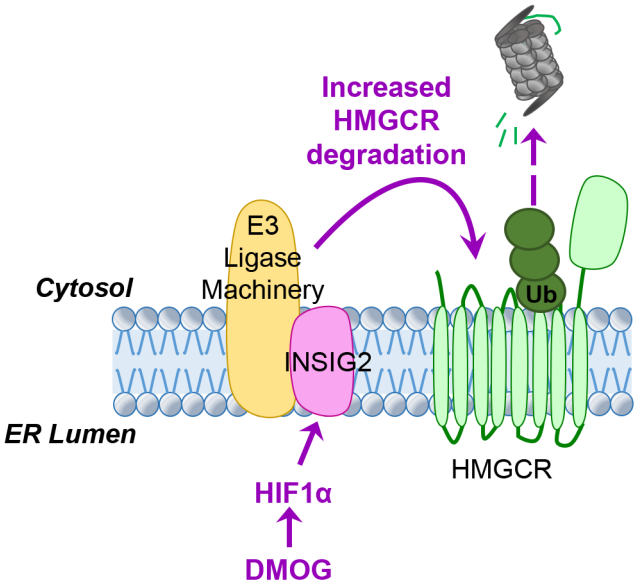

Figure 1.6. Schematic of the HIF1α dependent regulation of HMGCR.

Stabilisation of HIF1α by PHD inhibition through DMOG treatment, causes an upregulation of the HIF1α target gene, INSIG2. Increased INSIG2 within the ER membrane increases the likelihood of HMGCR interacting with its degradation machinery, even with a lack of sterols, therefore increased HMGCR degradation is observed.

Ub=Ubiquitin

Figure 1.6 (page 42) was originally published in the Journal of Biological Chemistry. Hwang. S., Nguyen. A. D., Jo. Y., Engelking. L. J., Brugarolas. J., DeBose-Boyd. R. A., Hypoxia-inducible factor-1α activates insig-2 transcription for degradation of HMG CoA reductase in the liver. J Biol Chem. 2017; 292:9382-9393. © The American Society for Biochemistry and Molecular Biology. (2017)

1.4. Forward genetic screens to study endoplasmic reticulum associated degradation

1.4.1. The development of forward genetic screens

Since the completion of the human genome project and the development of next generation sequencing, biological research has been able to focus much more on genetic manipulation in mammalian cells to understand the function of genes. Forward genetic screens are a powerful tool to determine a gene's function, and typically involve genome-wide mutagenesis to map the effects of individual gene mutations on specific phenotypes (Grimm, 2004). Forward genetic screens had previously been difficult to establish in human cells, principally due to the difficulty in mutagenizing both chromosomal copies. Carette *et al*., (2009) demonstrated that the near-haploid mammalian KBM7 cell line (apart from chromosome 8), could be used in forward genetic screens utilising gene-trap mutagenesis, as disruption of one gene locus is sufficient to create a knockout. This cell line and derivatives have been used successfully to elucidate the function of many previously unknown proteins and has revealed important insights into processes such as ERAD (Stefanovic-Barrett *et al*., 2018; Timms *et al*., 2016), the regulation of HIF1α (Burr *et al*., 2016; Miles *et al*., 2017) and the identification of host pathogen restriction factors (Carette *et al*., 2009).

The development of the CRISPR Cas9 system for use in mammalian cells has revolutionised the study of gene function within mammalian cells (Hsu *et al*., 2014). CRISPR enables the specific modification of a cell's genome utilising a technique based upon bacteria's adaptive immune system. In mammalian cells, a gene specific single guide RNA (sgRNA) is used which targets the Cas9 nuclease to induce site specific DNA cleavage (Barrangou *et al*., 2007; Wiedenheft *et al*., 2012). This double strand break is then repaired by cellular DNA repair mechanisms and can be used to create gene knock-outs (via non-homologous end joining) or knock-ins (via homology directed repair). This technique has advanced the field of forward genetic screens and has many advantages over the previously described screens in near-haploid cell lines, particularly the ability to generate bi-allelic mutations. This enables

forward genetic screens to be carried out in almost any cell type, including primary cell lines, allowing the most appropriate cell type for the phenotype to be selected (Shalem *et al.*, 2014; Wang *et al.*, 2015, Wang *et al.*, 2014).

1.4.2. Utilising the CL1 degron to study cytosolic proteasomal degradation at the ER

Forward genetic screens have proven to be a powerful unbiased approach to identify important genes involved protein quality control, but these have mainly been used to identify new components in budding yeast, *S. cerevisiae*. Many of these studies have utilised the cytosolic CL1 degron (Gilon *et al.*, 1998; Metzger *et al.*, 2008), however, the degradation machinery for the CL1 degron in mammalian cells had not been described. In an attempt to uncover the degradation machinery and membrane localisation of the CL1 degron in mammalian cells, Stephen Burr and Sandra Stefanovic-Barrett (Nathan laboratory) developed a fluorescent reporter using the amphipathic helical CL1 degron fused to mCherry **(Figure 1.7 A, B)**.

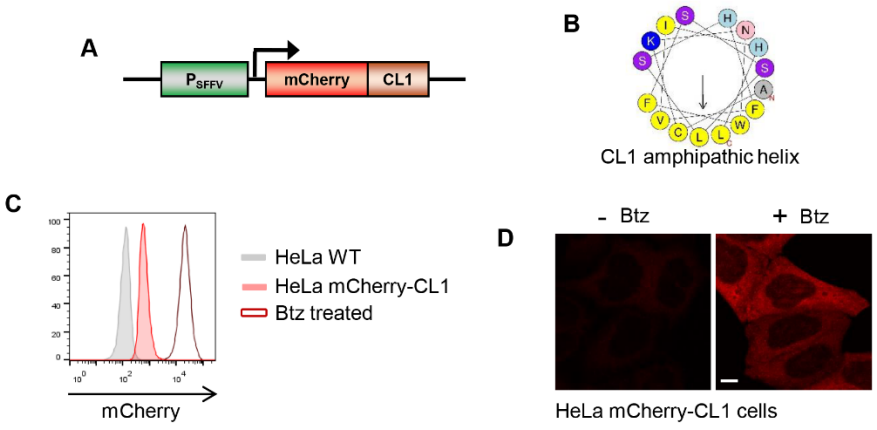

Figure 1.7. The cytosolic degron, CL1, is an amphipathic helix rapidly degraded by the proteasome. **(A)** Schematic of the mCherry-CL1 reporter construct used. **(B)** Prediction of the 16 amino acid amphipathic helix formed. HeLa mCherry-CL1 cells were treated with the proteasome inhibitor 20 nM Bortezomib (Btz) and analysed by flow cytometry **(C)** or immunofluorescence microscopy **(D)**.

As expected, in mammalian cells mCherry-CL1 was rapidly stabilised upon proteasome inhibition, and interestingly appeared to be localised to the ER membrane **(Figure 1.7 C, D)**. This reporter was then utilised in a gene trap retroviral forward genetic screen in the near-haploid KBM7 cell line, in an attempt to uncover the degradation machinery required. Although the screen was not saturating, it revealed some of the proteins involved in the ubiquitination and degradation of the CL1 degron in mammalian cells and highlighted the scope for further CRISPR/Cas9 forward genetic screens using this degron (Stefanovic-Barrett *et al*., 2018) **(see Chapter 3)**.

1.4.3. Studying the degradation of HMG-CoA reductase using CRISPR Cas9

Forward genetic screens can be used to study the regulation of other rapidly degraded proteins, such as the ERAD substrate HMGCR. Under sterol rich conditions, HMGCR is polyubiquitinated and degraded by the proteasome, however, the ligases involved remained elusive until recently. In an attempt to uncover the degradation machinery required, the Lehner laboratory opted to use two sequential unbiased CRISPR Cas9 forward genetic screens. Using an endogenous HMGCR knock-in reporter in HeLa cells, HMGCR_clover, Menzies *et al*., (2018) showed that the E2 enzyme, UBE2G2, and three E3 ligases, RNF145, gp78, and Hrd1 are required for degradation of HMGCR when sterols are present in 21% oxygen. Their studies revealed that the sterol sensitive ligase, RNF145 and gp78 predominantly regulate HMGCR, and that Hrd1 is able to partially regulate HMGCR in the absence of the other ligases. The effectiveness of HMGCR_clover in CRISPR Cas9 forward genetic screens has been demonstrated, and this reporter has been shown to dynamically respond to cellular sterol levels, making it an invaluable tool to study HMGCR degradation by flow cytometry. Here, I use the reporter to further understand how HMGCR is regulated, focusing on the role of oxygen in this pathway **(see Chapter 5)**.

1.5. Aims of this thesis

The overarching aim of my thesis is to increase our understanding about how different stressors affect endoplasmic reticulum (ER) associated degradation pathways and these systems as a whole. Within my thesis I focus on two main stressors; misfolded cytosolic proteins and limiting oxygen conditions.

Specifically my aims are:

- To establish a CRISPR/Cas9 forward genetic screen to study MARCH6 dependent degradation at the ER.
- To determine the role oxygen availability on the regulation of HMG-CoA Reductase (HMCGR).
- To elucidate the effect of hypoxia on the transcription factor for HMGCR, SREBP2.

Chapter 2: Materials and Methods

2.1. Reagents

2.1.1. Antibodies

(IB: Immunoblotting, FC: Flow Cytometry, IF: Immunofluorescence)

Primary Antibody	Species	Concentration	Source
β-actin	Mouse	IB: 1:30,000	Sigma-Aldrich, A2228
HA	Mouse	IB: 1:1,000	Covance, 16B12
HA	Rat	IB: 1:1,000	Roche, 11867423001
FLAG-M2	Mouse	IB: 1:3,000	Sigma, F3165
Squalene monooxygenase	Rabbit	IB: 1:2,000	Proteintech, 12544-1-AP
UBE2G2	Mouse	IB: 1:2,000	Santa Cruz, sc-100613
UBE2J2	Rabbit	IB: 1:2,000	Proteintech, 17713-1-AP
EMC6	Rabbit	IB: 1:4,000	Abcam, ab84902
HIF1α	Mouse	IB: 1:1,000	BD Transduction Laboratories, 610959
HIF1β	Rabbit	IB: 1:1,000	Cell Signaling, 5537S
CAIX (Carbonic Anhydrase 9) M75	Mouse	FC: 1:1,000 IB: 1:1,000	Obtained from E. Oosterwijk, Nijmegen
HMG CoA Reductase	Mouse	IB: 1:1,000	Santa Cruz Biotechnology, sc-271595
Hrd1	Rabbit	IB: 1:5,000	Abgent, AP2184a
RNF145	Mouse	IB: 1:1,000	ProteinTech
gp78	Rabbit	IB: 1:1,000	ProteinTech, 16675–1-AP
SREBP2	Goat	IB: 1:1,000	R&D Systems, AF7119
anti MHC Class I (W6/32)	Mouse	FC: 1:1,000	Gift from Paul Lehner, CITIID
Phospho-p70S6K	Rabbit	IB: 1:1,000	Gift from David Rubinsztein, CIMR

Total p70S6K	Rabbit	IB: 1:1,000	Gift from David Rubinsztein, CIMR
HIF2α	Rabbit	IB: 1:1,000	Cell Signaling, 7096S
S6 ribosomal protein	Mouse	IB: 1:1,000	Cell Signaling, 2317S
L4 ribosomal protein	Mouse	IB:1:1,000	Sigma, WH0006124M1
KDEL	Rat	WB: 1:5000	Gift from Geoff Butcher, Babraham

Table 1. List of primary antibodies

Secondary Antibodies	**Species**	**Concentration**	**Source**
Anti-goat HRP	Donkey	IB: 1:10,000	Jackson, 705-035-003
Anti-mouse HRP	Goat	IB: 1:10,000	Jackson, 115-035-146
Anti-rabbit HRP	Goat	IB: 1:10,000	Jackson, 111-035-045
Anti-rat HRP	Goat	IB: 1:10,000	Jackson, 112-035-003
Alexa Fluor Anti-mouse 647	Goat	FC: 1:2,000	Invitrogen
Alexa Fluor Anti-mouse 488	Goat	FC: 1:2,000	Invitrogen

Table 2. List of secondary antibodies

2.1.2. Chemical Reagents

Reagent List	**Final Concentration** (where appropriate)	**Source**
MG132	20 uM	Sigma-Aldrich
Bortezomib (Velcade)	20 nM	Gift from Alfred Goldberg
Lipoprotein-deficient serum (LPDS)	10% (v/v)	Biosera, FB-1001L/100
Digitonin	1% (w/v)	Calbiochem, 300410
Mevastatin	10 µM	Sigma-Aldrich, M2537
Mevalonolactone	-	Sigma-Aldrich, M4467
25-hydroxycholesterol	2 µg/ml	Sigma-Aldrich, H1015
Cholesterol	20 µg/ml	Sigma-Aldrich, C3045
DMOG	1 mM	Sigma-Aldrich, D3695
Roxadustat (FG-4592)	100 µM	Selleckchem, S1007
Blasticidin	2.5 µg/ml	Cambridge Bioscience
Hygromycin	100 µg/ml	Cambridge Bioscience
Puromycin	1 µg/ml	Cambridge Bioscience
Thapsigargin	50 nM	Gift from Paul Lehner
Tunicamycin	2 µg/ml	Gift from Stefan Marciniak, CIMR
Cycloheximide	1 or 100 µg/ml	Sigma Aldrich, 01810
Rapamycin	100 nM	MP Biomedicals, #159346

Table 3. List of reagents and chemicals

2.1.3. Oligonucleotides

CRISPR-Cas9 sgRNA targeting sequences

Target Gene	sgRNA sequence (5'-3')
AUP1	GAGCCCTAGCACCGCACACA
β2M	GGCCGAGATGTCTCGCTCCG
EMC6 guide 1	CCCCGACAGCGCTGACACCG
EMC6 guide 4	TCATTCTCAAGGCGGGAAGG
HIF1β	CAGTCCTCCGTCTCCTCACC
Hrd1	GGTGTTCTTTGGGCAACTGA
MARCH6	TATCATCCTTGTGTATGTAC
PCTP guide 1	TATAAAGTCTTTGGTGTTC
PCTP guide 2	CTCCACTAGGAGCTGCCAGT
PCTP guide 3	GGCCGCCGGAAGCTTCTCGG
SREBP2	AGTGCAACGGTCATTCACCC
TSC1 guide 1	CGAGATAGACTTCCGCCACG
TSC1 guide 2	ATTCGTTAATCCTGTCCAAG
TSC2 guide 1	CCAACGAAGACCTTCACGAA
TSC2 guide 2	GGTCGCGGATCTGTTGCAGC
TRC8	GCACGATGCAGAACCGGCTT
UBE2D3	GAATGACAGCCCATATCAAGG
UBE2J2	GAGAATCCTTACCTTCATAAG
UBE2G2	CATGGGCTACGAGAGCAGCG
UBE2K	GCAATGACAATAATACCGTG
YEATS4 guide 1	GATGGGCACACTCATCAG
YEATS4 guide 2	TCAGACACCAATGCAATGCT
YEATS4 guide 3	CAGCTTTAGCAAATGATACA

Table 4. List of CRISPR sgRNAs

Primers used for RT-qPCR

RT-qPCR primers **(Table 5)** were either previously validated in either the Nathan or Lehner laboratories or designed using PrimerBank (https://pga.mgh.harvard.edu/primerbank/) (Wang *et al*., 2012).

Target Gene	Forward Primer (5'-3')	Reverse Primer (5'-3')
β-actin	CTGGGAGTGGGTGGAGGC	TCAACTGGTCTCAAGTCAGTG
BiP	CGAGGAGGAGGACAAGAAGG	CACCTTGAACGGCAAGAACT
CAIX	GCCGCCTTTCTGGAGGA	TCTTCCAAGCGAGACAGCAA
CHOP	AGAACCAGGAAACGGAAACAGA	TCTCCTTCATGCGCTGCTTT
HMGCR	CGTGGAATGGCAATTTTAGGTCC	ATTTCAAGCTGACGTACCCCT
HMGCS1	GATGTGGGAATTGTTGCCCTT	ATTGTCTCTGTTCCAACTTCCAG
INSIG2	TAATGCGGTGTGTAGCAGTCT	GTCCAATGGATAGTGCAGCCA
LRLR	ACCAACGAATGCTTGGACAAC	ACAGGCACTCGTAGCCGAT
RNF145	AATCGGGGCATGACAGAAGG	AGCACGGAAGTGTTTCCACA
SREBP2	AACGGTCATTCACCCAGGTC	GGCTGAAGAATAGGAGTTGCC

Table 5. List of RT-qPCR primers

2.2. Molecular Biology

2.2.1. Plasmids

Viral packaging vectors: pMD.G (Lentiviral VSVG) (gift from Paul Lehner)

pCMVR8.91 (Lentiviral Gag/Pol), (gift from Paul Lehner).

CRISPR vectors: LentiCRISPR v2 (gift from F. Zhang, Addgene 52961). pKLV-U6sgRNApGKPuro-2A-BFP (gift from K. Yusa, Addgene #50946).
pSpCas9(BB)-T2A-Puro (gift from F. Zhang, Addgene #48139). pSpCas9(BB)-T2A-GFP (gift from F. Zhang, Addgene #48138).

Lentiviral Constructs: pHRSIN-C9AMarch6-HA-pGK-Puro (made by Sandra Stefanovic-Barrett; Stefanovic-Barrett *et al*., 2018).

pHRSIN-FLAG-NLS-CAS9-NLS-pGK-Hygro (gift from Paul Lehner). Lenti-Cas9-T2A-Blast (gift from Jason Moffat, Addgene #73310).

I.M.A.G.E. clone: Sequence verified SREBF2 image clone (Source Bioscience, IRATp970B0781D 6169568).

CRISPR libraries: Human Brunello CRISPR knockout pooled library (gift from David Root and John Doench, Addgene #73178, Doench *et al*., 2016).

Human CRISPR knockout library (gift from Michael Bassik, Addgene #101926-101934, Morgens *et al*., 2017).

Cell lines not generated in this thesis:

- HeLa_mCherry_CL1 and HeLa_mCherry_CL1_UBE2G2 KO clone cells were created by Sandra Stefanovic-Barrett (Stefanovic-Barrett *et al*., 2018).
- HeLa_EMC6 KO clone cells were created by Sandra Stefanovic-Barrett.
- Thp1_HLA-A2_GFP and Thp1_HLA-A2_GFP were created by Dick van den Boomen (Lehner lab).

- HeLa_HMGCR_clover knock-in cells, HeLa_HMGCR_clover_UBE2G2 null clone cells, HeLa_HMGCR_clover RNF145 null clone cells, HeLa_HMGCR_clover_RNF145/GP78 null cells were created by Sam Menzies (Lehner laboratory; Menzies *et al*., 2018).
- HeLa_HMGCR_clover SREBP2 KO population were created by Norbert Volkmar (Lehner laboratory).
- HeLa HIFα-GFP^{ODD} cells were created by Stephen Burr (Burr *et al*., 2016).
- HeLa HIFα-GFP^{ODD} HIF1α/HIF2α null cells were created by Peter Bailey.

2.2.2. Cloning

Cloning was performed using Gibson assembly® and primers designed accordingly using the NEBuilder assembly tool (NEB). Generally cloning was carried out as follows:

1. **PCR amplification** was performed in 20 µl reactions using Phusion® High-Fidelity DNA polymerase (NEB) following the manufacturer's guidelines **(Table 6)**. Typically a 30 cycle program was carried out; 98°C denature (10 seconds), gradient annealing temperature (30 seconds), extension (30 seconds per kb), and a final 10 minute extension. PRC products were purified using a QIAquick® PCR purification kit (Qiagen).

	Amount (µl)
GC buffer	4
dNTPs	0.4
DMSO	0.7
Forward primer	1
Reverse primer	1
Template DNA (10 ng/µl)	1
Phusion polymerase	0.2
H_2O	11.2

Table 6. Typical PCR protocol

2. **Restriction enzyme digests** were performed using Thermo Scientific FastDigest restriction enzymes according to manufacturer's guidelines. Backbones were gel purified typically using 1% agarose gel electrophoresis containing ethidium bromide in TAE buffer. DNA was extracted using the QIAquick® gel extraction kit (Qiagen).

3. **Gibson assembly® (NEB) ligation** of the backbone and PCR product was performed according to the manufacturer's instructions. Briefly, the digested vector and insert were incubated at 50°C for 50 minutes at a 1:1 or 1:3 ratio, with 50% of the reaction made up of the Gibson assembly master mix.

4. **Bacterial transformation** was carried out using α-select Silver Competent E. coli cells (Bioline) transformed with 2 µl ligated product. DNA was incubated with the E. coli for 30 minutes on ice, before being subjected to heat shock for 45 seconds in a 42°C water bath. Transformed E. coli were incubated with SOC (super optimal broth) media for 30 minutes at 37°C before being plated on LB agar plates containing appropriate antibiotic selection overnight.

5. **Plasmid purification** was carried out from a single bacterial colony. A single colony was inoculated into 5 ml LB (Lysogeny broth) media with the appropriate antibiotic selection and placed in a shaker overnight at 37°C. The final plasmid was purified using a QIAprep® spin miniprep kit according to manufacturer's instructions.

2.2.3. Generation of new plasmids

pHRSIN-FLAG-UBE2J2-pPGK-blasticidin

N-terminally flag tagged UBE2J2 was created by PCR amplification of pDEST17-UBE2J2, which was a gift from Wade Harper (Addgene plasmid #15794), using primers that incorporated the 5' BamHI and 3' NotI restricting sites and ligated using Gibson Assembly®.

Flag_BamHI_J2 Forward:

GACTACAAGGACGACGATGACAAGGGCGGATCCATGAGCAGCAGCAGTAAGAG

J2_Not1_Reverse:

GCCTGCAGGTCGACTCTAGAGTCGCGCGGCCGCTCACTCCTGCGCGATGCTC

pHRSIN_HA-SREBP2-pPGK-puromycin

N-terminally HA tagged SREBP2 was created by PCR amplification of the SREBF2 I.M.A.G.E clone and ligated into the backbone vector using Gibson Assembly®.

HA-SREBP2_FL Forward:

GCTTATCCTTACGACGTGCCTGACTACGCCGGATCCGACGACAGCGGCGAGCTGGGTGG

FL_SREBP2_FL Reverse:

GCCTGCAGGTCGACTCTAGAGTCGCTCAGGAGGCGGCAATGGCAGTG

2.2.4. sgRNA cloning

Gene specific CRISPR sgRNA were selected from either the GeCKO v2 library (Sanjana *et al*., 2014), Brunello library (Doench *et al*., 2016), Bassik library (Morgens *et al*., 2017) or designed using the Broad Institute design algorithm (https://portals.broadinstitute.org/gpp/public/analysis-tools/sgrna-design). Sense and

antisense sgRNAs oligonucleotides were designed with 5' CACC and 3' CAAA overhangs respectively. The sgRNAs were cloned into the pSpCas9(BB)-T2A-puro or pSpCas9(BB)-T2A-GFP vector for transient transfection (Ran *et al.*, 2013). LentiCRISPRv2 (sgRNA/Cas9, F. Zhang, Addgene #52961) or pKLV-U6gRNA(BbsI) PGKpuro2A-BFP were used for lentivirus production of the sgRNA (Koike-Yusa *et al.*, 2014; Sanjana *et al.*, 2014).

2.2.5. Real-time quantitative PCR (RT-qPCR)

Whole cell RNA was extracted and purified using the Qiagen RNeasy® Plus Mini Kit (Qiagen) following the manufacturer's instructions. 1 μg of RNA was used to generate 1 μg cDNA using photoscript reverse transcriptase. Mixture 1 was incubated for 5 minutes at 65°C to denature the sample, before mixture 2 was added **(Table 7)**. The whole mixture was incubated at 42°C for one hour before inactivating the transcriptase for 20 minutes at 65°C. Samples were either used immediately or stored at -20°C until needed.

		Volume (μl)
Mixture 1	Total RNA	1 μg
	Oligo $d(T)_{23}VN$ (100 μM)	1
	10 nM dNTPs	1
	Nuclease free H_2O	To a total of 10 μl
Mixture 2	5X PhotoScript II buffer	4
	0.1 M DTT	2
	PhotoScript RT (200 U/μl)	1
	RNase Inhibitor	0.2
	Nuclease free H_2O	2.8

Table 7. Protocol for creating cDNA

Transcript levels were determined in quadruplicate, using 15 µl reactions in 384 well plates, using SYBR Green PCR Master Mix (Applied Biosystems) with 10-20 ng starting cDNA sample per reaction **(Table 8)**. The reactions were carried out in either an ABI 7900 HT Real-Time PCR system (Applied Biosystems) or a QuantStudio 5 Real-Time PCR System (Thermo Fisher). RNA quantification was performed using the ΔΔCT method using housekeeping gene β-actin for normalisation.

Per 15 µl reaction	Volume (µl)
Nuclease free H_2O	3.25
SYBR Green PCR Master Mix	6.25
Forward Primer (10 µM)	0.25
Reverse Primer (10 µM)	0.25
cDNA	10-20 ng made up to 5 µl in nuclease free H_2O

Table 8. Protocol for RT-qPCR

2.3. Cell Biology

2.3.1. Cell culture

HeLa, Thp1 (gift from Paul Lehner), HepG2 and HEK293T/HEK293ET cells, were routinely cultured and maintained in DMEM or RPMI-1640 supplemented with 10% v/v fetal calf serum (FCS), 100 U/ml penicillin G and 100 μg/ml streptomycin, with the addition of 1 μg/ml puromycin, 2.5 μg/ml blasticidin or 100 μg/ml hygromycin where appropriate for selection. All experiments were performed in mycoplasma negative cells, confirmed using the MycoAlert™ Mycoplasma detection kit (Lonza). HeLa, HEK293ET and Thp1 cells were also authenticated (Eurofins).

2.3.2. Sterol depletion assays

Cells seeded at approximately 60% confluency were washed twice with PBS and before being incubated in starvation medium (DMEM, 10% LPDS, 10 μM mevastatin, penicillin/streptomycin (with the addition of 50 μM mevalonate if using SREBP2 KO cells in the experiment)). For hypoxic experiments, cells were sterol depleted for 24 hours in 21% oxygen, prior to being incubated in hypoxia for a further ~18 hours still under sterol depletion.

2.3.3. Preparation of compounds

Mevastatin was made up in DMSO (Dimethyl Sulfoxide) at a stock concentration of 10 mM and stored at -20°C. 25-hydroxycholesterol was made up in ethanol at a stock concentration of 2 mg/ml and stored at -20°C until further use. Mevalonate was prepared by adding 385 μl 2.04 M KOH to 100 mg mevalonolactone (Sigma). The solution was heated (1 hr, 37°C) and adjusted to a 50 mM stock solution. Mevalonate was used in any experiment where SREBP2 KO lines were used under sterol deplete conditions.

2.3.4. Cycloheximide chases in sterol deplete hypoxic conditions

Cells were seeded as previously described and sterol depleted for 42 hours. Where appropriate cells were incubated in hypoxia (1% oxygen) for the final 18 hours. Next, cycloheximide (1 μg/ml) and/or MG132 (20 μM) were added and cells were harvested at the defined intervals (0, 1, 2, 4, 6 or 8 hours) prior to further analysis by immunoblot. Alternatively, cells were sterol depleted for 24 hours, and then sterols were re-introduced to trigger HMGCR degradation (2 μg/ml 25-hydroxycholesterol and 20 μg/ml cholesterol). Cells were harvested at the indicated time points before analysis by immunoblot.

2.3.5. Transient Transfections of HeLa cells

Cells were passaged 24 hours prior to transient transfection to ensure they were in the exponential growth phase when transfected. Transient transfections in HeLa cells were carried out using TransIT-HeLaMonster® (Mirus) following the manufacturer's instructions. Briefly, the transfection mix (200 μl OptiMEM, 1 ug DNA, 5 μl TransIT and 1 μl Monster) was incubated for 30 minutes at room temperature before being added dropwise to cells at 70% confluency in a 3 cm dish. 24 hours post transfection, the cells were split 1:10 and the appropriate antibiotic selection added for up to 48 hours to enrich for successful transfection.

2.3.6. siRNA transfection

siRNA knock-downs were carried out using Lipofectamine RNAiMax (ThermoFisher Scientific) following the manufacturer's instructions. Briefly, HeLa cells were seeded so they were 50% confluent on the day of transfection. Cells were either untreated or treated with RNAiMAX only (mock), or 50 nM siRNA; β2M (Sigma Aldrich, NM_004048 #2), or SREBP2 (Dharmacon ON-TARGETplus SREBF2 siRNA, L-009549-00-0005) diluted in OptiMEM with 7.5 μl RNAiMAX. The siRNA/RNAiMAX/OptiMEM mix was incubated at room temperature for 20 minutes before being added dropwise to cells. The media was changed 24 hours following transfection

and expanded as required and harvested at 48 hours post transfection for further analysis.

2.3.7. Single Cell Cloning

Clonal populations of cells was achieved either by manual serial dilution of the cells or by single cell sorting by FACS **(see section 2.3.12)** if the desired cells contained a fluorescent reporter. Manual serial dilution was achieved by diluting the cells to a concentration of 1.5 cells/ml and 200 µl added to a flat-bottomed 96 well plate giving a final concentration of 0.3 cells/well. Cells were incubated at 37°C in 5% CO_2 for 2-4 weeks until individual colonies were formed. Successful clones were then expanded and phenotypically analysed.

2.3.8. Hypoxic culture

All hypoxic experiments were performed in either a Whitley H35 Hypoxystation (Don Whitley Scientific) or a SCI-tive Dual Hypoxia workstation (Baker Ruskinn) maintained at 1% oxygen, 94% N_2, 5% CO_2 at 37°C. Cells were kept upon ice when leaving the chamber for FACS and for mRNA and protein isolation the cells were harvested as much as possible within the hypoxic chamber to minimise re-oxygenation of samples.

2.3.9. Lentiviral production and transduction

Lentivirus was created in HEK293ET or HEK293T cells by transfection using Mirus Trans-IT-293 Transfection reagent according to manufacturer's instructions. Cells were transfected at approximately 70% confluency with pMD.G (VSVG envelope), the appropriate lentiviral transgene vector and pCMVR8.91 (gag/pol) at a ratio 2:3:4 prepared in Opti-MEM reduced serum medium. Viral supernatant was collected 48 hours post transfection and filtered through a 0.45 µm filter and stored at -80°C until further use or used immediately.

Cells were seeded in a 24 well plate immediately before being transduced using the appropriate volume of viral supernatant (typically 250 µl). Plates were then centrifuged at

750 xg, 37°C for 1 hour before being incubated at 37°C. Cells were selected for antibiotic resistance 24-48 hours post transduction.

2.3.10. CRISPR-Cas9 targeted deletions

The sgRNA's were cloned as described in sgRNA cloning **(section 2.2.4)** into either one of the viral vectors: LentiCRISPR v2 or pKLV-U6sgRNA-pGK- Puro-2A-BFP, or one of the transient vectors: pSpCas9(BB)-T2A or pSpCas9(BB)-T2A-GFP**.** Following transient transfection or viral transduction, the cells were assessed for specific knockdown from seven days. For cells transduced using the pKLV-U6sgRNA-pGK- Puro-2A-BFP vector, cells needed to firstly be stably expressing Cas9.

2.3.11. Flow Cytometry

Cells were harvested and washed twice with PBS by centrifugation before either being subjected to live cell flow cytometry (pDonor Clover) or being fixed in 3.6% PFA in PBS. Cells were run on an LSRFortessa™ (BD Biosciences). Resulting data was analysed using the FlowJo software.

2.3.12. Fluorescence activated cell sorting (FACS)

Cells were harvested before being washed in PBS/10 mM Hepes and re-suspended in sorting medium (10 mM Hepes, 2% FCS, PBS). The cell suspensions were then passed through a 50 μm filter (CellTrics®, Partec) and sorted through a High speed Influx Cell Sorter (BD Biosciences). Cells were collected in 10 mM Hepes, 50% DMEM, 50% FCS supplemented with penicillin/streptomycin.

2.3.13. Cell surface staining

Cells prepared for staining were trypsinised, washed in PBS and incubated with 100 µl of the primary antibody made up in PBS for 30 minutes at 4°C. The primary antibody was removed by a PBS wash by centrifugation (500 xg, 5 minutes) before incubation with the appropriate Alexa Fluor conjugated secondary antibody for 30 minutes at 4°C in the dark. Two final PBS washes were performed before cells were fixed in PBS with 3.7% PFA before analysis on a BD LSRFortessa™ (BD Biosciences).

2.3.14. CRISPR-Cas9 forward genetic screens

HeLa mCherry-CL1 screen

HeLa mCherry-CL1 UBE2G2 null cells were firstly transduced with Cas9-Blast and maintained under selected for at least 14 days. For the screen 50 x 10^6 HeLa mCherry-CL1_UBE2G2null_Cas9-blast cells were transduced with the CRISPR knockout Brunello library, which targets 19,114 human genes and contains 76,441 unique sgRNAs (Doench *et al*., 2016). Cells were transduced at an MOI of ~30% (approximately 15 x 10^6 cells) with transduced cells selected using puromycin for at least seven days. To maintain an even representation of the guides throughout the screen the unsorted library was routinely maintained in excess of 50 x 10^6 cells, this ensured approximately at least a 600X representation of each guide.

After 7 days, mCherry^{HIGH} cells were enriched by FACS as detailed in Fluorescence activated cell sorting (FACS) **section 2.3.12.** These cells were cultured for a further 9 days before a second round of FACS to select for the mCherry^{MEDIUM} and mCherry^{HIGH} cells was carried out. DNA was extracted from the control library (transduced cells which had not undergone FACS) and sorted cells using the Puregene® Core kit A (Qiagen) according to manufacturer's instructions. The sgRNA locus was amplified using two rounds of PCR as previously described (Timms *et al*., 2016), and the amplicons sequenced by Illumina HiSeq as previously described

(Timms *et al*., 2016) **(Table 9)**. The data was analysed using the MAGeCK algorithm with assistance from Peter Bailey and Stuart Bloor (Nathan and Lehner laboratories) (Li *et al.*, 2014).

sgRNA amplification primers (5'-3')	
Outer_Fwd	GCTTACCGTAACTTGAAAGTATTTCG
Outer_Rev	GTCTGTTGCTATTATGTCTACTATTCTTTCC
P5_inner_Fwd	AATGATACGGCGACCACCGAGATCTACACTCTCTTGTGGAAA GGACGAAACACCG
P5_*index*_inner_Rev	CAAGCAGAAGACGGCATACGAGA*nnnnnnn*GTGACTGGAGT TCAGACGTGTGCTCTTCCGATCTTCTACTATTCTTTCCCCTGCA CTGT
Illumina sequencing primer	ACACTCTCTTGTGGAAAGGACGAAACACCG

Table 9. Brunello CRISRP/Cas9 screen sgRNA amplification primers

HeLa HMGCR_clover screen

Hela HMGCR_clover cells were first transduced with Cas9-Hygro and maintained under selection for at least 14 days. For the screen 10^8 cells were transduced with the CRISPR knockout Bassik library which targets 20,500 genes and contains approximately 220,000 unique sgRNAs (Morgens *et al*., 2017). Cells were transduced at an MOI of ~30% with transduction efficiency determined by measurement of mCherry by flow cytometry 48 hours post transduction. Transduced cells were enriched by puromycin selection for at least seven days. To maintain an even representation of guides throughout the screen the unsorted library was routinely maintained in excess of 100 x 10^6 cells ensuring approximately 500X representation of each guide.

After eight days cells were seeded to approximately 30% confluency and allowed to settle before being sterol depleted (DMEM +10% LPDS+10 µM mevastatin +penicillin/streptomycin) overnight as detailed in Sterol depletion assays **(section 2.3.2)**. The next day the cells were placed in hypoxia for approximately 18 hours. Cells were prepared for FACS sort as detailed in **section 2.3.12**, and clover^{HIGH} cells were collected. These cells were cultured for a further six

days before being subjected to sterol depletion and hypoxia and FACS as detailed above, further enriching for clover^{Medium} and clover^{HIGH} cells. DNA was extracted from the control library (transduced cells which had not undergone FACS) and sorted cells using the Puregene® Core kit A (Qiagen) according to manufacturer's instructions. The sgRNA locus was amplified using two rounds of PCR as previously described (Timms *et al*., 2016), and the amplicons sequenced by Illumina MiniSeq and HiSeq as previously described (Timms *et al*., 2016) **(Table 10)**. The data was analysed using the MAGeCK algorithm with assistance from Peter Bailey and Stuart Bloor (Nathan and Lehner laboratories) (Li *et al*., 2014).

sgRNA amplification primers (5'-3')	
Outer_Fwd	AGGCTTGGATTTCTATAACTTCGTATAGCATACATTATAC
Outer_Rev	ACATGCATGGCGGTAATACGGTTATC
P5_inner_Fwd	AATGATACGGCGACCACCGAGATCTACAC TCTCTTGTGGAAAGGACGAAACACCG
P5_*index*_inner_Rev	CAAGCAGAAGACGGCATACGAGAT*nnnnnnn*GTGACTGGAGTTC AGACGTGTGCTCTTCCGATCCGACTCGGTGCCACTTTTTC
Illumina sequencing primer	AGACTATAAGTATCCCTTGGAGAACCACCTTGTTGG

Table 10. Bassik CRISPR/Cas9 screen sgRNA amplification primers

2.4. Biochemistry

2.4.1. Cell lysis and Immunoblotting

Polyacrylamide gels were prepared using the BioRad gel system (BioRad) or precast gradient (4-12%) gels were used (Invitrogen), and gels ran using either Tris-Glycine or MES buffer (Invitrogen) respectively. 4-12% gradient gels were routinely used for blots being probed for UBE2J2, RNF145 and SREBP2 due to the requirement for increased protein separation for clear visualisation. Cells were lysed using an appropriate volume of either Triton X-100 buffer (1% Triton X-100, 100 mM NaCl, 50 mM Hepes pH 7.4, 1 mM PMSF, protease inhibitors (Roche)), RIPA buffer (50 mM TRIS pH 8.0, 150 mM NaCl, 0.1% SDS, 1% NP40, 0.5% sodium deoxycholate, protease inhibitors), Digitonin buffer (1% digitonin, protease inhibitors) or 1X SDS buffer (1% SDS, 50 mM Tris pH7.4, 150 mM NaCl, 10% glycerol and 5 µl/ml benzonase nuclease). Phosphatase inhibitors (Calbiochem, phosphatase inhibitor cocktail set V, 50X) were used in the lysis buffer when immunoblotting using phospho-antibodies. Cells were lysed on ice for at least 15 minutes before being subjected to centrifugation at 16.9 xg for 10 minutes to remove the nuclear fraction. 6X SDS sample buffer (Laemmli) was added to the supernatant, and the samples typically heated at 75°C for 10 minutes prior to analysis. Samples to be probed for MARCH6(C9A)-HA, HMGCR and RNF145 were heated at 50°C for 30 minutes as higher temperatures result in protein aggregation, and samples lysed in 1X SDS buffer were subjected to a higher temperature of 95°C for 5 minutes to assist full denaturing.

Proteins were resolved using SDS-PAGE and transferred to methanol activated 0.45 µm PVDF membranes (Immobiolon-P) in BioRad mini-trans blot modules (Bio-Rad) for 1 hour at 100V. Membranes were blocked in PBS 0.2% Tween 20 (PBST) containing 5% (w/v) skimmed milk powder (Marvel), before being probed with the appropriate primary and secondary antibodies conjugated to HRP which were incubated for at least one hour each. Immunoblots were developed using Pierce™ enhanced chemiluminescence (ECL), SuperSignal™ West Pico or Dura Chemiluminescent Substrates (Thermo Scientific).

2.4.2. Immunoprecipitation

Co-immunoprecipitation of MARCH6(C9A)-HA and Flag-UBE2J2

HeLa cells overexpressing MARCH6(C9A)-HA and/or Flag-UBE2J2 (9×10^6) were harvested and washed twice with PBS before being lysed in 1 ml of 1% digitonin buffer (30 minutes on ice). Cells were centrifuged for 10 minutes (16.9 xg, 4°C). Supernatants were pre-cleared with Sepharose CL4B for 1 hour at 4°C, then 10% volumes were taken for the input sample. The pre-cleared supernatant was then incubated with 10 µl EZviewTM Red Anti-HA beads (Sigma-Aldrich) for 3 hours at 4°C with rotation. Resins were washed three times by centrifugation with 0.3-0.5% digitonin or 1% Triton X-100 and bound proteins were eluted using SDS sample buffer and heated at 75°C for 10 minutes before being analysed by SDS-PAGE and immunoblotting **(section 2.4.1)**.

2.4.3. Polysome profiling

Polysome profiling in HeLa cells was carried out in collaboration with Professor Ian Brierley (Department of Virology, Cambridge). Cells were plated in a 6 cm dish so that they would be 80% confluent on the day of harvest. Ten minutes before harvesting cycloheximide was added to a final concentration of 100 µg/ml. Cells were washed with PBS and harvested by scraping in 500 µl lysis buffer (20 mM Tris HCl pH 7.5, 100 mM KCl, 5 mM MgCl2, 1 mM DTT, 100 µg/ml CHX, 0.5 % (v/v) NP-40, 14 U of Turbo DNAse I, supplemented with protease inhibitors) and incubated for 15 minutes on ice. Lysates were homogenised by ten passes through a 27G needle and the nuclei removed by centrifugation at 13,000 xg for 20 minutes at 4°C. Samples were then frozen prior to use.

Sucrose gradients were made up by underlying 10% with 50% (w/v) sucrose solutions (20 mM Tris HCl pH 7.5, 100 mM KCl, 5 mM $MgCl_2$, 100 µg/CHX, 1 mM DTT, 0.1 mM EDTA, topped up with H_2O), and using a GradientMaster, before 350 µl of the sample was loaded on top.

The samples were centrifuged in a Beckman SW40Ti rotor at 200,000 xg for 90 minutes at 4°C. Gradients were fractionated at 4°C using an Isco fractionator by piercing at the bottom of the

tube and chasing the gradient upwards with 60% (w/v) sucrose containing bromophenol blue. The gradient is monitored by UV absorbance at 254 nm.

Proteins were collected from the 500 µl fractions using methanol chloroform precipitation. 200 µl of the fraction was mixed with 200 µl methanol and 50 µl chloroform by vortexing. Samples were centrifuged at 13,300 xg for 5 minutes before removing the top organic layer. 300 µl methanol was added to each sample and samples were centrifuged at 13,300 xg for 5 minutes before the supernatant was remove, and pellet air dried for 15 minutes prior to being dissolved in 1X SDS loading buffer and analysed by immunoblotting.

2.5. Statistical analysis

Unless specified in the figure legend, a minimum of three biological repeats were performed for each experiment with the appropriate controls. Immunoblots were quantified using ImageJ. Quantitative data is expressed as the mean from experimental technical replicates, with independent data points from at least three biological repeats unless specified in the figure legend. P-values were calculated using the appropriate statistical test, typically a one way ANOVA unless specified in the figure legend. A p-value of <0.05 was considered statistically significant.

Chapter 3: The role of UBE2J2 in protein quality control at the endoplasmic reticulum

3.1. Introduction

The degradation mechanism for the cytosolic CL1 degron in mammalian cells had been partially elucidated from the KBM7 screen that was carried out before I joined the Nathan laboratory. This screen identified two ER resident E3 ligases, MARCH6 and TRC8, the E2 conjugating enzyme UBE2G2, and the ubiquitin binding protein AUP1 **(Figure 3.1 A & B)**. Only combined depletion of the two ligases together was sufficient to fully stabilise the CL1 degron **(Figure 3.1 C)**. Additionally, it was shown that TRC8, UBE2G2 and AUP1 function in the same arm of the pathway for degrading the CL1 degron and that MARCH6 was still able to degrade the CL1 degron in the absence of AUP1 or UBE2G2 (Stefanovic-Barrett *et al.*, 2018) **(Figure 3.1 D)**. Therefore, the E2 enzyme, or any other proteins, involved in the MARCH6 arm of this pathway remained elusive.

The initial screen which uncovered the two E3 ligases was carried out in the near-haploid cell line, KBM7, using a gene trapping retrovirus. This approach did not provide full genome coverage **(Figure 3.1 B)** and it was likely that other genes involved in this degradative pathway remain to be identified. Therefore, we decided to develop the screening approach further using a genome wide CRISPR/Cas9 knockout library in mammalian cells.

In this chapter I use a CRISPR/Cas9 forward genetic screen in HeLa cells in an attempt to uncover new genes involved in intracellular protein quality control at the ER. I identify UBE2J2 as the predominant E2 enzyme working with MARCH6 for the degradation of the cytosolic degron CL1, and for squalene monooxygenase, an endogenous substrate. Additionally, I identify a potential role for the EMC in regulating the ER insertion of UBE2J2 under basal conditions.

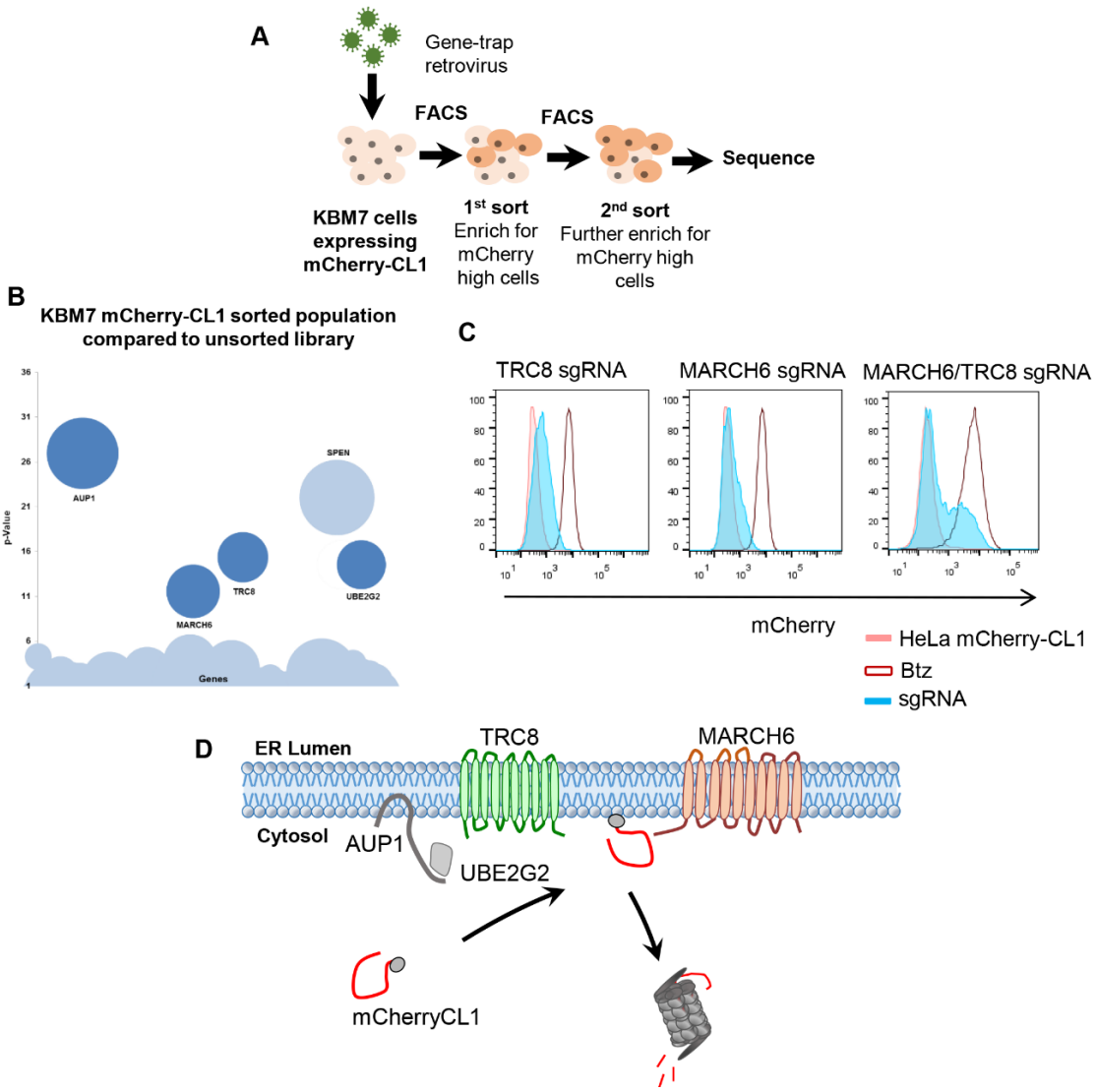

Figure 3.1. A forward genetic screen in KBM7 cells identifies ubiquitin machinery required for the degradation of a cytosolic degron.

(A) Schematic of the forward genetic screen carried out using gene trap retrovirus in the near-haploid cell line KBM7 expressing mCherry-CL1 degron. mCherry^{HIGH} cells were sorted by FACS from two sequential sorts 5 and 19 days post transduction. **(B)** Bubble plot showing genes enriched for gene-trapping insertions compared to non-phenotypically selected cells. 5457 different genes were mutagenized by the gene trap retrovirus. Bubble size is proportional to the number of independent gene-trap insertions. **(C)** HeLa cells expressing mCherry-CL1 were depleted of either TRC8, MARCH6 or both and analysed by flow cytometry. **(D)** Initial schematic for the degradation of mCherry-CL1 (red line = mCherry protein, circle = CL1 degron) at the ER membrane in mammalian cells utilising two independent E3 ligases.

Figure 3.1 (page 71) has been adapted from Stefanovic-Barrett et al, 2018 which is licenced under CC CY 4.0; EMBO reports. MARCH6 and TRC8 facilitate the quality control of cytosolic and tail-anchored proteins. Stefanovic-Barrett. S., Dickson. A. S., Burr. S. P., Williamson. J. C., Lobb. I. T., van den Boomen. D. J. H., Lehner. P. J., Nathan. J. A. © (2018). (Experiments carried out by Sandra Stefanovic-Barrett and Stephen Burr).

3.2. Results

3.2.1. Depleting UBE2G2 enables the specific study of MARCH6 dependent degradation of the CL1 degron

The near-haploid screen using gene trap retrovirus in KBM7 cells uncovered a novel pathway for cytosolic protein quality control at the ER membrane and identified some key components; MARCH6, TRC8, UBE2G2 and AUP1. However, it was likely that some components of this pathway were missed due to incomplete coverage of the genome by the gene-trapping retrovirus technology (Burr *et al*., 2016), so we decided to establish a CRISPR/Cas9 forward genetic screening approach to study this pathway in more detail, particularly focusing on other components working with the E3 ligase MARCH6.

To uncover genes involved in the MARCH6 arm of the degradative pathway for the cytosolic degron CL1, we decided to use a cell line where UBE2G2 was absent. Depleting UBE2G2 rendered the TRC8 pathway non-functional, so that the degradation of CL1 was solely dependent upon MARCH6.

Firstly, I transduced the HeLa mCherry-CL1 UBE2G2 null clone (created by Sandra Stefanovic-Barrett) with Cas9 and validated it was a true knockout **(Figure 3.2 A)**, and that the Cas9 was functional **(Figure 3.2 B)**. The functionality of the Cas9 was assessed using a sgRNA for Beta-2-Microglobulin (β2M). For the correctly folded MHC-1 to be expressed on the cell surface, the cell must express β2M which enables the complex to leave the ER and be trafficked to the cell surface. Cell surface staining, using an antibody specific for cell surface MHC-1, seven days following transduction with a β2M guide, demonstrated that 75.2% of the cells no longer expressed MHC-1 on the cell surface, showing that the Cas9 is functional and effective in these cells.

We have been unable to immunoblot for TRC8 and MARCH6 due to a lack of specific antibodies, however, mixed population knockouts of TRC8 or AUP1 in the HeLa mCherry-CL1 UBE2G2 null cells did not have any effect upon CL1 levels, whereas depletion of MARCH6 showed full CL1 stabilisation similar to full proteasome inhibition using Bortezomib (Btz)

(Figure 3.2 C). In comparison, HeLa mCherry-CL1 Wild type (WT) cells only show full CL1 stabilisation when both MARCH6 and TRC8 are depleted **(Figure 3.1 C)**. This confirmed that the degradation of CL1 in the UBE2G2 null cells was solely dependent upon MARCH6 and the cell line was appropriate to take forward into genome wide CRISPR/Cas9 forward genetic screen.

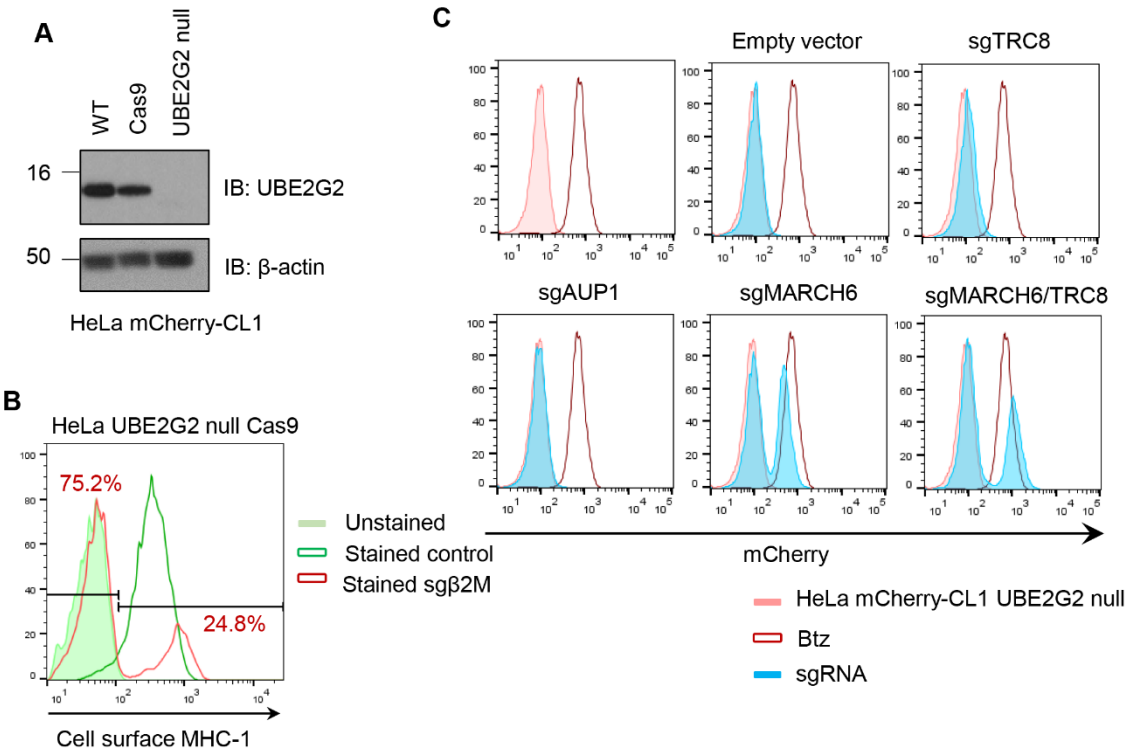

Figure 3.2. Depleting UBE2G2 enabled the specific study of MARCH6 dependent degradation of CL1 in Hela cells.

(A) Hela mCherry-CL1 cells were depleted of UBE2G2 and a clonal population isolated. **(B)** Hela mCherry-CL1 Cas9 UBE2G2 null cells were transduced with sgβ2M, seven days post transduction cells were stained with an antibody for cell surface MHC-1 and analysed by flow cytometry. **(C)** Hela mCherry-CL1 Cas9 UBE2G2 cells were transiently transfected with sgRNA and analysed seven days post transfection by flow cytometry. Cells were treated with 20 nM Bortezomib for 16 hours where appropriate.

3.2.2. A genome wide CRISPR Cas9 forward genetic screen in HeLa mCherry-CL1 UBE2G2 null cells identifies candidate E2 enzymes that work with MARCH6

A CRISPR/Cas9 genome wide forward genetic screen was carried out in the HeLa mCherry-CL1 UBE2G2 null cells to uncover genes not previously associated with this pathway **(Figure 3.3 A)**. We used the well validated Brunello CRISPR knockout library which contains 76,411 unique sgRNAs targeting 19,114 human genes (Doench *et al*., 2016).

Hela mCherry-CL1 UBE2G2 null cells were transduced with the Brunello library at a multiplicity of infection (MOI) of ~30% and selected with puromycin. The low MOI was to try and ensure that only one unique sgRNA would be transduced into a single cell and limit the possibility that two sgRNAs would be transduced into one cell which would confound the results.

The cells were subjected to two sequential FACS sorting steps to enrich for mCherry^{HIGH} cells 7 and 16 days post transduction. During the first sort 0.65% of cells were collected. During the second sort the cells were split into two populations; mCherry^{MEDIUM} (1.81%) and mCherry^{HIGH} (0.09%), due to two distinct populations being identified during the sort **(Figure 3.3 A)**. Following the second sort, cells were analysed by flow cytometry to assess the enrichment of mCherry, which seemed effective for both the mCherry^{MEDIUM} and mCherry^{HIGH} populations **(Figure 3.3 B)**. **Figure 3.3 C** shows the results from the Illumina sequencing of the extracted DNA from the mCherry^{MEDIUM} cells compared to an unsorted library of transduced cells.

Some of the top hits in the mCherry^{HIGH} and mCherry^{MEDIUM} populations included SPEN (Spen Family Transcriptional Repressor), UROD (Uroporphyrinogen Decarboxylase) and BCLAP (BLCAP Apoptosis Inducing Factor). These genes appear to be artefacts in a number of forward genetic screens, particularly those involving mCherry reporter proteins. SPEN is involved in transcriptional repression (McHugh *et al*., 2015), and UROD is involved in heme biosynthesis (Layer *et al*., 2010), therefore mutations in UROD may cause the cells red autofluorescence to increase which is why cells lacking UROD were enriched. BLCAP is involved in stimulating apoptosis (Zhao *et al*., 2016), and therefore depletion of UROD may promote cell survival, again increasing the likelihood of enrichment. Other genes enriched in the mCherry^{HIGH} population included transcription factors such as ZNF280B and the nuclear pore protein NUP50 which could be involved in increasing mCherry transcriptionally. We chose not to

analyse these hits further due to their already defined roles and likely indirect or non-specific effects.

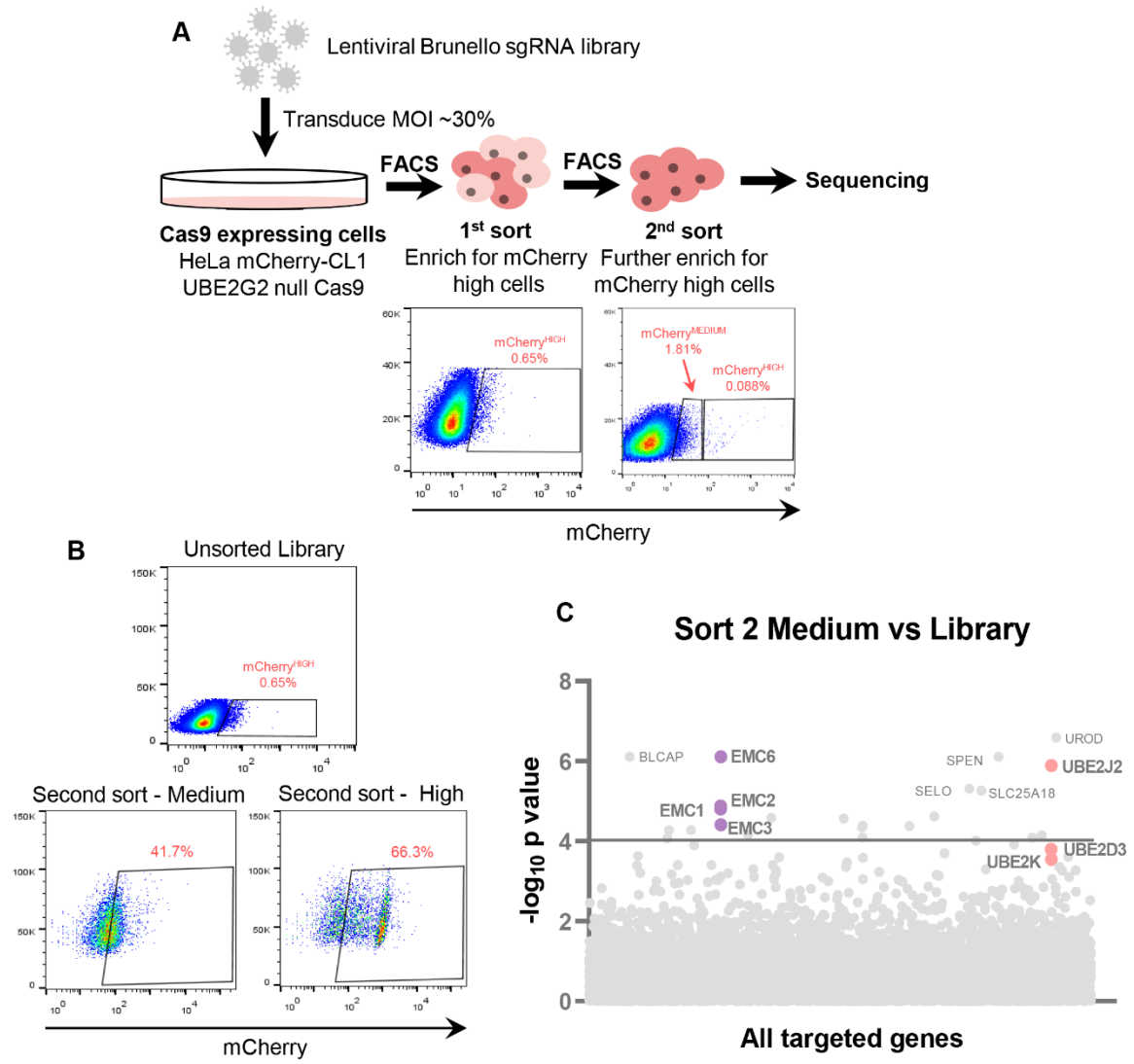

Figure 3.3. A CRISPR forward genetic screen in HeLa mCherry-CL1 UBE2G2 null cells identifies genes required for MARCH6 mediated degradation of the reporter.

(A) Schematic of the genome wide CRISPR screen carried out in Hela mCherry-CL1 cells using the Brunello CRISPR knockout library. Cells were sorted by FACS 7 days post transduction with 0.65% of cells collected as mCherry^{HIGH}. Nine days later these cells were subjected to a second sort with the collected cells split into two populations; mCherry^{MEDIUM} (1.81%) and mCherry^{HIGH} (0.09%). DNA was extracted from these cells and sequenced using Illumina sequencing. **(B)** Prior to sequencing cells from the second sort were analysed by flow cytometry to confirm the phenotype. mCherry^{MEDIUM} and mCherry^{HIGH} cells had ~42% and ~66% positive cells. **(C)** Bubble plot showing all the genes identified in the sort 2 mCherry^{MEDIUM} population compared to unsorted library. Bubbles represent the genes enriched in the mCherry^{MEDIUM} population compared to the unsorted library (significance threshold > -log(p)4). Data was analysed using the MAGeCK algorithm.

I chose to focus my attention on the hits in the mCherry^{MEDIUM} population as the approximate mCherry one fold shift on flow cytometry was similar to the observed shift following depletion of MARCH6 in these cells **(Figure 3.2 C)**, as opposed to the two fold shift observed in the mCherry^{HIGH} population. In addition, after analysis of the data from both the mCherry^{MEDIUM} and mCherry^{HIGH} populations, there were some E2 enzymes present in the mCherry^{MEDIUM} population and none detected in the mCherry^{HIGH} population **(Figure 3.3 C, red dots & see Appendix)**. Therefore overall, we thought the mCherry^{MEDIUM} population better represented our population of interest, and the very high level of mCherry-CL1 observed in mCherry^{HIGH} population was likely due to non-specific effects such as transcriptional upregulation.

From the hits in the mCherry^{MEDIUM} population UBE2J2 was of particular interest as it is a ER transmembrane E2 enzyme which has been previously implicated with ERAD substrates (van den Boomen *et al*., 2014; Wang *et al*., 2009). Additionally, both UBE2D3 and UBE2K, which were of lower statistical significance, were also potentially interesting. UBE2D3 (also known as UbcH5) is a soluble E2 enzyme, that has been implicated as an initiator of polyubiquitin chain formation by initiating the mono-ubiquitination of protein substrates (Duncan *et al*., 2006; Zhang *et al*., 2008). UBE2K (also known as HIP2 or E2-25K) is required for the autoubiquitination of the E3 ligase MARCH7 (Nathan *et al*., 2008), and has a putative role in the ER dislocation of MHC-1 in cells infected by the human cytomegalovirus gene product US11 (Flierman *et al*., 2006).

Perhaps surprisingly, MARCH6 was not picked up as a hit in this genome wide screen, although we know that depleting MARCH6 in these cells stabilises mCherry-CL1 levels **(Figure 3.2 C)**. Following further analysis of the screen data, I observed that only two out of the four possible MARCH6 sgRNAs were picked up in the library and sorted populations, and only one of these guides were enriched in the sorted populations. This suggested that only one of the MARCH6 sgRNAs in the library effectively depleted MARCH6. Therefore, the statistical power of MARCH6 depletion stabilising CL1 levels in the screen was dramatically reduced and is why MARCH6 is not amongst the top hits.

Four components of the ER membrane complex (EMC) were also identified as significantly enriched in the mCherry^{MEDIUM} population **(Figure 3.3 C, purple dots)**. The mammalian EMC proteins reside in a 10 protein complex (EMC1-10) at the ER membrane (Christianson *et al*.,

2011). Recent advances have shown that the EMC can act as an ER membrane insertase for moderately hydrophobic tail-anchored proteins (Guna *et al*., 2018) and the first TMD of G-protein-coupled receptors (Chitwood *et al*., 2018).

Following analysis of the screen, we decided to follow up the top hits that looked most likely to be involved in degradation of the CL1 degron; UBE2J2, UBE2D3 UBE2K and the components of the EMC.

3.2.3. UBE2J2 is the predominant E2 enzyme that is recruited by MARCH6

HeLa mCherry-CL1 and HeLa WT cells were used to validate whether the E2 enzymes identified in the screen were required for mCherry-CL1 degradation. Mixed knockout populations of UBE2J2, UBE2D3 and UBE2K were generated by transient transfection with plasmids co-expressing Cas9 and gene-specific sgRNA in HeLa mCherry-CL1 cells, and analysed by flow cytometry. UBE2J2 depletion partially stabilised mCherry-CL1, whereas depletion of UBE2D3 and UBE2K depletion had no effect by themselves **(Figure 3.4 A)**. In combination, depletion of multiple E2 enzymes caused an additive effect on CL1 stabilisation, with full CL1 stabilisation observed following combined depletion of UBE2G2, UBE2J2 and UBE2D3 **(Figure 3.4 B)**. This suggests a role for all these E2 enzymes in the degradation of mCherry-CL1. Overall, these data suggest that UBE2J2 is the predominant E2 enzyme working with MARCH6 in the stabilisation of CL1.

To determine if UBE2J2 was required for the degradation of other MARCH6 substrates, we chose to examine a validated endogenous substrate of MARCH6, squalene monooxygenase (squalene). Squalene an ER transmembrane protein which is a key enzyme in cholesterol synthesis and its endogenous turnover has been shown to rely upon MARCH6 and the UPS (Foresti *et al*., 2013; Zelcer *et al*., 2014). Mixed knockout populations of UBE2J2 in HeLa cells increased squalene levels to a comparable level observed with MARCH6 depletion or proteasomal inhibition **(Figure 3.4 C & D)**. Depletion of UBE2D3 or UBE2K by themselves had no effect on squalene levels compared to control cells. Additionally, CRISPR mediated depletion of UBE2D3 or UBE2K along with UBE2J2 had no additional effect upon squalene

above levels observed in the UBE2J2 deficient cells **(Figure 3.4 C & D)**, suggesting that UBE2J2 is the predominant E2 required for the MARCH6 ubiquitination of squalene.

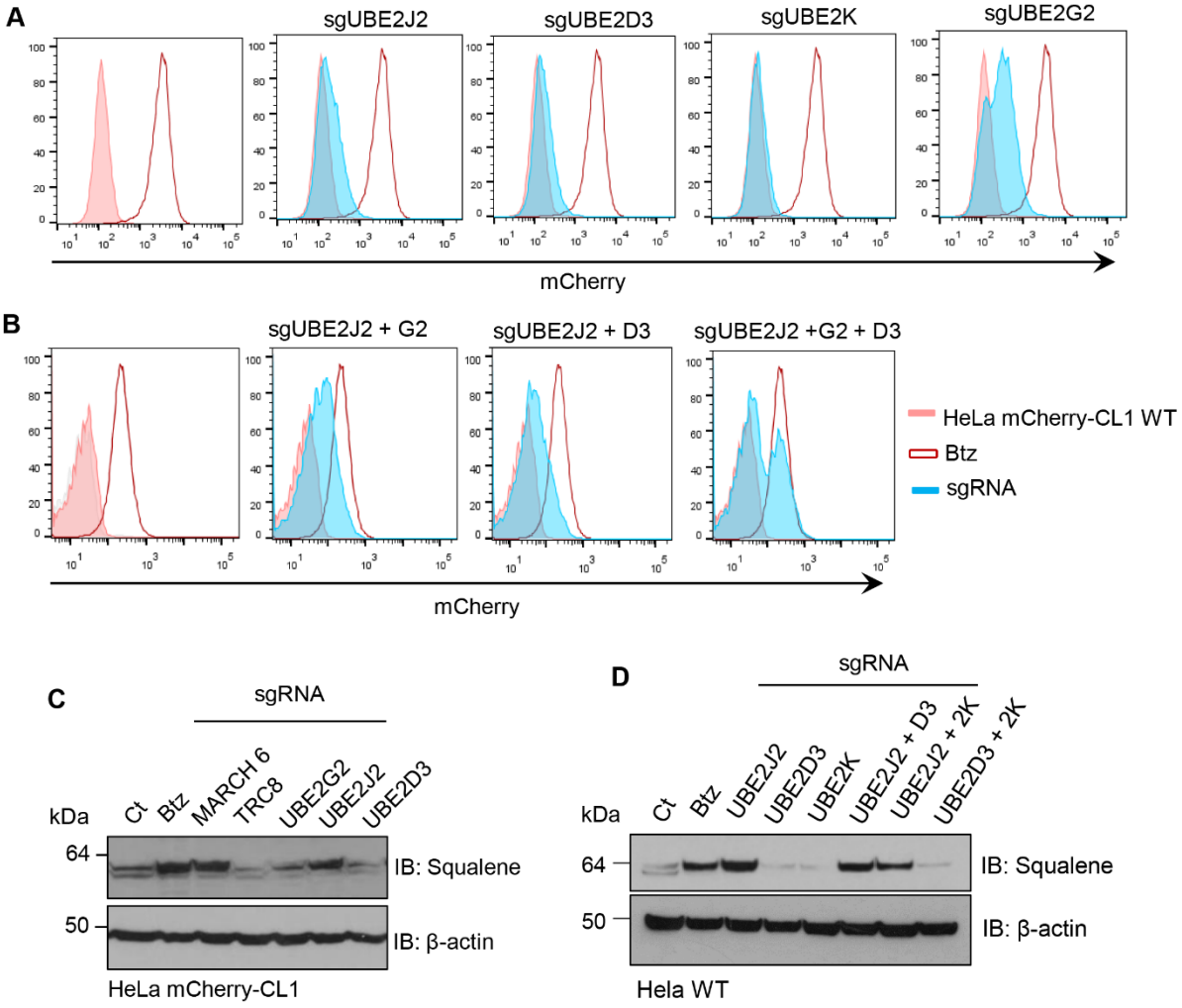

Figure 3.4. UBE2J2 is the predominant E2 enzyme that is recruited by MARCH6.

(A) Hela mCherry-CL1 cells were transiently transfected with sgRNA and Cas9 targeting UBE2G2, J2, D3 and K alone **(A)** or in combination **(B)** and analysed 7 days post transfection by flow cytometry. Cells were treated with 20 nM Bortezomib for 16 hours where appropriate. Hela mCherry-CL1 **(C)** or HeLa WT **(D)** cells were transiently transfected with sgRNA and Cas9 targeting the respective protein and cells were lysed 7 or 10 days post transfection in Triton X-100 buffer and immunoblotted. Cells were treated with 20 nM Bortezomib for 16 hours where appropriate.

To examine if MARCH6 could associate with UBE2J2, HeLa cells expressing HA tagged MARCH6 were immunoprecipitated with FLAG tagged UBE2J2 (the endogenous proteins could not be used to due to the lack of specific and appropriate antibodies for immunoprecipitation). As

MARCH6 rapidly undergoes autoubiquitination (Hassink *et al*., 2005) and is difficult to detect even when overexpressed, I used a catalytic inactive form of MARCH6, MARCH6(C9A)-HA. HeLa cells expressing MARCH6(C9A)-HA were immunoprecipitated with a resin bound HA antibody and the immunoblots probed for UBE2J2 using a FLAG antibody. FLAG-UBE2J2 was visualised in the MARCH6(C9A)-HA pull-downs when the cells were lysed in 1% digitonin lysis with 0.3-0.5% digitonin washes **(Figure 3.5 A)**. Moreover, this association was still observed using more stringent 1% Triton X-100 wash conditions in the immunoprecipitation **(Figure 3.5 B)**. Thus, UBE2J2 associates with the catalytically inactive form of MARCH6. However, whether the interaction is direct remains to be determined.

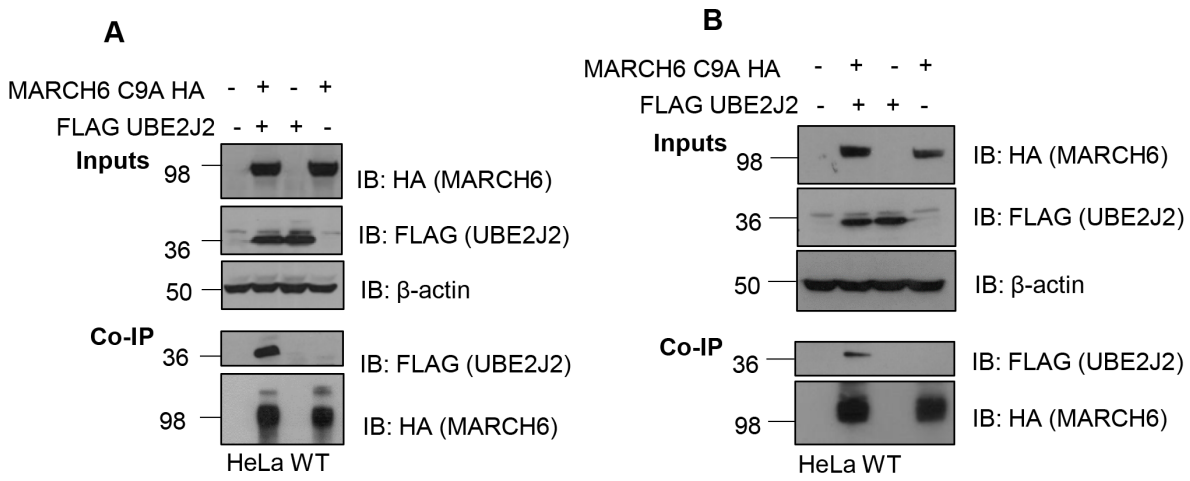

Figure 3.5. UBE2J2 and MARCH6 are in close proximity in the ER membrane.

Hela WT cells expressing either FLAG-UBE2J2 or MARCH6(C9A)-HA alone or in combination were lysed in 1% digitonin buffer and co-immunoprecipitated (Co-IP) using anti-HA beads. IP samples were washed with either 0.3-0.5% digitonin **(A)** or 1% Triton X-100 **(B)** and analysed by immunoblotting.

3.2.4. The UBE2J2 sgRNA specifically and efficiently depletes UBE2J2

To confirm that the sgRNA used against UBE2J2 was specific and efficient, I transduced HeLa mCherry-CL1 cells with UBE2J2 sgRNA and sorted for mCherry^{HIGH} cells seven days post transduction prior to immunoblotting for UBE2J2 **(Figure 3.6 A)**. The decreased levels of UBE2J2 observed in the mCherry^{HIGH} cells correlated with an increase in squalene as expected from previous experiments **(Figure 3.6 B)**. UBE2J2 is known to be regulated by the proteasome

therefore a slight increase in UBE2J2 levels following Btz treatment was not unexpected, although as yet, the ligases involved in this are unknown (Lam *et al.*, 2014).

The UBE2J2 sgRNA was also validated in a different cell line and using a different biological system where UBE2J2 is known to function. US11 is a viral protein which hijacks ERAD to degrade the human leukocyte antigen (HLA)-A2 (one form of MHC-1), using the E3 ligase TMEM129 and the E2 enzyme UBE2J2 (van den Boomen *et al.*, 2014). Depletion of UBE2J2 in this system prevented the US11-mediated degradation of HLA-A2, whilst depletion of UBE2D3 had no effect on HLA-A2 levels **(Figure 3.6 C)**.

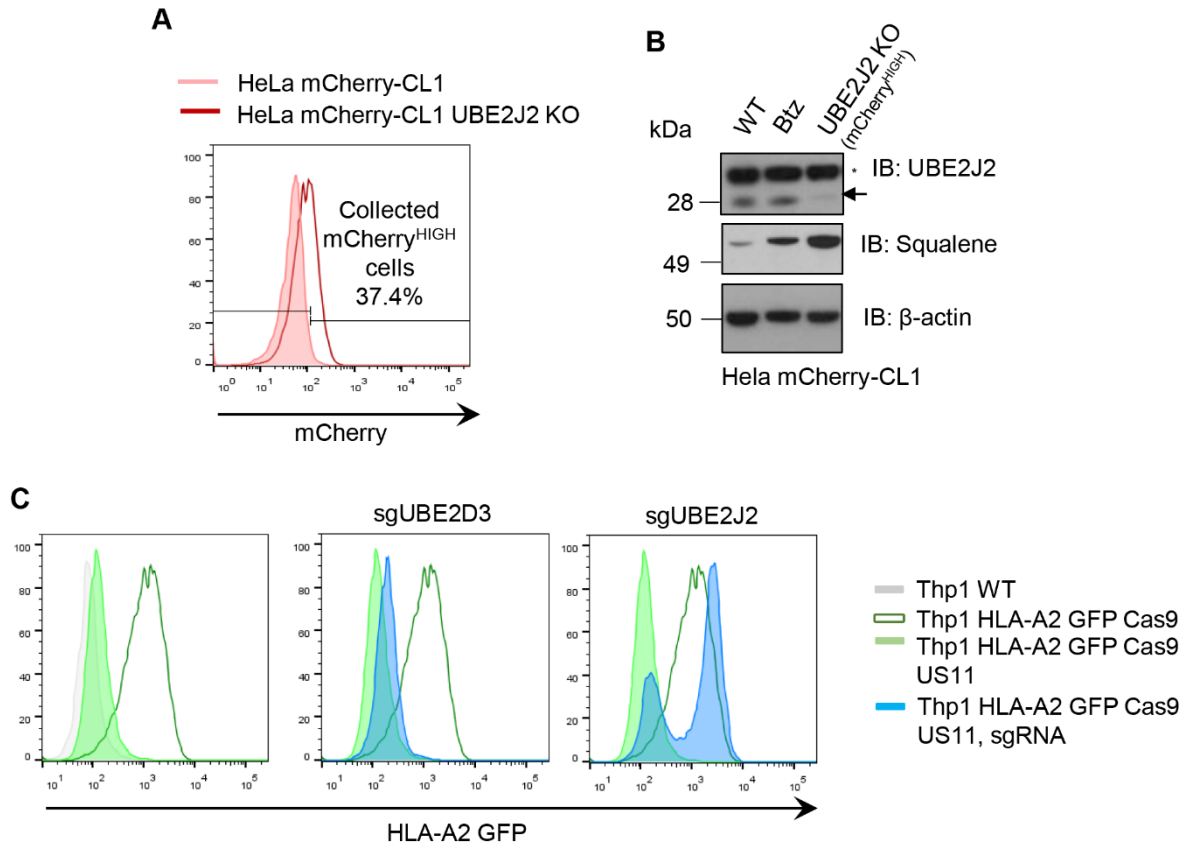

Figure 3.6. The UBE2J2 sgRNA specifically and efficiently depletes UBE2J2.

(A) HeLa mCherry-CL1 cells were transduced with UBE2J2 sgRNA and mCherry^{HIGH} cells were collected by FACS. **(B)** Hela mCherry-CL1 UBE2J2 KO mCherry^{HIGH} cells were blotted for UBE2J2 to confirm specific depletion. **(C)** THP1 HLA-A2 GFP US11 cells were transduced with UBE2J2 or UBE2D3 sgRNA and analysed by flow cytometry 7 days post transduction.

*represents non-specific bands

3.2.5. Overexpression of UBE2J2 promotes mCherry-CL1 degradation in UBE2J2 null cells.

To ensure that the phenotype observed with UBE2J2 depletion was specific to loss of UBE2J2 and not due to any off-target effects of the sgRNA, I reconstituted the UBE2J2 null cells. HeLa mCherry-CL1 UBE2J2 mixed population null cells (sorted for mCherry^{HIGH}) were transduced with a CRISPR resistant FLAG-UBE2J2 construct. The increase in mCherry-CL1 and squalene observed in UBE2J2 null cells was reverted back to WT levels upon overexpression of FLAG-UBE2J2 **(Figure 3.7 A & B)**. In addition, these cells still responded to treatment with proteasome inhibitors, showing that overexpression of UBE2J2 did not alter the proteasome mediated degradation of mCherry-CL1.

Together, these experiments show that UBE2J2 is the predominant E2 enzyme for MARCH6 in the proteasome mediated degradation of the CL1 degron and squalene. UBE2D3 and UBE2K appear to have some additive effects, particularly with mCherry-CL1 degradation, and may be able to work with MARCH6 under certain conditions, but do not appear to be predominant E2 enzymes in this pathway.

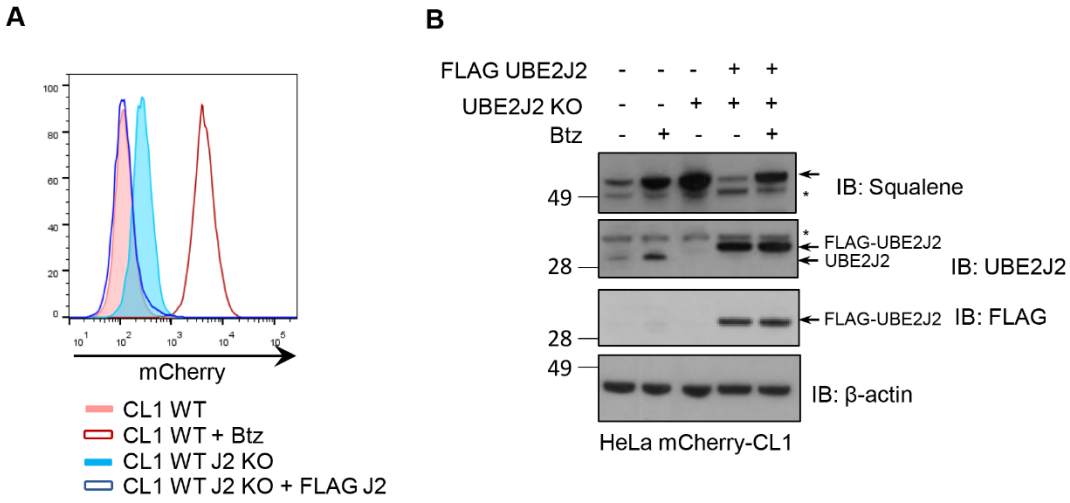

Figure 3.7. Overexpression of UBE2J2 promotes mCherry-CL1 and squalene monooxygenase degradation in UBE2J2 null cells.

HeLa mCherry CL1 UBE2J2 KO mCherry^{HIGH} cells were transduced with FLAG-UBE2J2 and analysed by flow cytometry **(A)** and immunoblot **(B)**. Cells were treated with 20 nM bortezomib for 16 hours where appropriate.

*represents non-specific bands

3.2.6. The ER membrane complex may be involved in the insertion of UBE2J2 into the ER membrane

Since the discovery of the highly conserved EMC in yeast (Jonikas *et al*., 2009), the EMC has been associated with a multitude of phenotypes, including depletion being shown to hinder lipid transfer from the ER to mitochondria (Lahiri *et al*., 2014). In mammals, the EMC has 10 subunits and was identified in an interaction network of proteins associated with ERAD (Christianson *et al*., 2011). Subsequently, recently published data has highlighted the role of the EMC complex in the ER insertion of tail-anchored proteins with a moderately hydrophobic transmembrane domain (Guna *et al*., 2018).

As four components of the EMC were identified in the screen **(Figure 3.3 C)**, I decided to assess how the EMC could be directly or indirectly involved in mCherry-CL1 degradation. I hypothesised that the EMC could be involved in the insertion of UBE2J2 into the ER membrane, as the EMC has recently been shown to be involved in the ER insertion of some tail-anchored proteins (Guna *et al*., 2018; Volkmar *et al*., 2019), or it could facilitate degradation of the membrane associated CL1 degron independently of its role in ER insertion. To test this, I chose to delete EMC6 as loss of EMC6 has been shown to severely disrupt the whole complex sufficiently to hinder the ER insertion of one of its target proteins squalene synthase and is therefore termed one of the 'core' subunits of the EMC (Guna *et al*., 2018; Volkmar *et al*., 2019). EMC6 was also the top EMC subunit identified in my screen **(Figure 3.3 C)**.

Depletion of EMC6 in HeLa mCherry-CL1 cells produced a modest increase in mCherry-CL1 levels **(Figure 3.8 A, top panel)**, similar to the effect observed when depleting UBE2J2 **(Figure 3.4 A)**. Interestingly, EMC6 depletion in UBE2J2 null cells had little effect on mCherry-CL1 levels, suggesting that the EMC has no additional effect on CL1 degradation beyond the loss of UBE2J2 **(Figure 3.8 A)**. A similar effect was observed following depletion of EMC6 in HeLa WT cells **(Figure 3.8 B)**. Following depletion of EMC6 a decrease in basal UBE2J2 levels were observed, which was at least partially rescued with proteasome inhibition **(Figure 3.8 B & C)**. These findings suggest that EMC6 depletion stabilises mCherry-CL1 by

reducing the UBE2J2 levels in HeLa cells, consistent with the requirement for the EMC to facilitate UBE2J2 membrane insertion.

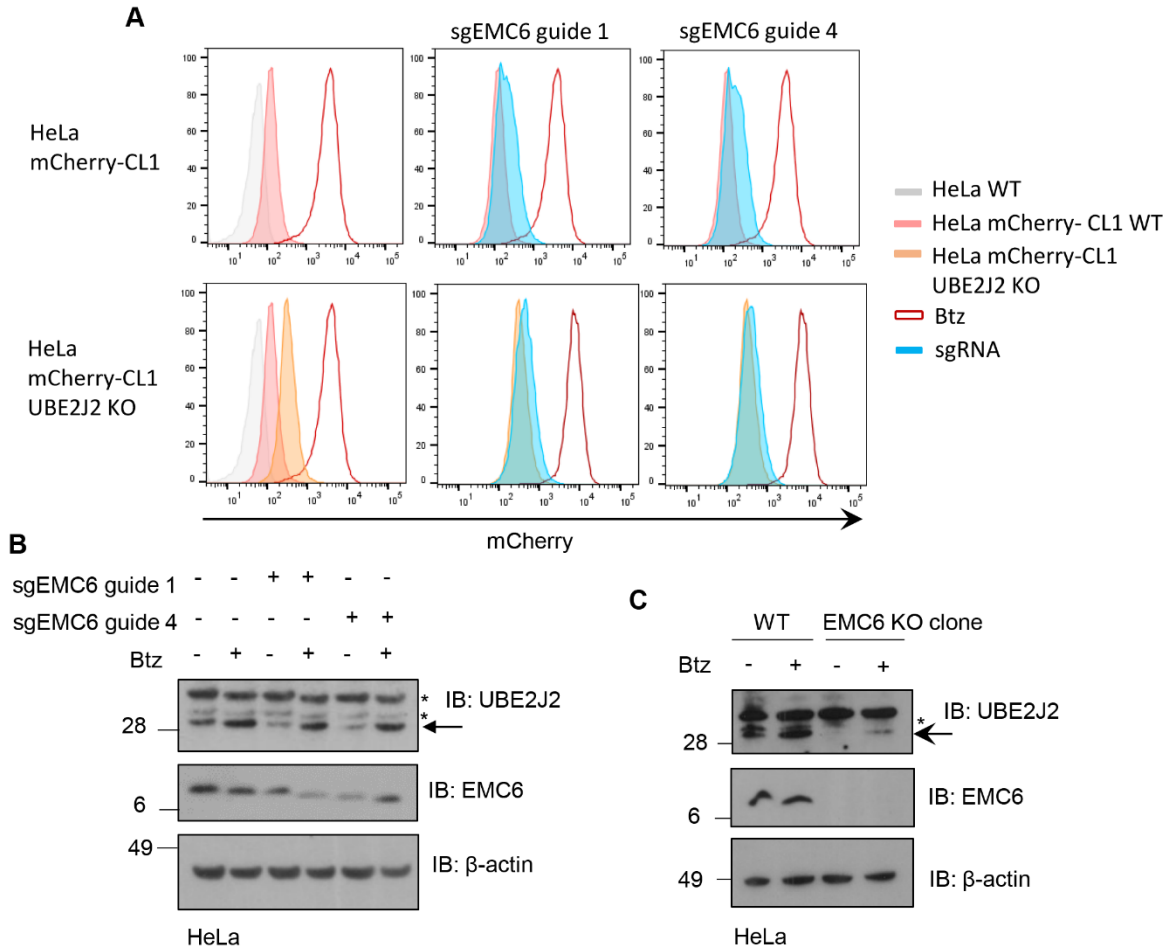

Figure 3.8. The ER membrane complex may be involved in the insertion of UBE2J2 into the ER membrane.

(A) HeLa mCherry-CL1 WT and UBE2J2 KO or Hela WT cells **(B)** were transiently transfected with two separate sgRNAs with Cas9 against EMC6 and analysed 7 days post transfection by flow cytometry **(A)** or immunoblotting **(B)**. **(C)** HeLa WT or Hela EMC6 KO clone cells were analysed by immunoblotting. Cells were treated with 20 nM Btz where appropriate.

*represents non-specific bands

Figure 3.9 shows my proposed model for how the E3 ligases, E2 enzymes and the EMC work together to regulate CL1 levels. My data has also shown that the MARCH6 and UBE2J2 arm of this pathway is akin to the regulation of the endogenous MARCH6 substrate squalene.

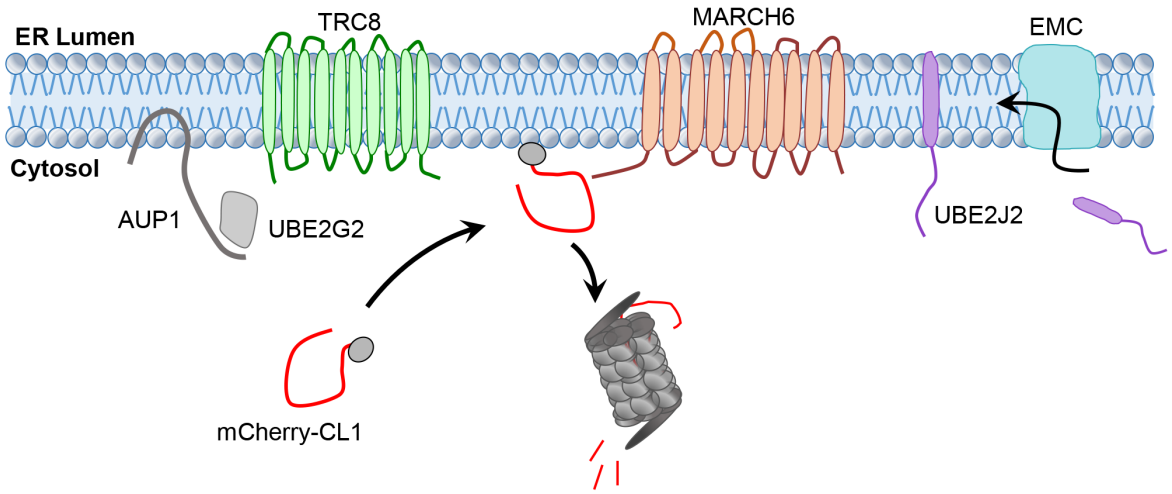

Figure 3.9. Schematic showing the degradation of mCherry-CL1 at the ER membrane in mammalian cells utilising two independent E3 ligases working with separate E2 enzymes.

In mammalian cells the mCherry-CL1 degron (red line = mCherry protein, circle = CL1 degron) is recruited to the ER membrane via its amphipathic helix, here it is targeted for proteasomal degradation. The two ER E3 ligases MARCH6 and TRC8 work with the E2 enzymes, UBE2J2 and UBE2G2, respectively, and both pathways are required for the complete degradation of CL1. The EMC appears to be required for UBE2J2 insertion into the ER and is therefore also required for full CL1 degradation.

3.3. Discussion

3.3.1. Limitations of the CRISPR/Cas9 forward genetic screen

The cells enriched for mCherry in the CRISPR screen using HeLa mCherry-CL1 UBE2G2 null cells were split into two populations; mCherry^{MEDIUM} and mCherry^{HIGH}. No new significant genes of interest were identified in the mCherry^{HIGH} population, with only a couple of genes involved in transcription and growth inhibition detected. Furthermore, putative genes involved in degradation were not detected. The reasons for these discrepancies between the mCherry^{MEDIUM} and mCherry^{HIGH} populations is not clear, but they suggest that the very high levels of mCherry-CL1 observed in the screen may relate to non-degradative pathways. Therefore, we focused our attention on the mCherry^{MEDIUM} population where the E2 enzymes of interest were identified.

The fact that the E2 enzymes were only identified in the mCherry^{MEDIUM} population, is probably due to the partial mCherry-CL1 stabilisation observed when the E2 enzymes are depleted. For example, depletion of UBE2J2, even alongside UBE2G2 did not stabilise mCherry-CL1 levels to those observed following proteasome inhibition **(Figure 3.4 B)**. Full stabilisation of mCherry-CL1 was only achieved when UBE2J2, UBE2G2 and UBE2D3 were depleted **(Figure 3.4 B)**. The other candidate genes in the mCherry^{MEDIUM} population included UROD, SPEN and BLCAP which appear to be artefacts in a number of forward genetic screens (Stefanovic-Barrett *et al.*, 2018; Thijn Brummelkamp, personal communications) and are involved in pathways such as transcriptional repression and apoptosis stimulation so appear to be non-specific to this pathway.

3.3.2. Degradation of the CL1 degron at the ER membrane

Whether mCherry-CL1 is actively recruited to the membrane or associates stochastically due to its amphipathic helix is not clear. Cell fractionation and microscopy studies show that mCherry-CL1 is mainly cytosolic, but following proteasome inhibition or depletion of

MARCH6/TRC8 it accumulates at the ER membrane (Stefanovic-Barrett *et al*., 2018). In yeast, Metzger *et al*., (2008) showed that ER-associated chaperones (Ssa1p and Ydj1p) bind to CL1 and are required for its ubiquitination and degradation, however, they do not seem to be required for the membrane association of the degron. Furthermore, we did not identify any cytosolic chaperones in the near-haploid or CRISPR/Cas9 genetic screens. This may be due to a limitation of screening in mammalian cells, as there could be a large amount of redundancy here and depletion of one gene may not show an identifiable phenotype, or it could be because no chaperones are required in this process. Our results currently suggest that no particular chaperones are required to bring CL1 to the membrane and this may occur stochastically when the hydrophobic portion of CL1 comes into close contact to the ER membrane, which may offer a new mechanism for cytosolic protein quality control.

3.3.3. The role of UBE2J2 in the MARCH6 mediated degradation of CL1 and squalene monooxygenase

The identification of UBE2J2 as the top candidate E2 enzyme in the screen suggests that UBE2J2 is the predominant E2 enzyme for MARCH6 mediated degradation of mCherry-CL1. This is supported by partial mCherry-CL1 stabilisation following UBE2J2 depletion in HeLa mCherry-CL1 WT cells. In addition, the role of UBE2J2 with MARCH6 is further supported by the stabilisation of squalene following UBE2J2 depletion in HeLa cells to comparable levels observed by MARCH6 depletion or proteasome inhibition **(Figure 3.4 C & D)**. Although UBE2D3 and UBE2K do not appear to be involved in squalene stabilisation, the depletion of UBE2D3 in particular did seem to have some effect on mCherry-CL1 stabilisation and these E2 enzymes may be able to somewhat compensate for the loss of UBE2J2 **(Figure 3.4 A)**. Furthermore, depletion of UBE2J2 and UBE2G2 in combination did not fully stabilise mCherry-CL1 to levels observed with proteasome inhibition, supporting a potential role for the other E2 enzymes identified in compensating for the loss of one E2. Indeed, the combined depletion of UBE2J2, UBE2G2 and UBE2D3 stabilised mCherry-CL1 to the levels observed with combined loss of TRC8 and MARCH6, and full proteasomal inhibition, suggesting that UBE2D3 may also be recruited by the E3 ligases **(Figure 3.4 B)**. For example, it is possible that either

UBE2D3 or UBE2K are required to monoubiquitinate mCherry-CL1, before the chain is elongated prior to degradation. This has been previously demonstrated for UBE2D3, in the monoubiquitination of the viral ubiquitin E3 ligase K3, (from KSHV (Kaposi's sarcoma-associated herpesvirus)) associated with MHC-1 receptors prior to internalisation and degradation of the MHC-1 receptor through the endolysosome system, to propagate the viral infection (Duncan *et al*., 2006), and for the monoubiquitination of PCNA, which is involved in the DNA damage tolerance pathway (Zhang *et al*., 2008). However, as we do not have antibodies to confirm depletion of UBE2K or UBE2D3 we cannot be completely confident of their efficient depletion in our experiments.

Although it has been shown that overexpressed forms of UBE2J2 and MARCH6 are in close proximity with each other in the ER membrane **(Figure 3.5)**, this does not confirm a direct interaction. To confirm a direct interaction a crosslinking experiment would need to be performed to covalently link interacting proteins and enable isolation through stringent lysis conditions. However, independent depletion of MARCH6 or UBE2J2 stabilises both the CL1 degron and squalene monooxygenase, which is rescued by their overexpression, suggesting that they function within the same pathway and supports a probable interaction.

Several approaches could be used to further determine how these different E2 enzymes function with TRC8 and MARCH6. It could be possible that they are preferentially involved in different ubiquitination steps (monoubiquitination or chain elongation), or that they allow the formation of different lysine linked ubiquitin chains on mCherry-CL1. This could be identified using ubiquitin containing lysine mutants and assessing ubiquitin chain formation. Additionally, it may be possible *in vitro* to reconstitute the ubiquitination of mCherry-CL1 at membranes and assess the preferential role of the E2s identified, which may help understand any compensation that may occur.

3.3.4. The role of the EMC in UBE2J2 ER insertion

Four members of the EMC were identified as being significantly enriched in the mCherry^{MEDIUM} population. The EMC proteins reside in a 10 protein complex (EMC1-10) at the ER membrane (Christianson *et al*., 2011), and their function is now beginning to be understood. The EMC has

recently been described as an ER membrane insertase for tail-anchored proteins with a moderately hydrophobic transmembrane domain (Guna *et al*., 2018; Volkmar *et al*., 2019), and G-protein coupled receptors (GPCRs) (Chitwood *et al*., 2018).

A tail-anchored protein is a protein which is anchored into the ER membrane via a hydrophobic stretch at its 'tail' (C-terminus) and is therefore post translationally inserted into the ER. UBE2J2 is a tail-anchored protein in the ER membrane which contains a stretch of moderately hydrophobic amino acids, this is unlike UBE2G2 which does not span the ER membrane and is only associated with the membrane through AUP1. Therefore, it seemed possible that the EMC could be acting as an insertase for UBE2J2 and that members of this complex were picked up in the screen indirectly through their effect on UBE2J2 levels.

My data supports this hypothesis as depleting EMC6 decreases the basal level of UBE2J2 which is partially rescued by proteasome inhibition, suggesting that some UBE2J2 not inserted into the membrane is degraded via the proteasome upon EMC loss **(Figure 3.8 B & C).** The EMC is therefore probably involved in regulating the basal levels of UBE2J2 through regulating its ER insertion.

Further work would be needed to confirm the link between the EMC and UBE2J2. The effect of EMC depletion on other UBE2J2 substrates, for example squalene monooxygenase, could be assessed and mutations could be incorporated into the transmembrane domain of UBE2J2 to increase its hydrophobicity and its reliance on the EMC for ER insertion could be tracked. If significantly increasing the hydrophobicity decreases its reliance on the EMC then this data fits with Guna *et al*., (2018) and would be consistent with the rest of our data suggesting that the stabilisation of the CL1 degron upon EMC depletion is indirect through the MARCH6 arm of this pathway due to the effect on UBE2J2 levels.

3.3.5. Endogenous substrates for MARCH6 and their role in the cholesterol synthesis pathway

To search for new endogenous substrates for MARCH6 and TRC8, mass spectrometry was carried out in HeLa mCherry-CL1 WT and MARCH6/TRC8 null cells by Sandra, a previous

post-doc in the Nathan laboratory (Stefanovic-Barrett *et al*., 2018). Squalene monoxygenase was identified as one of the top hits, which I have additionally shown relies on the E2 enzyme UBE2J2 **(Figure 3.10)**. Another protein of interest enriched in the double ligase knockouts was heme oxygenase-1 (HO-1), which our group has shown is a substrate of these ligases (Stefanovic-Barrett *et al*., 2018).

Interestingly, this analysis also revealed a number of proteins enriched in the MARCH6/TRC8 double knockout population that are involved in the cholesterol synthesis pathway, namely squalene monooxygenase, sterol regulatory element-binding protein (SREBP) 1 and SREBP2. Squalene monooxygenase is an important enzyme involved in the cellular generation of cholesterol from acetyl Co-A (Gill *et al*., 2011), and SREBP2 is a sterol sensitive transcription factor which is activated upon the cell's depletion of cholesterol (Brown & Goldstein, 1997). Upon activation, SREBP2 is involved in the transcription of a number of genes involved in the cholesterol synthesis pathway including the enzyme involved in the rate limiting step, HMG-CoA Reductase (HMGCR) (Horton *et al*., 2002). SREBP1 is another member of this family which primarily controls the transcription of genes involved in fatty acid synthesis such as fatty acid synthase (Horton *et al*., 2002).

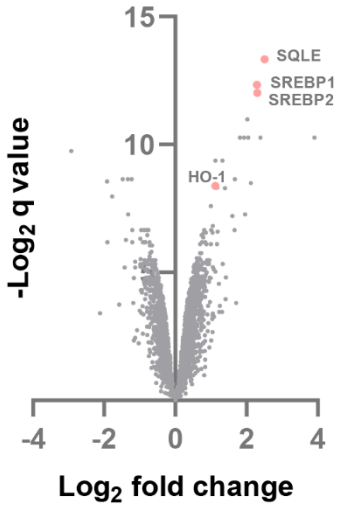

Figure 3.10. Volcano plot showing mass spectrometry analysis comparing HeLa mCherry-CL1 WT cells compared to MARCH6/TRC8 knockout cells.

Figure 3.10 (page 89) has been adapted from Stefanovic-Barrett et al, 2018 which is licenced under CC CY 4.0; EMBO reports. MARCH6 and TRC8 facilitate the quality control of cytosolic and tail-anchored proteins. Stefanovic-Barrett. S., Dickson. A. S., Burr. S. P., Williamson. J. C., Lobb. I. T., van den Boomen. D. J. H., Lehner. P. J., Nathan. J. A. © (2018).

Interestingly, the EMC has also been implicated in cholesterol homeostasis. Volkmar *et al*., (2019), recently showed that the EMC is involved in the ER insertion of squalene synthase, an enzyme involved in the cholesterol synthesis pathway prior to squalene monooxygenase. Volkmar *et al*., additionally showed that cells depleted of the EMC display reduced viability under conditions of limiting the cells extracellular cholesterol as they are unable to create their own cholesterol to sustain survival due to the lack of components involved in the pathway.

The links between MARCH6 and TRC8 mediated degradation and the cholesterol synthesis pathway were very intriguing to us. The cholesterol synthesis pathway is of huge importance for cell growth and survival and this is evident throughout evolution (Burg & Espenshade, 2011). Therefore, stringent regulation pathways must exist for many of the pathway's components. The regulation of a key rate limiting step of this pathway, HMGCR, has been extensively studied (Goldstein & Brown, 1990), but the regulation and turnover of other components, such as SREBP2, remain largely unknown. Additionally, several studies have shown that varying oxygen tensions may affect the cholesterol synthesis pathway (Hwang *et al*., 2017; Nguyen *et al*., 2007). This was of particular interest as a major focus of the Nathan group is understanding how cells respond to oxygen and nutrients. Therefore, I chose to focus my further studies on understanding how ERAD pathways and low oxygen environments affected the cholesterol synthesis pathway.

3.4. Summary

By utilising a near haploid gene trap mutagenesis screen to search for new regulators of protein quality control in mammalian cells we have previously demonstrated that that the soluble CL1 degron, which is analogous to a misfolded cytosolic protein, is degraded at the ER membrane by two ER resident E3 ligases MARCH6 and TRC8 (Stefanovic-Barrett *et al*., 2018). Here, using a CRISPR/Cas9 forward genetic approach, I have shown that UBE2J2 is the predominant E2 enzyme recruited by MARCH6 in degrading both the CL1 degron and the endogenous substrate squalene monooxygenase. I have also shown that the EMC may be the ER insertase for UBE2J2, thereby indirectly affect the degradation of UBE2J2 substrates.

Additionally, we observed that these degradative pathways are involved in the regulation of proteins involved in the cholesterol synthesis pathway, such as SREBP2. Given the importance of oxygen for cholesterol synthesis and our incomplete understanding of how oxygen may regulate cholesterol synthesis and associated ERAD pathways, this is the avenue I continued to study.

Chapter 4: The relationship between hypoxia and HMG-CoA Reductase

4.1. Introduction

The cholesterol biosynthetic pathway in mammalian cells is highly oxygen dependent with 11 molecules of oxygen required for the generation of one molecule of cholesterol. In less diverse organisms such as fission yeast, cholesterol synthesis and oxygen sensing pathways remain connected with stimulation of either pathway activating the transcription of the same target genes (Hughes *et al.*, 2005). The connection between these pathways throughout evolution highlights the importance of studying them together to understand their significance for cell survival.

In mammalian cells, to control the cellular availability of cholesterol, HMG-CoA reductase (HMGCR), the therapeutic target of statins and a rate-limiting enzyme of this pathway, is highly regulated at both the transcriptional level by SREBP2, and post translationally by ERAD (Goldstein *et al.*, 2006; Menzies *et al.*, 2018). Prior studies have proposed some regulatory links between the oxygen sensing and cholesterol synthesis pathways in mammalian cells, relating HIF1α transcription and lanosterol accumulation under low oxygen tensions, with increased HGMCR degradation (Hwang *et al.*, 2017; Nguyen *et al.*, 2007).

In this chapter I use a dynamic endogenous knock-in reporter construct, HMGCR_clover **(Figure 4.1)** (Menzies *et al.*, 2018), to further study the effects of varying oxygen tensions upon HMGCR regulation. In accordance with previous studies, I corroborate a modest role for HIF1α mediated transcription inducing HMGCR degradation under conditions of hypoxia, but also uncover that hypoxia has an additional effect on HMGCR regulation that is independent of HIFs.

4.2. Results

4.2.1. HMG-CoA reductase levels are reduced under sterol deplete condition in hypoxia

The HeLa HMGCR_clover cell line created by Sam Menzies (Lehner laboratory) **(Figure 4.1)** has been effective in studying HMGCR regulation and has uncovered new genes involved in HMGCR degradation under sterol rich conditions (Menzies *et al*., 2018). Due to the links described between the sterol synthesis pathway and oxygen availability, we decided to explore the relationship further using the HeLa HMGCR_clover cell line.

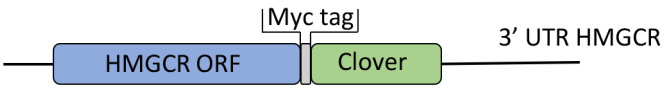

Figure 4.1. Schematic of the HMG CoA-Reductase (HMGCR)_clover knock-in construct used, with clover at the C-terminus of HMGCR.

Figure 4.1 (page 93) has been adapted from Menzies et al., 2018 which is licenced under CC CY 4.0. ELife. The sterol-responsive RNF145 E3 ubiquitin ligase mediates the degradation of HMG-CoA reductase together with gp78 and hrd1. Menzies. S. A., Volkmar. N., van den Boomen. D. J. H.,Timms. R. T., Dickson. A. S., Nathan. J. A., Lehner. P. J. © (2018).

As previously shown by Menzies *et al*., (2018), HeLa HMGCR_clover cells respond dynamically to 24 hours of sterol depletion resulting in a large accumulation of HMGCR_clover **(Figure 4.2 A (i))**. This accumulation is due to the increased transcription, and decreased proteasomal degradation of HMGCR. To fully stabilise HMGCR a combination of 10% lipoprotein deficient serum (LPDS) and treatment with a statin (10 μM Mevastatin) is required, thereby preventing any *de novo* cholesterol synthesis and any cholesterol uptake from the media.

Previous studies have shown that stabilising HIF1α increases the proteasomal degradation of HMGCR under sterol deplete conditions, due to the transcriptional upregulation of INSIG2 (Hwang *et al*., 2017). In accordance with this data, incubating HeLa HMGCR_clover cells with PHD inhibitors, DMOG or Roxadustat, combined with sterol depletion showed a modest decrease in HMGCR_clover levels when compared to sterol depletion in 21% oxygen

(Figure 4.2 A (ii), (iii)). Interestingly, following co-incubation with sterol depletion and hypoxia (1% oxygen), HMGCR_clover levels were further reduced in comparison to levels achieved with the PHD inhibitors **(Figure 4.2 A (iv))**. This effect was also observed with endogenous HMGCR in HeLa WT **(Figure 4.2 B, F)**, HepG2 **(Figure 4.2.C)** and HEK293ET **(Figure 4.2 D)** cells. The striking difference between the levels of HMGCR following sterol depletion with PHD inhibition or hypoxia (1% oxygen) suggested that low oxygen tensions had an additional effect upon HMGCR regulation that is independent of HIF stabilisation.

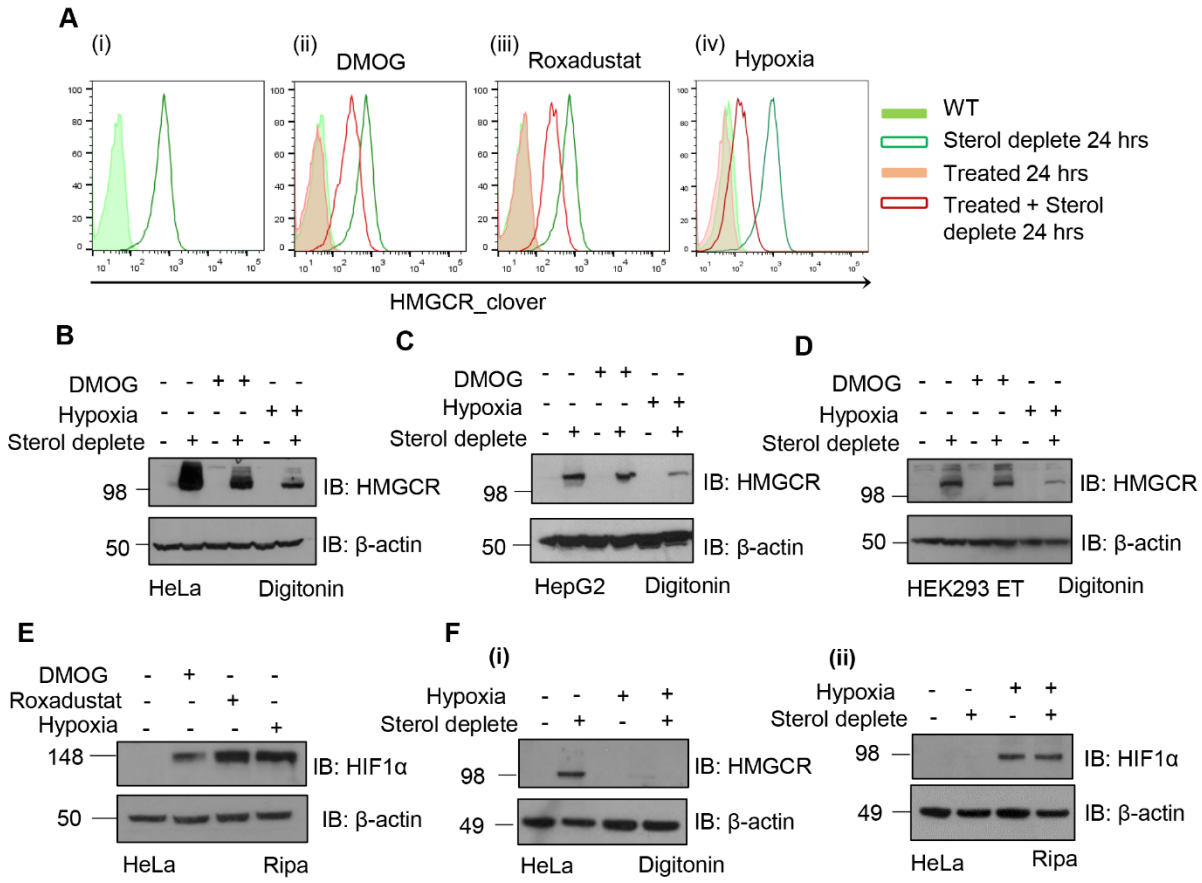

Figure 4.2. HMGCR levels are reduced under sterol deplete conditions in hypoxia.

HeLa HMGCR_clover **(A)**, HeLa WT **(B)**, HepG2 **(C)** or HEK293ET **(D)** cells were placed under sterol deplete conditions (DMEM supplemented with 10% lipid depleted FCS and 10 µM mevastatin) for 24 hours either in 21% oxygen, hypoxia (1% oxygen) or in combination with 1 mM DMOG or 100 µM Roxadustat. Cells were then subjected to live flow cytometry **(A)** or lysis in 1% digitonin buffer **(B-D)** and immunoblotted to assess for cellular HMGCR levels. **(E)** HeLa WT cells were treated for 24 hours with either hypoxia (1% oxygen), 1 mM DMOG or 100 µM Roxadustat, lysed in RIPA buffer and immunoblotted to assess for cellular levels of HIF1α. **(F)** HeLa WT cells were placed under sterol deplete conditions for 24 hours either in 21% oxygen or hypoxia (1% oxygen), lysed in 1% digitonin **(i)** or RIPA **(ii)** buffer and immunoblotted.

Unfortunately, it proved very challenging to effectively immunoblot both HMGCR and HIF1α using the same cell lysis conditions due to the different cellular localisation and membrane interactions of these two proteins. As HIF1α is not membrane bound and is typically located in the nucleus when active, a detergent that effectively solubilises the nuclear membrane needed to be used. Therefore, I used an SDS buffer at either 1% or 0.1% for HIF1α, and used a 1% digitonin buffer to blot for HMGCR. Digitonin is a weaker non-denaturing and non-ionic buffer so is able to keep large multi-pass transmembrane proteins intact during lysis and produced clean bands following immunoblotting for HMGCR, but HIF1α was unable to be visualised using these conditions as digitonin does not permeabilise the nuclear membrane.

PHD inhibition through DMOG or Roxadustat treatment stabilised HIF1α to a higher level than hypoxia (1% oxygen), suggesting that the lower level of HMGCR observed under conditions of sterol depletion with hypoxia was not due to increased HIF1α causing increased degradation **(Figure 4.2 E)**. Additionally, simultaneous lysis conditions and immunoblots were carried out to confirm that treatment with sterol depletion did not increase HIF1α stabilisation under hypoxia in HeLa cells **(Figure 4.2 F)**.

As levels of HMGCR are tightly regulated by ERAD and through transcription by the transcription factor SREBP2, I wanted to try and study these pathways as separately as possible, with an initial focus on degradation. To study the degradation dynamics of HMGCR I used a similar workflow described in Menzies *et al*., (2018), whereby HMGCR_clover cells were sterol depleted overnight, then sterols re-introduced for a few hours the next day to promote HMGCR degradation. However, the reduction of HMGCR levels under conditions of hypoxia (1% oxygen) occurred over 18 hours, so the workflow needed to be modified. I firstly assessed whether incubating HeLa HMGCR_clover cells with sterol depletion prior to hypoxia (1% oxygen) produced the same phenotype as simultaneous sterol depletion and hypoxia (1% oxygen) treatment. **Figure 4.3** shows that these two workflows, termed ‘same time’ and ‘pre-sterol deplete’ produced the same end phenotype by flow cytometry, both resulting in lower HMGCR_clover levels when compared to sterol depletion alone.

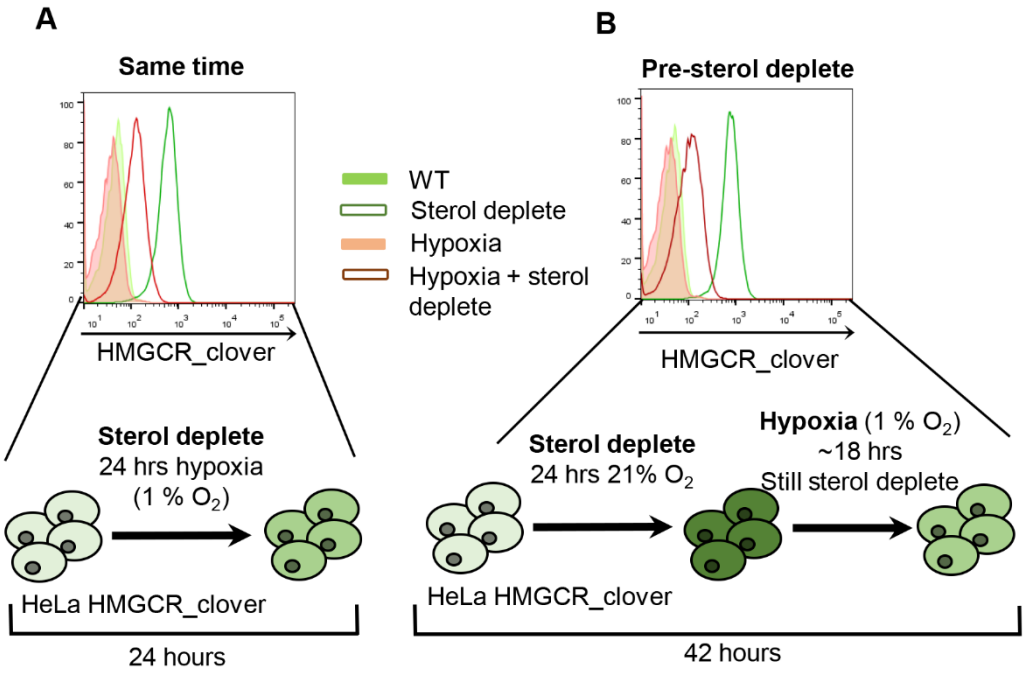

Figure 4.3. Pre-incubating cells with sterol depletion prior to hypoxia produces the same phenotype as simultaneous incubation.

HeLa HMGCR_clover cells were either placed under sterol deplete conditions (DMEM supplemented with 10% lipid depleted FCS and 10 µM mevastatin) for 24 hours either in 21% O_2 or hypoxia (1% O_2) **(A)**, or placed under sterol deplete conditions for 42 hours, and where appropriate cells were subjected to hypoxia (1% O_2) for the final 18 hours **(B)**, before being analysed by live flow cytometry.

Following the first set of experiments which were carried out using the 'same time' workflow **(Figure 4.3 A)**, I decided to continue my experimental work using the 'pre-sterol deplete' workflow **(Figure 4.3 B)**, as this workflow enabled me to study the dynamics of HMGCR degradation following its accumulation. I could also genetically manipulate the cells to see which genes were required for this process.

4.2.2. The reduction of HMG-CoA reductase levels under sterol deplete conditions in hypoxia occurs independently of HIF1α mediated transcription

The reduction of HMGCR observed under sterol deplete condition in hypoxia was far greater than following the chemical stabilisation of HIF1α through PHD inhibition **(Figure 4.2 A)**. This suggested that a HIF1α independent mechanism for lowering HMGCR levels may be occurring in hypoxia (1% oxygen). To investigate this further, HMGCR_clover cells expressing Cas9 were transduced with a HIF1β sgRNA. Following selection, the cells were subjected to either sterol depletion alone, sterol depletion and DMOG, or sterol depletion and hypoxia. In a mixed population of HMGCR_clover Cas9 HIF1β KOs, sterol depletion with hypoxia still produced a dramatic reduction in HMGCR_clover levels comparable to that observed in WT cells **(Figure 4.4 A, red lines)**. To confirm this effect was not due to any residual HIF1β present in these cells, I created a clonal population of the HMGCR_clover Cas9 HIF1β KOs. The levels of HMGCR_clover following sterol depletion and hypoxia in the HIF1β KO clonal population were comparable to the WT **(Figure 4.4 B)**, consistent with the hypoxic decrease in HMGCR levels being HIF independent. DMOG treatment had no effect on HMGCR_clover levels in the HIF1β KO population when compared to sterol depletion alone, whilst a modest decrease in HMGCR_clover levels was observed following DMOG treatment in HMGCR_clover WT cells **(Figure 4.4 A, blue lines)**.

Efficient depletion of HIF1β was confirmed using cell surface staining of the HIF1α target gene carbonic anhydrase 9 (CAIX) (Wykoff *et al.*, 2000). Whilst WT cells have high cell surface levels of CAIX following stabilisation of HIF1α **(Figure 4.4 C first panel)**, the HIF1β KO mixed population only had a small amount of CAIX stabilisation **(Figure 4.4 C middle panel)**, and the HIF1β KO clonal population had no noticeable CAIX stabilisation **(Figure 4.4 C third panel)**. These results confirmed effective depletion of HIF1α mediated transcription in HIF1β KO cells, and supported the hypothesis that hypoxia (1% oxygen) is having an additional HIF1α independent effect on HMGCR levels under sterol deplete conditions.

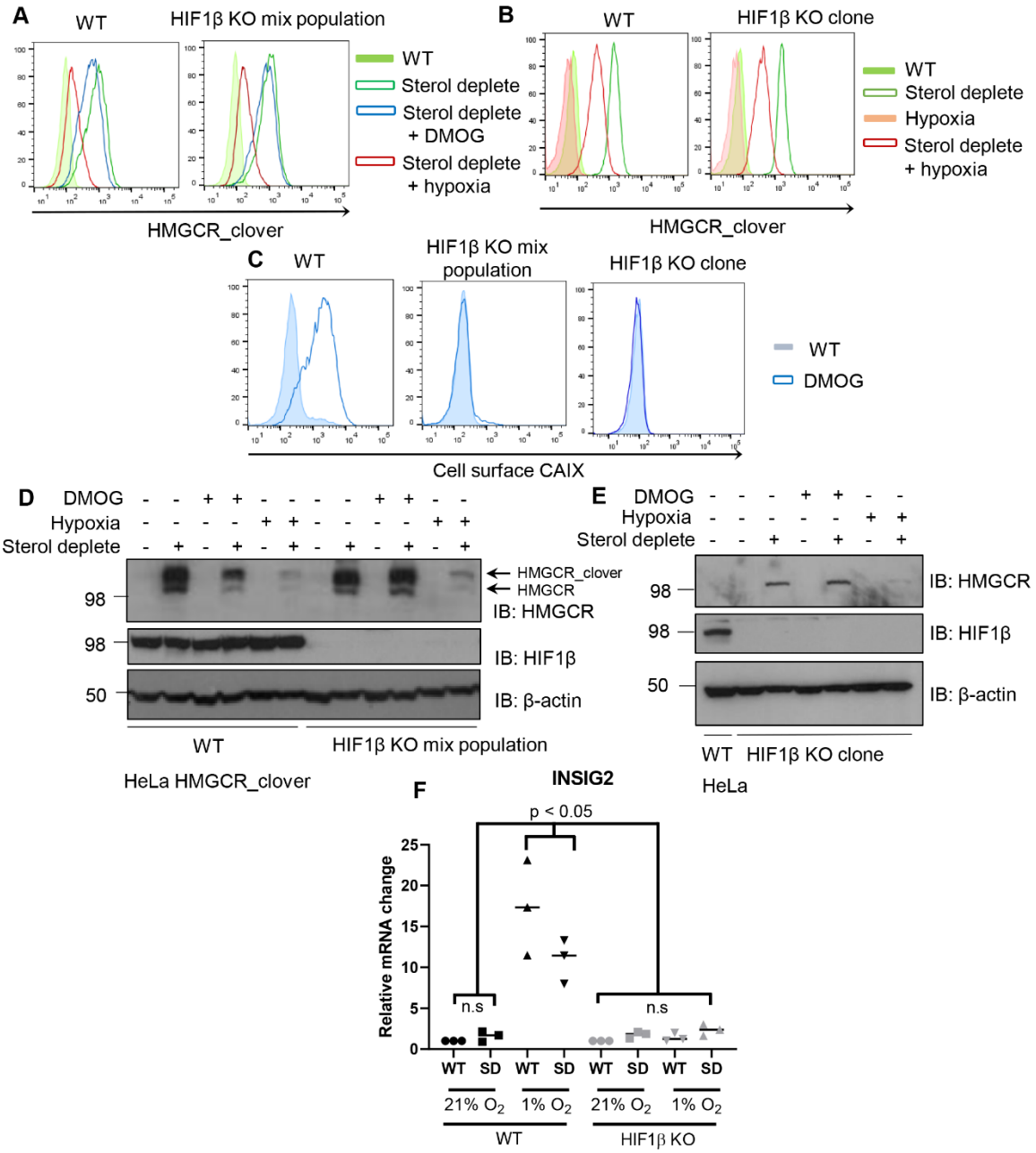

Figure 4.4. The reduction of HMGCR under sterol deplete condition in hypoxia is independent of HIF1β mediated transcription.

HeLa HMGCR_clover WT and mixed population of HIF1β KOs **(A, D)** or a clonal population of HMGCR_clover HIF1β null **(B)** were placed under sterol deplete conditions for 42 hours, and where appropriate cells were subjected to hypoxia (1% O_2) or 1 mM DMOG for the final 18 hours before being analysed by live flow cytometry **(A, B)** or lysed in 1% digitonin buffer and immunoblotted **(D)**. **(C)** HeLa HMGCR_clover WT and mixed or clonal populations of HIF1β knock-outs were treated with 1 mM DMOG for 18 hours before being stained for cell surface CAIX and analysed by flow cytometry. **(E, F)** HeLa WT or HIF1β KO clone were placed under sterol deplete conditions for 42 hours, and where appropriate cells were subjected to hypoxia (1% O_2) or 1 mM DMOG for the final 18 hours before being lysed in 1% digitonin buffer and immunoblotted **(E)** or analysed by RT-qPCR **(F)**.

To confirm the flow cytometry findings the levels of HMGCR were also measured by immunoblot in both HeLa HMGCR_clover **(Figure 4.4 D)** and HeLa WT cells **(Figure 4.4 E)**. Hela HMGCR_clover cells encode at least one allele of HMGCR that is not tagged with clover (Menzies *et al*., 2018), so visualisation of both the clover tagged and endogenous HMGCR is possible by western blot. In accordance with the flow cytometry data **(Figure 4.4 B)**, the same effect was observed, with a marked reduction of HMGCR in both the HIF1β depleted and WT cells following incubation with sterol depletion and hypoxia (1% oxygen) **(Figure 4.4 D, E)**. DMOG treatment partially reduced HMGCR levels in WT cells, but had no effect on HMGCR levels in the HIF1β null cells **(Figure 4.4 D)**, demonstrating that HIF1α activation was not responsible for the large decrease in HMGCR in hypoxia.

Hwang *et al*., (2017) showed that HIF1α stabilisation by DMOG treatment activated the transcription of INSIG2. Following increased expression, INSIG2 accumulates in the ER membrane and increases the likelihood of interaction between HMGCR and its E3 ligase machinery, therefore causing increased degradation under sterol deplete conditions in hypoxia. I therefore examined if INSIG2 levels were transcriptionally upregulated in WT and clonal HIF1β KO HeLa cells. **Figure 4.4 F** shows that INSIG2 was transcribed in a HIF1α dependent manner, with transcript levels significantly increasing in hypoxia (1% oxygen), and transcription being blocked in HIF1β KO cells. Therefore, INSIG2 was not responsible for the reduction of HMGCR observed in the HIF1β KO cells. Additionally, INSIG2 levels were not increased by sterol depletion. These finding supports my previous data indicating that there is a HIF1α and INSIG2 independent mechanism occurring in hypoxia under sterol deplete conditions resulting in lower levels of HMGCR.

Although I had shown that the HIF1β KO cells did not mount a transcription response mediated through HIF1α using two different target genes (CAIX and INSIG2), I wanted to confirm that the effect was independent of the both HIF1α and HIF2α mediated transcription. Therefore, I used cell lines expressing a HIF fluorescent reporter (HeLa HIF1α GFP^{ODD}), which were clonally depleted of both HIF1α and HIF2α (which were previously created in the Nathan laboratory by Stephen Burr and Peter Bailey). Following sterol depletion with hypoxia both the HeLa HIF1α GFP^{ODD} WT (Burr *et al*., 2016) and HeLa GFP^{ODD} HIF1/2α null clones showed reduced levels of HMGCR **(Figure 4.5)**, confirming the reduction of HMGCR observed under sterol depletion in hypoxia is independent of any HIF1α or HIF2α mediated transcription.

Together these results show that hypoxia (1% oxygen) has an additional effect on HMGCR levels that is independent of the previously reported HIF1α mediated transcriptional regulation of INSIG2 (Hwang *et al.*, 2017).

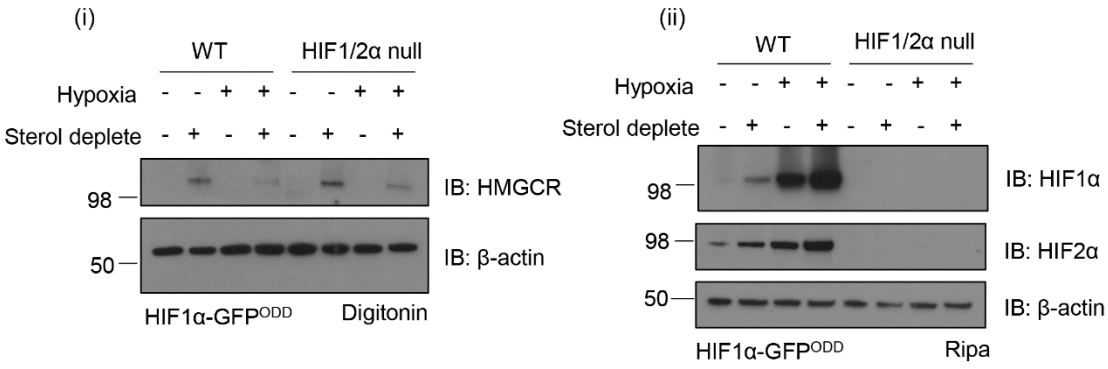

Figure 4.5. The reduction of HMGCR under sterol deplete condition in hypoxia is independent of HIF1 or 2 mediated transcription.

HeLa HIF1α-GFP^{ODD} WT (Burr *et al*, 2016) or HIF1α/2α null cells were placed under sterol deplete conditions for 42 hours, and where appropriate cells were subjected to hypoxia (1% oxygen) for the final 18 hours before being lysed in either 1% digitonin **(i)** or RIPA **(ii)** buffer and analysed by immunoblotting.

4.2.3. HMGCR is being degraded under sterol deplete conditions in hypoxia

One way in which HMGCR is tightly regulated is through ubiquitination and ERAD. The Lehner laboratory have recently shown that under 21% oxygen the E3 ligases RNF145, gp78 and Hrd1, and the E2 enzyme UBE2G2 are the predominant enzymes involved in HMGCR degradation under sterol replete conditions (Menzies *et al.*, 2018). This is due to increased interaction between HMGCR with the INSIG proteins when sterol are present **(Figure 1.4)**. As I have observed a decrease in HMGCR levels under sterol deplete conditions in hypoxia (1% oxygen), I wanted to assess whether HMGCR was being proteasomally degraded, similarly to sterol repletion when oxygen is present. **Figure 4.6 A** shows a schematic of the experimental set up, where cells were sterol depleted for 42 hours in total, and where appropriate, treated for the final 18 hours with a proteasome inhibitor and hypoxia (1% oxygen). Proteasome inhibition rescued HMGCR levels following sterol depletion combined with hypoxia (1% oxygen)

(Figure 4.6 B), suggesting that HMGCR was being degraded under sterol deplete conditions in hypoxia (1% oxygen). Consistent with our previous results suggesting there is a HIF independent effect, the rescue of HMGCR with the addition of a proteasome inhibitor also occurred in the absence of HIF1β **(Figure 4.6 C)**. These results suggested that hypoxia promoted HMGCR degradation under sterol deplete conditions, overriding the normal sterol sensing response leading to HMGCR stabilisation.

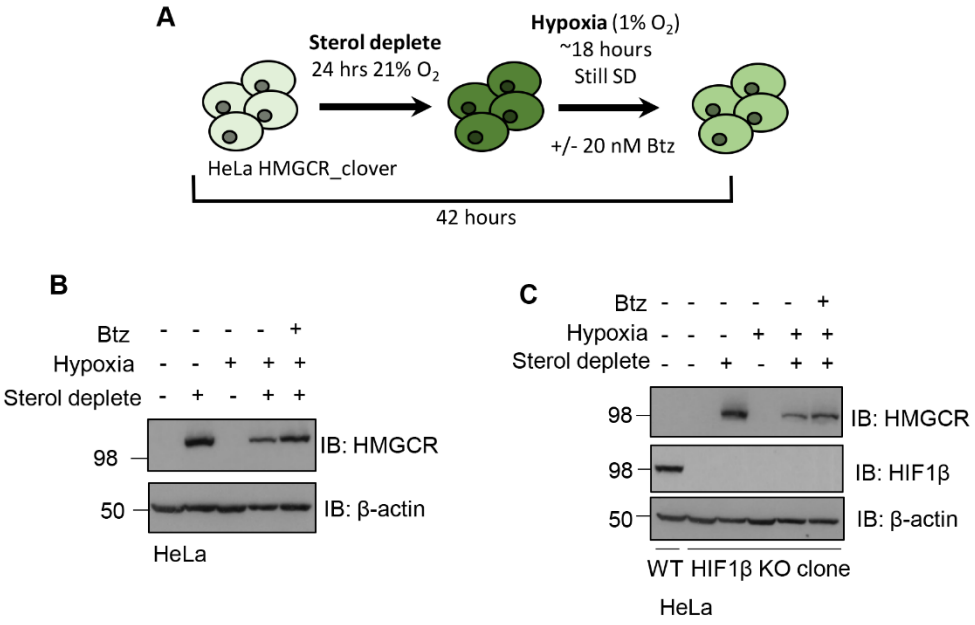

Figure 4.6. HMGCR is being degraded in hypoxia under sterol deplete conditions.

(A) Schematic of the experimental set up looking at degradation of HMGCR in hypoxia (1% O_2). **(B, C)** HeLa WT and clonal HIF1β KO cells were placed under sterol deplete conditions for 42 hours, and where appropriate cells were subjected to hypoxia (1% O_2) for the final 18 hours with the addition of 20 nM Bortezomib as the cells were placed in hypoxia.

4.3. Discussion

4.3.1. The hypoxic response and HMGCR regulation

My data suggests that low oxygen tensions have an additional effect on HMGCR regulation beyond that of HIF1α mediated transcription. The reduction of HMGCR under sterol deplete conditions and hypoxia (1% oxygen) in HIF1β **(Figure 4.4)** or combined HIF1α, and HIF2α **(Figure 4.5)** deficient cells is comparable to that in HeLa WT cells. These findings suggest that the HIF1α mediated induction of INSIG2 alone is not responsible for the decrease in HMGCR protein levels, as previously reported by Hwang *et al*., (2017). In their studies Hwang and colleagues focused on HIF1α mediated effects on HMGCR regulation, predominantly using DMOG to stimulate an effect. They did not focus on low oxygen tensions in their studies and therefore would not have observed any HIF1α independent effects on HMGCR regulation. My data confirms that HIF1α stabilisation through PHD inhibition does increase INSIG2 mRNA levels, and does modestly reduce HMGCR levels under sterol deplete conditions; however, there is an additional role for low oxygen tensions further reducing HMGCR levels in a HIF independent manner **(Figure 4.2 A-D)**.

Activation of the HIFs is a very well described response to hypoxia, and although this pathway promotes the transcription of a myriad of genes involved in cell survival under conditions of low oxygen, it is not the only cellular response to low oxygen tensions.

The *de novo* cholesterol synthesis pathway is highly oxygen dependent, requiring 11 molecules of oxygen to create one molecule of cholesterol **(Figure 1.3)** (reviewed in DeBose-Boyd, 2008). Therefore limiting oxygen tensions could potentially affect cholesterol synthesis at oxygen consuming steps. How much this pathway or other pathways and reactions which require oxygen are affected at different oxygen concentrations is currently unknown, but it is likely that with reducing oxygen concentrations their activities will decrease, and will be fully prevented when no oxygen is present. The part of the cholesterol synthesis pathway which requires the most oxygen is the series of reactions converting lanosterol to cholesterol as it requires ten oxygen molecules (Summons *et al*., 2006) **(Figure 1.3)**. Lanosterol has been shown to accumulate in cells under conditions of low oxygen, probably due to the

requirement of oxygen to convert lanosterol to cholesterol. This accumulation has been reported to accelerate HMGCR degradation with lanosterol shown to interact with the SSD of HMGCR and initiate the interaction with the degradation machinery for HMGCR (Nguyen *et al*., 2007). Lanosterol is downstream of HMGCR in the cholesterol synthesis pathway, and therefore the hypoxic effect of lanosterol accumulation on HMGCR degradation can be inhibited with statin treatment (Nguyen *et al*., 2007). My studies exclude a role of lanosterol accumulation as I combined sterol depletion using lipid depleted FCS with statin treatment. Therefore the regulation of HMGCR in hypoxia occurs upstream or at the level of HMGCR degradation.

4.3.2. The role of 2-oxoglutarate dependent dioxygenases

An alternative explanation for my findings relates to the role of other oxygen sensitive enzymes outside the canonical HIF response in the cholesterol synthesis pathway. PHDs form the oxygen sensing component of the HIF pathway, but they also form part of a larger family of oxygen sensing enzymes, termed 2-oxoglutarate dependent dioxygenases (2-OGDD, α-ketoglutarate dependent dioxygenases) which have diverse roles in the cell (Schofield & Ratcliffe, 2004). One family of human 2-OGDDs are of particular interest to sterol synthesis, as their orthologue in fission yeast is required for oxygen sensing (Hughes & Espenshade, 2008).

In fission yeast, a 2-OGDD family member, Ofd1, regulates the stability of the transcription factor Sre1, the orthologue of SREBP (Hughes & Espenshade, 2008; Lee *et al*., 2009; Lee *et al*., 2011). Like SREBP2, Sre1 is stabilised and activated following sterol depletion, but is also activated under conditions of hypoxia, and activates genes required for adaptation in both conditions (Hughes *et al*., 2005). There are three mammalian orthologues of Ofd1, OGFOD1-3, however, as yet no link with the cholesterol synthesis or oxygen sensing pathways have been described. It is therefore possible that the OGFOD family was responsible for modulating the oxygen sensitivity of HMGCR levels in HeLa cells. However, all 2-OGDDs require iron and 2-oxyglutarate (2-OG) for their catalytic activity and can be inhibited by DMOG, a cell permeable competitive inhibitor (Jaakkola *et al*., 2001), or by limiting the availability of

extracellular iron (Schofield & Ratcliffe, 2004). In my experiments, DMOG and Roxadustat (FG-5495), a PHD selective inhibitor (Maxwell & Eckardt, 2016), treatment had the same effect on HMGCR levels under sterol deplete conditions in hypoxia **(Figure 4.2 A)**, suggesting that DMOG is not inhibiting any other 2-OGDDs beyond that of the PHDs that is causing a reduction in HMGCR levels. Additionally I have carried out some preliminary experiments looking at iron chelation and my data shows that following sterol depletion and iron chelation, levels of HMGCR are comparable to that following DMOG and Roxadustat treatment.

These data do not exclude a role for other 2-OGDDs in regulating HMGCR levels, but do suggest that a DMOG sensitive 2-OGDD was not solely responsible for the reduced levels of HMGCR observed under sterol deplete conditions in hypoxia. Therefore, due to the involvement of 2-OGDDs in fission yeast, I decided that an unbiased way to study this further, would be to carry out a genome wide forward genetic screen which should reveal any genes involved in the hypoxia regulation of HMGCR, including any 2-OGDDs **(see Chapter 5)**.

4.3.3. Why is degradation occurring under sterol deplete conditions in hypoxia?

Normally, under sterol deplete conditions HMGCR is stabilised through increased transcription and decreased degradation, in an attempt to restore the cells cholesterol levels. However, under sterol deplete conditions in hypoxia, my data shows that levels of HMGCR are reduced, and that this reduction is almost fully rescued with proteasome inhibition **(Figure 4.6 B)**.

There were two likely possibilities for these observations. Firstly, under conditions of hypoxia the degradation machinery for HMGCR could be altered or activated. Secondly, as the reduction in HMGCR levels occurs over 18 hours, it is possible that HMGCR transcription or translation is reduced, and proteasome inhibition may be preventing the steady state turnover of HMGCR. HMGCR degradation still occurs under sterol deplete conditions, albeit slowly, with the half-life reported to increase from under 2 hours (in sterol rich conditions) to over 10 hours following sterol depletion (Brown *et al*., 1973; Gil *et al*., 1985; Goldstein & Brown, 1990). Therefore, to uncover the explanation for the degradation observed, I wanted to explore any changes in steady state degradation and assess what happens to the degradation machinery for HMGCR under conditions of hypoxia.

4.4. Summary

Prior studies have shown that stabilisation of HIF1α through PHD inhibition or lanosterol accumulation in low oxygen conditions, causes HMGCR to be degraded under sterol deplete conditions. By utilising a dynamic endogenous knock-in reporter construct, HMGCR_clover, in HeLa cells I have uncovered an additional role for hypoxia which causes a greater reduction in HMGCR levels compared to PHD inhibition alone, and is regulating HMGCR levels independent of HIF1α or lanosterol accumulation.

My data also shows that degradation is still active under conditions of sterol depletion in hypoxia, and prior reports from fission yeast suggest that 2-OGDDs outside of the HIF pathway may play a role in the hypoxic regulation of cholesterol synthesis. Therefore, to uncover the mechanisms involved I proposed two strategies: (i) an unbiased CRISPR/Cas9 forward genetic screen in HeLa HMGCR_clover cells to search for any genes responsible for the hypoxic degradation of the reporter, and (ii) biochemical studies to determine whether HMGCR is regulated at a transcriptional, translational or post-translational level in hypoxia.

Chapter 5: HMG CoA-Reductase regulation under sterol deplete conditions in hypoxia

5.1. Introduction

In sterol deplete conditions HMGCR is typically increased due to decreased proteasomal degradation and increased transcription through SREBP2 **(Figure 1.4)**. My data suggests that hypoxia is able to override sterol depletion, causing HMGCR levels to be reduced in conditions of 1% oxygen combined with sterol depletion **(Figure 4.2)**. How this occurs is currently unclear, but my previous data has shown that the effect is independent of HIF1α mediated transcription **(Figure 4.4)**.

It was possible that low oxygen conditions was causing the activation or change of function of a protein within the cell, possibly a 2-OGDD or additional degradation machinery, that was leading to the reduction of HMGCR observed under these conditions. Therefore, I decided to assess this in an unbiased way.

In this chapter I use a CRISPR/Cas9 forward genetic screen in HeLa HMGCR_clover cells under sterol deplete conditions in hypoxia to try and uncover any new genes involved in HMGCR regulation. The screen identified components of the degradation machinery for HMGCR, which I have shown to be the same as the ubiquitin enzymes involved when oxygen was not limiting. However, the screen did not robustly reveal any new genes involved in HMGCR regulation. In this chapter I also begin to look at the transcriptional regulation of HMGCR under hypoxia and observe that the transcription of some SREBP2 target genes are reduced under sterol deplete conditions in 1% oxygen. I show that these effects are independent of ER stress or activation of the mammalian target of rapamycin (mTOR) pathway, suggesting that SREBP2 itself may be regulated in an oxygen dependent manner.

5.2. Results

5.2.1. CRISPR/Cas9 forward genetic screen to identify new genes involved in regulating HMG CoA-Reductase in conditions of sterol depletion in low oxygen tensions

To try and uncover new genes involved in regulating HMGCR under sterol deplete conditions in 1% oxygen, I decided to utilise a genome wide CRISPR/Cas9 forward genetic screen in HeLa HMGCR_clover cells. For this screen I used the well validated Bassik genome wide CRISPR knockout library which targets 20,500 genes and contains approximately 220,000 unique sgRNAs (Morgens *et al*., 2017). The Bassik library was chosen over the Brunello library which I used in **Chapter 3**, as this newer library has 10 unique sgRNAs per gene instead of 4, increasing the likelihood of an effective knockout.

The screen is depicted in **Figure 5.1 A**. HeLa HMGCR_clover cells expressing Cas9 were transduced with the Bassik library at an MOI of ~30% and selected with puromycin. The cells were subjected to two sequential FACS sorting steps. Seven days post transduction the cells were sterol depleted for 42 hours, with the cells being incubated in hypoxia for the final 18 hours. The cells were then sorted by FACS with 0.93% of the cells collected as clover^{HIGH} and cultured appropriately. Seven days later, these cells were subjected to the same treatment before being sorted by FACS again with the collected cells split into two populations; clover^{MEDIUM} (5.07%) and clover^{HIGH} (0.1%) **(Figure 5.1 A)**. **Figure 5.1 B** shows the Illumina sequencing results comparing sort 2 clover^{MEDIUM} with the unsorted library following sequencing on the Illumina MiniSeq **(Figure 5.1 B (i))** or HiSeq **(Figure 5.1 B (ii))** platforms. Genes enriched that have previously been associated with HMGCR degradation are highlighted in red and genes which have not been previously implicated in HMGCR regulation are highlighted in purple. The screen identified the E2 conjugating enzyme UBE2G2 and its accessory factor AUP1, which have been shown to be required for the degradation of HMGCR (Menzies et al., 2018), and the UBX domain containing protein FAF2 (UBXD8), which has been

implicated in the extraction of HMGCR from the ER membrane prior to proteasomal degradation, through its recruitment of VCP/p97 via its UBX domain (Loregger *et al.*, 2017).

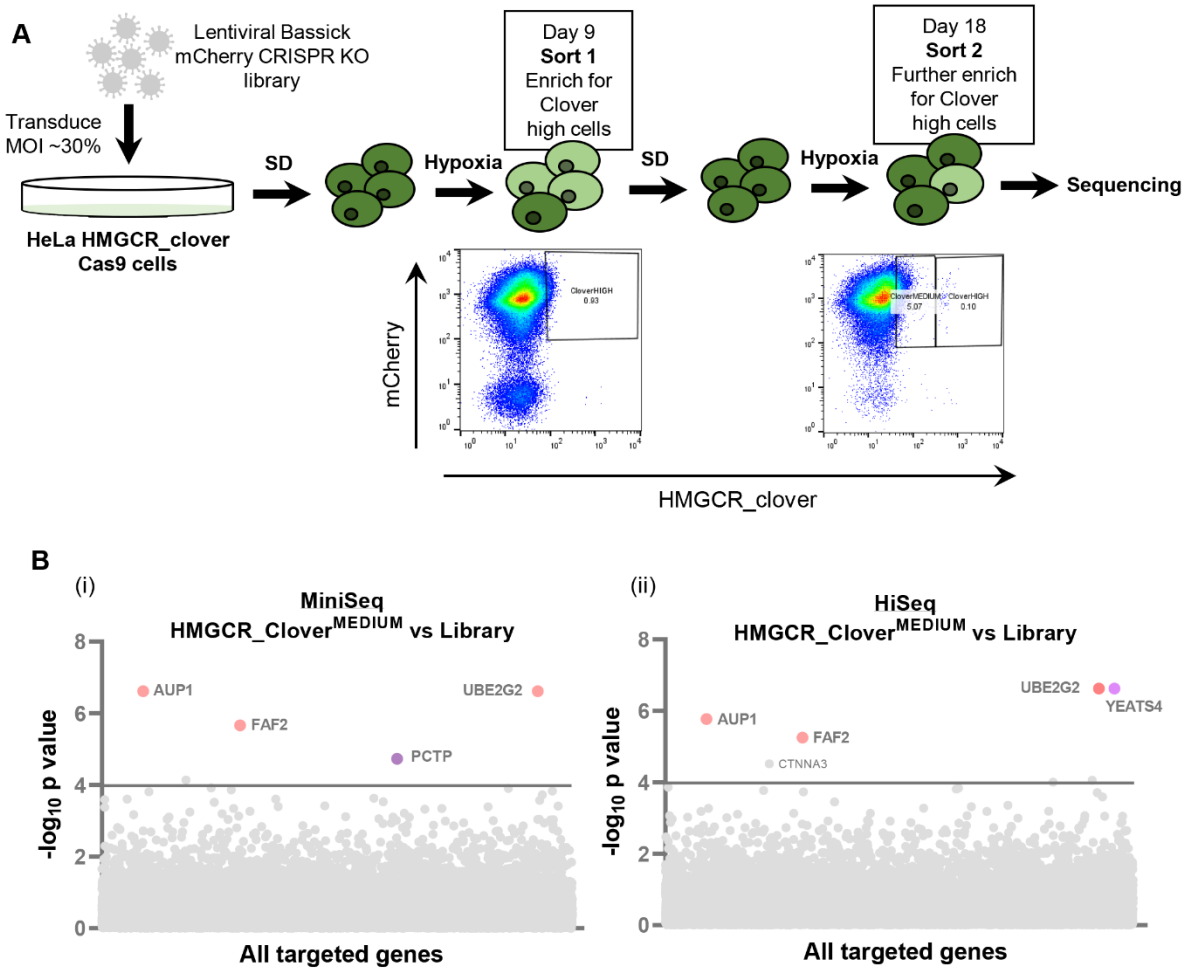

Figure 5.1. Designing a CRISPR/Cas9 forward genetic screen to search for novel regulators of HMGCR under sterol deplete conditions in hypoxia.

(A) Schematic of the genome wide CRISPR screen carried out in HeLa HMGCR_clover cells using the Bassik mCherry CRISPR knockout library. Seven days post transduction the cells were sterol depleted (SD) for 42 hours, and incubated in hypoxia (1% O_2) for the final 18 hours. The cells were then sorted by FACS with 0.93% of the cells collected as clover^{HIGH} and cultured as appropriate. Seven days later, the cells were subjected to the same treatment before being sorted by FACS again, with the collected cells split into two populations; clover^{MEDIUM} (5.07%) and clover^{HIGH} (0.1%). DNA was extracted from these cells and sequenced using Illumina sequencing. **(B)** Bubble plots showing all the genes identified in the sort 2 clover^{MEDIUM} population compared to unsorted library (significance threshold > -log(p)4), from the MiniSeq **(i)** and HiSeq **(ii)** analysis. Red bubbles indicate genes that are known to be involved in HMGCR degradation, while purple bubbles indicate genes with unknown roles in this pathway. Data was analysed using the MAGeCK algorithm.

I chose to focus my attention on the mCherry^{MEDIUM} population rather than the mCherry^{HIGH} population, as the hits in the mCherry^{HIGH} analysis appeared less relevant to HMGCR regulation. Although UBE2G2 was identified in the mCherry^{HIGH} analysis, AUP1 and FAF2 were not, and other hits included genes involved in general transcriptional regulation such as a histone protein and a zinc finger protein **(see Appendix)**, which may be upregulating HMGCR_clover none specifically. However, it was reassuring to see that most of the top hits in the mCherry^{MEDIUM} population were consistent between sequencing using the two Illumima platforms, with the only exceptions being Phosphatidylcholine Transfer Protein (PCPT) and YEATS (Yaf9, ENL, AF9, Taf14, Sas5) 4 which were only amongst the top hits in the MiniSeq and HiSeq analysis, respectively **(Figure 5.1 B)**. These proteins had not previously been implicated in the cholesterol synthesis pathway or HMGCR regulation. CTNNA3 (Catenin alpha 3) was identified as a borderline hit in the HiSeq analysis just above the cut of level for significance. This was very likely to be an unrelated protein as it is involved in cell-cell adhesion in muscle cells and defects are involved in cardiomyopathy (Chiarella *et al*., 2018). As it had no apparent link to the cholesterol synthesis pathway, I chose not to look into this protein further.

PCTP (StARD2) is a lipid binding protein which catalyses the transfer of lipids, specifically phosphatidylcholine, between membranes (Kang *et al*., 2010). YEATS4 (GAS41) is a relatively unstudied protein but the YEATS domain is conserved throughout yeast and eukaryotes and seems to be involved in chromatin remodelling (Schulze *et al*., 2009). YEATS4 has been identified as a histone acetylation reader with links to non-small cell lung carcinomas (Hsu *et al*., 2018). I decided to try and validate these two proteins as potentially PCTP could be involved in some sterol movement within the membrane, and YEATS4 could be involved in altering transcriptional activity.

To validate PCPT and YEATS4 I created three sgRNAs for each, one sgRNA was taken from the Bassik library that appeared enriched in my sorted sample, and two were designed using the Broad Institute sgRNA design tool. HMGCR_clover cells were transduced with guides against PCTP, YEATS4, β2M (negative control) and UBE2G2 (positive control) and selected using puromycin for at least seven days. The cells were then subjected to sterol depletion for 42 hours, and where appropriate the cells were incubated in 1% oxygen for the final 18 hours before analysis. Unfortunately, none of the sgRNAs produced an effect that was any different to the control or negative control, suggesting that PCTP or YEATS4 depletion is not sufficient

to rescue the reduction of HMGCR levels under sterol deplete conditions in hypoxia **(Figure 5.2 A (top panels), C)**. Blue fluorescent protein (BFP) levels was monitored in the transduced cells to confirm efficient transduction **(Figure 5.2 A (lower panels))**. As expected from the screen results, depletion of UBE2G2 rescued HMGCR levels under conditions of sterol depletion and hypoxia **(Figure 5.2 C)**. To confirm that the Cas9 was functional in these cells, the cells transduced with β2M were stained for cell surface MHC-1. Indeed, following β2M transduction cells over 60% of the cells had reduced cell surface MHC-1 **(Figure 5.2 B).**

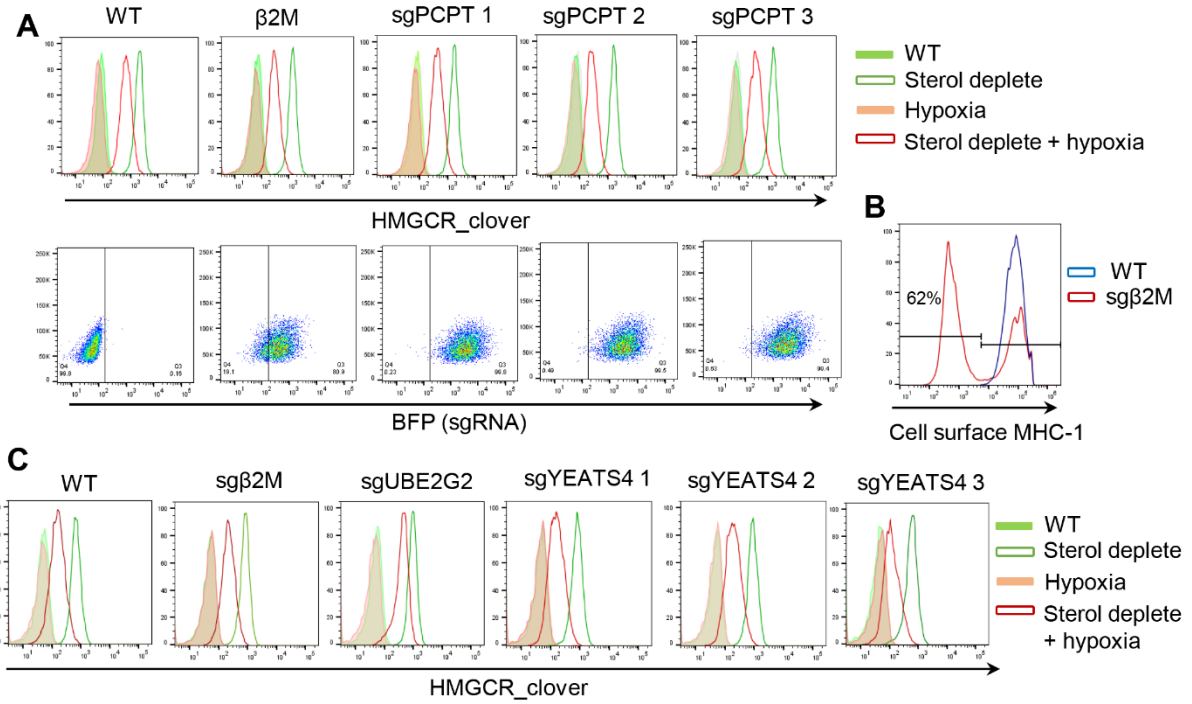

Figure 5.2. Validating the top hits from the CRISPR/Cas9 screen in HeLa HMGCR_clover cells.

(A, C) HeLa HMGCR_clover Cas9 cells were transduced with three sgRNAs (the vector includes BFP) to the two top novel hits from the screen, PCPT and YEATS4. 11 days post transduction cells were sterol depleted for 42 hours, and incubated in hypoxia (1% O_2) for the final 18 hours where appropriate before analysis by live flow cytometry. **(B)** Cells were treated with β2M sgRNA and the cell surface expression of MHC-1 assessed using flow cytometry.

5.2.2. The degradation machinery and kinetics of HMG-CoA Reductase following sterol depletion does not change with varying oxygen tensions

Known components of HMGCR degradation (UBE2G2, AUP1 and FAF2) were identified as hits in the CRISPR screen **(Figure 5.1 A)**, whilst no other degradation machinery was identified. This suggested that no new degradation machinery was involved in degrading HMGCR under sterol deplete conditions in hypoxia (1% oxygen). Menzies *et al*., (2018) showed that the three E3 ligases required for HMGCR degradation under sterol replete conditions were RNF145, gp78 and Hrd1, which all relied on the E2 enzyme UBE2G2. To assess whether this machinery was the same under low oxygen conditions, I utilised two cell lines created by Sam Menzies (Menzies *et al*., 2018); HMGCR_clover UBE2G2 null and HMGCR_clover RNF145/gp78 null. Indeed, under sterol deplete condition in 1% oxygen, the UBE2G2 null cells showed an almost complete rescue of HMGCR_clover when compared to sterol depletion in 21% oxygen. Additionally this rescue was comparable to proteasomal inhibition under these conditions, suggesting that UBE2G2 is the sufficient E2 enzyme involved in this pathway **(Figure 5.3 A (i))**. Partial rescue of HMGCR_clover was observed in the double ligase KO (RNF145/gp78) **(Figure 5.3 A (i) and (ii))**, however, once Hrd1 was additionally depleted, a complete rescue of HMGCR was observed **(Figure 5.3 A (ii))**. Protein depletions were confirmed by immunoblotting **(Figure 5.3 B)**. Overall this data suggested that that the degradation machinery required for HMCGR was unaffected by different oxygen tensions and that hypoxia did not initiate a new degradative pathway.

Interestingly, the protein levels of one of the main E3 enzymes involved in HMGCR degradation, RNF145, was reduced following incubation in hypoxia (1% oxygen), independent of sterol depletion **(Figure 5.3 C)**, while gp78 and UBE2G2 protein levels remain largely unaffected **(Figure 5.3 C)**. The reasons for this were not clear, and how RNF145 may be regulated requires further investigation.

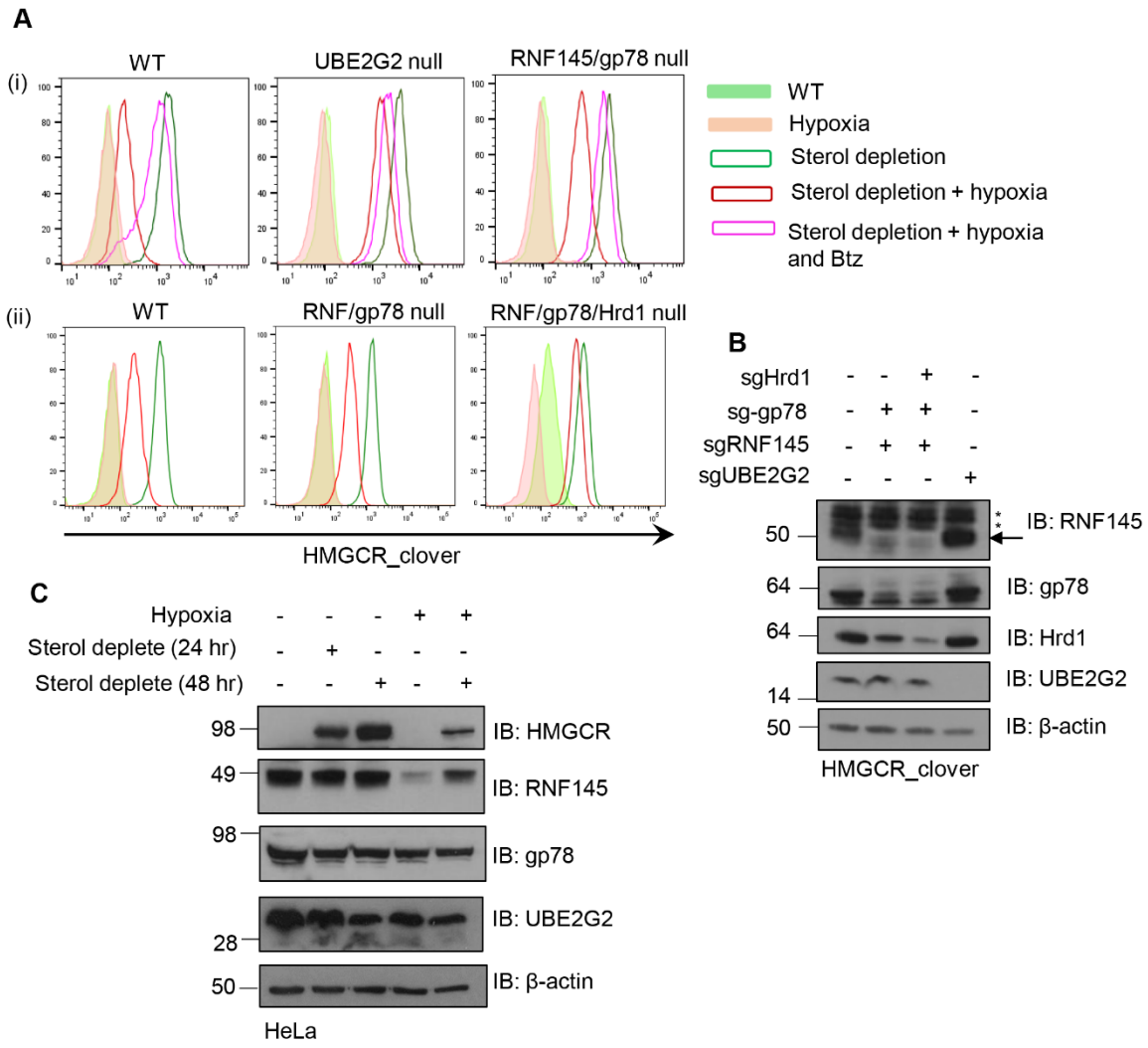

Figure 5.3. The degradation machinery for HMGCR is the same under sterol deplete conditions in 21% oxygen and hypoxia.

HeLa HMGCR_clover WT, UBE2G2 null, RNF145/gp78 null, RNF145/gp78/HRD1 null **(A, B)** or HeLa WT cells **(C)** were placed under sterol deplete conditions for 42 hours, and where appropriate cells were subjected to hypoxia (1% oxygen) for the final 18 hours with the addition of 20nM Bortezomib as the cells were placed in hypoxia, before being analysed by live flow cytometry **(A)** or being lysed in 1% digitonin buffer and immunoblotted **(B, C)**.

* represents non-specific bands observed when using the RNF145 antibody for immunoblotting in HeLa cells.

As the majority of required HMGCR degradation machinery appeared to be unaffected by different oxygen tensions, I next wanted to assess if the degradation kinetics of HMGCR was affected using a cycloheximide (CHX) chase. The half-life of HMGCR under normal sterol (or sterol replete) conditions is reported to be under 2 hours, whilst sterol depletion increases

this to over 10 hours (Brown *et al.*, 1973; Gil *et al.*, 1985; Goldstein & Brown, 1990). Therefore, following overnight sterol depletion and then the reintroduction of sterols (cholesterol and 25-hydroxycholesterol), there should be rapid HMGCR degradation, a technique used in (Menzies *et al.*, 2018). As expected within 4 hours following the addition of CHX and the reintroduction of sterols, HMGCR was rapidly degraded **(Figure 5.4 A)**.

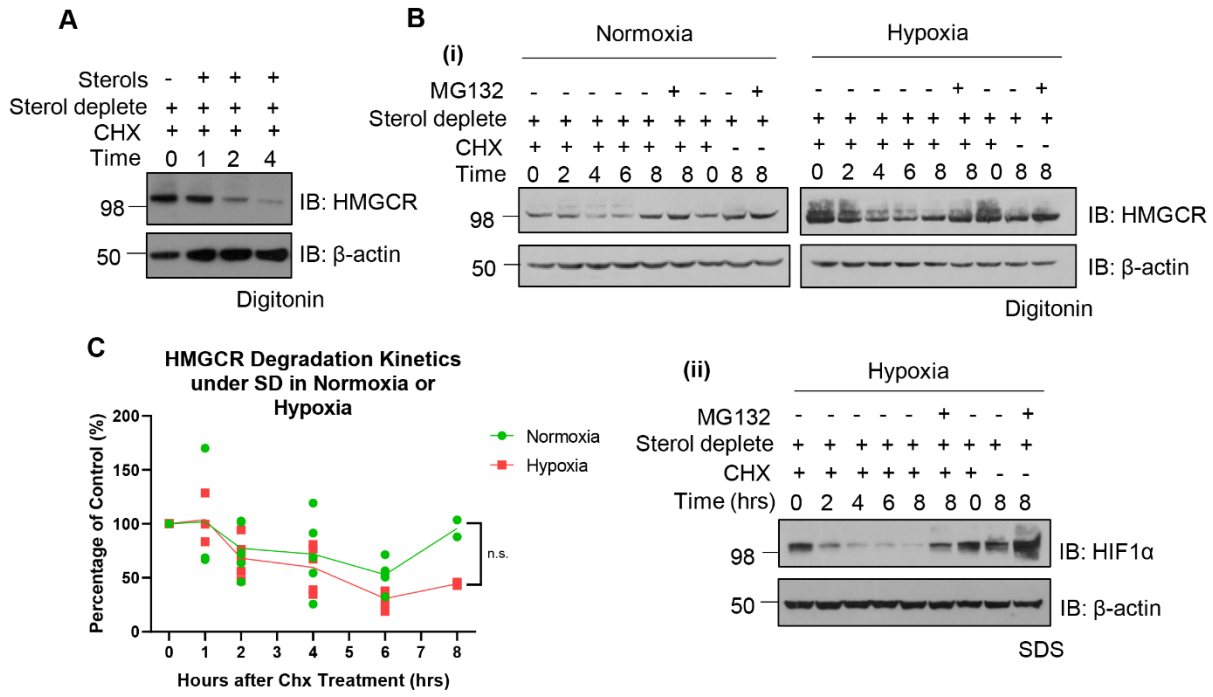

Figure 5.4. The degradation kinetics of HMGCR did not vary significantly with different oxygen tensions.

(A) HeLa WT cells were sterol depleted for 24 hours before the reintroduction of sterol (2 μg/ml 25-hydroxycholesterol and 20 μg/ml cholesterol) and 1 μg/ml cycloheximide (CHX). Samples were harvested at appropriate time points before being lysed in 1% digitonin buffer and immunoblotted. **(B)** HeLa WT cells were sterol depleted for 42 hours, for the final 18 hours cells were subjected to hypoxia (1% oxygen) where appropriate. Cells were then treated with 1 μg/ml CHX and 20 μM MG132 were appropriate and harvested at sequential time points, lysed in 1% digitonin **(i)** or SDS lysis buffer **(ii)** and immunoblotted. **(C)** A minimum of three blots (8 hours only has two) were quantified using ImageJ and HMGCR levels normalised to the housekeeping gene, actin. Significance was calculated using a two-way ANOVA using Bonferroni multiple comparisons.

n.s. = not significant.

To investigate if there was a significant difference between the degradation of HMGCR under sterol deplete conditions in 21% or 1% oxygen (hypoxia), I compared the kinetics of HMGCR degradation using CHX. HeLa cells were sterol depleted overnight, before being placed in 1% oxygen where appropriate for a further 18 hours. Cells were then chased for 8 hours with CHX **(Figure 5.4 B (i))**. Some degradation of HMGCR was observed under both oxygen tensions, which is more indicative of steady state degradation rather than the rapid degradation observed when adding sterols back in **(Figure 5.4 A)**. Proteasome inhibition prevented this degradation occurring as expected **(Figure 5.4 B (i))**.

Alongside HMGCR degradation I also assessed the degradation kinetics of HIF1α under hypoxia as a treatment control. The half-life of HIF1α in 21% oxygen is <10 minutes (Wang *et al*., 1995), due to its rapid degradation through the PHD-VHL axis, however, under hypoxic conditions HIF1α is stabilised, increasing its half-life (Huang *et al*., 1996). Following the 8 hour CHX chase, the initial pool of HIF1α in hypoxia was almost completely degraded and the levels were rescued appropriately with proteasome inhibition **(Figure 5.4 B (ii))**. HIF1α is known to still undergo degradation in hypoxia and this time course is consistent with prior degradation studies (Kong et al., 2007).

Quantification of these experiments showed that there was no significant difference in the degradation kinetics of HMGCR under sterol deplete conditions with varying oxygen tensions **(Figure 5.4 C)**. Although degradation of HMGCR was perhaps slightly faster under conditions of hypoxia, the changes were not significant. Additionally, it is known that the increase of INSIG2 transcription through HIF1α under conditions of low oxygen will increase HMGCR degradation, so the small increase in degradation kinetics observed here is probably explained through this mechanism (Hwang *et al*., 2017). Overall, the levels of HMGCR decreased in both oxygen tensions at a similar rate consistent with steady state degradation rather than induced degradation **(Figure 5.4 C)**.

5.2.3. Selected SREBP2 targets are downregulated transcriptionally following sterol depletion in hypoxia

HMGCR is regulated at the transcriptional level by the sterol regulated transcription factor, SREBP2, which is activated under conditions of low sterols. Therefore I decided to investigate how hypoxia (1% oxygen) and sterol depletion alters the transcription of SREBP2 target genes.

As expected, the three SREBP2 target genes investigated (HMGCR, HMG CoA synthase 1 (HMGCS1) and the low-density lipoprotein receptor (LDLR)) were upregulated transcriptionally following sterol depletion **(Figure 5.5 A)**. Following 18 hours incubation in hypoxia (1% oxygen) alone there was a very slight increase in the mRNA levels of these genes. Interestingly, following incubation with sterol depletion and 1% oxygen, the transcript levels of HMGCR and HMGCS1 were both significantly reduced when compared to sterol depletion in 21% oxygen, suggesting that low oxygen levels are somehow hindering the transcriptional upregulation typically observed under sterol depletion.

Interestingly, not all SREBP2 target genes seem to be transcriptionally reduced following sterol depletion in hypoxia. The LDLR was modestly increased following sterol depletion, but transcript levels are not significantly altered under conditions of sterol depletion in hypoxia. The reason for this is currently unclear, but we know that hypoxia does not downregulate all gene transcription, as HIF1α target genes are known to be upregulated. The HIF1α target gene CAIX was hugely upregulated in hypoxia **(Figure 5.5 A)**, and additionally, this increase remained unchanged under sterol depletion in hypoxia, suggesting that this combination did not reduce general transcription.

This transcriptional effect was independent of HIF1α mediated transcription, as the same effect was observed in all SREBP2 target genes in HIF1β null clones **(Figure 5.5 B)**, but as expected, transcription of CAIX was not induced in these cells. Consistent with the RT-qPCR data in **Figure 5.5 A and B**, the lack CAIX expression is confirmed by immunoblotting **(Figure 5.5 C)**. It is worth noting that HIF1α was still stabilised following hypoxia in these cells but it is unable to activate transcription due to the lack of its binding partner HIF1β.

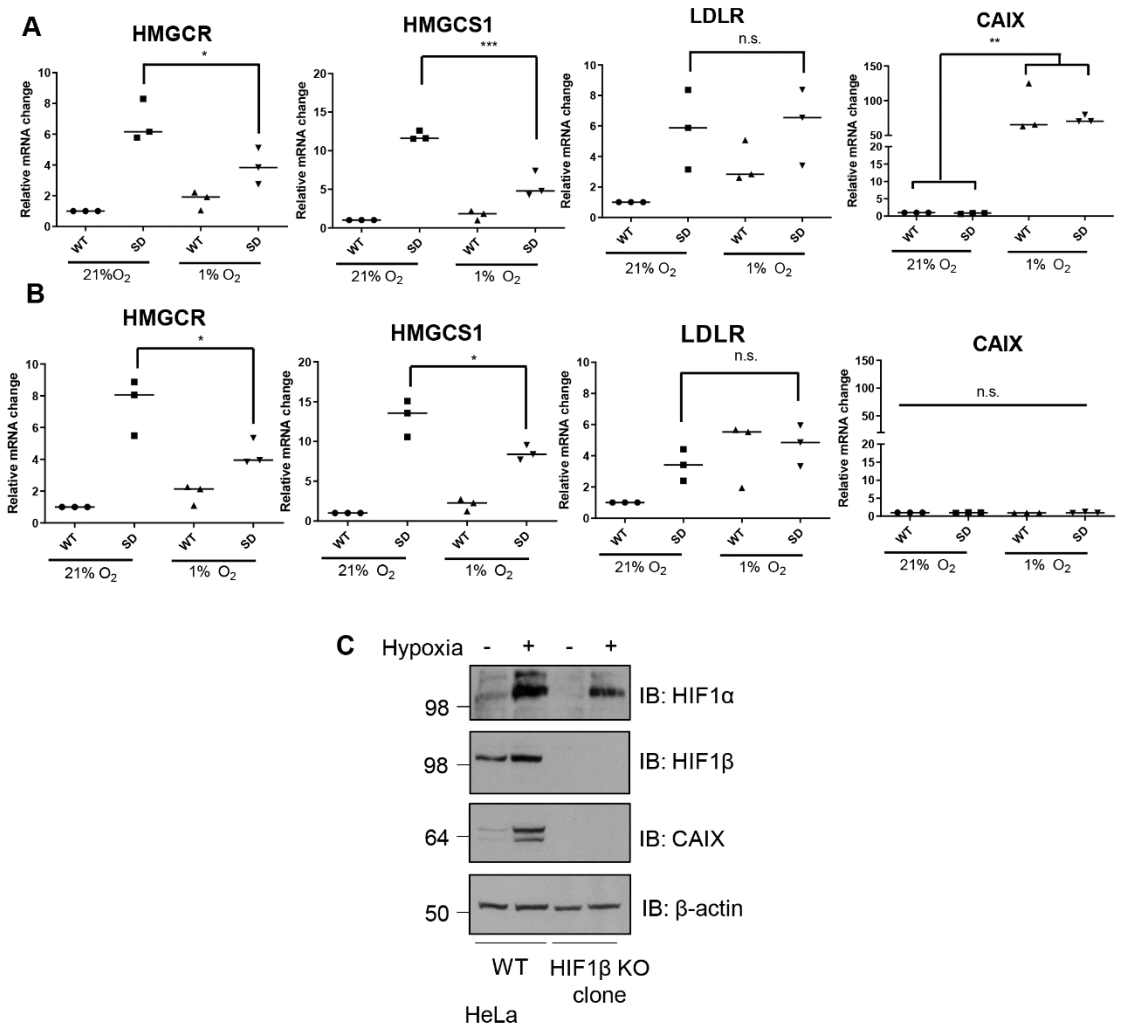

Figure 5.5. Selected SREBP2 targets are down regulated transcriptionally under sterol depletion in hypoxia.

HeLa WT **(A)** or clonal HIF1β null **(B)** cells were sterol depleted for 42 hours and where appropriate, for the final 18 hours the cells were subjected to hypoxia (1% oxygen), before being analysed using RT-qPCR. **(C)** HeLa WT and HIF1β null clone cells were treated with hypoxia (1% oxygen) where appropriate for 18 hours before being lysed in RIPA buffer and immunoblotted.

All mRNA levels were normalised using the ΔΔCT method using the housekeeping gene, actin. *= P<0.05, **= P<0.01, *** = P<0.001, n.s. = not significant.

To investigate the kinetics of this transcriptional response, the mRNA levels of each protein were assessed at various time points in hypoxia (1% oxygen) following overnight incubation in sterol deplete media. Slowly, over a period of 24 hours, the mRNA levels of HMGCR and HMGCS1 decreased by >50% when compared to their transcription level without incubation

in hypoxia **(Figure 5.6 (top panels))**. In accordance with my previous data, the levels of the LDLR did not significantly change over a 24 hour period in hypoxia, and as expected, the transcription of the HIF1α target gene, CAIX, significantly increased **(Figure 5.6 (bottom panels))**.

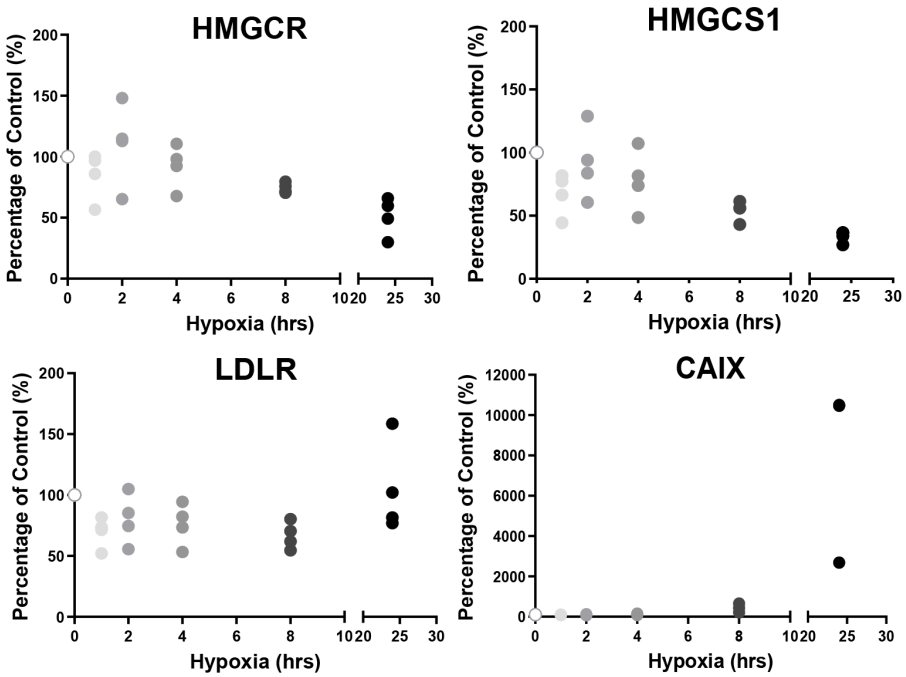

Figure 5.6. The transcriptional downregulation of some SREBP2 targets occurs slowly.

HeLa WT cells were treated with sterol depletion for 24 hours before being placed in hypoxia (1% O_2) and harvested at sequential time points (0, 1, 2, 4, 8 and 24 hours) before being analysed by RT-qPCR. mRNA levels were normalised to 100%, which was taken as the transcript level following 24 hours sterol depletion (0 hours hypoxia).

All mRNA levels were normalised using the ΔΔCT method using the housekeeping gene, actin.

5.2.4. The reduction of HMGCR in hypoxia is not due to the unfolded protein response

Protein flux through the ER is variable depending on the cellular environment, therefore the cell needs a homeostatic mechanism to adjust the protein folding capacity of the ER, which is termed the unfolded protein response (UPR). Upon ER stress, the accumulation of misfolded proteins within the ER, the UPR is initiated with the primary aim of restoring ER homeostasis (Hetz, 2012). Homeostasis is achieved by reducing the protein load on the ER by decreasing general transcription and translation, whilst simultaneously increasing the levels of ER protein folding chaperones such as BiP (also known as GRP-78), Grp94 (heat shock protein 90) and PDI (protein disulphide-isomerase) to increase the folding capacity of the ER (Ni & Lee, 2007). In cases of prolonged damage due to ER stress the cell undergoes apoptosis, CHOP (C/EBP homologous protein) is a transcription factor induced during ER stress which sensitizes the cell to UPR mediated death if required (Marciniak *et al*., 2004). Changes in transcription are a hallmark of the UPR, therefore, I wanted to assess whether ER stress was playing a role in the reduced transcription observed for some SREBP2 target genes.

Tunicamycin and thapsigargin are two well described chemicals which induce ER stress in cells. Tunicamycin inhibits essential protein modifications in the ER thereby blocking efficient protein folding and hindering protein exit (Oslowski & Urano, 2011), and thapsigargin treatment results in decreased ER calcium levels (Treiman *et al*., 1998) thereby decreasing the activity of calcium dependent ER chaperones including BiP, Grp94 and PDI (Coe & Michalak, 2009). If the induction of ER stress under sterol deplete conditions in hypoxia was driving the reduction in HMGCR observed, then chemically inducing ER stress under sterol deplete conditions in 21% oxygen should phenocopy this.

Firstly I confirmed that overnight treatment with tunicamycin or thapsigargin was sufficient to induce ER stress. This is shown through the transcriptional activation of the ER chaperone BiP and the transcription factor CHOP **(Figure 5.7 C (bottom panels))**, and the increased protein levels of some ER chaperones **(Figure 5.7 B (ii))**.

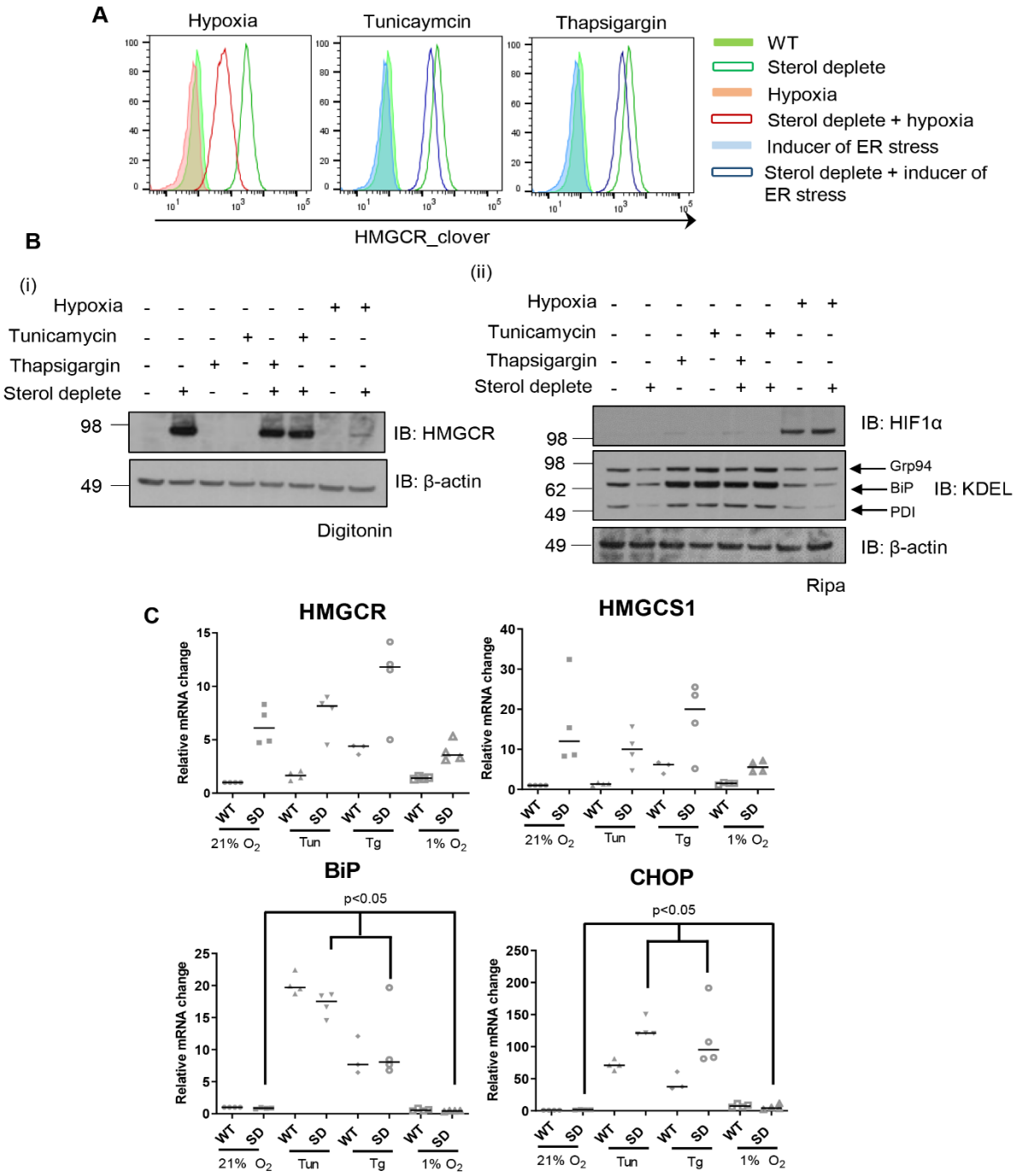

Figure 5.7. The decreased transcription of some SREBP2 targets is not due to ER stress.

HeLa HMGCR_clover **(A)** or HeLa WT **(B, C)** cells were treated with sterol depletion for 42 hours, where appropriate the cells were incubated with hypoxia (1% O_2), 2 μg/ml tunicamycin or 50 nM thapsigargin for the final 18 hours and analysed by flow cytometry **(A)** immunoblotting **(B)** or RT-qPCR **(C)**. *Tun= tunicamycin. Tg= Thapsigargin*

All mRNA levels were normalised using the ΔΔCT method using the housekeeping gene, actin.

Next I wanted to assess the effect ER stress had on HMGCR levels. Inducing ER stress had no effect on basal levels of HMGCR_clover, and did not cause any reduction in HMGCR levels when incubated with sterol depletion **(Figure 5.7 A)**. This was also observed with endogenous HMGCR levels **(Figure 5.7 B (i))**, suggesting that activating ER stress was not sufficient to reduce HMGCR under sterol deplete conditions. In accordance with this, HMGCR and HMGCS1 were not reduced transcriptionally following ER stress and sterol depletion, dissimilar to what was observed following sterol depletion and hypoxia **(Figure 5.7 C (top panels))**. Overall, these data suggested that ER stress was not the mechanism by which SREBP2 target genes were reduced at the protein and transcription level under sterol deplete conditions in hypoxia.

Some studies have shown the induction of ER stress under conditions of hypoxia which is reported to have a role in tumour progression (reviewed in Chipurupalli *et al.*, 2019; Wouters & Koritzinsky, 2008). However, in my experiments, under conditions of hypoxia (1% oxygen), independent of sterol depletion, I did not observe any increase in the protein level of the ER chaperones BiP, Grp94 or PDI **(Figure 5.7 B (ii)),** and did not see any transcriptional upregulation of BiP or CHOP **(Figure 5.7 C, (bottom panels))** suggesting that ER stress is not being activated strongly in this system.

5.2.5. Manipulating the mammalian target of rapamycin (mTOR) signalling pathway has no effect on HMGCR levels

My previous data shows a reduction in protein and transcript levels of components of the cholesterol synthesis pathway under sterol deplete conditions and low oxygen tensions, that is independent of induced degradation and HIF1α mediated transcription. Low oxygen tensions are known to reduce the activity of the mammalian target of rapamycin (mTOR) signalling pathway with one outcome being reduced protein translation. Therefore I wanted to assess if a reduction in mTOR activity was driving reduced translation of proteins involved in the cholesterol synthesis pathway.

The mTOR signalling pathway integrates extracellular signalling factors, such as growth factors and nutrients, to coordinate an intracellular response, regulating cell growth, metabolism and

survival. Activation of mTOR typically induces cell growth and protein translation, and decreases catabolic processes. Due to its importance for cell growth and survival, this pathway is often over activated during disease states such as cancer and diabetes, and is therefore an attractive therapeutic target (Laplante & Sabatini, 2009). mTOR acts in two distinct complexes; complex 1 (mTORC1) and complex 2 (mTORC2). mTORC1 has been well studied, whereas much less is known about mTORC2 but both are known to play important roles in cell survival, growth and metabolism.

Activate mTORC1 signalling leads to the phosphorylation of its downstream targets. Two target proteins include p70S6K1 and 4E-BP1. Phosphorylation of p70S6K1 at threonine 389, activates the kinase and promotes protein translation, whilst phosphorylation of 4E-BP1 prevents binding to eukaryotic translation initiation factor (eIF) 4E, enabling eIF4E to initiate protein translation (Laplante & Sabatini, 2009) **(Figure 5.8 A)**.

Rapamycin is an inhibitor of mTOR (Sabatini *et al*., 1994), and has been shown to be effective against complex 1, but less effective for complex 2 (Laplante & Sabatini, 2012). To assess if hypoxia was reducing protein translation through the mTOR pathway under sterol deplete conditions, I inhibited the mTOR pathway using rapamycin and assessed HMGCR levels. Firstly, the effectiveness of rapamycin treatment was confirmed by the loss of phosphorylated-p70S6K1 (P-p70S6K1), whilst total p70S6K1 levels remained constant, showing mTOR inhibition **(Figure 5.8 B (ii))**. To assess HMGCR levels, cells were treated with sterol depletion and rapamycin. Following treatment, levels of HMGCR were not reduced when compared to sterol depletion alone **(Figure 5.8 B (i)),** suggesting that inhibiting mTOR, and therefore reducing protein translation through this pathway, was not sufficient to cause a reduction in HMGCR levels.

Tuberous Sclerosis Complex (TSC) is a heterodimeric complex, comprising of Tsc1 and Tsc2, which is a GTPase activating protein (GAP) for the GTPase Rheb (Castro *et al*., 2003), and therefore negatively regulates the activity of mTOR **(Figure 5.8 A)**. Within this complex, Tsc2 is the catalytic GAP subunit (The European Chromosome 16 Tuberous Sclerosis Consortium, 1993), whilst Tsc1 stabilises Tsc2 by inhibiting its degradation by the HERC1 ubiquitin ligase (Chong-Kopera *et al*., 2006).

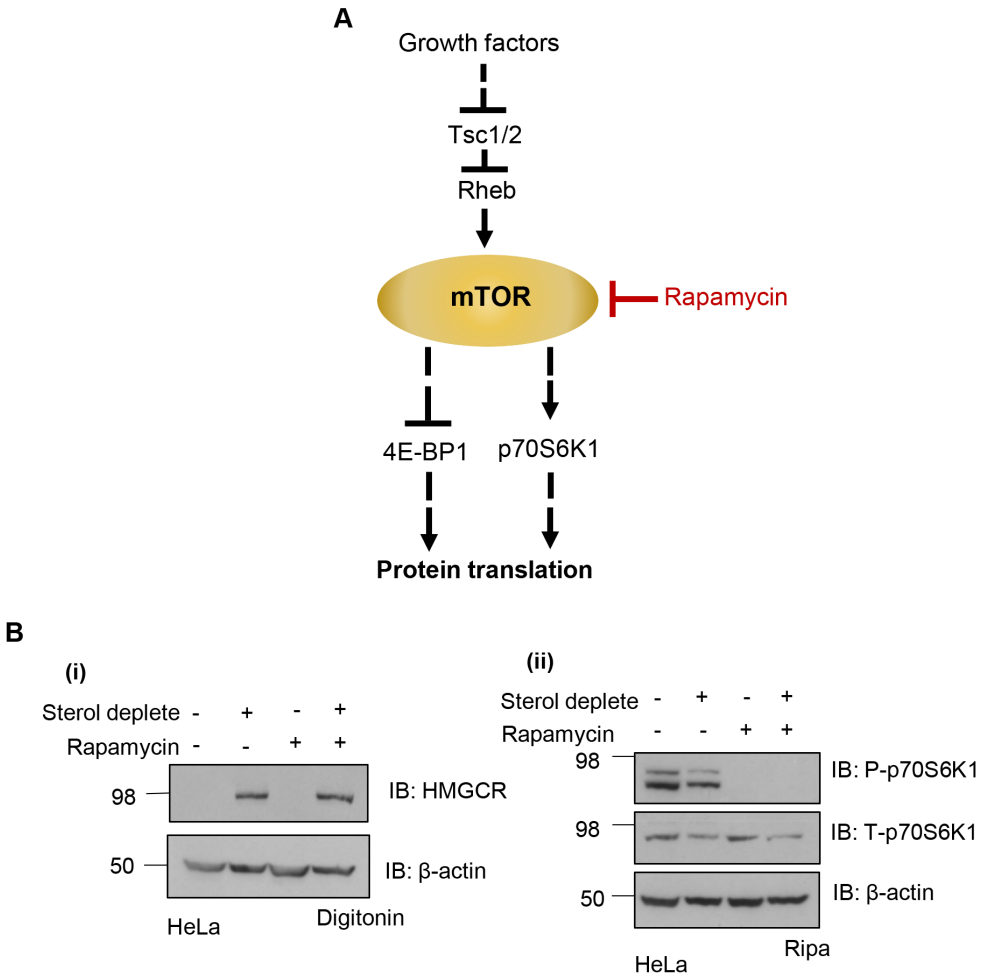

Figure 5.8. HMGCR levels are not affected by the inhibition of mTOR signalling.

(A) A basic schematic of two ways in which the mTOR pathway regulates protein translation. mTOR signalling is triggered by extracellular growth factors, which leads to the inactivation of the GTPase activating protein (GAP) complex Tsc1/2. Inactivation of Tsc1/2 leads to the GTPase Rheb being in the active GTP bound form, thereby activating mTOR which leads to the phosphorylation of its downstream targets including 4E-BP1 and p70S6K1. **(B)** HeLa WT cells were treated with sterol depletion for 42 hours, for the final 18 hours where appropriate cells treated with 100 nM rapamycin before lysis in 1% digitonin **(i)** or RIPA **(ii)** buffer and immunoblotted.

Depletion of either Tsc1/2 causes mTOR to be constitutively active. Depletion using two separate sgRNAs for each protein, was confirmed indirectly through an increase in phosphorylated mTOR targets such as p70S6K1 **(Figure 5.9 A)**, as I was unable to immunoblot for Tsc1/2 directly due to the lack of specific antibodies. Tsc1 sgRNA 2 and Tsc2 sgRNA 1

appeared to be most effective, so these were used in subsequent experiments. To assess whether causing constitutive activation of the mTOR pathway could overcome the reduction of HMGCR levels observed under sterol deplete conditions in hypoxia, Tsc1/2 mixed population KOs were subjected to these conditions. Depleting either Tsc1/2 had no effect upon HMGCR levels, which were comparable to that observed in WT cells **(Figure 5.9 B (i))**, whilst mTOR activation was observed in these cells by an increase in P-p70S6K1 **(Figure 5.9 B (ii))**.

Some studies have shown that low oxygen tensions reduce the activity of the mTOR signalling at multiple points in the pathway, to conserve energy and limit cell growth (reviewed in (Wouters & Koritzinsky, 2008). My data corroborates these studies as incubation in 1% oxygen reduced the level of P-p70S6K1 in WT cells **(Figure 5.9 B (ii), C)**. Low oxygen tensions also reduced levels of P-p70S6K1 in cells where the mTOR pathway was active (Tsc1/2 KOs) **(Figure 5.9 B (ii), C)**, suggesting that low oxygen tensions are able to override mTOR activation induced by Tsc1/2 depletion, and that hypoxia can act downstream of the Tsc1/2 complex.

Interestingly, my preliminary results showed increased levels of HIF1α in the Tsc1/2 KO populations compared to WT cells and that mTOR inhibition with rapamycin treatment was able to override this response and reduce HIF1α levels **(Figure 5.9 C)**. This suggested that the mTOR pathway was able to drive HIF1α expression when activated. This effect was also observed by a previous post-doc in the Nathan laboratory, Ian Lobb, but the findings are still preliminary and require further investigation.

Overall this data shows that activation or inhibition of the mTOR pathway does not greatly affect HMGCR levels, suggesting that the decrease in HMGCR levels following hypoxia and sterol depletion is not driven my mTOR induced protein translation. However, other protein translation pathways may be involved. These results also highlighted a potential interesting role for the mTOR pathway increasing HIF1α stabilisation.

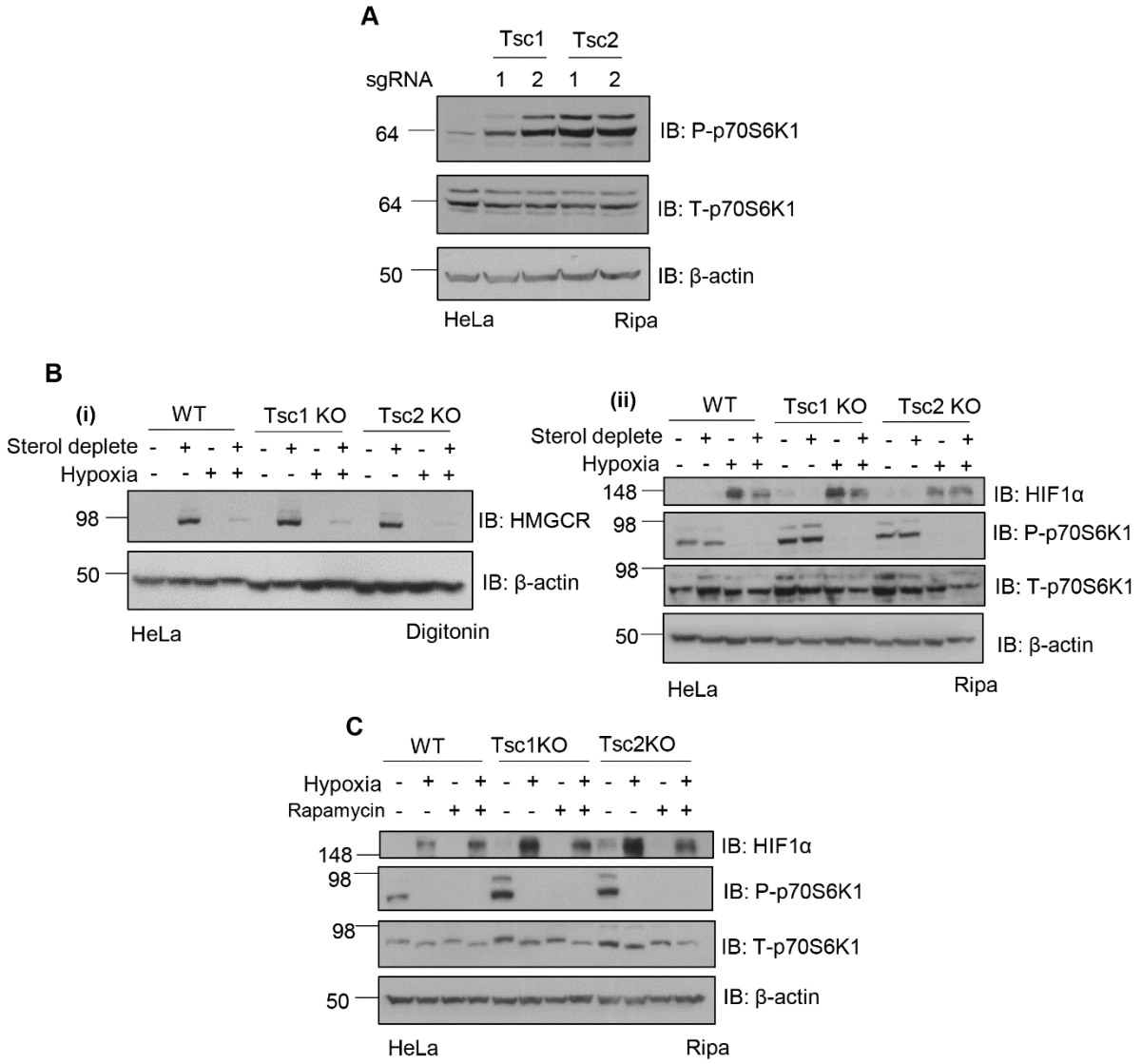

Figure 5.9. HMGCR levels are not affected by the activation of mTOR signalling.

(A) Tsc1 and Tsc2 CRISPR/Cas9 mixed population KO lines were created following transduction into HeLa WT cells. Depletion was confirmed by lysis in RIPA buffer and immunoblotting following selection. **(B)** HeLa WT, or mixed population Tsc1 KO (sgRNA 2), or Tsc2 KO (sgRNA 1) cells were sterol depleted for 42 hours, for the final 18 hours where appropriate cells were placed in hypoxia (1% O_2) before lysis in 1% digitonin **(i)** or RIPA **(ii)** buffer and analysis by immunoblotting. **(C)** HeLa WT, or mixed population Tsc1 or Tsc2 KO cells were either treated with hypoxia (1% O_2) for 18 hours or 100 nM rapamycin for 18 hours alone or in combination, before lysis in RIPA buffer and analysis by immunoblotting.

5.3. Discussion

5.3.1. Challenges and limitations of the genome wide CRISPR/Cas9 genetic screen in HeLa HMGCR_clover cells

Similarly to the CRISPR/Cas9 forward genetic screen carried out in HeLa mCherry-CL1 cells in **Chapter 3**, the screen carried out in HeLa HMGCR_clover cells was split into two populations; clover^{MEDIUM} and clover^{HIGH}. I chose to focus my attention on the clover^{MEDIUM} population, due to the identification of known components of the HMGCR degradation pathway, whilst the majority of hits in the clover^{HIGH} population seemed to be associated with general transcription and not relevant to HMGCR regulation. Unfortunately, the CRISPR/Cas9 forward genetic screen did not reveal any new genes involved in reducing HMGCR levels under conditions of sterol depletion in 1% oxygen **(Figure 5.1)**. This could have been due to a number of biological and experimental reasons.

Firstly, the failure to identify new genes in the genetic screen suggested that the reduction in HMGCR observed under conditions of sterol depletion in 1% oxygen was not due to the effects of a single gene, although could be due to a group of genes displaying redundancy. Secondly, some gene deletions may have been lethal and these gene knockouts would have been lost over the duration of the screen and not identified in the sequencing. Alternatively, more global effects such as changes in protein translation may be involved, which would also not be represented in the screen. Finally, although the screen was successful in identifying known genes required for the degradation of HMGCR, such as UBE2G2, some experimental limitations may have caused genes with subtler effects on HMGCR levels to be missed. All available cell sorting machines were at atmospheric oxygen, and due to formaldehyde fixation quenching the clover signal, all cells had to be sorted live by FACS, and were therefore exposed to higher oxygen tensions. Although the cells were maintained in 1% oxygen and subsequently on ice for as long as possible, any oxygen exposure may have limited the scope of the screen, although this was unfortunately unavoidable.

Another technical challenge from the screen was analysing the sequencing data from the two different Illumina platforms. The same DNA pool was analysed on the MiniSeq and HiSeq

platforms predictably giving very similar results, both identifying UBE2G2, FAF2 and AUP1 as the top hits. However, some discrepancies were observed such as PCTP and YEATS4 only being identified in the MiniSeq or HiSeq analysis respectively. These small difference in the data could be due to the depth or variability of the sequencing on the two platforms, or because the control libraries used to analyse the data were different due to not being able to sequence the unsorted library on the MiniSeq. Therefore, it would be helpful to reanalyse these data using the same control library to assess for significance. Additionally I was only able to validate these two genes phenotypically, due to a lack of access to specific antibodies. Therefore, it would also be beneficial to assess the knockout efficiency of these guides using a different method such as Inference of CRISPR edits (ICE) which is able to assess the efficiency of the CRISPR knockout (Hsiau et al., 2018), to conclusively rule out any role for these genes in the hypoxic regulation of HMGCR.

I had hypothesised that 2-OGDDs may be involved in the hypoxic regulation of the cholesterol synthesis pathway, similarly to fission yeast, but there was no evidence to demonstrate any involvement of 2-OGDDs from the screen as no family members were identified. It is likely that this pathway has diverged from fission yeast, and agrees with my previous data showing that DMOG, which should inhibit all 2-OGDDs, had no effect on this system in mammalian cells beyond that of HIF1α stabilisation **(Figure 4.4)**. Furthermore, no additional degradation machinery was identified in the screen suggesting that hypoxia was not inducing an alternative degradative route for HMGCR, which fits with my data showing that HMGCR is degraded in 1% oxygen using the same machinery as in 21% oxygen **(Figure 5.3)** (Menzies *et al*., 2018).

It is known that the E3 ligases RNF145, gp78 and Hrd1, and the E2 enzyme UBE2G2 (which requires AUP1 for its ER membrane localisation) are required for HMGCR degradation under sterol rich conditions in 21% oxygen (Jiang *et al*., 2018; Menzies *et al*., 2018). My results also show that these enzymes are sufficient to degrade HMGCR under sterol deplete conditions in 1% oxygen **(Figure 5.3 A)**. However, in the CRISPR/Cas9 forward genetic screen, only UBE2G2 and AUP1 were identified from this pathway **(Figure 5.1 B)**, and none of the ligases featured in the top hits. This was probably due to redundancy between the three E3 ligases, RNF145, gp78 and Hrd1, as full stabilisation of HMGCR under sterol deplete conditions in hypoxia was only observed when all three ligases were depleted **(Figure 5.3 A)**. Supporting this, Menzies *et al*., (2018) only see partial stabilisation of HMGCR following depletion of either ligase

individually under conditions of sterol repletion in 21% oxygen, and indeed only identified gp78 as being involved in HMGCR degradation, when carrying out a CRISPR/Cas9 forward genetic screen in cells lacking RNF145. Conversely, depletion of UBE2G2 alone is enough to stabilise HMGCR under conditions of sterol repletion (Menzies *et al*., 2018) and sterol depletion in hypoxia **(Figure 5.3 A)**, supporting a lack of redundancy here and that all ligases appear to work with this E2 enzyme in this pathway.

5.3.2. Why is HMGCR degraded under sterol deplete conditions in hypoxia?

My data suggests that hypoxia is overriding sterol depletion, causing a reduction in the cholesterol synthesis pathway even when cellular sterols are limiting. This has been shown through the degradation and lack of transcription of HMGCR under sterol deplete conditions in hypoxia.

The degradation of HMGCR observed under sterol deplete conditions in 1% oxygen was likely to be steady state degradation rather than induced degradation, as no significant difference between the degradation kinetics was observed in sterol deplete conditions under different oxygen tensions (21% vs 1%) **(Figure 5.4)**. There appeared to be a slight increase in the degradation of HMGCR under conditions of 1% oxygen. However, it has been previously reported that HIF1α stabilisation causes an increase in HMGCR degradation via INSIG2 transcription (Hwang *et al*., 2017). As this experiment was carried out in HeLa WT cells, HIF1α was present, so it was likely that this slight increase in degradation was mediated through HIF1α stabilisation **(Figure 4.2 A)**. To confirm this, the experiment would need to be repeated using clonal HIF1β KO cells where no HIF1α effect would be observed.

Chun *et al*., (1990) reported that a high concentration of cycloheximide (~140 μg/ml) affected the sterol induced degradation of HMGCR. Therefore, I opted to use a lower concentration in my experiments (1 μg/ml) that had been used to previously study HMGCR degradation (Menzies *et al*., 2018). Additionally, I validated this concentration by following HIF1α **(Figure 5.4 B (ii))**, and the sterol mediated induction of HMGCR **(Figure 5.4 A)** degradation alongside. Whilst studying the degradation kinetics of HMGCR using cycloheximide is effective, it would be beneficial to carry out radioactive pulse chase experiments alongside to

confirm the results. Unfortunately, this is not currently possible, due to the complexity of the experimental conditions and the current limitations of where radioactivity can be used in the institute. There are benefits and limitations of using both cycloheximide and radioactive pulse chase experiments to study protein degradation. Cycloheximide inhibits the synthesis of any new proteins and therefore degradation of the target protein can be followed. However, the lack of protein synthesis will also affect the levels of any short lived proteins, including ubiquitin and some E3 ligases within the cell (Hanna *et al*., 2003). This could confound the results and leads to some of the toxicity caused by prolonged cycloheximide treatment. Additionally, detection following a cycloheximide chase is through immunoblotting and is therefore very antibody dependent. Radioactive pulse chase experiments are typically more sensitive and do not cause any other cellular change, however, conducting these radioactive experiments in the hypoxic chamber would be challenging.

The E3 ligase RNF145 has been shown by Menzies *et al*., (2018) to be a sterol regulated ligase with a half-life of approximately 2 hours and auto-regulated by UBE2G2 **(Figure 5.3 B)**. My data showed that RNF145 protein levels are significantly reduced in response to 1% oxygen **(Figure 5.3 C)**. Levels of other components of the degradation machinery for HMGCR, such as gp78 or UBE2G2 did not change under conditions of low oxygen **(Figure 5.3 C)**. Therefore, it was possible that the degradation of HMGCR observed of under conditions of sterol depletion and 1% oxygen is mediated by the other two E3 ligases involved in its degradation, with the likelihood that gp78 is the predominant enzyme. To confirm this, the kinetics of HMGCR degradation would need to be studied in cells depleted of RNF145, gp78 and Hrd1 individually and in combination. It would also be interesting to understand why RNF145 is degraded under low oxygen conditions whilst other ligases remain stable.

5.3.3. Why is the transcription of selected SREBP2 target genes decreased under conditions of sterol depletion in hypoxia?

SREBP2 is a sterol regulated transcription factor that regulates genes involved in the cholesterol synthesis pathways such as HMGCR, HMGCS1 and the LDLR. Selected SREBP2 target genes, including HMGCR and HMGCS1 were downregulated transcriptionally under

sterol deplete conditions in 1% oxygen when compared to sterol depletion in 21% oxygen **(Figure 5.5, Figure 5.6)**.

This downregulation is consistent with low oxygen tensions overriding sterol depletion in HeLa cells. However, the transcriptional reduction of HMGCR and HMGCS1 under sterol deplete conditions in 1% oxygen was slow, taking about 20 hours for transcription to be reduced by about 50% when compared to sterol depletion in 21% oxygen **(Figure 5.6)**. Similar to my results, following incubation in lipid depleted serum and <0.5% oxygen, Lewis *et al*., (2015) observed a transcriptional reduction in HMGCS1, but not HMGCR in glioblastoma cells. The mechanism for the transcriptional decrease under sterol deplete conditions in low oxygen is currently unknown, but could be due to reduced SREBP2 levels under low oxygen conditions which would result in reduced transcription of its target genes.

Interestingly, transcript levels of the LDLR did not significantly change with varying oxygen tensions **(Figure 5.5, Figure 5.6)**. The reasons for the discrepancies between SREBP2 target genes are currently unclear, but could be due to a number of explanations including; (i) that there is a difference in how oxygen regulates the *de novo* cholesterol synthesis pathway and the cholesterol uptake pathway, or (ii) that another transcription factor is also driving transcription of the LDLR.

The LDLR acts in the cholesterol uptake pathway, and is increased under sterol deplete conditions in an attempt to increase cholesterol uptake from the cells environment, whereas HMGCR and HMGCS1 are involved in the *de novo* cholesterol synthesis pathway, where cholesterol is generated from acetyl-CoA intracellularly. It is possible that the mechanism regulating components of the cholesterol synthesis pathway under low oxygen conditions is specific for the cholesterol synthesis pathway and not the cholesterol uptake pathway. Therefore, it would be of interest in further studies to explore how cell surface LDLR levels respond to low oxygen conditions and whether differential regulation of LDLR by SREBP1 compared to SREBP2 may account for the differences in gene transcription observed in my studies. Although SREBP2 is thought to be the predominant transcription factor for the LDLR, SREBP1 can mediate LDLR transcription (Guo *et al*., 2011; Horton *et al*., 2003), and has been shown to be more stable than SREBP2 under low oxygen conditions (Furuta *et al*., 2008; Lewis *et al*., 2015; J. Li *et al*., 2005).

5.3.4. Links between oxygen tensions, the mTOR pathway and the cholesterol synthesis pathway

As the screen did not uncover a genetic cause of decreased HMGCR levels following sterol depletion in low oxygen conditions, I assessed whether changes in the mTOR pathway may be accounting for my observations.

The mTOR pathway regulates many extracellular and intracellular signals to control cell growth, survival and metabolism, therefore it is unsurprising that the pathway is sensitive to oxygen levels. Low oxygen conditions have been shown to inhibit mTOR through multiple pathways, in both HIF1α dependent (Brugarolas et al., 2004; Li et al., 2007), and independent manners (Arsham et al., 2003; Bernardi et al., 2006; Liu et al., 2006). Upregulation of AMPK (Liu *et al*., 2006) and REDD1 (Brugarolas *et al*., 2004) under low oxygen conditions increase Tsc1/2 activity, thereby inactivating mTOR. Other pathways have been shown to act downstream of the Tsc1/2 complex. Promyelocytic leukaemia (PML) represses mTOR in a HIF1α and Tsc1/2 independent manner by inhibiting the interaction of mTOR with the GTPase Rheb (Bernardi *et al*., 2006). Similarly, Bnip3, a HIF1α target gene, inhibits the interaction between Rheb and mTOR under low oxygen conditions (Li *et al*., 2007). Here I have shown that overnight incubation in 1% oxygen conditions decreased the activity of the mTOR pathway in HeLa WT cells, consistent with prior studies. Interestingly this occurred even in cells where mTOR was activated through Tsc1/2 depletion **(Figure 5.9 B (ii), C))**, highlighting how hypoxia can inhibit the mTOR pathway at multiple positions, including downstream of Tsc1/2. Furthermore, HIF1α levels were dependent on mTOR. Levels of HIF1α were increased in Tsc1/2 deficient cells, with the accumulation reversed upon mTOR inhibition with rapamycin **(Figure 5.9 C)**. This observation is consistent with prior studies (Brugarolas *et al*., 2004), although the full mechanism by which this occurs is currently unclear.

Irrespective of the hypoxic regulation of mTOR, activating or inhibiting the pathway through Tsc1/2 depletion or rapamycin treatment did not appear to affect HMGCR levels **(Figure 5.8 B (i), Figure 5.9 B (i))**, suggesting that altered mTOR signalling was not solely responsible for the inhibition of the cholesterol synthesis pathway in hypoxia. However, my

experiments used mixed population Tsc1/2 KOs, so although mTOR activity appears to be increased, it would be beneficial to generate clonal KOs to confirm these results.

5.3.5. The role of ER stress on the cholesterol synthesis pathway

The majority of cholesterol synthesis occurs at the ER membrane, and hallmarks of the UPR, driven by ER stress, are decreased general transcription and translation. Therefore, I assessed whether activation of the UPR was involved in altering the cholesterol synthesis pathway, as prior studies have shown that the UPR is activated under conditions of low oxygen (reviewed by Chipurupalli *et al*., 2019; Wouters & Koritzinsky, 2008). One proposed mechanism for how oxygen levels influence ER stress is that some post-translation modifications within the ER have been shown to require oxygen. Extreme hypoxia has been shown to limit the folding capacity of the ER, thereby accumulating misfolded proteins and activating the UPR (Koritzinsky *et al*., 2013). Additionally, low oxygen conditions have been shown to activate the UPR in other ways, resulting in decreased general protein translation (Koumenis *et al*., 2002) and increased transcription of ER chaperones (Romero-Ramirez *et al*., 2004).

My data does not show much activation of the UPR in 1% oxygen conditions, however, I only assessed the activation in HeLa cells following 1% oxygen for 18 hours, and different conditions and cell types are likely to produce different effects. Additionally, induction of the UPR following thapsigargin or tunicamycin treatment did not appear to have any effect on HMGCR levels **(Figure 5.7)**, and therefore ER stress did not appear to be the main driver of the reduction in the cholesterol synthesis pathway I observe following sterol depletion in 1% oxygen.

5.4. Summary

Levels of HMGCR are reduced under conditions of sterol depletion in low oxygen conditions, however, the mechanism by which this occurs is currently unknown. In this chapter I have used a CRISPR/Cas9 forward genetic screen in HeLa HMGCR_clover cells to search for new

regulators of HMGCR under low oxygen conditions. The screen did not uncover new genes involved in downregulating HMGCR under sterol deplete conditions in 1% oxygen suggesting that the reduced levels of HMGCR were not due to any one specific protein. However, the genetic approach did identify known HMGCR degradation machinery, confirming that the same ERAD E3 ligases were involved in regulating HMGCR levels. Kinetic cycloheximide chase experiments suggested that HMGCR degradation under sterol deplete conditions in hypoxia is similar to steady state degradation of HMGCR in 21% oxygen.

While HMGCR degradation alone did not account for its decreased levels in sterol deplete conditions in 1% oxygen, I observed a decrease in the transcript levels of selected SREBP2 target genes. Therefore, I next wanted to explore the levels and regulation of SREBP2 under sterol depletion in 1% oxygen, to investigate whether this transcription factor was responsible for the reduction of HMGCR in hypoxia when sterols were limiting.

Chapter 6: Regulation of the transcription factor SREBP2 in hypoxia

6.1. Introduction

Activity of the *de novo* cholesterol synthesis pathway is reduced under conditions of hypoxia, with the enzyme involved in the rate limiting step, HMGCR, reduced at both the protein and transcriptional level. As no new genes were identified as being involved in the regulation of HMGCR under sterol deplete conditions in 1% oxygen, and that these changes appeared to be independent of both ER stress and mTOR activity **(see Chapter 5)**, I decided to focus on the transcription factor SREBP2.

In fission yeast, the SREBP2 orthologue, Sre1, is the principle regulator of anaerobic and sterol limiting gene expression. In conditions where oxygen or sterols are limited, Sre1 becomes stabilised and is able to activate the transcription of its target genes which are required for survival in both low oxygen and low sterol conditions (Hughes *et al.*, 2005; Todd *et al.*, 2006). Due to the significance of SREBP2 in the oxygen sensitivity of the cholesterol synthesis pathway in fission yeast, and the decrease I observed in the transcription of selected SREBP2 target genes under sterol deplete conditions in hypoxia **(Figure 5.5)**, I decided to focus on the regulation of SREBP2 itself.

In this chapter I show that SREBP2 decreases at the protein, but not mRNA, level under conditions of low oxygen and that this is partially rescued by proteasome inhibition. I show that exogenous SREBP2 is able to partially rescue HMGCR levels, and similar observations were observed by hindering endogenous degradation of SREBP2 through the two E3 ligases MARCH6 and TRC8. However, a decrease in SREBP2 protein level was still observed in low oxygen conditions. This focused my attention on translation, and here I begin to look at protein translation under low oxygen conditions.

6.2. Results

6.2.1. Sterol depletion combined with hypoxia decreases SREBP2 protein levels

The transcription of selected SREBP2 target genes were decreased under sterol deplete conditions in 1% oxygen when compared to sterol depletion in 21% oxygen **(Figure 5.5)**, therefore I decided to investigate whether SREBP2 itself was changed under conditions of low oxygen.

There are two forms of SREBP2 in the cell, the full length form, which is in the ER membrane, and the cleaved form, which is the active transcription factor produced by cleavage in the Golgi **(Figure 1.4)**. As expected, under steady state high sterol conditions there were low levels of the cleaved form of SREBP2. However, following sterol depletion, increased cleavage of SREBP2 was observed with a corresponding decrease in the full length form **(Figure 6.1 A (compare lanes 1 and 2))**. Interestingly, following incubation with hypoxia (1% oxygen) alone there was a decrease in the full length form of SREBP2 **(Figure 6.1 A (compare lanes 1 and 3))**. Similarly, under sterol deplete conditions in hypoxia there was a comparable reduction in full length SREBP2 **(Figure 6.1 A (compare lanes 3 and 4))**, but also a decrease in the cleaved form when compared to sterol depletion in 21% oxygen **(Figure 6.1 A (compare lanes 2 and 4))**. This was independent of HIF1α mediated transcription as I observed the same pattern in cells lacking HIF1β **(Figure 6.1 B)**. These findings suggested that hypoxia overrides the normal sterol depletion response of SREBP2 activation, with a marked reduction of SREBP2 protein levels. The lack of SREBP2 observed under conditions of hypoxia could be due to three possible reasons: decreased transcription, increased degradation, or decreased translation.

To first assess whether SREBP2 transcription was affected under low oxygen conditions I assessed the transcript levels of SREBP2 using RT-qPCR. An increase in SREBP2 mRNA was observed following sterol depletion in 21% oxygen, **(Figure 6.1 C)**, which was in agreement with prior studies that have shown that SREBP2 mRNA levels are regulated through self-activation (Sato *et al*., 1996). Interestingly, SREBP2 transcription increased with hypoxia alone **(Figure 6.1 C)**, which may explain the very modest increase in HMGCR, HMGCS1 and LDLR transcript levels also observed in 1% oxygen **(Figure 5.5 A)**. There was no significant difference

between the transcript levels of SREBP2 under sterol deplete conditions in 21% or 1% oxygen, suggesting that the changes in SREBP2 protein levels observed in **Figure 6.1 A** were not due to transcriptional changes. Additionally, SREBP2 transcription in hypoxia was independent of the HIF response as the same effect was observed in cells lacking HIF1β **(Figure 6.1 C).**

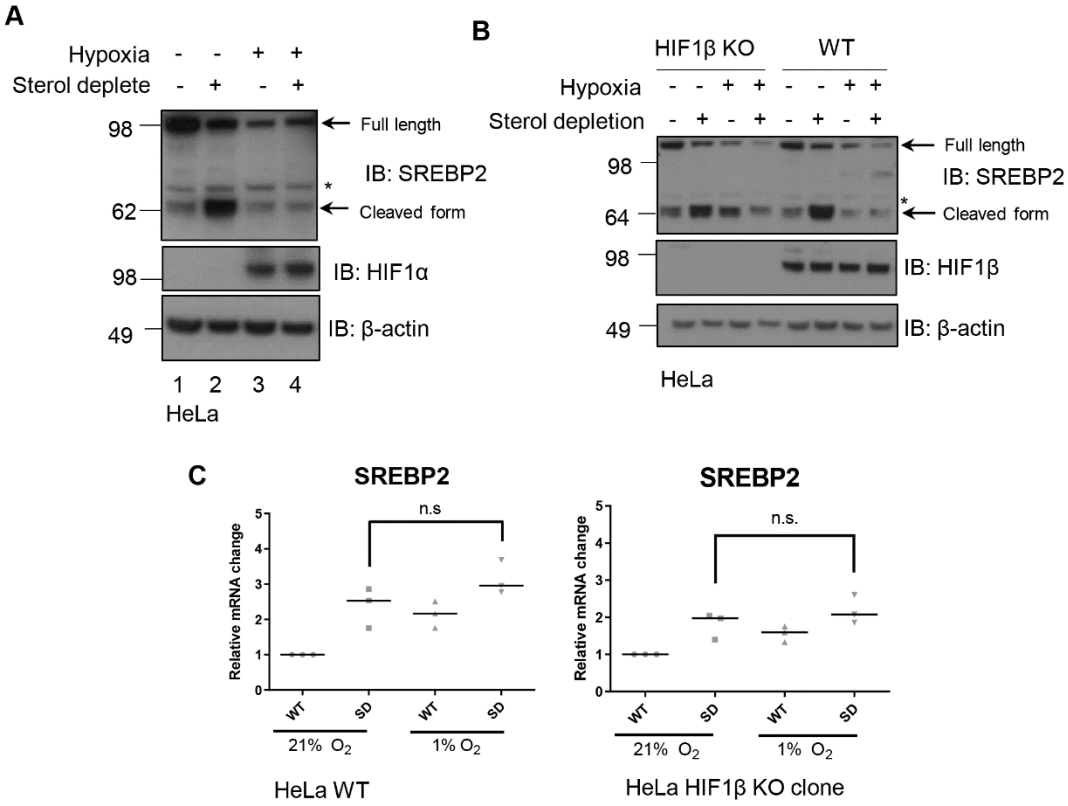

Figure 6.1. SREBP2 decreases at the protein, but not mRNA level under sterol deplete conditions in hypoxia.

HeLa WT **(A)** or HIF1β KO clone **(B)** cells were treated with sterol depletion for 42 hours, and where appropriate for the final 18 hours cells were placed in hypoxia (1% O_2) before being lysed in RIPA buffer and analysed by immunoblotting. **(C)** HeLa WT or HeLa HIF1β KO clone cells were treated with sterol depletion for 42 hours, and where appropriate for the final 18 hours cells were placed in hypoxia (1% O_2) before being analysed by RT-qPCR. mRNA levels were normalised using the ΔΔCT method using the housekeeping gene, actin.

* Represents non-specific bands, n.s= not significant.

To confirm that the primers used for the RT-qPCR in **Figure 6.1 C** recognised SREBP2 mRNA, in addition to checking for a single peak on the melt curve, I depleted SREBP2 using siRNA and assessed knockdown efficiency by RT-qPCR. 48 hours following siRNA transfection, SREBP2

had been efficiently depleted at both the protein level **(Figure 6.2 A)** and mRNA level **(Figure 6.2 B)**. To check for transfection efficiency, I used an siRNA which had been previously well validated in the Nathan laboratory, β2M. I confirmed that β2M was efficiently depleted, by showing the loss of cell surface MHC-1 48 hours after transfection **(Figure 6.2 C)**. Together, these results confirmed that the primer used for RT-qPCR recognised SREBP2 mRNA.

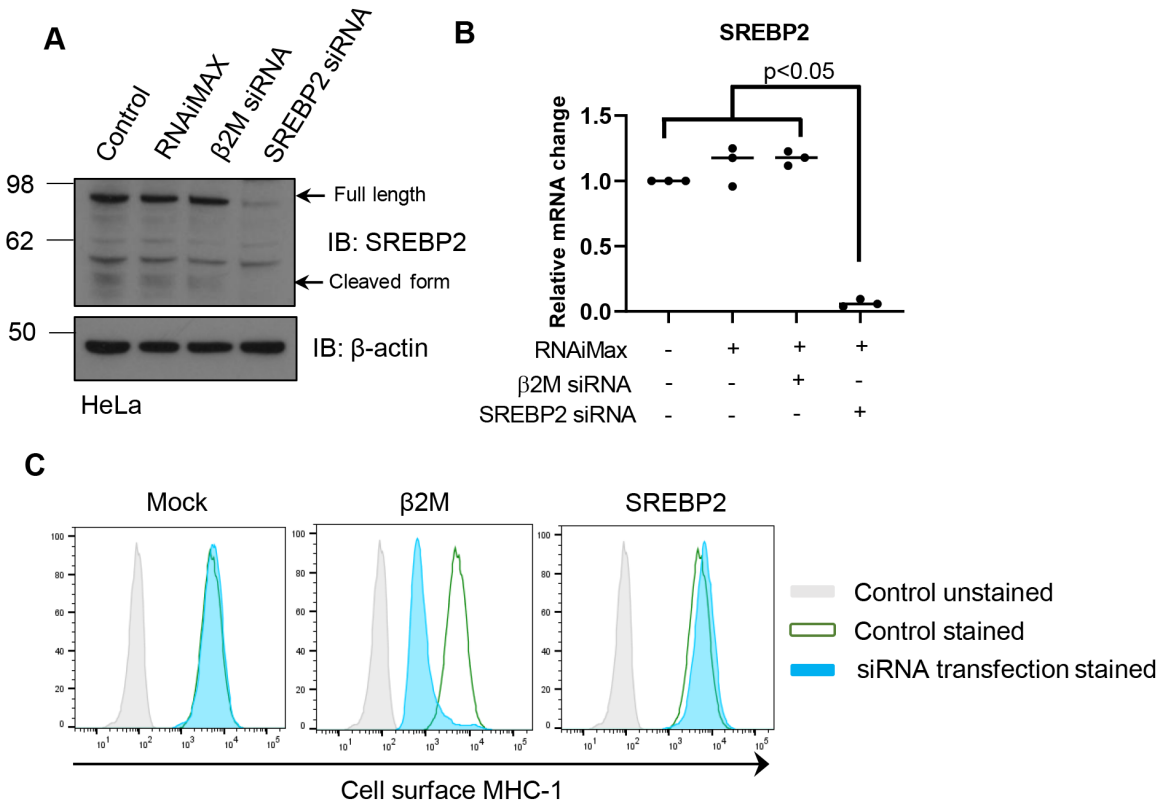

Figure 6.2. The SREBP2 RT-qPCR primer recognises SREBP2.

HeLa WT cells were transfected with siRNA against β2M, SREBP2 or mock (no siRNA) 48 hours prior to analysed by immunoblotting **(A)**, RT-qPCR **(B)** or cell surface staining for MHC-1 and flow cytometry **(C)**.

The change in SREBP2 protein level was not due to any transcriptional modifications, therefore there were two other likely possibilities for how SREBP2 was being regulated: (i) that SREBP2 was regulated through proteasomal degradation; or (ii) that translation of SREBP2 was being affected in low oxygen conditions. Due to previous work carried out in the Nathan laboratory, we had data which suggested that SREBP2 was regulated under steady state conditions by the E3 ligases MARCH6 and TRC8 **(Figure 3.10)** (Stefanovic-Barrett *et al.*, 2018). Therefore, next I decided to investigate whether SREBP2 was being proteasomally degraded in hypoxia.

Following proteasome inhibition using either MG132 (20 μM, 4 hours) **(Figure 6.3 A)** or Btz (20 nM, 16 hours) **(Figure 6.3 B)**, both the full length and cleaved form of SREBP2 were rescued under high sterol conditions in 21% oxygen **(Figure 6.3 A & B (lanes 1 and 2)).** However, under sterol deplete conditions, proteasome inhibition only rescued the cleaved form of SREBP2 by immunoblot **(Figure 6.3 A & B (compare lanes 3 and 4))**. The predominant rescue of the cleaved form was likely due to either stabilisation of the cleaved form, or as a result of high levels of SREBP2 cleavage under sterol deplete conditions.

Hypoxia (1% oxygen) reduced both the full length and cleaved form of SREBP2, as previously described **(Figure 6.1 A; Figure 6.3 A & B (compare lanes 1 and 5))**. Proteasome inhibition predominantly rescued the cleaved form of SREBP2, which was most evident in sterol deplete conditions **(Figure 6.3 A & B (lanes 3 and 4, & 7 and 8))**. Interestingly, proteasome inhibition had little effect on full length SREBP2 in hypoxia, although some rescue was observed with Btz **(Figure 6.3 B, lane 6)**. However, proteasome inhibition also preferentially stabilised the cleaved form in cells incubated in 21% oxygen. While proteasome inhibition did not fully overcome the reduction of SREBP2 in hypoxia, these results suggest that proteasome inhibition could partially rescue SREBP2 levels in hypoxia combined with sterol depletion.

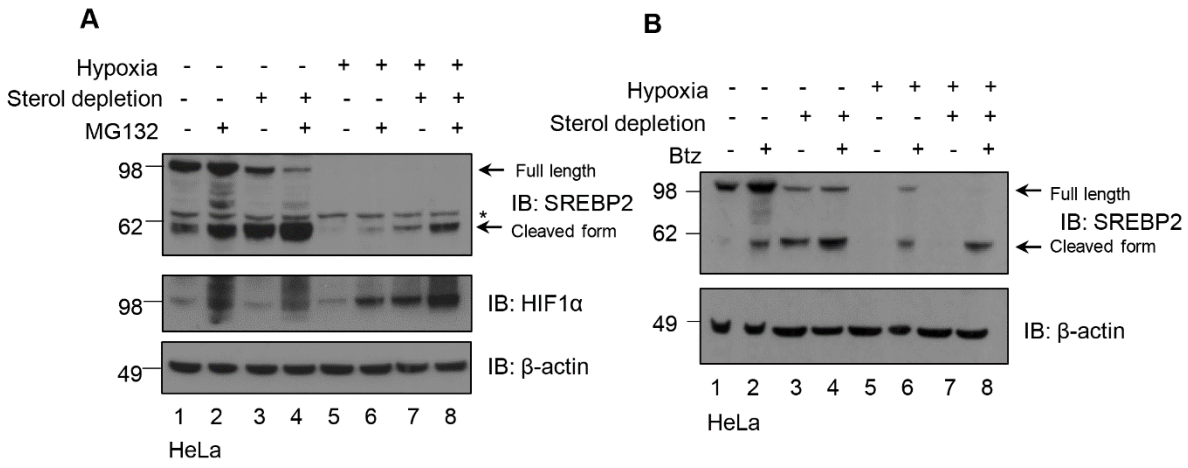

Figure 6.3. SREBP2 levels are rescued by proteasome inhibition.

HeLa WT cells were treated with sterol depletion for 42 hours, with or without hypoxia (1% O_2) for the final 18 hours. Where appropriate cells were treated with 20 μM MG132 four hours prior to harvest **(A)** or 20 nM Btz 18 hours prior to harvest **(B)** before lysis in RIPA buffer and immunoblotting.

* Represents non-specific bands.

6.2.2. The reduction of HMG-CoA reductase following sterol depletion in hypoxia is partially rescued by the overexpression of SREBP2

The reduced protein levels of SREBP2 observed under conditions of hypoxia could explain the reduction of HMGCR transcription previously observed. Therefore I wanted to assess whether overexpressing SREBP2 could overcome this reduction. HeLa HMGCR_clover WT cells were transduced with pHRSIN_HA-SREBP2 (HA-SREBP2) and selected using puromycin. A partial rescue of HMGCR_clover was consistently observed under sterol deplete conditions in hypoxia **(Figure 6.4 A)**, suggesting that increased SREBP2 levels could overcome the reduction of HMGCR_clover.

Next I determined the effect of reconstituting SREBP2 in hypoxia in SREBP2 deficient HeLa HMGCR_clover cells. Mixed population HMGCR_clover SREBP2 KO cells were created by Norbert Volkmar (Lehner laboratory) by transfecting cells with a sgRNA against SREBP2. SREBP2 KO cells displayed a significantly diminished increase in HMGCR_clover following sterol depletion in 21% oxygen as they were unable to mount any transcriptional response **(Figure 6.4 B)**. A small population of these cells were still able to stabilise HMGCR_clover following sterol depletion, revealing that a few were still expressing SREBP2, as would be expected with mixed KO populations **(Figure 6.4 B)**. HA-SREBP2 was well expressed in both control HMGCR_clover and SREBP2 KO cells, demonstrated by the increased HMGCR levels observed following sterol depletion when compared to the corresponding non-transduced control **(Figure 6.4 A, B)**, with only a small population in the SREBP2 KO cells not expressing HA-SREBP2 **(Figure 6.4 B)**. A partial rescue of HMGCR_clover was seen in the reconstituted SREBP2 KO cells following sterol depletion in hypoxia **(Figure 6.4 B)**. However, even in the absence of SREBP2 a small reduction of HMGCR_clover under sterol deplete conditions in hypoxia was still observed **(Figure 6.4 B)**, suggesting that additional factors aside from SREBP2 may still be involved in HMGCR regulation in low oxygen conditions.

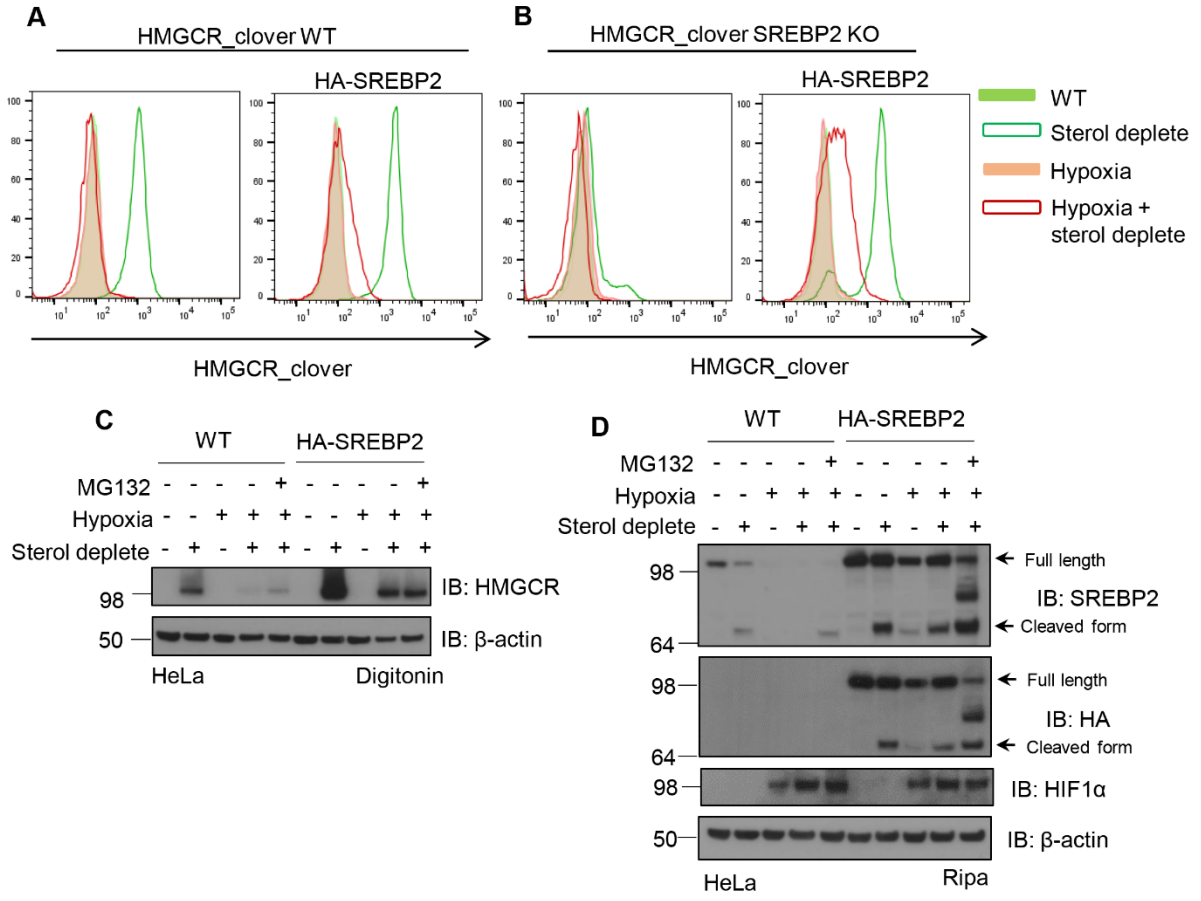

Figure 6.4. The reduction of HMGCR in sterol deplete conditions in hypoxia is partially rescued by SREBP2 overexpression.

HeLa HMGCR_clover **(A),** HMGCR_clover mixed population SREBP2 KO, **(B)** or HeLa WT **(C, D)** cells were transduced with pHRSIN_HA-SREBP2 and selected using puromycin. Following selection WT and HA-SREBP2 expressing cells were treated with sterol depletion for 42 hours, with the appropriate cells being incubated in hypoxia (1% O_2) for the final 18 hours. Cells were then analysed by live cell flow cytometry **(A, B)** or lysed in 1% digitonin **(C)** or RIPA **(D)** buffer and immunoblotted. Cells were treated with 10 μM MG132 4 hours prior to harvest where appropriate.

The ability of exogenous SREBP2 to restore HMGCR levels were also assessed in HeLa WT cells. Overexpression of HA-SREBP2 caused increased HMGCR stabilisation following sterol depletion, due to an increased transcriptional response. A partial rescue of HMGCR was also seen under sterol deplete conditions in hypoxia when compared to WT cells **(Figure 6.4 C)**, similarly to the HMGCR_clover cells.

Interestingly, protein levels of HA-SREBP2 were slightly reduced in low oxygen conditions but to a lesser extent than endogenous SREBP2 **(Figure 6.4 D)**. This finding supports data in **Figure 6.1**, and suggests that SREBP2 may be proteasomally degraded. Proteasome inhibition rescued HA-SREBP2, with a preference for the cleaved form, as previously observed. A slower migrating HA-SREBP2 species was also observed **(Figure 6.4 D)**. The identity of this species is not known, but it could be the C-terminus of SREBP2 following cleavage or a ubiquitinated intermediate.

6.2.3. SREBP2 is degraded by MARCH6 and TRC8

As proteasome inhibition partially rescued SREBP2 levels in hypoxia combined with sterol depletion, I wanted to determine which ubiquitin E3 ligases may be involved in SREBP2 degradation. As previously shown in **Chapter 3**, Sandra Stefanovic-Barrett (Nathan laboratory), carried out some mass spectrometry analysis in cells lacking two ER E3 ligases MARCH6 and TRC8 **(Figure 3.10)** (Stefanovic-Barrett *et al.*, 2018). This analysis showed that SREBP2 was enriched in cells depleted of these ligases, suggesting that they were involved in the basal degradation of SREBP2 in HeLa cells.

As SREBP2 protein levels were reduced in hypoxia, and this reduction was partially rescued by proteasome inhibition **(Figure 6.3)**, it was possible that MARCH6 and TRC8 were degrading SREBP2 under sterol deplete conditions in hypoxia. To investigate the potential role of MARCH6 and TRC8 degradation I used HeLa mCherry-CL1 WT and double MARCH6/TRC8 clonal KOs cells (created by Sandra Stefanovic-Barrett), and compared SREBP2 levels following sterol depletion combined with hypoxia. Full length SREBP2 levels were increased in the MARCH6/TRC8 null cells when compared to WT cells **(Figure 6.5 A)**, consistent with our prior mass spectrometry results (Stefanovic-Barrett *et al.*, 2018) **(Figure 3.10)**.

In conditions of hypoxia (1% oxygen), levels of SREBP2 were reduced in HeLa mCherry-CL1 WT cells, and although to a lesser extent, SREBP2 levels were also reduced in the MARCH6/TRC8 null cells **(Figure 6.5 A)**. This occurred predominantly under conditions of sterol depletion, but suggested that depletion of MARCH6 and TRC8 alone could not completely rescue SREBP2 levels in 1% oxygen. Interestingly, levels of SREBP2 were largely unchanged following

incubation in 1% oxygen alone in the MARCH6/TRC8 null cells, suggesting that perhaps degradation of SREBP2 was limited in these conditions **(Figure 6.5 A)**.

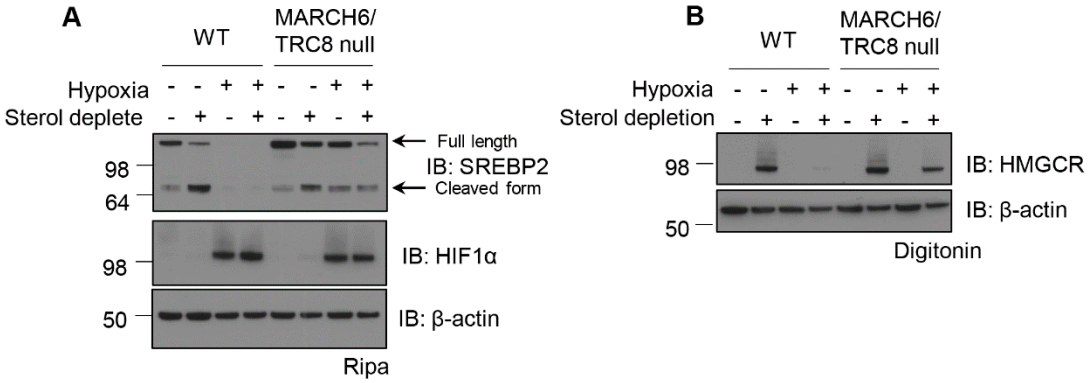

Figure 6.5. The turnover of SREBP2 is mediated by the E3 ligases MARCH6 and TRC8.

HeLa mCherry-CL1 WT and MARCH6/TRC8 double knockout clone cells (Stefanovic-Barrett *et al*, 2018) were sterol depleted for 42 hours, where appropriate cells were incubated in hypoxia (1% O_2) for the final 18 hours before being lysed in RIPA **(A)** or 1% digitonin **(B)** buffer and immunoblotted.

In accordance with increased SREBP2 levels, HMGCR levels were increased in the MARCH6/TRC8 null cells in 21% oxygen following sterol depletion **(Figure 6.5 B)**. Following sterol depletion combined with 1% oxygen, the MARCH6/TRC8 null cells showed a partial rescue of HMGCR when compared to WT cells **(Figure 6.5 B)**. This rescue was similar to that observed following HA-SREBP2 overexpression in HeLa WT cells **(Figure 6.5 D)**, further suggesting that increased levels of SREBP2 were able to partially compensate for the effect driven by low oxygen conditions.

Overall, these data suggested that MARCH6 and TRC8 were important for SREBP2 degradation in different oxygen tensions. However, as HMGCR levels were not fully rescued and some decrease in SREBP2 was observed in the MARCH6/TRC8 null cells, perhaps the reduction of SREBP2 observed in low oxygen conditions was not solely due to a lack of protein degradation.

6.2.4. Levels of active translation are decreased under conditions of hypoxia

To explore if other pathways may be important for the reduction of SREBP2 in hypoxia, I hypothesised that SREBP2 translation may be altered. Proteins are synthesised following a specific interaction between mRNA and ribosomes, which enables the incorporation of amino acids into a growing protein chain. For more efficient translation, mRNAs can be translated simultaneously by multiple ribosomes to form a 'polysome' (Warner *et al*., 1962; Noll, 2008). Polysomes are associated with active, efficient translation and can be studied using a technique called polysome profiling. Polysome profiling demonstrates the activity of cellular translational machinery at a specific point in time. It separates the actively translating transcripts (which are associated with polysomes) from the poorly translating transcripts using a sucrose gradient, and can be combined with immunoblotting or RNA analysis to assess which genes are associated with active translation. Prior studies have shown that polysomes are reduced under condtisions of low oxygen in multiple cell types, but further work is needed to understand the mechanism and specificity of this effect (Koritzinsky *et al*., 2007; Koumenis *et al*., 2002; Thomas & Johannes, 2007; Young *et al*., 2008).

Polysome profiles were generated from Hela WT cells in four different conditions: (i) normal media **(Figure 6.6 A)**, (ii) 42 hours sterol depletion **(Figure 6.6 B)**, (iii) 1% oxygen overnight **(Figure 6.6 C)**, and (iv) 42 hours sterol depletion with the final 18 hours additionally incubated in 1% oxygen **(Figure 6.6 D)**. The HeLa WT profile showed multiple polysome peaks suggesting an abundance of translation **(Figure 6.6 A)**, which was as expected and similar to that observed in other studies (Coudert *et al*., 2014). Following sterol depletion for 42 hours there appeared to be a slight reduction, but not ablation of polysomes suggesting active translation was still occurring, but perhaps slightly less efficiently **(Figure 6.6 B)**. Following overnight 1% oxygen incubation, polysomes were significantly reduced, coinciding with a dramatic increase in the 80S monomer ribosome **(Figure 6.6 C, D)**, suggesting that active translation was reduced in in low oxygen conditions and this was largely independent of sterol depletion.

Proteins were precipitated following polysome profiling **(Figure 6.6, fractions indicated by dotted purple lines)**, and immunoblotted. RPL4 (ribosomal protein L4) and RPS6 (ribosomal protein S6) are components of the 60S and 40S ribosomal subunits respectively, and were

correspondingly observed in fractions where the subunits are present. The majority of polysome fractions in the WT and sterol deplete sample contained both subunits **(Figure 6.6 A, B)**, whilst significantly less were observed in the hypoxic samples **(Figure 6.6 C, D)**, as expected from the lack of peaks in the corresponding profiles. Overall, these results suggested that active translation was reduced under conditions of hypoxia.

The immunoblots looking specifically at the SREBP2 protein level in the polysomes were unfortunately very difficult to interpret due to some fractions containing inconsistent protein levels and perhaps also due to the low steady state translation of SREBP2. Some translating SREBP2 was observed in WT cells **(Figure 6.6 A)**, whereas no translating SREBP2 was observed in hypoxia **(Figure 6.6 C, D)**, matching the general observed reduction in translation. To fully understand the extent in which translation is affecting proteins involved in the cholesterol synthesis pathway, these experiments would need to be repeated and the levels of RNA in the polysome fractions would need to be assessed and quantified. However, together my studies suggest that both SREBP2 degradation and translation are important for the reduced HMGCR levels observed in hypoxia, which overrides the normal sterol depletion response, inhibiting the cholesterol synthetic pathway when oxygen is limiting.

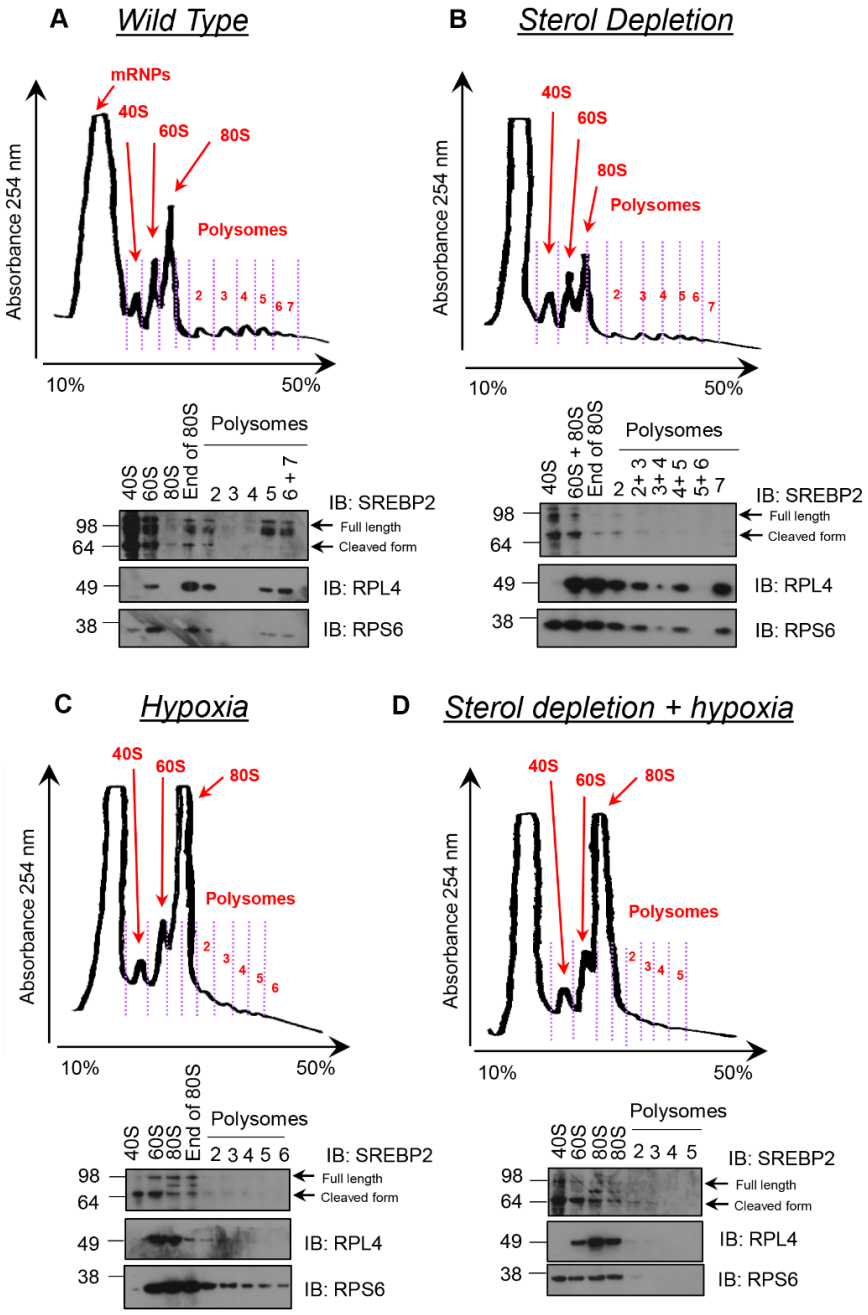

Figure 6.6. Translation is reduced in low oxygen conditions.

HeLa WT cells (A) were treated with sterol depletion for 42 hours (B, D), and where appropriate for the final 18 hours cells were incubated in hypoxia (1% O_2) (C, D). Cells were treated with 100 µg cyclohexamide for 10 minutes prior to harvesting in an NP40 based buffer. Samples were centrifuged on a 10-50% (w/v) sucrose gradient before being fractionated using an Isco fractionator and absorbance measured at 254 nm. Proteins were precipitated from the fractions using a methanol-chloroform precipitation before being analysed by immunoblotting. Polysome profiles were traced from the original profile (original profiles in Appendix). Polysome profiling was carried out twice, with representative traces used. Protein extraction was carried out from one experiment. *mRNPs = messenger ribosomal ribonucleoprotein particles (inactive mRNAs).*

6.3. Discussion

6.3.1. The dynamics of SREBP2 regulation

My data showed that protein levels of SREBP2 were decreased under low oxygen conditions. No change was observed in SREBP2 transcription **(Figure 6.1)**, suggesting that SREBP2 levels were likely to be regulated either by protein degradation or changes in translation. These results are consistent with the findings of Lewis *et al*., (2015) which showed that following incubation with lipid depleted FCS and hypoxia, SREBP2 mRNA levels did not significantly change when compared to lipid depleted FCS alone, whilst levels of activated SREBP2 were reduced. However, I observed a decrease in HMGCR transcription, but Lewis *et al*., (2015) did not. This discrepancy may relate to the method of sterol depletion. I used lipid depleted FCS combined with a statin, whereas Lewis *et al*., (2015) used lipid depleted FCS alone enabling the cells to still synthesise cholesterol.

Expression of exogenous SREBP2, partially rescued HMGCR levels under sterol deplete conditions in 1% oxygen when compared to WT cells **(Figure 6.4)**. However, exogenous SREBP2 was still reduced under conditions of low oxygen, suggesting that hypoxia is acting upstream of HMGCR and altering SREBP2 levels through decreased translation or increased protein degradation.

6.3.2. The role of MARCH6 and TRC8 in the regulation of SREBP2

Prior studies have shown individual roles for the ER E3 ligases, MARCH6 and TRC8, in the regulation of SREBP2 (Lee *et al*., 2010; Loregger *et al*., 2015), and work from the Nathan laboratory has recently suggested that both ligases together are required for its basal turnover (Stefanovic-Barrett *et al*., 2018) **(Figure 3.10; Figure 6.5 A)**. Loregger *et al*., (2015) showed that depletion of MARCH6 led to increased levels of SREBP2 target genes, and depletion of TRC8 has been shown to reduce levels of full length SREBP2 and subsequent target gene transcription (Lee *et al*., 2010). Additionally, TRC8 has a predicted SSD (Gemmill *et al*., 1998),

which leads to its stabilisation under conditions of low sterols (Lee *et al*., 2010), highlighting its potential importance in membrane lipid homeostasis. Our work showing that both MARCH6 and TRC8 are required for the full proteasomal degradation of selected tail-anchored proteins and those with amphipathic helices (Stefanovic-Barrett *et al*., 2018), may help explain why both ligases are involved in the degradation of SREBP2. However, the mechanism by which these ligases degrade SREBP2 must differ as SREBP2 is not a tail-anchored protein and is not thought to contain an amphipathic helical region.

SREBP2 is an ER membrane protein which is inserted into the ER co-translationally into a hairpin topology. SREBP2 has two transmembrane domains, a short ER luminal loop, and its N- and C-terminus reside within the cytosol (Hua *et al*., 1995) **(Figure 1.4)**. The intramembrane cleaving signal peptide peptidase (SPP) has been implicated in the cleavage of tail-anchored proteins, such as HO-1, within the ER membrane. The cleavage of HO-1 by SPP is required for its subsequent proteasomal degradation by MARCH6 and TRC8 (Boname *et al*., 2014; Stefanovic-Barrett *et al*., 2018). It is possible that SPP is able to cleave other proteins within the ER membrane such as SREBP2, and that this is required or enhances its proteasomal degradation. To assess whether SPP is involved in SREBP2 cleavage and degradation, treatment with a specific SPP inhibitor ($(Z\text{-}LL)_2$ ketone) could be used. Additionally, it is currently unclear which E2 enzymes are working with MARCH6 and TRC8 to degrade SREBP2, but UBE2G2 or UBE2J2 are likely candidates and this could be assessed using genetic depletions.

While proteasome inhibition or loss of MARCH6 and TRC8 increased SREBP2 levels and subsequent HMGCR levels, it is currently unclear whether this relates to increased degradation under conditions of low oxygen, or whether the stabilisation observed is from interrupting steady state degradation **(Figure 6.3; Figure 6.5 A)**. Increased basal levels of SREBP2 in the MARCH6/TRC8 null cells could result in increased HMGCR transcription, and therefore any steady state degradation of SREBP2 would take longer to reduce HMGCR transcription to WT levels. Alternatively, if MARCH6 and TRC8 were increasing the degradation of SREBP2 in low oxygen conditions causing a reduction in the *de novo* cholesterol synthesis pathway, then depletion of these ligases would consistently show increased HMGCR transcription in hypoxia.

Although depletion of MARCH6 and TRC8 partially stabilised SREBP2 under low oxygen conditions, full stabilisation was not observed, suggesting that SREBP2 levels were still being reduced independently of MARCH6 and TRC8. It is possible that another ligase is required for SREBP2 stabilisation under conditions of low oxygen, however, the CRISPR screen in **Chapter 3** did not pick up any E3 ligases, suggesting that depletion of a single ligase could not restore the loss of HMGCR. To fully assess the role of steady state or induced degradation of SREBP2 under conditions of low oxygen, the kinetics of SREBP2 need to be studied, particularly focusing on the full length form. This could be done by carrying out cycloheximide or radioactive pulse chase experiments and assessing the degradation of SREBP2 in both WT and MARCH6/TRC8 null cells under different oxygen tensions. It will also be important to assess the protein and transcript levels of both MARCH6 and TRC8 under low oxygen conditions, although there is no current evidence that they are regulated by oxygen levels.

The MARCH6 and TRC8 studies were carried out in HeLa cells which contained the mCherry-CL1 reporter **(Chapter 3)**. I decided to use these cells as they were confirmed MARCH6 and TRC8 null clones and were the cells used in the mass spectrometry analysis **(Figure 3.10)** (Stefanovic-Barrett *et al*., 2018). Although it is unlikely that this reporter had any effect on levels of HMGCR or SREBP2 in low oxygen tensions, future experiments should be carried out in WT cells where possible.

6.3.3. What does the reduction in polysomes in hypoxia mean for the cholesterol synthesis pathway?

Gene expression is regulated through transcription, translation and protein degradation, with each process regulated at multiple points. The mRNA being translated at any specific point in time reflects the functionality of the cell and can be quickly changed in response to any cellular stressors. Polysome profiling is a methodology to infer the translation status of a cell, and levels of polysomes are known to be reduced under certain stressors such as ER stress (Gülow *et al*., 2002).

SREBP2 protein levels are reduced in hypoxia, resulting in the transcriptional reduction of its target genes **(Figure 6.1; Figure 5.5)**. While proteasome inhibition or depletion of MARCH6 and TRC8 rescue SREBP2 levels, this is a partial rescue and changes in SREBP2 translation may also be involved. The polysome profiling suggested that active translation was significantly reduced under conditions of low oxygen largely independent of sterol depletion **(Figure 6.6)**. It is known that in addition to changes in transcription, mammalian cells also respond to low oxygen conditions by reducing their overall rate of protein translation, and that this is at least partially due to limited ATP availability (Liu *et al*., 2006). However, the degree to which specific mRNA species are affected vary greatly, with the translation of HIF target genes increasing under low oxygen conditions, whilst global translation is reduced, suggesting that there is some specificity (reviewed in Koritzinsky & Wouters, 2007).

Prior studies have shown that polysomes decrease following short periods of extreme hypoxia (<0.2% oxygen), and that the inhibition of protein translation is independent of HIF1α (Koritzinsky *et al*., 2007; Koumenis *et al*., 2002). I observed a reduction in polysomes in HeLa cells following incubation in 1% oxygen for 18 hours, suggesting that higher oxygen concentrations over a longer period of time can produce the same effect. Supporting this, Koumenis *et al*., (2002) observed a modest reduction in polysomes following incubation in 1% oxygen for 8 hours, whilst a further reduction was observed following 20 hours incubation (Thomas & Johannes, 2007). Phosphorylation of eIF2α reduces general protein synthesis during cellular stress such as activation of the UPR (reviewed by Wek *et al*., 2006) and has been previously shown to occur during extreme hypoxia (Koritzinsky *et al*., 2007; Koumenis *et al*., 2002). To assess if I was observing any reduction in translation driven by eIF2α phosphorylation, cells could be treated with ISRIB (integrated stress response inhibitor). ISRIB is a small molecule which specifically reverses the effects of eIF2α phosphorylation (Sidrauski *et al*., 2013, Sidrauski *et al*., 2015). Following ISRIB treatment, levels of components of the cholesterol synthesis pathway could be assessed to see if their protein levels were stabilised, or whether this effect was eIF2α independent.

Along with the decrease in polysomes observed following incubation in 1% oxygen, I also observed an increase in the 80S monomer, when compared to cells in 21% oxygen. This phenotype has been associated with defects in translation initiation (Coudert *et al*., 2014), and initiation defects have been reported to occur under low oxygen conditions (reviewed in

Fähling, 2009). In addition, a reduction in general translation under low oxygen conditions will correspond with a loss of most short lived proteins. This could begin to explain why the E3 ligase RNF145 is lost following overnight incubation in hypoxia **(Figure 5.3 C)**.

The collected fractions form the polysome profiling can be analysed in multiple ways. Here I precipitated the proteins to try to analyse what proteins were present in the polysome fractions. This technique had some limitations which made it difficult to draw many conclusions from my results. The main limitation was the lack of protein precipitated form certain samples. The protein from some fractions may have been lost during the precipitation process, however, the polysome fractions from the hypoxia samples had a very low protein concentration to begin with, so interpreting changes was challenging. Although the immunoblots do appear to match the polysome profiles, showing that general translation was reduced under low oxygen conditions. As I was specifically interested in SREBP2 translation, I assessed the levels of SREBP2 proteins in these fractions. The immunoblots show SREBP2 in some polysome fractions from the WT cells, but not in the other conditions, suggesting that SREBP2 translation was reduced **(Figure 6.6)**. However, due to limitations of the immunoblots and a lack of control proteins, these results are inconclusive and need repeating to assess any specificity. Additionally, the immunoblots appear to show both the full length and cleaved form of SREBP2 in some of the fractions. The presence of the cleaved form of SREBP2, could be due to the active translation of SREBP2 at the time of cycloheximide treatment prior to cell lysis, rather than the cleaved form itself being associated with ribosomes, as the cleaved form is the N-terminus and is recognised by the antibody. Another way these fractions could be analysed is by purifying the RNA and carrying out a northern blot or RT-qPCR which may give more accurate and quantitative results, and enable analysis of multiple genes of interest.

There is a clear reduction in translation under conditions of low oxygen, but it is as yet unclear how this impacts the *de novo* cholesterol synthesis pathway. Due to current experimental limitations it unclear whether SREBP2 is reduced translationally under low oxygen conditions, and if it is, whether this is a specific or general reduction. RNA analysis of the polysome fractions and assessing the abundance of SREBP2 mRNA in in the fractions under different oxygen tensions may help distinguish if this is a selective decrease in SREBP2 translation. Alternatively, RNA translation profiling would be a more sensitive method to examine if SREBP2 translation is selectively reduced in hypoxia. However, irrespective of the role of

SREBP2 translation in hypoxia, my studies do confirm that SREBP2 abundance is the principal determinant of HMGCR levels and activation of the cholesterol synthetic pathway under sterol deplete conditions in hypoxic environments.

6.4. Summary

In this chapter I have shown that cellular levels of SREBP2 were reduced at the protein level, but were not altered transcriptionally, under low oxygen conditions, and that this was partially rescued by increasing SREBP2 levels through exogenous expression. The decrease in SREBP2 observed in hypoxia was also partially rescued by proteasome inhibition and combined depletion of MARCH6 and TRC8, confirming that protein degradation is involved in the hypoxic regulation of SREBP2. However, a full rescue of SREBP2 or its target gene HMGCR, was never observed, suggesting that SREBP2 protein levels may also be regulated by translation. Polysome profiling showed that active translation, appeared to be reduced under low oxygen conditions, but these preliminary experiments did not conclusively show any specificity for proteins in the cholesterol synthesis pathway. While further work is needed to determine the relative contribution of impaired SREBP2 translation to the decrease in HMGCR levels following sterol depletion in hypoxic environments, my studies demonstrate a key role for SREBP2 in the hypoxic regulation of the cholesterol synthesis pathway.

Chapter 7: Summary and Discussion

7.1. Summary

In this thesis I have used genome wide CRISPR Cas9 forward genetic screens, and other biochemical approaches to study the regulation of two ERAD substrates, the CL1 degron and HMGCR. I have studied the regulation of these proteins in mammalian cells in response to two different stressors, accumulation of misfolded cytosolic proteins and low oxygen tensions.

The forward genetic screen in KBM7 cells carried out by Stephen Burr and Sandra Stefanovic-Barrett (Nathan Laboratory), was successful in identifying some components of the CL1 degradation machinery in mammalian cells. The components identified included the ER E3 ligases, MARCH6 and TRC8, the E2 ubiquitin conjugating enzyme, UBE2G2, and the ubiquitin binding protein, AUP1 (Stefanovic-Barrett *et al*., 2018). However, this screen was not saturating, so I sought to uncover novel components of this degradation pathway using a CRISPR/Cas9 forward genetic screen in HeLa cells. This screen identified another ER E2 ubiquitin conjugating enzyme, UBE2J2, and the recently identified ER insertase for moderately hydrophobic tail-anchored proteins, the EMC (Guna *et al*., 2018; Stefanovic-Barrett *et al*., 2018). I went on to show that UBE2J2 is the predominant E2 enzyme working with MARCH6 to degrade both the CL1 degron, and the endogenous MARCH6 substrate squalene monooxygenase. I also identified that the EMC was indirectly affecting CL1 degradation through its role in the ER insertion of UBE2J2 **(Figure 3.10)**. Additionally, mass spectrometry analysis in cells lacking MARCH6 and TRC8, carried out by Sandra Stefanovic-Barrett (Nathan Laboratory), identified that some components of the cholesterol synthesis pathway such as squalene monooxygenase, SREBP1 and SREBP2 were enriched in the ligase null cells, which started to focus my attention on this pathway (Stefanovic-Barrett *et al*., 2018) **(Figure 3.10)**.

HMGCR, the enzyme involved in the rate limiting step of cholesterol synthesis, is regulated at the transcriptional level by SREBP2, and at the post translational level by ERAD (Goldstein *et al*., 2006). The regulation of this pathway has been studied extensively under 21% oxygen. However, the cholesterol synthesis pathway is very oxygen dependent requiring 11 molecules

of oxygen to generate one molecule of cholesterol, and recently some studies have shown that HMGCR is degraded under sterol deplete conditions when oxygen is limited in a HIF1α dependent manner (Hwang *et al*., 2017; Nguyen *et al*., 2007). Utilising an endogenous fluorescent knock-in reporter construct, HMGCR_clover (Menzies *et al*., 2018), I demonstrate here that HMGCR levels are reduced under sterol deplete conditions in 1% oxygen, beyond the reduction of HMGCR observed following the chemical stabilisation of HIF1α using the PHD inhibitors DMOG or Roxadustat. In an attempt to uncover how oxygen was regulating HMGCR levels independently of HIF1α, I carried out a CRISPR Cas9 forward genetic screen in HeLa cells. Unfortunately this screen did not identify any novel regulators of HMGCR, so I started to focus my attention onto the regulation of HMGCR transcription by SREBP2. I uncovered that selected SREBP2 target genes were transcriptionally repressed under sterol deplete conditions in 1% oxygen, and that protein, but not mRNA, levels of SREBP2 were also decreased. Proteasome inhibition or depletion of the ER E3 ligases MARCH6 and TRC8 partially rescued SREBP2 levels under conditions of low oxygen. However, a complete rescue was never observed, suggesting that hindered degradation was not sufficient to fully overcome the effect of hypoxia. Prior studies have demonstrated that protein translation is reduced in conditions of low oxygen, therefore, I decided to assess this in sterol deplete and 1% oxygen conditions, with an initial focus on SREBP2. My data suggests that active translation is reduced in low oxygen conditions, however, further work is needed to assess any specificity for proteins involved in the cholesterol synthesis pathway.

To conclude, I propose a model whereby low oxygen tensions regulate the mammalian synthesis pathway in two ways **(Figure 7.1)**. Firstly, a HIF1α dependent mechanism described by Hwang *et al*., (2017), whereby transcription of the HIF1α target gene, INSIG2, increases HMGCR degradation under sterol deplete conditions **(Figure 7.1, left)**. Secondly, from my studies, I propose a HIF1α independent mechanism, whereby low oxygen tensions reduce the protein level of SREBP2, either through increased proteasomal degradation, decreased protein translation or a combination of both, which subsequently leads to a decrease in selected SREBP2 target genes, such as HMGCR, thereby reducing the *de novo* cholesterol synthesis pathway **(Figure 7.1, right)**.

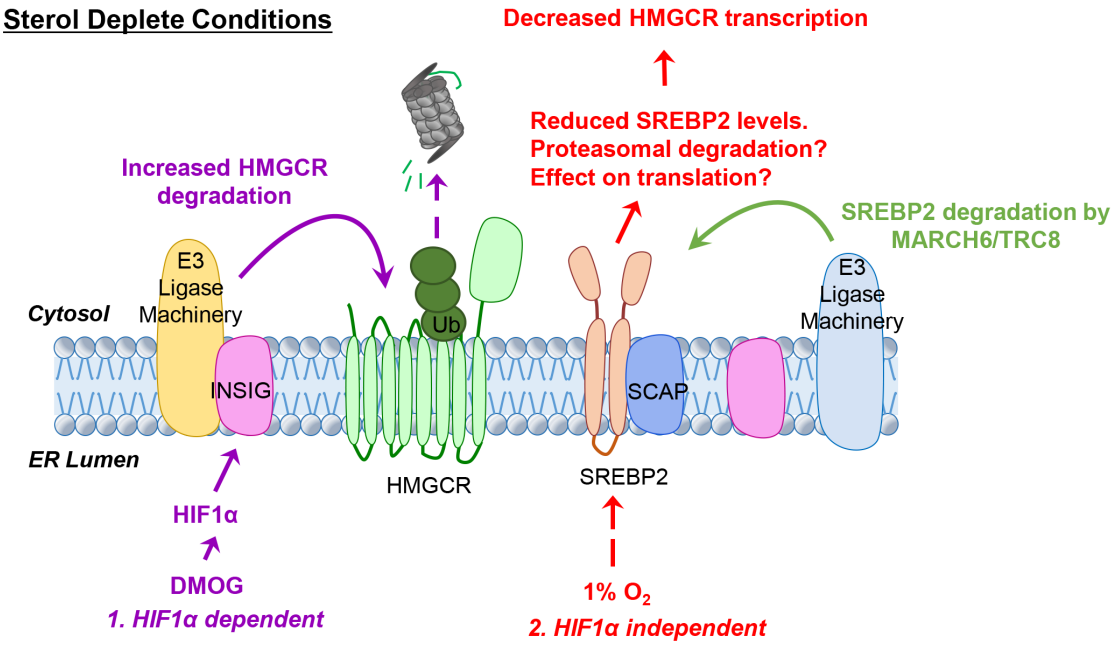

Figure 7.1. The role of hypoxia in regulating the cholesterol synthesis pathway

Proposed model showing how low oxygen conditions can regulate the *de novo* cholesterol synthesis pathway in mammalian cells under sterol deplete conditions. The HIF1α dependent pathway (left) described by Hwang *et al*, (2017). Stabilisation of HIF1α activates the transcription of Insig2, which increases the degradation of HMGCR through ERAD. The HIF1α independent pathway (right), whereby low oxygen tensions decrease the protein levels of SREBP2, either through increased proteasomal degradation or a reduction in protein translation. This reduction in SREBP2 leads to decreased transcription and therefore protein levels of its target genes including HMGCR, therefore reducing the activity of the *de novo* cholesterol synthesis pathway.

7.2. Discussion

7.2.1. Other methods to study the cholesterol synthesis pathway

I have predominantly studied the regulation of HMGCR and SREBP2 to indirectly interpret the activity of the *de novo* cholesterol synthesis pathway in mammalian cells. Although assessing levels of these proteins is important for understanding their regulation and should correlate with synthesis activity, alongside this it would be beneficial to investigate other components of the pathway. Looking at cholesterol itself though microscopy could increase our understanding of its localisation and total cellular levels, although visualising ER cholesterol is intrinsically challenging due to its low concentration. Filipin and theonellamides (TNM) labelled with fluorescent dyes such as BODIPY (TNM-BF), can be used to visualise cellular sterols using techniques such as immunofluorescence (IF) and immuno-gold electron microscopy (Edgar *et al*., 2016; Nishimura *et al*., 2013). These fluorescent probes could help to show any global changes in cholesterol levels under different oxygen tensions and give an idea of its cellular localisation. I have attempted IF microscopy using TNM-BF, however, due to the low level of cholesterol in the ER my preliminary experiments were inconclusive. This was likely due to insufficient sensitivity, and therefore any future microscopy experiments would need higher resolution in order to observe smaller changes. Another way to assess cellular levels of cholesterol and other sterols is through lipidomic experiments, where cellular lipids are extracted and identified through mass spectrometry analysis (Lydic & Goo, 2018). This is something I have also attempted using a fractionation protocol to isolate the ER membrane as described in Radhakrishnan *et al*., (2008). However, in my preliminary experiments controlling for the changes in cholesterol in different oxygen tensions proved challenging, but it is something that could be optimised for future experiments. Finally, rates of cholesterol synthesis could also be assessed by tracking the generation of cholesterol. Supporting my findings in other organisms, one study used ^{14}C-acetate incorporation to show that cholesterol biosynthesis was attenuated under conditions of low oxygen in the mouse fibroblast cell line, 3T3L1 (Zhu *et al*., 2014).

Throughout my thesis I have used treatment with a statin and LPDS over a period of up to 42 hours to deplete the cells of cholesterol by reducing the activity of both the cholesterol uptake and synthesis pathways. Another method that is widely used to deplete cholesterol from cells is with the cyclodextrin, methyl-β-cyclodextrin (MBCD). Although MBCD is able to deplete cholesterol much quicker than incubation with a statin and LPDS, it is not specific for cholesterol and is only able to remove sterols from the plasma membrane (López *et al.*, 2011; Mahammad & Parmryd, 2015). Therefore, treatment with MBCD is less physiologically relevant than a statin and LPDS, and is predominantly used for studying functions of cholesterol at the plasma membrane, not focusing on the cholesterol synthesis pathway.

7.2.2. Can statins be used to treat cancer?

Statins exert their pharmacological effect through inhibiting HMGCR. Not only does this inhibition reduce the amount of cholesterol synthesised, it also causes upregulation of SREBP mediated transcription of the LDLR, enabling the cell to uptake more circulating cholesterol to restore cholesterol homeostasis. Some studies have shown that statins display effects beyond that of lowering cholesterol levels, including decreasing oxidative stress, improving endothelial cell function, and modulating the immune system. These effects may be driven by the reduction of the mevalonate and isoprenoid pathway which are downstream of HMGCR, or by statins binding to and impacting other pathways in the cell (reviewed in Liao & Laufs, 2005).

For a long time the role of statins in cancer has been inconclusive. One study inappropriately suggested that statins and other lipid lowering drugs could be carcinogenic (Newman & Hulley, 1996). However, since then many studies have shown that this is not the case, citing factors including the studies use of elevated drug concentrations, and inadequate assays to interpret an effect in humans, as to why the effects are not conclusive (Dalen & Dalton, 1996). Additionally, later studies have not shown any association between statins and increased risk of cancer (Boudreau *et al.*, 2010). More recently there have been discrepancies as to whether statin treatment is protective against tumour development or whether they have no significant effect. A number of studies have shown an association between statin treatment

and a reduced risk of cancers including: colorectal (Poynter *et al*., 2005), breast (Beckwitt *et al*., 2018; Kochhar *et al*., 2005), prostate (Solomon & Freeman, 2008) and lung (Khurana *et al*., 2007). Additionally, Clendening *et al*., (2010) showed that increased levels of HMGCR drives tumour formation in mice and high HMGCR levels appear to correlate with poor prognosis in breast cancer patients, supporting a role for targeting HMGCR to treat some cancers. However, three large retrospective meta-analyses (Browning & Martin, 2007; Dale *et al*., 2006; Farooqi *et al*., 2018) and a comprehensive clinical trial review (Boudreau *et al*., 2010), concluded that there were no significant effects of statin treatment on incidence or death rate of any of the cancer subtypes studied including breast, colorectal, and prostate. Therefore, the topic still remains controversial and unresolved.

Many regions of tumours experience hypoxia and nutrient depletion, particularly their centres where there are likely to be fewer blood vessels and necrosis (Petrova *et al*., 2018). If statins exert their cholesterol synthesis lowering property on cancer cells, then my studies suggest that statins would not have a significant effect in hypoxic regions of the tumour, as the activity of this pathway would already be reduced. In less hypoxic regions of tumours, statins may be able to reduce the cholesterol synthesis pathway further, potentially having an effect on their growth. Therefore, my results may help to explain some of the discrepancies observed in the effect of statins in cancers, however, further research is needed to understand the effect of targeting the cholesterol synthesis pathway in cancers.

7.2.3. The cholesterol synthesis pathway in glioblastoma tumours

The brain is a cholesterol rich environment containing almost 20% of the body's total cholesterol, however, as circulating cholesterol is unable to readily cross the blood brain barrier, under normal conditions cells in the brain rely on *de novo* cholesterol synthesis (Björkhem & Meaney, 2004). This creates a unique environment to study the cholesterol synthesis pathway independently of cholesterol uptake. Glioblastoma (GBM) tumours are an aggressive form of cancer that originate in glial cells in the brain, and studies have shown the importance of cholesterol levels in GBM progression. Increasing GBM cell cholesterol efflux, through the activation of the transcription factor liver X receptor (LXR), was shown to induce

GBM cell death (Villa *et al*., 2016), whilst poor GBM patient prognosis has been associated with the upregulation of the cholesterol synthesis pathway (Kambach *et al*., 2017; Lewis *et al*., 2015). In addition, Lewis *et al*., (2015) studied GBM cells in conditions of low oxygen, and demonstrated that in hypoxia combined with sterol depletion, SREBP activity, particularly SREBP1, was induced and necessary for cell survival, proposing that modulating SREBP activity could be a potential therapeutic target.

Amplification or mutation of the epidermal growth factor receptor (EGFR) is observed in some GBM patients. Interestingly, increased EGFR signalling in GBM cells leads to increased cholesterol uptake through the LDLR in an SREBP1 dependent manner, and a concurrent decrease cholesterol synthesis (Guo *et al*., 2011). This clever adaptation of GBM cells to switch from relying on cholesterol synthesis to cholesterol uptake is thought to occur to conserve energy, and remove feedback mechanisms associated with the cholesterol synthesis pathway, to potentiate GBM cell growth (reviewed in Liu & Mischel, 2018). Utilising this adaptation of GBM cells could be particularly useful for increasing our understanding of how low oxygen tensions independently affects the both the cholesterol synthesis and uptake pathway in WT and EGFR mutated cells. This could help uncover the role hypoxia plays in altering disease states, and whether targeting cholesterol pathways could be beneficial therapeutically.

7.2.4. How is protein translation affected in hypoxia?

Changes in protein translation produce a quicker response than transcriptional changes, enabling cells to rapidly adapt to their environment. It is known that general protein translation is reduced in hypoxia, however, selected mRNAs remain efficiently translated to drive the hypoxia response mediated by the HIFs. In eukaryote cells, protein translation can be initiated through cap-dependent or cap-independent mechanisms. The majority of protein translation is initiated through cap-dependent mechanisms, which requires machinery such as the eIFs. Cap-independent translation involves an internal ribosome entry site (IRES) within the 5' untranslated region (UTR) of the mRNA which is able to recruit ribosomal subunits to initiate translation independent of the eIFs (reviewed by Hellen & Sarnow, 2001). Studies have shown that cap-dependent, but not IRES dependent, translation is reduced in hypoxia through

the activation of ER stress leading to eIF2α phosphorylation, and inhibition of the mTOR pathway **(Figure 5.9 A)** (Lai *et al*., 2016; Liu *et al*., 2006; reviewed by Liu & Simon, 2004). IRES mediated translation is thought to account for the translation of some genes in hypoxia (Stein *et al*., 1998), however, a study suggested that this is unlikely to be the case for all hypoxic genes (Young *et al*., 2008), so the precise mechanism by which specific proteins are translated in hypoxia is still largely unknown.

Damiano *et al*., (2010) identified an IRES site in the 5' UTR of SREBP1, and showed that translation was protected under conditions when global cap-dependent translation was reduced. This supports other studies suggesting that SREBP1 is more stable in hypoxia (Lewis *et al*., 2015) and is essential for hypoxic survival (Jain *et al*., 2020). No IRES site has been identified in SREBP2 and supporting this, in my studies I observe a decrease in SREBP2 protein level suggesting that it is not stabilised. As SREBP1 is able to activate the transcription of the LDLR, it would be interesting to assess if the stabilisation of this transcription factor was responsible for the transcription of the LDLR under sterol deplete conditions in hypoxia and what effect this has on the cholesterol uptake pathway.

7.3. Future directions

I have uncovered a HIF1α independent mechanism in mammalian cells, whereby low oxygen tensions reduce the levels of proteins involved in the cholesterol synthesis pathway. However, several questions remain unresolved, including:

- How does the regulation of SREBP2 in low oxygen conditions affect the cholesterol synthesis pathway?
- How does a reduction in protein translation in hypoxia affect cholesterol synthesis?
- What is the role of the hypoxic regulation of cholesterol synthesis in disease?

7.3.1. Understanding the degradation dynamics of SREBP2

I have shown that SREBP2 protein levels, are reduced under conditions of 1% oxygen, and this appears to be somewhat independent of cellular sterol levels. It will be interesting to properly assess the dynamics of SREBP2 degradation in hypoxia, to try and understand whether the decrease observed under low oxygen conditions is due to steady state turnover, or induced degradation of SREBP2. This could be initially achieved by carrying out cycloheximide or radioactive pulse chase experiments under conditions of 21% and 1% oxygen tensions, to analyse any change in the half-life of SREBP2. Additionally, to try and understand the involvement of the E3 ligases MARCH6 and TRC8, these experiments could be carried out in ligase null cells to see if the degradation dynamics of SREBP2 are altered.

7.3.2. How is translation affected in low oxygen conditions and how does this affect the cholesterol synthesis pathway?

Consistent with prior studies, my experiments showed that active translation, in the form of polysomes, is dramatically reduced under conditions of 1% oxygen. However, my results following protein precipitation of the fractions had several limitations and it was not possible

to conclusively show how this affected proteins in the cholesterol synthesis pathway and whether there was any protein specificity. Therefore, it will be beneficial to carry out further experiments focusing on translation. Initially, extracting the mRNA from the polysome profiling fractions and carrying out RT-qPCR on proteins of interest such as SREBP2, SREBP1, HMGCR and the LDLR will provide more specificity. However, it may also be of interest to analyse the full spectrum of mRNAs associated with actively translating ribosomes under the conditions of interest using deep sequencing and ribosomal profiling.

7.3.3. The importance of the hypoxic regulation of the cholesterol synthesis pathway in disease

My studies suggest that the relative abundance of cholesterol, or oxygen availability within the cellular environment will determine the ability of a cell to synthesise cholesterol. The biological implications of these findings will be broad but GBM tumours appear to be an intriguing biological system to examine further. Delineating the cholesterol synthesis and cholesterol uptake pathways using GBM cells with EGFR mutations (which predominantly rely on cholesterol uptake) or without (which rely on cholesterol synthesis), may help to clarify the role of HMGCR inhibition as a potential treatment in GBM. Speculating from my data, hypoxia should not have a large effect on GBM cells with mutant EGFR, as their cholesterol synthesis pathway is already downregulated, whereas hypoxia should have an effect on cells without mutant EGFR, potentially affecting cell survival, as these cells rely on cholesterol synthesis. As well as increasing our understanding of how oxygen concentrations affect cholesterol synthesis and uptake, this could be important for developing further treatment strategies for patients with GBM.

7.3.4. Other future directions and outstanding questions

Most tissues experience a range of oxygen concentrations, and the extent to which hypoxia plays a physiological or pathological role in adapting to oxygen concentrations differs between

tissues. My studies have focused on the extremes of oxygen availability (21% and 1%), but it would be interesting to assess how this pathway is affected in a range of oxygen concentrations, from 21-0%. I would expect an intermediate effect in moderate oxygen concentrations, whilst severe effects in anoxic (0% oxygen) conditions, and this could be informative for different disease states.

Additionally, it may become important to delineate the effect of hypoxia on cholesterol uptake. This could be done both through analysis of GBM cells, but also through analysing the cholesterol uptake pathway in other cell types. I have observed that transcription of the LDLR, which is a target gene of both SREBP1 and SREBP2, does not decrease under low oxygen conditions, but the cellular levels of the LDLR and the processing of LDL within cells has not been examined. This could be done through cell surface staining of the LDLR or tracking the uptake of cholesterol through this pathway by microscopy or labelling. As SREBP1 is involved in regulating transcription of the LDLR, and is known to contain an IRES site which is likely to be responsible for its increased stability in hypoxia over SREBP2, it will be interesting to assess levels of SREBP1 under my experimental conditions. Understanding the differences in the translation or stability of the two SREBP transcription factors may help explain the role of the cholesterol uptake pathway under low oxygen conditions.

Finally, it would also be interesting to assess what happens to other proteins involved in the cholesterol synthesis pathway in conditions of hypoxia. Squalene monooxygenase, similarly to SREBP2, is an endogenous substrate of MARCH6 (Stefanovic-Barrett *et al*., 2018; Zelcer *et al*., 2014), and is the enzyme involved in the second rate limiting step of cholesterol synthesis. The degradation of squalene monooxygenase, mediated by UBE2J2 and MARCH6, is regulated by its amphipathic N-terminus **(Chapter 3)**, which promotes its degradation when levels of cholesterol are high or squalene (the substrate for the reaction catalysed squalene monooxygenase) are low within the ER membrane (Gill *et al*., 2011; Yoshioka *et al*., 2020). Squalene monooxygenase is already therapeutically targeted in yeast as an anti-fungal (Rodrigues, 2018), and is a promising candidate for future clinical studies with the development of human specific inhibitors (Horie *et al*., 1990; Padyana *et al*., 2019). Given the role of MARCH6 and TRC8 in SREBP2 degradation, it is possible that hypoxia may also alter the abundance of squalene monooxygenase and provide a further hypoxic regulated step within the cholesterol synthetic pathway.

In summary, exploring the role of oxygen gradients in the regulation of other components of the cholesterol synthesis and uptake pathway including SREBP1, the LDLR and squalene monooxygenase, could provide a more mechanistic insight into how low oxygen conditions regulate cholesterol synthesis and its role in disease.

Appendix

Top hits from the CRISPR Cas9 forward genetic screens

1. HeLa mCherry-CL1 mCherry^{MEDIUM} vs unsorted library

Hit	*Gene name*	*p-value (-log)*	*FDR*	*Comment*
1	UROD	6.58	0.0037	Uroporphyrinogen Decarboxylase
2	SPEN	6.11	0.0037	Transcriptional Repressor
3	EMC6	6.11	0.0037	Component of EMC
4	BLCAP	6.11	0.0037	Apoptosis Inducing Factor
5	UBE2J2	5.89	0.0050	ER membrane E2 enzyme
6	SELO	5.31	0.015	Mitochondrial selenoprotein
7	SLC25A18	5.26	0.015	Mitochondrial solute carrier Family
8	EMC2	4.88	0.032	Component of EMC
9	EMC1	4.80	0.034	Component of EMC
10	PTGER3	4.62	0.043	Prostaglandin E Receptor 3
11	HAO2	4.58	0.043	Peroxisome Hydroxyacid Oxidase 2
12	MFNG	4.57	0.043	glycosyltransferase
13	EMC3	4.41	0.054	Component of EMC
14	NBPF4	4.39	0.054	Neuroblastoma Breakpoint Family Member 4
15	PI4KA	4.37	0.054	phosphatidylinositol (PI) 4-kinase
27	UBE2D3	3.80	0.11	Cytosolic E2 enzyme
33	UBE2K	3.54	0.17	Cytosolic E2 enzyme

Supplementary table 1. **Top hits from the HeLa mCherry-CL1 UBE2G2 null screen, mCherry^{MEDIUM}**

List of top 15 hits, with the addition of two E2 enzymes of interest, form the HeLa mCherry-CL1 UBE2G2 null screen, sort 2 mCherry^{MEDIUM} population, analysed using the MAGECK algorithm**.**

2. HeLa mCherry-CL1 mCherry^{HIGH} vs unsorted library

Hit	*Gene name*	*p-value (-log)*	*FDR*	*Comment*
1	SPEN	6.57	0.0025	Transcriptional Repressor
2	UROD	6.57	0.0025	Uroporphyrinogen Decarboxylase
3	TBC1D10A	6.11	0.0037	TBC1 Domain Family Member 10A
4	LMF2	6.11	0.0037	Lipase protein maturation factor
5	YDJC	5.74	0.0069	Carbohydrate Deacetylase
6	BLCAP	5.63	0.0074	Apoptosis Inducing Factor
7	MFNG	5.26	0.013	glycosyltransferase
8	SELO	5.26	0.013	Mitochondrial selenoprotein
9	SUSD2	5.22	0.013	Sushi Domain-Containing Protein 2 – potential cytokine receptor
10	NUP50	4.88	0.024	Nuclear pore protein
11	SDF2L1	4.86	0.024	Stromal Cell Derived Factor 2 Like 1
12	ZNF280B	4.77	0.027	Transcription factor
13	SEC14L2	4.60	0.037	Lipid-binding protein
14	KLHDC7B	4.48	0.045	Kelch Domain-Containing Protein 7B
15	CRYBB1	4.43	0.047	Crystallins

Supplementary table 2. Top hits from the HeLa mCherry-CL1 UBE2G2 null screen, mCherry^{HIGH}

List of top 15 hits form the HeLa mCherry-CL1 UBE2G2 null screen, sort 2 mCherry^{HIGH} population, analysed using the MAGECK algorithm.

3. HeLa HMGCR_clover clover^{MEDIUM} vs unsorted library - MiniSeq

Hit	*Gene name*	*p-value (-log)*	*FDR*	*Comment*
1	UBE2G2	6.62	0.0025	ER membrane associated E2 enzyme
2	AUP1	6.62	0.0025	ER ubiquitin binding protein
3	FAF2	5.66	0.015	Fas Associated Factor Family Member 2
4	PCTP	4.73	0.095	Phosphatidylcholine Transfer Protein
5	CFD	4.14	0.3	Complement Factor D

Supplementary table 3. Top hits from MiniSeq analysis of the HeLa HMGCR_clover screen, clover^{MEDIUM}

List of top hits from the HMGCR_clover screen, sort 2 clover^{MEDIUM}, under sterol deplete conditions in hypoxia from the MiniSeq analysed using the MAGECK algorithm**.**

4. HeLa HMGCR_clover clover^{MEDIUM} vs unsorted library - HiSeq

Hit	*Gene name*	*p-value (-log)*	*FDR*	*Comment*
1	UBE2G2	6.62	0.0017	ER membrane associated E2 enzyme
2	YEATS4	6.62	0.0017	YEATS Domain-Containing Protein 4
3	AUP1	5.77	0.0087	ER ubiquitin binding protein
4	FAF2	5.25	0.023	Fas Associated Factor Family Member 2
5	CTNNA3	4.52	0.10	Catenin Alpha 3

Supplementary table 4. Top hits from HiSeq analysis of the HeLa HMGCR_clover screen, clover^{MEDIUM}

List of top hits from the HMGCR_clover screen, sort 2 clover^{MEDIUM}, under sterol deplete conditions in hypoxia from the HiSeq analysed using the MAGECK algorithm**.**

5. HeLa HMGCR_clover clover^{HIGH} vs unsorted library - HiSeq

Hit	*Gene name*	*p-value (-log)*	*FDR*	*Comment*
1	UBE2G2	6.62	0.0025	ER membrane associated E2 enzyme
2	HIST1H3I	6.62	0.0025	Histone Cluster 1 H3 Family Member I
3	PGA3	5.58	0.018	Pepsinogen A3
4	TMEM14C	4.76	0.90	Transmembrane Protein 14C
5	AL590714.1	4.19	0.26	Novel transcript
6	ZNF862	4.12	0.26	Zinc Finger Protein 862

Supplementary table 5. Top hits from HiSeq analysis of the HeLa HMGCR_clover screen, clover^{HIGH}

List of top hits from the HMGCR_clover screen, sort 2 clover^{HIGH}, under sterol deplete conditions in hypoxia from the HiSeq analysed using the MAGECK algorithm**.**

Polysome profiling original traces

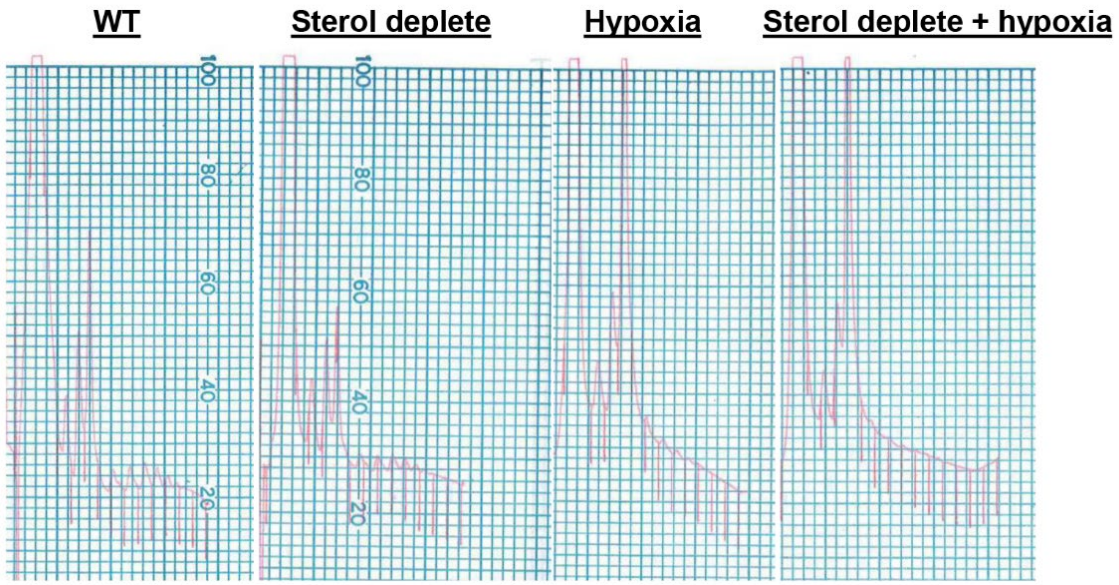

Supplementary figure 1. Original polysome profile traces from the spectrometer

These traces were traced and scanned to create **Figure 6.6.** The regular interspaced vertical lines represent the change of fraction collected and subsequently used for western blot analysis.

References

Aguzzi, A., & O'Connor, T. (2010). Protein aggregation diseases: pathogenicity and therapeutic perspectives. *Nature Reviews Drug Discovery*.

Arsham, A. M., Howell, J. J., & Simon, M. C. (2003). A novel hypoxia-inducible factor-independent hypoxic response regulating mammalian target of rapamycin and its targets. *Journal of Biological Chemistry*, *278*(32), 29655–29660.

Balchin, D., Hayer-Hartl, M., & Hartl, F. U. (2016). In vivo aspects of protein folding and quality control. *Science*. 353(6294).

Baldridge, R. D., & Rapoport, T. A. (2016). Autoubiquitination of the Hrd1 Ligase Triggers Protein Retrotranslocation in ERAD. *Cell*, *166*(2), 394–407.

Barrangou, R., Fremaux, C., Deveau, H., Richards, M., Boyaval, P., Moineau, S., Romero, D. A., & Horvath, P. (2007). CRISPR provides acquired resistance against viruses in prokaryotes. *Science*. 315(5819).

Bays, N. W., Gardner, R. G., Seelig, L. P., Joazeiro, C. a, & Hampton, R. Y. (2001). Hrd1p/Der3p is a membrane-anchored ubiquitin ligase required for ER-associated degradation. *Nature Cell Biology*.

Beckwitt, C. H., Brufsky, A., Oltvai, Z. N., & Wells, A. (2018). Statin drugs to reduce breast cancer recurrence and mortality 11 Medical and Health Sciences 1112 Oncology and Carcinogenesis. In *Breast Cancer Research* (Vol. 20, Issue 1). BioMed Central Ltd.

Bence, N. F., Bennett, E. J., & Kopito, R. R. (2005). Application and Analysis of the GFPu Family of Ubiquitin-Proteasome System Reporters. In *Methods in enzymology* (Vol. 399, pp. 481–490).

Bennett, E. J., Bence, N. F., Jayakumar, R., & Kopito, R. R. (2005). Global Impairment of the Ubiquitin-Proteasome System by Nuclear or Cytoplasmic Protein Aggregates Precedes Inclusion Body Formation. *Molecular Cell*, *17*(3), 351–365.

Bernardi, R., Guernah, I., Jin, D., Grisendi, S., Alimonti, A., Teruya-Feldstein, J., Cordon-Cardo, C., Celeste Simon, M., Rafii, S., & Pandolfi, P. P. (2006). PML inhibits HIF-1α translation and neoangiogenesis through repression of mTOR. *Nature*, *442*(7104), 779–785.

Berra, E., Benizri, E., Ginouvès, A., Volmat, V., Roux, D., & Pouysségur, J. (2003). HIF prolyl-hydroxylase 2 is the key oxygen sensor setting low steady-state levels of HIF-1α in normoxia. *EMBO Journal*, *22*(16).

Björkhem, I., & Meaney, S. (2004). Brain Cholesterol: Long Secret Life Behind a Barrier. *Arteriosclerosis, Thrombosis, and Vascular Biology*, *24*(5), 806–815.

Bloch, K. (1965). The Biological Synthesis of Cholesterol. *Science*, *150*(3692), 19–28.

Bloch, Konrad, & Rittenberg, D. (1942). *ON THE UTILIZATION OF ACETIC ACID FOR CHOLESTEROL FORMATION*. J. Biol. Chem. 145, 625-636.

Boname, J. M., Bloor, S., Wandel, M. P., Nathan, J. A., Antrobus, R., Dingwell, K. S., Thurston, T. L., Smith, D. L., Smith, J. C., Randow, F., & Lehner, P. J. (2014). Cleavage by signal peptide peptidase is required for the degradation of selected tail-anchored proteins. *The Journal of Cell Biology*, *205*(6), 847–862.

Boudreau, D. M., Yu, O., & Johnson, J. (2010). Statin use and cancer risk: A comprehensive review. In *Expert Opinion on Drug Safety* (Vol. 9, Issue 4, pp. 603–621). NIH Public Access.

Brodsky, J. L., & Vembar, S. S. (2008). One step at a time: endoplasmic reticulum-associated degradation. *Nature Reviews. Molecular Cell Biology*.

Brown, M. S., Dana, S. E., & Goldstein, J. L. (1973). *Regulation of 3-Hydroxy-3-Methylglutaryl Coenzyme A Reductase Activity in Human Fibroblasts by Lipoproteins (cholesterol biosynthesis/enzyme suppression and stimulation/low-density and high-density lipoproteins)* (Vol. 70, Issue 7).

Brown, M. S., & Goldstein, J. L. (1976). Receptor-mediated control of cholesterol metabolism. Study of human mutants has disclosed how cells regulate a substance that is both vital and lethal. *Science*, *191*(4223), 150–154.

Brown, M. S., & Goldstein, J. L. (1997). The SREBP pathway: Regulation of cholesterol metabolism by proteolysis of a membrane-bound transcription factor. In *Cell* (Vol. 89, Issue 3, pp. 331–340). Cell Press.

Browning, D. R. L., & Martin, R. M. (2007). Statins and risk of cancer: A systematic review and metaanalysis. In *International Journal of Cancer* (Vol. 120, Issue 4, pp. 833–843). Int J Cancer.

Brugarolas, J., Lei, K., Hurley, R. L., Manning, B. D., Reiling, J. H., Hafen, E., Witters, L. A., Ellisen, L. W., & Kaelin, W. G. (2004). Regulation of mTOR function in response to hypoxia by REDD1 and the TSC1/TSC2 tumor suppressor complex. *Genes and Development*, *18*(23), 2893–2904.

Bruick, R. K., & McKnight, S. L. (2001). A conserved family of prolyl-4-hydroxylases that modify HIF. *Science*, *294*(5545), 1337–1340.

Burg, J. S., & Espenshade, P. J. (2011). Regulation of HMG-CoA reductase in mammals and yeast. In *Progress in Lipid Research* (Vol. 50, Issue 4, pp. 403–410). NIH Public Access.

Burg, J. S., Powell, D. W., Chai, R., Hughes, A. L., Link, A. J., & Espenshade, P. J. (2008). Insig Regulates HMG-CoA Reductase by Controlling Enzyme Phosphorylation in Fission Yeast. *Cell Metabolism*, *8*(6), 522–531.

Burr, S. P., Costa, A. S. H., Grice, G. L., Timms, R. T., Lobb, I. T., Freisinger, P., Dodd, R. B., Dougan, G., Lehner, P. J., Frezza, C., & Nathan, J. A. (2016). Mitochondrial Protein Lipoylation and the 2-Oxoglutarate Dehydrogenase Complex Controls HIF1α Stability in Aerobic Conditions. *Cell Metabolism*, *24*(5), 740–752.

Byrne, P., Cullinan, J., & Smith, S. M. (2019). Statins for primary prevention of cardiovascular disease. In *The BMJ* (Vol. 367). BMJ Publishing Group.

Carette, J. E., Guimaraes, C. P., Varadarajan, M., Park, A. S., Wuethrich, I., Godarova, A., Kotecki, M., Cochran, B. H., Spooner, E., Ploegh, H. L., & Brummelkamp, T. R. (2009). Haploid genetic screens in human cells identify host factors used by pathogens. *Science (New York, N.Y.)*.

Carreau, A., Hafny-Rahbi, B. El, Matejuk, A., Grillon, C., & Kieda, C. (2011). Why is the partial oxygen pressure of human tissues a crucial parameter? Small molecules and hypoxia. *Journal of Cellular and Molecular Medicine*, *15*(6), 1239–1253.

Carvalho, P., Goder, V., & Rapoport, T. A. (2006). Distinct Ubiquitin-Ligase Complexes Define Convergent Pathways for the Degradation of ER Proteins. *Cell*, *126*(2), 361–373.

Carvalho, P., Stanley, A. M., & Rapoport, T. A. (2010). Retrotranslocation of a misfolded luminal ER protein by the ubiquitin-ligase hrd1p. *Cell*, *143*(4), 579–591.

Castro, A. F., Rebhun, J. F., Clark, G. G., & Quilliam, L. A. (2003). Rheb binds TSC2 and promotes S6 kinase activation in a rapamycin- and farnesylation-dependent manner. *J Biol Chem*, *278*, 32493–32496.

Chen, N., Hao, C., Peng, X., Lin, H., Yin, A., Hao, L., Tao, Y., Liang, X., Liu, Z., Xing, C., Chen, J., Luo, L., Zuo, L., Liao, Y., Liu, B.-C., Leong, R., Wang, C., Liu, C., Neff, T., … Yu, K.-H. P. (2019). Roxadustat for Anemia in Patients with Kidney Disease Not Receiving Dialysis. *New England Journal of Medicine*, *381*(11), 1001–1010.

Chen, S., & Sang, N. (2016). Hypoxia-Inducible Factor-1: A Critical Player in the Survival Strategy of Stressed Cells. *Journal of Cellular Biochemistry*, *117*(2), 267–278.

Chiarella, S. E., Rabin, E. E., Ostilla, L. A., Flozak, A. S., & Gottardi, C. J. (2018). αT-catenin: A developmentally dispensable, disease-linked member of the α-catenin family. *Tissue Barriers*, *6*(2), e1463896.

Chilov, D., Camenisch, G., Kvietikova, I., Ziegler, U., Gassmann, M., & Wenger, R. H. (1999). Induction and nuclear translocation of hypoxia-inducible factor-1 (HIF-1): Heterodimerization with ARNT is not necessary for nuclear accumulation of HIF-1α. *Journal of Cell Science*, *112*(8).

Chipurupalli, S., Kannan, E., Tergaonkar, V., D'andrea, R., & Robinson, N. (2019). Hypoxia induced ER stress response as an adaptive mechanism in cancer. In *International Journal of Molecular Sciences* (Vol. 20, Issue 3). MDPI AG.

Chitwood, P. J., Juszkiewicz, S., Guna, A., Shao, S., & Hegde, R. S. (2018). EMC Is Required to Initiate Accurate Membrane Protein Topogenesis. *Cell*, *175*(6).

Chong-Kopera, H., Inoki, K., Li, Y., Zhu, T., Garcia-Gonzalo, F. R., Rosa, J. L., & Guan, K. L. (2006). TSC1 stabilizes TSC2 by inhibiting the interaction between TSC2 and the HERC1 ubiquitin ligase. *Journal of Biological Chemistry*, *281*(13), 8313–8316.

Christianson, J. C., Olzmann, J. A., Shaler, T. A., Sowa, M. E., Bennett, E. J., Richter, C. M., Tyler, R. E., Greenblatt, E. J., Wade Harper, J., & Kopito, R. R. (2011). Defining human ERAD networks through an integrative mapping strategy. *Nature Cell Biology*, *14*(1), 93–105.

Christianson, J. C., & Ye, Y. (2014). Cleaning up in the endoplasmic reticulum: ubiquitin in charge. *Nature Structural & Molecular Biology*.

Chua, N. K., Hart-Smith, G., & Brown, A. J. (2019). Non-canonical ubiquitination of the cholesterol-regulated degron of squalene monooxygenase. *Journal of Biological Chemistry*, *294*(20).

Chun, K. T., Bar-Nun, S., & Simoni, R. D. (1990). The regulated degradation of 3-hydroxy-3-methylglutaryl-CoA reductase requires a short-lived protein and occurs in the endoplasmic reticulum. *The Journal of Biological Chemistry*, *265*(35), 22004–22010.

Clendening, J. W., Pandyra, A., Boutros, P. C., El Ghamrasni, S., Khosravi, F., Trentin, G. A., Martirosyan, A., Hakem, A., Hakem, R., Jurisica, I., & Penn, L. Z. (2010). Dysregulation of the mevalonate pathway promotes transformation. *Proceedings of the National Academy of Sciences of the United States of America*, *107*(34), 15051–15056.

Coe, H., & Michalak, M. (2009). R e v i e w Calcium binding chaperones of the endoplasmic reticulum. In *F96 Gen. Physiol. Biophys* (Vol. 28).

Collins, G. A., & Goldberg, A. L. (2017). The Logic of the 26S Proteasome. In *Cell* (Vol. 169, Issue 5, pp. 792–806). Cell Press.

Compernolle, V., Brusselmans, K., Acker, T., Hoet, P., Tjwa, M., Beck, H., Plaisance, S., Dor, Y., Keshet, E., Lupu, F., Nemery, B., Dewerchin, M., Van Veldhoven, P., Plate, K., Moons, L., Collen, D., & Carmeliet, P. (2002). Loss of HIF-2α and inhibition of VEGF impair fetal lung maturation, whereas treatment with VEGF prevents fatal respiratory distress in premature mice. *Nature Medicine*, *8*(7), 702–710.

Coudert, L., Adjibade, P., & Mazroui, R. (2014). Analysis of translation initiation during stress conditions by polysome profiling. *Journal of Visualized Experiments*, *87*.

Dale, K. M., Coleman, C. I., Henyan, N. N., Kluger, J., & White, C. M. (2006). Statins and cancer risk: A meta-analysis. In *Journal of the American Medical Association* (Vol. 295, Issue 1, pp. 74–80). American Medical Association.

Dalen, James E., Dalton, W. S. (1996). Does Lowering Cholesterol Cause Cancer? *JAMA: The Journal of the American Medical Association*, *275*(1), 67.

Damiano, F., Alemanno, S., Gnoni, G. V., & Siculella, L. (2010). Translational control of the sterol-regulatory transcription factor SREBP-1 mRNA in response to serum starvation or ER stress is mediated by an internal ribosome entry site. *Biochemical Journal*, *429*(3), 603–612.

DeBose-Boyd, R. A. (2008). Feedback regulation of cholesterol synthesis: Sterol-accelerated ubiquitination and degradation of HMG CoA reductase. *Cell Research*, *18*(6), 609–621.

Dengler, V. L., Galbraith, M. D., & Espinosa, J. M. (2014). Transcriptional regulation by hypoxia inducible factors. In *Critical Reviews in Biochemistry and Molecular Biology* (Vol. 49, Issue 1, pp. 1–15).

Doench, J. G., Fusi, N., Sullender, M., Hegde, M., Vaimberg, E. W., Donovan, K. F., Smith, I., Tothova, Z., Wilen, C., Orchard, R., Virgin, H. W., Listgarten, J., & Root, D. E. (2016). Optimized sgRNA design to maximize activity and minimize off-target effects of CRISPR-Cas9. *Nature Biotechnology*, *34*(2), 184–191.

Dong, X. Y., & Tang, S. Q. (2010). Insulin-induced gene: A new regulator in lipid metabolism. In *Peptides* (Vol. 31, Issue 11, pp. 2145–2150). Elsevier.

Duncan, L. M., Piper, S., Dodd, R. B., Saville, M. K., Sanderson, C. M., Luzio, J. P., & Lehner, P. J. (2006). Lysine-63-linked ubiquitination is required for endolysosomal degradation of class I molecules. *The EMBO Journal*, *25*(8), 1635–1645.

Edgar, J. R., Manna, P. T., Nishimura, S., Banting, G., & Robinson, M. S. (2016). *Tetherin is an exosomal tether*.

Eguchi, H., Ikuta, T., Tachibana, T., Yoneda, Y., & Kawajiri, K. (1997). A nuclear localization signal of human aryl hydrocarbon receptor nuclear translocator/hypoxia-inducible factor 1β is a novel bipartite type recognized by the two components of nuclear pore-targeting complex. *Journal of Biological Chemistry*, *272*(28), 17640–17647.

Ema, M., Taya, S., Yokotani, N., Sogawa, K., Matsuda, Y., & Fujii-Kuriyama, Y. (1997). A novel bHLH-PAS factor with close sequence similarity to hypoxia-inducible factor 1α regulates the VEGF expression and is potentially involved in lung and vascular development. *Proceedings of the National Academy of Sciences of the United States of America*, *94*(9), 4273–4278.

Endo, A. (2010). A historical perspective on the discovery of statins. In *Proceedings of the Japan Academy Series B: Physical and Biological Sciences* (Vol. 86, Issue 5, pp. 484–493). The Japan Academy.

Endo, A., Kuroda, M., & Tanzawa, K. (1976). Competitive inhibition of 3-hydroxy-3-methylglutaryl coenzyme a reductase by ML-236A and ML-236B fungal metabolites, having hypocholesterolemic activity. *FEBS Letters*, *72*(2), 323–326.

Epstein, A. C. R., Gleadle, J. M., McNeill, L. A., Hewitson, K. S., O'Rourke, J., Mole, D. R., Mukherji, M., Metzen, E., Wilson, M. I., Dhanda, A., Tian, Y. M., Masson, N., Hamilton, D. L., Jaakkola, P., Barstead, R., Hodgkin, J., Maxwell, P. H., Pugh, C. W., Schofield, C. J., & Ratcliffe, P. J. (2001). C. elegans EGL-9 and mammalian homologs define a family of dioxygenases that regulate HIF by prolyl hydroxylation. *Cell*.

Espenshade, P. J., Li, W. P., & Yabe, D. (2002). Sterols block binding of COPII proteins to SCAP, thereby controlling SCAP sorting in ER. *Proceedings of the National Academy of Sciences of the United States of America*, *99*(18), 11694–11699.

Fähling, M. (2009). Surviving hypoxia by modulation of mRNA translation rate. In *Journal of Cellular and Molecular Medicine* (Vol. 13, Issue 9 A, pp. 2770–2779). Wiley-Blackwell.

Fang, S., Ferrone, M., Yang, C., Jensen, J. P., Tiwari, S., & Weissman, A. M. (2001). The tumor autocrine motility factor receptor, gp78, is a ubiquitin protein ligase implicated in degradation from the endoplasmic reticulum. *Proceedings of the National Academy of Sciences of the United States of America*.

Farooqi, M. A. M., Malhotra, N., Mukherjee, S. D., Sanger, S., Dhesy-Thind, S. K., Ellis, P., & Leong, D. P. (2018). Statin therapy in the treatment of active cancer: A systematic review and meta-analysis of randomized controlled trials. In *PLoS ONE* (Vol. 13, Issue 12). Public Library of Science.

Fisher, E. A., Khanna, N. A., & McLeod, R. S. (2011). Ubiquitination regulates the assembly of VLDL in HepG2 cells and is the committing step of the apoB-100 ERAD pathway. *Journal of Lipid Research*, *52*(6), 1170–1180.

Flierman, D., Coleman, C. S., Pickart, C. M., Rapoport, T. A., & Chau, V. (2006). E2-25K mediates US11-triggered retro-translocation of MHC class I heavy chains in a permeabilized cell system.

Proceedings of the National Academy of Sciences of the United States of America, *103*(31), 11589–11594.

Foresti, O., Rodriguez-Vaello, V., Funaya, C., & Carvalho, P. (2014). Quality control of inner nuclear membrane proteins by the Asi complex. *Science*, *346*(6210), 751–755.

Foresti, O., Ruggiano, A., Hannibal-Bach, H. K., Ejsing, C. S., & Carvalho, P. (2013). Sterol homeostasis requires regulated degradation of squalene monooxygenase by the ubiquitin ligase Doa10/Teb4. *ELife*, *2*, e00953.

Furuta, E., Pai, S. K., Zhan, R., Bandyopadhyay, S., Watabe, M., Mo, Y. Y., Hirota, S., Hosobe, S., Tsukada, T., Miura, K., Kamada, S., Saito, K., Iiizumi, M., Liu, W., Ericsson, J., & Watabe, K. (2008). Fatty acid synthase gene is up-regulated by hypoxia via activation of Akt and sterol regulatory element binding protein-1. *Cancer Research*, *68*(4), 1003–1011.

Gemmill, R. M., West, J. D., Boldog, F., Tanaka, N., Robinson, L. J., Smith, D. I., Li, F., & Drabkin, H. A. (1998). The hereditary renal cell carcinoma 3;8 translocation fuses FHIT to a patched-related gene, TRC8. *Proceedings of the National Academy of Sciences of the United States of America*, *95*(16), 9572–9577.

Gidding, S. S., & Allen, N. B. (2019). Cholesterol and Atherosclerotic Cardiovascular Disease: A Lifelong Problem. *Journal of the American Heart Association*, *8*(11).

Gil, G., Faust, J. R., Chin, D. J., Goldstein, J. L., & Brown, M. S. (1985). Membrane-bound domain of HMG CoA reductase is required for sterol-enhanced degradation of the enzyme. *Cell*, *41*(1), 249–258.

Gill, S., Stevenson, J., Kristiana, I., & Brown, A. J. (2011). Cholesterol-dependent degradation of squalene monooxygenase, a control point in cholesterol synthesis beyond HMG-CoA reductase. *Cell Metabolism*, *13*(3), 260–273.

Gilon, T., Chomsky, O., & Kulka, R. G. (1998). Degradation signals for ubiquitin system proteolysis in Saccharomyces cerevisiae. *The EMBO Journal*, *17*(10), 2759–2766.

Glick, D., Barth, S., & Macleod, K. F. (2010). Autophagy: Cellular and molecular mechanisms. In *Journal of Pathology*.

Goldstein, J L, & Brown, M. S. (1990). Regulation of the mevalonate pathway. *Nature*.

Goldstein, Joseph L., & Brown, M. S. (2009). The LDL receptor. In *Arteriosclerosis, Thrombosis, and Vascular Biology* (Vol. 29, Issue 4, pp. 431–438). NIH Public Access.

Goldstein, Joseph L., DeBose-Boyd, R. A., & Brown, M. S. (2006). Protein sensors for membrane sterols. In *Cell*.

Goldstein, Joseph L, & Brown, M. S. (1973). *Familial Hypercholesterolemia: Identification of a Defect in the Regulation of 3-Hydroxy-3-Methylglutaryl Coenzyme A Reductase Activity Associated with Overproduction of Cholesterol* (Vol. 70, Issue 10).

Goldstein, Joseph L, & Brown, M. S. (1990). *Regulation of the mevalonate pathway*.

Görlich, D., Prehn, S., Hartmann, E., Kalies, K. U., & Rapoport, T. A. (1992). A mammalian homolog of SEC61p and SECYp is associated with ribosomes and nascent polypeptides during translocation. *Cell*, *71*(3), 489–503.

Grice, G. L., & Nathan, J. A. (2016). The recognition of ubiquitinated proteins by the proteasome. In *Cellular and Molecular Life Sciences* (Vol. 73, Issue 18, pp. 3497–3506). Birkhauser Verlag AG.

Grimm, S. (2004). The art and design of genetic screens: mammalian culture cells. *Nature Reviews. Genetics*.

Gu, Y. Z., Moran, S. M., Hogenesch, J. B., Wartman, L., & Bradfield, C. A. (1998). Molecular characterization and chromosomal localization of a third α- class hypoxia inducible factor subunit, HIF3α. *Gene Expression*, *7*(3), 205–213.

Gülow, K., Bienert, D., & Haas, I. G. (2002). BiP is feed-back regulated by control of protein translation efficiency. *Journal of Cell Science*, *115*(11).

Guna, A., Volkmar, N., Christianson, J. C., & Hegde, R. S. (2018). The ER membrane protein complex is a transmembrane domain insertase. *Science*.

Guo, D., Reinitz, F., Youssef, M., Hong, C., Nathanson, D., Akhavan, D., Kuga, D., Amzajerdi, A. N., Soto, H., Zhu, S., Babic, I., Tanaka, K., Dang, J., Iwanami, A., Gini, B., DeJesus, J., Lisiero, D. D., Huang, T. T., Prins, R. M., … Mischel, P. S. (2011). An LXR agonist promotes glioblastoma cell death through inhibition of an EGFR/AKT/ SREBP-1/LDLR-dependent pathway. *Cancer Discovery*, *1*(5), 442–456.

Haglund, K., & Dikic, I. (2005). Ubiquitylation and cell signaling. *The EMBO Journal*.

Haglund, K., & Dikic, I. (2012). The role of ubiquitylation in receptor endocytosis and endosomal sorting. In *Journal of Cell Science* (Vol. 125, Issue 2, pp. 265–275). The Company of Biologists Ltd.

Hampton, R. Y., & Bhakta, H. (1997). Ubiquitin-mediated regulation of 3-hydroxy-3-methylglutaryl-CoA reductase. *Proceedings of the National Academy of Sciences of the United States of America*, *94*(24), 12944–12948.

Hampton, R. Y., Gardner, R. G., & Rine, J. (1996). Role of 26S Proteasome and HRD Genes in the Degradation of 3-Hydroxy-3-Methylglutaryl-CoA Reductase, an Integral Endoplasmic Reticulum Membrane Protein. In *Molecular Biology of the Cell* (Vol. 7).

Hampton, R. Y., & Rine, J. (1994). Regulated degradation of HMG-CoA reductase, an integral membrane protein of the endoplasmic reticulum, in yeast. *Journal of Cell Biology*, *125*(2), 299–312.

Hanna, J., Leggett, D. S., & Finley, D. (2003). Ubiquitin Depletion as a Key Mediator of Toxicity by Translational Inhibitors. *Molecular and Cellular Biology*, *23*(24), 9251–9261.

Hara, S., Hamada, J., Kobayashi, C., Kondo, Y., & Imura, N. (2001). Expression and characterization of hypoxia-inducible factor (HIF)-3α in human kidney: Suppression of HIF-mediated gene expression by HIF-3α. *Biochemical and Biophysical Research Communications*, *287*(4), 808–813.

Hartl, F. U., & Hayer-Hartl, M. (2009). Converging concepts of protein folding in vitro and in vivo. In *Nature Structural and Molecular Biology* (Vol. 16, Issue 6).

Hassink, G., Kikkert, M., Voorden, S. Van, Lee, S.-J., Spaapen, R., Laar, T. Van, Coleman, C. S., Bartee, E., Uh, K. F., Chau, V., & Wiertz, E. (2005). TEB4 is a C4HC3 RING finger-containing ubiquitin ligase of the endoplasmic reticulum. *Biochem. J*.

Hellen, C. U. T., & Sarnow, P. (2001). Internal ribosome entry sites in eukaryotic mRNA molecules. In *Genes and Development* (Vol. 15, Issue 13, pp. 1593–1612). Cold Spring Harbor Laboratory Press.

Hershko, A., Heller, H., Elias, S., & Ciechanover, A. (1983). Components of ubiquitin-protein ligase system. Resolution, affinity purification, and role in protein breakdown. *Journal of Biological Chemistry*.

Hetz, C. (2012). The unfolded protein response: Controlling cell fate decisions under ER stress and beyond. In *Nature Reviews Molecular Cell Biology* (Vol. 13, Issue 2, pp. 89–102). Nature Publishing Group.

Horie, M., Tsuchiya, Y., Hayashi, M., Iida, Y., Iwasawa, Y., Nagata, Y., Sawasaki, Y., Fukuzumi, H., Kitani, K., & Kamei, T. (1990). NB-598: A potent competitive inhibitor of squalene epoxidase. *Journal of Biological Chemistry*, *265*(30).

Horton, J. D., Goldstein, J. L., & Brown, M. S. (2002). SREBPs: activators of the complete program of cholesterol and fatty acid synthesis in the liver. *Journal of Clinical Investigation*, *109*(9), 1125–1131.

Horton, J. D., Shah, N. A., Warrington, J. A., Anderson, N. N., Park, S. W., Brown, M. S., & Goldstein, J. L. (2003). Combined analysis of oligonucleotide microarray data from transgenic and knockout mice identifies direct SREBP target genes. *Proceedings of the National Academy of Sciences of the United States of America*, *100*(21), 12027–12032.

Hsiau, T., Maures, T., Waite, K., Yang, J., Kelso, R., Holden, K., & Stoner, R. (2018). Inference of CRISPR Edits from Sanger Trace Data. *BioRxiv*, 251082.

Hsu, C. C., Shi, J., Yuan, C., Zhao, D., Jiang, S., Lyu, J., Wang, X., Li, H., Wen, H., Li, W., & Shi, X. (2018). Recognition of histone acetylation by the GAS41 YEATS domain promotes H2A.Z deposition in non-small cell lung cancer. *Genes and Development*, *32*(1), 58–69.

Hsu, P. D., Lander, E. S., & Zhang, F. (2014). Development and Applications of CRISPR-Cas9 for Genome Engineering. *Cell*. 157(6): 1262-1278.

Hua, X., Sakai, J., Ho, Y. K., Goldstein, J. L., & Brown, M. S. (1995). Hairpin orientation of sterol regulatory element-binding protein-2 in cell membranes as determined by protease protection. *Journal of Biological Chemistry*, *270*(49), 29422–29427.

Hua, Xianxin, Nohturfft, A., Goldstein, J. L., & Brown, M. S. (1996). Sterol resistance in CHO cells traced to point mutation in SREBP cleavage-activating protein. *Cell*, *87*(3), 415–426.

Huang, L. E., Arany, Z., Livingston, D. M., & Franklin Bunn, H. (1996). Activation of hypoxia-inducible transcription factor depends primarily upon redox-sensitive stabilization of its α subunit. *Journal of Biological Chemistry*, *271*(50), 32253–32259.

Huang, L. E., Gu, J., Schau, M., & Bunn, H. F. (1998). Regulation of hypoxia-inducible factor 1α is mediated by an O2-dependent degradation domain via the ubiquitin-proteasome pathway. *Proceedings of the National Academy of Sciences of the United States of America*, *95*(14), 7987–7992.

Hughes, A. L., Todd, B. L., & Espenshade, P. J. (2005). SREBP pathway responds to sterols and functions as an oxygen sensor in fission yeast. *Cell*, *120*(6), 831–842.

Hughes, B. T., & Espenshade, P. J. (2008). Oxygen-regulated degradation of fission yeast SREBP by Ofd1, a prolyl hydroxylase family member. *EMBO J*.

Hwang, S., Nguyen, A. D., Jo, Y., Engelking, L. J., Brugarolas, J., & DeBose-Boyd, R. A. (2017). Hypoxia-inducible factor-1α activates insig-2 transcription for degradation of HMG CoA reductase in the liver. *The Journal of Biological Chemistry*.

Iwai, K., Yamanaka, K., Kamura, T., Minato, N., Conaway, R. C., Conaway, J. W., Klausner, R. D., & Pause, A. (1999). Identification of the von Hippel-Lindau tumor-suppressor protein as part of an active E3 ubiquitin ligase complex. *Proceedings of the National Academy of Sciences of the United States of America*, *96*(22), 12436–12441.

Jaakkola, P., Mole, D. R., Tian, Y. M., Wilson, M. I., Gielbert, J., Gaskell, S. J., Von Kriegsheim, A., Hebestreit, H. F., Mukherji, M., Schofield, C. J., Maxwell, P. H., Pugh, C. W., & Ratcliffe, P. J. (2001). Targeting of HIF-α to the von Hippel-Lindau ubiquitylation complex by O2-regulated prolyl hydroxylation. *Science*, *292*(5516), 468–472.

Jain, I. H., Markhard, A. L., Skinner, O. S., To, T., Ast, T., Mootha, V. K., Calvo, S. E., Markhard, A. L., Skinner, O. S., To, T., & Ast, T. (2020). Genetic Screen for Cell Fitness in High or Low Oxygen Highlights Mitochondrial and Lipid Resource Genetic Screen for Cell Fitness in High or Low Oxygen Highlights Mitochondrial and Lipid Metabolism. *Cell*, 1–12.

Jiang, B. H., Rue, E., Wang, G. L., Roe, R., & Semenza, G. L. (1996). Dimerization, DNA binding, and transactivation properties of hypoxia-inducible factor 1. *The Journal of Biological Chemistry*, *271*(30), 17771–17778.

Jiang, L. Y., Jiang, W., Tian, N., Xiong, Y. N., Liu, J., Wei, J., Wu, K. Y., Luo, J., Shi, X. J., & Song, B. L. (2018). Ring finger protein 145 (RNF145) is a ubiquitin ligase for sterol-induced degradation of HMG-CoA reductase. *Journal of Biological Chemistry*, *293*(11), 4047–4055.

Jo, Y., Lee, P. C. W., Sguigna, P. V., & DeBose-Boyd, R. A. (2011). Sterol-induced degradation of HMG CoA reductase depends on interplay of two Insigs and two ubiquitin ligases, gp78 and Trc8. *Proceedings of the National Academy of Sciences*, *108*(51), 20503–20508.

Jonathan Warner, B. R., Knopf, P. M., & Rich, Alexande. (1962). 12 Wahba, A. In *PROCEEDINGS* (Vol. 48).

Jonikas, M. C., Collins, S. R., Denic, V., Oh, E., Quan, E. M., Schmid, V., Weibezahn, J., Schwappach, B., Walter, P., Weissman, J. S., & Schuldiner, M. (2009). Comprehensive characterization of genes required for protein folding in the endoplasmic reticulum. *Science*, *323*(5922).

Kaelin, W. G., & Maher, E. R. (1998). The VHL tumour-suppressor gene paradigm. *Trends in Genetics.* 14(10), 423–426.

Kambach, D. M., Halim, A. S., Gesine Cauer, A., Sun, Q., Tristan, C. A., Celiku, O., Kesarwala, A. H., Shankavaram, U., Batchelor, E., & Stommel, J. M. (2017). Disabled cell density sensing leads to dysregulated cholesterol synthesis in glioblastoma. *Oncotarget*, *8*(9), 14860–14875.

Kamura, T., Koepp, D. M., Conrad, M. N., Skowyra, D., Moreland, R. J., Iliopoulos, O., Lane, W. S., Kaelin, W. G., Elledge, S. J., Conaway, R. C., Harper, J. W., & Conaway, J. W. (1999). Rbx1, a component of the VHL tumor suppressor complex and SCF ubiquitin ligase. *Science*, *284*(5414), 657–661.

Kang, H. W., Wei, J., & Cohen, D. E. (2010). PC-TP/StARD2: Of membranes and metabolism. In *Trends in Endocrinology and Metabolism* (Vol. 21, Issue 7, pp. 449–456).

Khmelinskii, A., Blaszczak, E., Pantazopoulou, M., Fischer, B., Omnus, D. J., Dez, G. Le, Brossard, A., Gunnarsson, A., Barry, J. D., Meurer, M., Kirrmaier, D., Boone, C., Huber, W., Rabut, G., Ljungdahl, P. O., & Knop, M. (2014). Protein quality control at the inner nuclear membrane. *Nature*, *516*(7531), 410–413.

Khurana, V., Bejjanki, H. R., Caldito, G., & Owens, M. W. (2007). Statins reduce the risk of lung cancer in humans: A large case-control study of US Veterans. *Chest*, *131*(5), 1282–1288.

Kikkert, M., Doolman, R., Dai, M., Avner, R., Hassink, G., Van Voorden, S., Thanedar, S., Roitelman, J., Chau, V., & Wiertz, E. (2004). Human HRD1 Is an E3 Ubiquitin Ligase Involved in Degradation of Proteins from the Endoplasmic Reticulum. *Journal of Biological Chemistry*.

Kochhar, R., Khurana, V., Bejjanki, H., Caldito, G., & Fort, C. (2005). Statins to reduce breast cancer risk: A case control study in U.S. female veterans. *Journal of Clinical Oncology*, *23*(16_suppl), 514–514.

Koike-Yusa, H., Li, Y., Tan, E.-P., Velasco-Herrera, M. D. C., & Yusa, K. (2014). Genome-wide recessive genetic screening in mammalian cells with a lentiviral CRISPR-guide RNA library. *Nature Biotechnology*.

Komander, D., & Rape, M. (2012). The Ubiquitin Code. *Annual Review of Biochemistry*, *81*(1), 203–229.

Kong, X., Alvarez-Castelao, B., Lin, Z., Castaño, J. G., & Caro, J. (2007). Constitutive/hypoxic degradation of HIF-α proteins by the proteasome is independent of von Hippel Lindau protein ubiquitylation and the transactivation activity of the protein. *Journal of Biological Chemistry*, *282*(21), 15498–15505.

Koritzinsky, M., Levitin, F., Van Den Beucken, T., Rumantir, R. A., Harding, N. J., Chu, K. C., Boutros, P. C., Braakman, I., & Wouters, B. G. (2013). Two phases of disulfide bond formation have differing requirements for oxygen. *Journal of Cell Biology*, *203*(4), 615–627.

Koritzinsky, M., Rouschop, K. M. A., van den Beucken, T., Magagnin, M. G., Savelkouls, K., Lambin, P., & Wouters, B. G. (2007). Phosphorylation of eIF2α is required for mRNA translation inhibition and survival during moderate hypoxia. *Radiotherapy and Oncology*, *83*(3), 353–361.

Koritzinsky, M., & Wouters, B. G. (2007). Hypoxia and Regulation of Messenger RNA Translation. In *Methods in Enzymology* (Vol. 435, pp. 247–273). Academic Press.

Kotch, L. E., Iyer, N. V., Laughner, E., & Semenza, G. L. (1999). Defective vascularization of HIF-1α-null embryos is not associated with VEGF deficiency but with mesenchymal cell death. *Developmental Biology*, *209*(2), 254–267.

Koumenis, C., Naczki, C., Koritzinsky, M., Rastani, S., Diehl, A., Sonenberg, N., Koromilas, A., & Wouters, B. G. (2002). Regulation of Protein Synthesis by Hypoxia via Activation of the Endoplasmic Reticulum Kinase PERK and Phosphorylation of the Translation Initiation Factor eIF2α. *Molecular and Cellular Biology*, *22*(21), 7405–7416.

Lahiri, S., Chao, J. T., Tavassoli, S., Wong, A. K. O., Choudhary, V., Young, B. P., Loewen, C. J. R., & Prinz, W. A. (2014). A Conserved Endoplasmic Reticulum Membrane Protein Complex (EMC) Facilitates Phospholipid Transfer from the ER to Mitochondria. *PLoS Biology*, *12*(10).

Lai, M. C., Chang, C. M., & Sun, H. S. S. (2016). Hypoxia Induces Autophagy through Translational Up-Regulation of Lysosomal Proteins in Human Colon Cancer Cells. *PLoS ONE*, *11*(4).

Lam, S. Y., Murphy, C., Foley, L. A., Ross, S. A., Wang, T. C., & Fleming, J. V. (2014). The human ubiquitin conjugating enzyme UBE2J2 (Ubc6) is a substrate for proteasomal degradation. *Biochemical and Biophysical Research Communications*, *451*(3), 361–366.

Laplante, M., & Sabatini, D. M. (2009). mTOR signaling at a glance. *Journal of Cell Science*, *122*(20), 3589–3594.

Laplante, M., & Sabatini, D. M. (2012). MTOR signaling in growth control and disease. In *Cell* (Vol. 149, Issue 2, pp. 274–293). NIH Public Access.

Latif, F., Tory, K., Gnarra, J., Yao, M., Duh, F. M., Orcutt, M. Lou, Stackhouse, T., Kuzmin, I., Modi, W., Geil, L., Schmidt, L., Zhou, F., Li, H., Wei, M. H., Chen, F., Glenn, G., Choyke, P., Walther, M. M., Weng, Y., … Lerman, M. I. (1993). Identification of the von Hippel-Lindau disease tumor suppressor gene. *Science*, *260*(5112), 1317–1320.

Layer, G., Reichelt, J., Jahn, D., & Heinz, D. W. (2010). Structure and function of enzymes in heme biosynthesis. *Protein Science : A Publication of the Protein Society*, *19*(6), 1137–1161.

Lee, C.-Y. S., Stewart, E. V, Hughes, B. T., & Espenshade, P. J. (2009). Oxygen-dependent binding of Nro1 to the prolyl hydroxylase Ofd1 regulates SREBP degradation in yeast. *The EMBO Journal*, *28*(2), 135–143.

Lee, C. Y. S., Yeh, T. L., Hughes, B. T., & Espenshade, P. J. (2011). Regulation of the Sre1 hypoxic transcription factor by oxygen-dependent control of DNA binding. *Molecular Cell*.

Lee, J. P., Brauweiler, A., Rudolph, M., Hooper, J. E., Drabkin, H. A., & Gemmill, R. M. (2010). The TRC8 ubiquitin ligase is sterol regulated and interacts with lipid and protein biosynthetic pathways. *Molecular Cancer Research*, *8*(1), 93–106.

Lewis, C. A., Brault, C., Peck, B., Bensaad, K., Griffiths, B., Mitter, R., Chakravarty, P., East, P., Dankworth, B., Alibhai, D., Harris, A. L., & Schulze, A. (2015). SREBP maintains lipid biosynthesis and viability of cancer cells under lipid- and oxygen-deprived conditions and defines a gene signature associated with poor survival in glioblastoma multiforme. *Oncogene*, *34*(40), 5128–5140.

Li, J., Thorne, L. N., Punjabi, N. M., Sun, C.-K., Schwartz, A. R., Smith, P. L., Marino, R. L., Rodriguez, A., Hubbard, W. C., O'Donnell, C. P., & Polotsky, V. Y. (2005). Intermittent hypoxia induces hyperlipidemia in lean mice. *Circulation Research*, *97*(7), 698–706.

Li, W., Bengtson, M. H., Ulbrich, A., Matsuda, A., Reddy, V. A., Orth, A., Chanda, S. K., Batalov, S., & Joazeiro, C. A. P. (2008). Genome-Wide and Functional Annotation of Human E3 Ubiquitin Ligases Identifies MULAN, a Mitochondrial E3 that Regulates the Organelle's Dynamics and Signaling. *PLoS ONE*, *3*(1), e1487.

Li, W., Xu, H., Xiao, T., Cong, L., Love, M. I., Zhang, F., Irizarry, R. A., Liu, J. S., Brown, M., & Liu, X. S. (2014). MAGeCK enables robust identification of essential genes from genome-scale CRISPR/Cas9 knockout screens. *Genome Biology*, *15*(12), 554.

Li, Y., Wang, Y., Kim, E., Beemiller, P., Wang, C. Y., Swanson, J., You, M., & Guan, K. L. (2007). Bnip3 mediates the hypoxia-induced inhibition on mammalian target of rapamycin by interacting with Rheb. *Journal of Biological Chemistry*, *282*(49), 35803–35813.

Liao, J. K., & Laufs, U. (2005). PLEIOTROPIC EFFECTS OF STATINS. *Annual Review of Pharmacology and Toxicology*, *45*(1), 89–118.

Liu, F., & Mischel, P. S. (2018). Targeting epidermal growth factor receptor co-dependent signaling pathways in glioblastoma. *Wiley Interdisciplinary Reviews: Systems Biology and Medicine*, *10*(1).

Liu, L., Cash, T. P., Jones, R. G., Keith, B., Thompson, C. B., & Simon, M. C. (2006). Hypoxia-induced energy stress regulates mRNA translation and cell growth. *Molecular Cell*, *21*(4), 521–531.

Liu, L., & Simon, M. C. (2004). Regulation of transcription and translation by hypoxia. In *Cancer Biology and Therapy* (Vol. 3, Issue 6).

Loenarz, C., & Schofield, C. J. (2008). Expanding chemical biology of 2-oxoglutarate oxygenases. In *Nature Chemical Biology* (Vol. 4, Issue 3, pp. 152–156). Nature Publishing Group.

Lonergan, K. M., Iliopoulos, O., Ohh, M., Kamura, T., Conaway, R. C., Conaway, J. W., & Kaelin, W. G. (1998). Regulation of Hypoxia-Inducible mRNAs by the von Hippel-Lindau Tumor Suppressor Protein Requires Binding to Complexes Containing Elongins B/C and Cul2. *Molecular and Cellular Biology*, *18*(2), 732–741.

López-Barneo, J., Ortega-Sáenz, P., Pardal, R., Pascual, A., & Piruat, J. I. (2008). Carotid body oxygen sensing. *European Respiratory Journal*, *32*(5), 1386–1398.

López, C. A., de Vries, A. H., & Marrink, S. J. (2011). Molecular mechanism of cyclodextrin mediated cholesterol extraction. *PLoS Computational Biology*, *7*(3).

Loregger, A., Cook, E. C. L., Nelson, J. K., Moeton, M., Sharpe, L. J., Engberg, S., Karimova, M., Lambert, G., Brown, A. J., & Zelcer, N. (2015). A MARCH6 and IDOL E3 ubiquitin ligase circuit uncouples cholesterol synthesis from lipoprotein uptake in hepatocytes. *Molecular and Cellular Biology*, *36*(2), MCB.00890-15.

Loregger, A., Raaben, M., Tan, J., Scheij, S., Moeton, M., Van Den Berg, M., Gelberg-Etel, H., Stickel, E., Roitelman, J., Brummelkamp, T., & Zelcer, N. (2017). Haploid mammalian genetic screen identifes UBXD8 as a key determinant of HMGCR degradation and cholesterol biosynthesis. *Arteriosclerosis, Thrombosis, and Vascular Biology*, *37*(11), 2064–2074.

Lydic, T. A., & Goo, Y.-H. (2018). Lipidomics unveils the complexity of the lipidome in metabolic diseases. *Clinical and Translational Medicine*, *7*(1).

Mahammad, S., & Parmryd, I. (2015). Cholesterol depletion using methyl-β-cyclodextrin. *Methods in Molecular Biology (Clifton, N.J.)*, *1232*, 91–102.

Makino, Y., Cao, R., Svensson, K., Bertilsson, G., Asman, M., Tanaka, H., Cao, Y., Berkenstam, A., & Poellinger, L. (2001). Inhibitory PAS domain protein is a negative regulator of hypoxia-inducible gene expression. *Nature*, *414*(6863), 550–554.

Marciniak, S. J., Yun, C. Y., Oyadomari, S., Novoa, I., Zhang, Y., Jungreis, R., Nagata, K., Harding, H. P., & Ron, D. (2004). CHOP induces death by promoting protein synthesis and oxidation in the stressed endoplasmic reticulum. *Genes and Development*, *18*(24), 3066–3077.

Maxfield, F. R., & van Meer, G. (2010). Cholesterol, the central lipid of mammalian cells. In *Current Opinion in Cell Biology* (Vol. 22, Issue 4, pp. 422–429). NIH Public Access.

Maxwell, P. H., & Eckardt, K. U. (2016). HIF prolyl hydroxylase inhibitors for the treatment of renal anaemia and beyond. *Nature Reviews Nephrology*, *12*(3), 157–168.

Maxwell, P. H., & Ratcliffe, P. J. (2002). Oxygen sensors and angiogenesis. *Seminars in Cell and Developmental Biology*, *13*(1), 29–37.

Maxwell, P. H., Wlesener, M. S., Chang, G. W., Clifford, S. C., Vaux, E. C., Cockman, M. E., Wykoff, C. C., Pugh, C. W., Maher, E. R., & Ratcliffe, P. J. (1999). The tumour suppressor protein VHL targets hypoxia-inducible factors for oxygen-dependent proteolysis. *Nature*, *399*(6733), 271–275.

McHugh, C. A., Chen, C.-K., Chow, A., Surka, C. F., Tran, C., McDonel, P., Pandya-Jones, A., Blanco, M., Burghard, C., Moradian, A., Sweredoski, M. J., Shishkin, A. A., Su, J., Lander, E. S., Hess, S., Plath, K., & Guttman, M. (2015). The Xist lncRNA interacts directly with SHARP to silence transcription through HDAC3. *Nature*, *521*(7551), 232–236.

Menzies, S. A., Volkmar, N., van den Boomen, D. J. H., Timms, R. T., Dickson, A. S., Nathan, J. A., & Lehner, P. J. (2018). The sterol-responsive RNF145 E3 ubiquitin ligase mediates the degradation of HMG-CoA reductase together with gp78 and hrd1. *ELife*, *7*.

Metzger, Meredith B, Hristova, V. A., & Weissman, A. M. (2012). HECT and RING finger families of E3 ubiquitin ligases at a glance. *Journal of Cell Science*, *125*(Pt 3), 531–537.

Metzger, Meredith Boyle, Maurer, M. J., Dancy, B. M., & Michaelis, S. (2008). Degradation of a Cytosolic Protein Requires Endoplasmic Reticulum-associated Degradation Machinery. *Journal of Biological Chemistry*, *283*(47), 32302–32316.

Miles, A. L., Burr, S. P., Grice, G. L., & Nathan, J. A. (2017). The vacuolar-ATPase complex and assembly factors, TMEM199 and CCDC115, control HIF1α prolyl hydroxylation by regulating cellular iron levels. *ELife*, *6*.

Minami, R., Hayakawa, A., Kagawa, H., Yanagi, Y., Yokosawa, H., & Kawahara, H. (2010). BAG-6 is essential for selective elimination of defective proteasomal substrates. *Journal of Cell Biology*, *190*(4), 637–650.

Mole, D. R., Blancher, C., Copley, R. R., Pollard, P. J., Gleadle, J. M., Ragousis, J., & Ratcliffe, P. J. (2009). Genome-wide association of hypoxia-inducible factor (HIF)-1α and HIF-2α DNA binding with expression profiling of hypoxia-inducible transcripts. *Journal of Biological Chemistry*, *284*(25), 16767–16775.

Morgens, D. W., Wainberg, M., Boyle, E. A., Ursu, O., Araya, C. L., Kimberly Tsui, C., Haney, M. S., Hess, G. T., Han, K., Jeng, E. E., Li, A., Snyder, M. P., Greenleaf, W. J., Kundaje, A., & Bassik, M. C. (2017). Genome-scale measurement of off-target activity using Cas9 toxicity in high-throughput screens. *Nature Communications*, *8*.

Mueller, B., Klemm, E. J., Spooner, E., Claessen, J. H., & Ploegh, H. L. (2008). SEL1L nucleates a protein complex required for dislocation of misfolded glycoproteins. *Proceedings of the National Academy of Sciences of the United States of America*, *105*(34), 12325–12330.

Nadav, E., Shmueli, A., Barr, H., Gonen, H., Ciechanover, A., & Reiss, Y. (2003). A novel mammalian endoplasmic reticulum ubiquitin ligase homologous to the yeast Hrd1. *Biochemical and Biophysical Research Communications*.

Nathan, J. A., Sengupta, S., Wood, S. A., Admon, A., Markson, G., Sanderson, C., & Lehner, P. J. (2008). The ubiquitin E3 ligase MARCH7 is differentially regulated by the deubiquitylating enzymes USP7 and USP9X. *Traffic (Copenhagen, Denmark)*, *9*(7), 1130–1145.

Nathan, J. A., Tae Kim, H., Ting, L., Gygi, S. P., & Goldberg, A. L. (2013). Why do cellular proteins linked to K63-polyubiquitin chains not associate with proteasomes? *EMBO Journal*, *32*(4).

Newman, Thomas B., Hulley, S. B. (1996). Carcinogenicity of Lipid-Lowering Drugs. *JAMA: The Journal of the American Medical Association*, *275*(1), 55.

Nguyen, A. D., McDonald, J. G., Bruick, R. K., & DeBose-Boyd, R. A. (2007). Hypoxia stimulates degradation of 3-hydroxy-3-methylglutaryl-coenzyme A reductase through accumulation of lanosterol and hypoxia-inducible factor-mediated induction of insigs. *Journal of Biological Chemistry*.

Ni, M., & Lee, A. S. (2007). ER chaperones in mammalian development and human diseases. In *FEBS Letters* (Vol. 581, Issue 19, pp. 3641–3651). NIH Public Access.

Nishimura, S., Ishii, K., Iwamoto, K., Arita, Y., Matsunaga, S., Ohno-Iwashita, Y., Sato, S. B., Kakeya, H., Kobayashi, T., & Yoshida, M. (2013). Visualization of Sterol-Rich Membrane Domains with Fluorescently-Labeled Theonellamides. *PLoS ONE*, *8*(12), e83716.

Noll, H. (2008). The discovery of polyribosomes. *BioEssays*, *30*(11–12), 1220–1234.

Ohashi, K., Osuga, J. I., Tozawa, R., Kitamine, T., Yagyu, H., Sekiya, M., Tomita, S., Okazaki, H., Tamura, Y., Yahagi, N., Iizuka, Y., Harada, K., Gotoda, T., Shimano, H., Yamada, N., & Ishibashi, S. (2003). Early Embryonic Lethality Caused by Targeted Disruption of the 3-Hydroxy-3-methylglutaryl-CoA Reductase Gene. *Journal of Biological Chemistry*, *278*(44), 42936–42941.

Ohh, M., Park, C. W., Ivan, M., Hoffman, M. A., Kim, T. Y., Huang, L. E., Pavletich, N., Chau, V., & Kaelin, W. G. (2000). Ubiquitination of hypoxia-inducible factor requires direct binding to the β-domain of the von Hippel - Lindau protein. *Nature Cell Biology*, *2*(7), 423–427.

Osborne, A. R., Rapoport, T. A., & van den Berg, B. (2005). PROTEIN TRANSLOCATION BY THE SEC61/SECY CHANNEL. *Annual Review of Cell and Developmental Biology*, *21*(1), 529–550.

Osborne, T. F. (1991). Single nucleotide resolution of sterol regulatory region in promoter for 3-hydroxy-3-methylglutaryl coenzyme A reductase. *The Journal of Biological Chemistry*, *266*(21), 13947–13951.

Oslowski, C. M., & Urano, F. (2011). Measuring ER stress and the unfolded protein response using mammalian tissue culture system. In *Methods in Enzymology* (Vol. 490, Issue C, pp. 71–92). Academic Press Inc.

Padyana, A. K., Gross, S., Jin, L., Cianchetta, G., Narayanaswamy, R., Wang, F., Wang, R., Fang, C., Lv, X., Biller, S. A., Dang, L., Mahoney, C. E., Nagaraja, N., Pirman, D., Sui, Z., Popovici-Muller, J., & Smolen, G. A. (2019). Structure and inhibition mechanism of the catalytic domain of human squalene epoxidase. *Nature Communications*, *10*(1), 1–10.

Pause, A., Lee, S., Worrell, R. A., Chen, D. Y. T., Burgess, W. H., Linehan, W. M., & Klausner, R. D. (1997). The von Hippel-Lindau tumor-suppressor gene product forms a stable complex with

human CUL-2, a member of the Cdc53 family of proteins. *Proceedings of the National Academy of Sciences of the United States of America*, *94*(6), 2156–2161.

Petrova, V., Annicchiarico-Petruzzelli, M., Melino, G., & Amelio, I. (2018). The hypoxic tumour microenvironment. In *Oncogenesis* (Vol. 7, Issue 1, pp. 1–13). Nature Publishing Group.

Pickart, C. M. (2001). Mechanisms Underlying Ubiquitination. *Annual Review of Biochemistry*.

Poynter, J. N., Gruber, S. B., Higgins, P. D. R., Almog, R., Bonner, J. D., Rennert, H. S., Low, M., Greenson, J. K., & Rennert, G. (2005). Statins and the risk of colorectal cancer. *New England Journal of Medicine*, *352*(21), 2184–2192.

Radhakrishnan, A., Goldstein, J. L., McDonald, J. G., & Brown, M. S. (2008). Switch-like Control of SREBP-2 Transport Triggered by Small Changes in ER Cholesterol: A Delicate Balance. *Cell Metabolism*.

Radhakrishnan, A., Sun, L. P., Kwon, H. J., Brown, M. S., & Goldstein, J. L. (2004). Direct binding of cholesterol to the purified membrane region of SCAP: Mechanism for a sterol-sensing domain. *Molecular Cell*, *15*(2), 259–268.

Ran, F., Hsu, P., Wright, J., & Agarwala, V. (2013). Genome engineering using the CRISPR-Cas9 system. *Nat. Protoc.*

Ravid, T., Doolman, R., Avner, R., Harats, D., & Roitelman, J. (2000). The ubiquitin-proteasome pathway mediates the regulated degradation of mammalian 3-hydroxy-3-methylglutaryl-coenzyme A reductase. *Journal of Biological Chemistry*.

Rodrigues, M. L. (2018). The multifunctional fungal ergosterol. In *mBio* (Vol. 9, Issue 5). American Society for Microbiology.

Romero-Ramirez, L., Cao, H., Nelson, D., Hammond, E., Lee, A. H., Yoshida, H., Mori, K., Glimcher, L. H., Denko, N. C., Giaccia, A. J., Le, Q. T., & Koong, A. C. (2004). XBP1 is essential for survival under hypoxic conditions and is required for tumor growth. *Cancer Research*, *64*(17), 5943–5947.

Ron, D., & Walter, P. (2007). Signal integration in the endoplasmic reticulum unfolded protein response. In *Nature Reviews Molecular Cell Biology* (Vol. 8, Issue 7).

Sabatini, D. M., Erdjument-Bromage, H., Lui, M., Tempst, P., & Snyder, S. H. (1994). RAFT1: A mammalian protein that binds to FKBP12 in a rapamycin-dependent fashion and is homologous to yeast TORs. *Cell*, *78*(1), 35–43.

Sakai, J., Duncan, E. A., Rawson, R. B., Hua, X., Brown, M. S., & Goldstein, J. L. (1996). Sterol-regulated release of SREBP-2 from cell membranes requires two sequential cleavages, one within a transmembrane segment. *Cell*, *85*(7), 1037–1046.

Salceda, S., & Caro, J. (1997). Hypoxia-inducible factor 1α (HIF-1α) protein is rapidly degraded by the ubiquitin-proteasome system under normoxic conditions. Its stabilization by hypoxia depends on redox-induced changes. *Journal of Biological Chemistry*, *272*(36), 22642–22647.

Sanjana, N. E., Shalem, O., & Zhang, F. (2014). Improved vectors and genome-wide libraries for CRISPR screening. *Nature Methods*, *11*(8), 783–784.

Sato, R., Inoue, J., Kawabe, Y., Kodama, T., Takano, T., & Maeda, M. (1996). Sterol-dependent transcriptional regulation of sterol regulatory element-binding protein-2. *Journal of Biological Chemistry*, *271*(43), 26461–26464.

Sawkar, A. R., D'Haeze, W., & Kelly, J. W. (2006). Therapeutic strategies to ameliorate lysosomal storage disorders - A focus on Gaucher disease. In *Cellular and Molecular Life Sciences* (Vol. 63, Issue 10, pp. 1179–1192). Springer.

Schoebel, S., Mi, W., Stein, A., Ovchinnikov, S., Pavlovicz, R., DImaio, F., Baker, D., Chambers, M. G., Su, H., Li, D., Rapoport, T. A., & Liao, M. (2017). Cryo-EM structure of the protein-conducting ERAD channel Hrd1 in complex with Hrd3. *Nature*, *548*(7667).

Schofield, C. J., & Ratcliffe, P. J. (2004). Oxygen sensing by HIF hydroxylases. *Nature Reviews Molecular Cell Biology*, *5*(5), 343–354.

Schubert, U., Antón, L. C., Gibbs, J., Norbury, C. C., Yewdell, J. W., & Bennink, J. R. (2000). Rapid degradation of a large fraction of newly synthesized proteins by proteasomes. *Nature*, *404*(6779).

Schulze, J. M., Wang, A. Y., & Kobor, M. S. (2009). YEATS domain proteins: A diverse family with many links to chromatin modification and transcription. In *Biochemistry and Cell Biology* (Vol. 87, Issue 1, pp. 65–75).

Semenza, G L, & Wang, G. L. (1992). A nuclear factor induced by hypoxia via de novo protein synthesis binds to the human erythropoietin gene enhancer at a site required for transcriptional activation. *Molecular and Cellular Biology*, *12*(12), 5447–5454.

Semenza, Gregg L. (2014). Hypoxia-Inducible Factor 1 and Cardiovascular Disease. *Annual Review of Physiology*, *76*(1).

Seo, H. S., & Choi, M. H. (2015). Cholesterol homeostasis in cardiovascular disease and recent advances in measuring cholesterol signatures. *Journal of Steroid Biochemistry and Molecular Biology*, *153*, 72–79.

Sever, N., Song, B. L., Yabe, D., Goldstein, J. L., Brown, M. S., & DeBose-Boydb, R. A. (2003b). Insig-dependent Ubiquitination and Degradation of Mammalian 3-Hydroxy-3-methylglutaryl-CoA Reductase Stimulated by Sterols and Geranylgeraniol. *Journal of Biological Chemistry*, *278*(52), 52479–52490.

Sever, N., Yang, T., Brown, M. S., Goldstein, J. L., & DeBose-Boyd, R. A. (2003a). Accelerated degradation of HMG CoA reductase mediated by binding of insig-1 to its sterol-sensing domain. *Molecular Cell*.

Shalem, O., Sanjana, N. E., Hartenian, E., Shi, X., Scott, D. A., Mikkelsen, T. S., Heckl, D., Ebert, B. L., Root, D. E., Doench, J. G., & Zhang, F. (2014). Genome-Scale CRISPR-Cas9 Knockout Screening in Human Cells. *Science*, *343*(6166), 84–87.

Sidrauski, C., Acosta-Alvear, D., Khoutorsky, A., Vedantham, P., Hearn, B. R., Li, H., Gamache, K., Gallagher, C. M., Ang, K. K. H., Wilson, C., Okreglak, V., Ashkenazi, A., Hann, B., Nader, K., Arkin, M. R., Renslo, A. R., Sonenberg, N., & Walter, P. (2013). Pharmacological brake-release of mRNA translation enhances cognitive memory. *ELife*, *2013*(2).

Sidrauski, C., McGeachy, A. M., Ingolia, N. T., & Walter, P. (2015). The small molecule ISRIB reverses the effects of eIF2α phosphorylation on translation and stress granule assembly. *ELife*, *2015*(4).

Simons, K., & Ikonen, E. (2000). How cells handle cholesterol. In *Science* (Vol. 290, Issue 5497).

Solomon, K. R., & Freeman, M. R. (2008). Do the cholesterol-lowering properties of statins affect cancer risk? *Trends in Endocrinology and Metabolism*, *19*(4), 113–121.

Song, B. L., Sever, N., & DeBose-Boyd, R. A. (2005b). Gp78, a membrane-anchored ubiquitin ligase, associates with Insig-1 and couples sterol-regulated ubiquitination to degradation of HMG CoA reductase. *Molecular Cell*, *19*(6), 829–840.

Song, B. L., Javitt, N. B., & DeBose-Boyd, R. A. (2005a). Insig-mediated degradation of HMG CoA reductase stimulated by lanosterol, an intermediate in the synthesis of cholesterol. *Cell Metabolism*, *1*(3), 179–189.

Spandl, J., Lohmann, D., Kuerschner, L., Moessinger, C., & Thiele, C. (2011). Ancient Ubiquitous Protein 1 (AUP1) Localizes to Lipid Droplets and Binds the E2 Ubiquitin Conjugase G2 (Ube2g2) via Its G2 Binding Region. *Journal of Biological Chemistry*, *286*(7), 5599–5606.

Stagg, H. R., Thomas, M., van den Boomen, D., Wiertz, E. J. H. J., Drabkin, H. A., Gemmill, R. M., & Lehner, P. J. (2009). The TRC8 E3 ligase ubiquitinates MHC class I molecules before dislocation from the ER. *The Journal of Cell Biology*, *186*(5), 685–692.

Stefanovic-Barrett, S., Dickson, A. S., Burr, S. P., Williamson, J. C., Lobb, I. T., Boomen, D. J., Lehner, P. J., & Nathan, J. A. (2018). MARCH6 and TRC8 facilitate the quality control of cytosolic and tail-anchored proteins. *EMBO Reports*, *19*(5).

Stefanovic, S., & Hegde, R. S. (2007). Identification of a Targeting Factor for Posttranslational Membrane Protein Insertion into the ER. *Cell*, *128*(6), 1147–1159.

Stein, I., Itin, A., Einat, P., Skaliter, R., Grossman, Z., & Keshet, E. (1998). Translation of Vascular Endothelial Growth Factor mRNA by Internal Ribosome Entry: Implications for Translation under Hypoxia. *Molecular and Cellular Biology*, *18*(6), 3112–3119.

Stopsack, K. H., Gerke, T. A., Sinnott, J. A., Penney, K. L., Tyekucheva, S., Sesso, H. D., Andersson, S. O., Andrén, O., Cerhan, J. R., Giovannucci, E. L., Mucci, L. A., & Rider, J. R. (2016). Cholesterol metabolism and prostate cancer lethality. *Cancer Research*, *76*(16), 4785–4790.

Summons, R. E., Bradley, A. S., Jahnke, L. L., & Waldbauer, J. R. (2006). Steroids, triterpenoids and molecular oxygen. In *Philosophical Transactions of the Royal Society B: Biological Sciences* (Vol. 361, Issue 1470, pp. 951–968). Royal Society.

Sun, L. P., Li, L., Goldstein, J. L., & Brown, M. S. (2005). Insig required for sterol-mediated inhibition of Scap/SREBP binding to COPII proteins in vitro. *Journal of Biological Chemistry*, *280*(28), 26483–26490.

Sun, Z., & Brodsky, J. L. (2019). Protein quality control in the secretory pathway. In *Journal of Cell Biology* (Vol. 218, Issue 10, pp. 3171–3187). Rockefeller University Press.

Swanson, R., Locher, M., & Hochstrasser, M. (2001). A conserved ubiquitin ligase of the nuclear envelope/endoplasmic reticulum that functions in both ER-associated and Matα2 repressor degradation. *Genes and Development*.

Taylor, C. T., & Colgan, S. P. (2017). Regulation of immunity and inflammation by hypoxia in immunological niches. In *Nature Reviews Immunology* (Vol. 17, Issue 12, pp. 774–785). Nature Publishing Group.

The European Chromosome 16 Tuberous Sclerosis Consortium. (1993). Identification and characterization of the tuberous sclerosis gene on chromosome 16. *Cell*, *75*(7), 1305–1315.

Thomas, J. D., & Johannes, G. J. (2007). Identification of mRNAs that continue to associate with polysomes during hypoxia. *RNA*, *13*(7), 1116–1131.

Timms, R. T., Menzies, S. A., Tchasovnikarova, I. A., Christensen, L. C., Williamson, J. C., Antrobus, R., Dougan, G., Ellgaard, L., & Lehner, P. J. (2016). Genetic dissection of mammalian ERAD through comparative haploid and CRISPR forward genetic screens. *Nature Communications*.

Todd, B. L., Stewart, E. V., Burg, J. S., Hughes, A. L., & Espenshade, P. J. (2006). Sterol Regulatory Element Binding Protein Is a Principal Regulator of Anaerobic Gene Expression in Fission Yeast. *Molecular and Cellular Biology*, *26*(7), 2817–2831.

Treiman, M., Caspersen, C., & Christensen, S. B. (1998). A tool coming of age: Thapsigargin as an inhibitor of sarco-endoplasmic reticulum Ca2+-ATPases. *Trends in Pharmacological Sciences*, *19*(4), 131–135.

Tsai, Y. C., Leichner, G. S., Pearce, M. M. P., Wilson, G. L., Wojcikiewicz, R. J. H., Roitelman, J., & Weissman, A. M. (2012). Differential regulation of HMG-CoA reductase and Insig-1 by

enzymes of the ubiquitin-proteasome system. *Molecular Biology of the Cell*, *23*(23), 4484–4494.

Van den Boomen, D. J.H., & Lehner, P. J. (2015). Identifying the ERAD ubiquitin E3 ligases for viral and cellular targeting of MHC class I. *Molecular Immunology*, *68*(2).

van den Boomen, Dick J H, Timms, R. T., Grice, G. L., Stagg, H. R., Skødt, K., Dougan, G., Nathan, J. a, & Lehner, P. J. (2014). TMEM129 is a Derlin-1 associated ERAD E3 ligase essential for virus-induced degradation of MHC-I. *Proceedings of the National Academy of Sciences of the United States of America*.

Villa, G. R., Hulce, J. J., Zanca, C., Bi, J., Ikegami, S., Cahill, G. L., Gu, Y., Lum, K. M., Masui, K., Yang, H., Rong, X., Hong, C., Turner, K. M., Liu, F., Hon, G. C., Jenkins, D., Martini, M., Armando, A. M., Quehenberger, O., … Mischel, P. S. (2016). An LXR-Cholesterol Axis Creates a Metabolic Co-Dependency for Brain Cancers. *Cancer Cell*, *30*(5), 683–693.

Volkmar, N., Thezenas, M. L., Louie, S. M., Juszkiewicz, S., Nomura, D. K., Hegde, R. S., Kessler, B. M., & Christianson, J. C. (2019). The ER membrane protein complex promotes biogenesis of sterol-related enzymes maintaining cholesterol homeostasis. *Journal of Cell Science*, *132*(2).

Wang, G. L., Jiang, B.-H., Rue, E. A., & Semenza, G. L. (1995). Hypoxia-inducible factor 1 is a basic-helix-loop-helix-PAS heterodimer regulated by cellular 02 tension (dioxin receptor/erythropoietin/hypoxia/transcription). In *Genetics* (Vol. 92).

Wang, G. L., & Semenza, G. L. (1995). Purification and characterization of hypoxia-inducible factor. *Journal of Biological Chemistry*, *270*(3), 1230–1237.

Wang, T., Birsoy, K., Hughes, N. W., Krupczak, K. M., Post, Y., Wei, J. J., Lander, E. S., & Sabatini, D. M. (2015). Identification and characterization of essential genes in the human genome. *Science (New York, N.Y.)*, *350*(6264), 1096–1101.

Wang, T., Wei, J. J., Sabatini, D. M., & Lander, E. S. (2014). Genetic screens in human cells using the CRISPR-Cas9 system. *Science*.

Wang, X, & Athanasia Spandidos, 2,3 Huajun Wang,2,3 and Brian Seed2,3,*. (2012). *PrimerBank: a PCR primer database for quantitative gene expression analysis, 2012 update*.

Wang, Xiaoli, Herr, R. A., Rabelink, M., Hoeben, R. C., Wiertz, E. J. H. J., & Hansen, T. H. (2009). Ube2j2 ubiquitinates hydroxylated amino acids on ER-associated degradation substrates. *The Journal of Cell Biology*, *187*(5), 655–668.

Ward, C. L., Omura, S., & Kopito, R. R. (1995). Degradation of CFTR by the Ubiquitin-Proteasome Pathway. In *Cell* (Vol. 83).

Wek, R. C., Jiang, H.-Y., & Anthony, T. G. (2006). Coping with stress: eIF2 kinases and translational control. *Biochemical Society Transactions*, *34*(1), 7.

Wenger, R. H., Stiehl, D. P., & Camenisch, G. (2005). Integration of oxygen signaling at the consensus HRE. In *Science's STKE : signal transduction knowledge environment* (Vol. 2005, Issue 306, pp. re12–re12). American Association for the Advancement of Science.

Wiedenheft, B., Sternberg, S. H., & Doudna, J. a. (2012). RNA-guided genetic silencing systems in bacteria and archaea. *Nature*.

Wielockx, B., & Meneses, A. (2016). PHD2: from hypoxia regulation to disease progression. *Hypoxia*, *4*, 53.

Wiertz, E. J. H. J., Jones, T. R., Sun, L., Bogyo, M., Geuze, H. J., & Ploegh, H. L. (1996). The human cytomegalovirus US11 gene product dislocates MHC class I heavy chains from the endoplasmic reticulum to the cytosol. *Cell*, *84*(5), 769–779.

Wiesener, M. S., Turley, H., Allen, W. E., Willam, C., Eckardt, K. U., Talks, K. L., Wood, S. M., Gatter, K. C., Harris, A. L., Pugh, C. W., Ratcliffe, P. J., & Maxwell, P. H. (1998). Induction of endothelial PAS domain protein-1 by hypoxia: Characterization and comparison with hypoxia-inducible factor-1α. *Blood*, *92*(7).

Wiesener, Michael S., Jürgensen, J. S., Rosenberger, C., Scholze, C. K., Hörstrup, J. H., Warnecke, C., Mandriota, S., Bechmann, I., Frei, U. A., Pugh, C. W., Ratcliffe, P. J., Bachmann, S., Maxwell, P. H., & Eckardt, K. U. (2003). Widespread hypoxia-inducible expression of HIF-2alpha in distinct cell populations of different organs. *The FASEB Journal : Official Publication of the Federation of American Societies for Experimental Biology*, *17*(2), 271–273.

Wouters, B. G., & Koritzinsky, M. (2008). Hypoxia signalling through mTOR and the unfolded protein response in cancer. In *Nature Reviews Cancer* (Vol. 8, Issue 11, pp. 851–864). Nature Publishing Group.

Wu, X., & Rapoport, T. A. (2018). Mechanistic insights into ER-associated protein degradation. In *Current Opinion in Cell Biology* (Vol. 53, pp. 22–28). Elsevier Ltd.

Wykoff, C. C., Beasley, N. J. P., Watson, P. H., Turner, K. J., Pastorek, J., Sibtain, A., Wilson, G. D., Turley, H., Talks, K. L., Maxwell, P. H., Pugh, C. W., Ratcliffe, P. J., & Harris, A. L. (2000). Hypoxia-inducible expression of tumor-associated carbonic anhydrases. *Cancer Research*, *60*(24).

Yamashita, T., Ohneda, O., Nagano, M., Iemitsu, M., Makino, Y., Tanaka, H., Miyauchi, T., Goto, K., Ohneda, K., Fujii-Kuriyama, Y., Poellinger, L., & Yamamoto, M. (2008). Abnormal Heart Development and Lung Remodeling in Mice Lacking the Hypoxia-Inducible Factor-Related Basic Helix-Loop-Helix PAS Protein NEPAS. *Molecular and Cellular Biology*, *28*(4), 1285–1297.

Yang, T., Espenshade, P. J., Wright, M. E., Yabe, D., Gong, Y., Aebersold, R., Goldstein, J. L., & Brown, M. S. (2002). Crucial step in cholesterol homeostasis: sterols promote binding of SCAP to INSIG-1, a membrane protein that facilitates retention of SREBPs in ER. *Cell*, *110*(4), 489–500.

Ye, Y., Meyer, H. H., & Rapoport, T. A. (2001). The AAA ATPase Cdc48/p97 and its partners transport proteins from the ER into the cytosol. *Nature*, *414*(6864), 652–656.

Yoshioka, H., Coates, H. W., Chua, N. K., Hashimoto, Y., Brown, A. J., & Ohgane, K. (2020). A key mammalian cholesterol synthesis enzyme, squalene monooxygenase, is allosterically stabilized by its substrate. *Proceedings of the National Academy of Sciences of the United States of America*, *117*(13), 7150–7158.

Young, R. M., Wang, S. J., Gordan, J. D., Ji, X., Liebhaber, S. A., & Simon, M. C. (2008). Hypoxia-mediated selective mRNA translation by an internal ribosome entry site-independent mechanism. *Journal of Biological Chemistry*, *283*(24), 16309–16319.

Zelcer, N., Sharpe, L. J., Loregger, A., Kristiana, I., Cook, E. C. L., Phan, L., Stevenson, J., & Brown, A. J. (2014). The E3 Ubiquitin Ligase MARCH6 Degrades Squalene Monooxygenase and Affects

3-Hydroxy-3-Methyl-Glutaryl Coenzyme A Reductase and the Cholesterol Synthesis Pathway. *Molecular and Cellular Biology*, *34*(7), 1262–1270.

Zhang, S., Chea, J., Meng, X., Zhou, Y., Lee, E. Y. C., & Lee, M. Y. W. T. (2008). PCNA is ubiquitinated by RNF8. *Cell Cycle*.

Zhao, M., Zhang, L., Qiu, X., Zeng, F., Chen, W., An, Y., Hu, B., Wu, X., & Wu, X. (2016). BLCAP arrests G1/S checkpoint and induces apoptosis through downregulation of pRb1 in HeLa cells. *Oncology Reports*, *35*(5), 3050–3058.

Zhu, J., Jiang, X., & Chehab, F. F. (2014). FoxO4 interacts with the sterol regulatory factor SREBP2 and the hypoxia inducible factor HIF2α at the CYP51 promoter. *Journal of Lipid Research*, *55*(3), 431–442.